Dimitrios Gyalistras & Markus Gwerder (Eds.)

Use of Weather and Occupancy Forecasts For Optimal Building Climate Control (OptiControl): Two Years Progress Report

Reporting Period May 2007–April 2009

Terrestrial Systems Ecology ETH Zurich
Building Technologies Division, Siemens Switzerland Ltd., Zug
27. September 2010

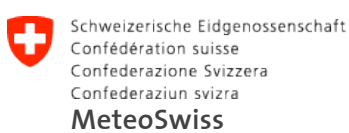

Imprint

OptiControl Project Two Years Progress Report
(Period May 2007–April 2009)

Published by

Terrestrial Systems Ecology, ETH Zurich, Switzerland
Building Technologies Division, Siemens Switzerland Ltd., Zug, Switzerland

May 2009 / September 2010

Available online from

www.opticontrol.ethz.ch

Please use the following reference to the whole report:

Gyalistras, D. & Gwerder, M. (Eds.) (2010). Use of weather and occupancy forecasts for optimal building climate control (OptiControl): Two years progress report. Terrestrial Systems Ecology ETH Zurich, Switzerland and Building Technologies Division, Siemens Switzerland Ltd., Zug, Switzerland, 158 pp, Appendices. ISBN 978-3-909386-37-6.

PREFACE

The needed transition towards a sustainable energy system opens up new business opportunities also in the Building Automation sector. The development of corresponding products and solutions poses however significant scientific-technical challenges that make a close collaboration between academia and industry necessary.

Such an effort was undertaken in the framework of the interdisciplinary project OptiControl (http://www.opticontrol.ethz/) that was launched in May 2007. The project deals with the development of predictive control technologies for buildings. This report summarizes the findings from the first two project years.

As of May 2009 the OptiControl project involved the following persons and institutions:

D. Gyalistras [1+2], A. Fischlin [1]
M. Morari, C.N. Jones, F. Oldewurtel, A. Parisio [2]
T. Frank, S. Carl, V. Dorer, B. Lehmann, K. Wirth [3]
P. Steiner, F. Schubiger, V. Stauch [4]
J. Tödtli, C. Gähler & M. Gwerder [5]

[1] Terrestrial Systems Ecology Group, ETH Zurich, Switzerland
[2] Automatic Control Laboratory, ETH Zurich, Switzerland
[3] Building Technologies Laboratory, Empa Dübendorf, Switzerland
[4] Federal Office of Meteorology and Climatology (MeteoSwiss), Zurich, Switzerland
[5] Building Technologies Division, Siemens Switzerland Ltd., Zug, Switzerland

The OptiControl project is sponsored by

- swiss*electric* research
  The applied research & development program by swiss*electric*, an organization of Swiss electricity grid companies.
  http://www.swisselectric-research.ch/
- CCEM-CH
  The Competence Center Energy and Mobility, Switzerland, a center of competence of the ETH Domain, the union of the two Swiss Federal Institutes of Technology and four application-oriented research institutes.
  http://ccem-ch.web.psi.ch/, http://www.ethrat.ch/
- Building Technologies Division, Siemens Switzerland Ltd., Zug
  Siemens BT is one of the building automation industry's leading players. It is active worldwide at more than 500 locations in 51 countries, with annual revenues in the order of 6 billion Euros and a divisional profit of ca. 0.45 billion Euros.
  http://www.buildingtechnologies.siemens.ch/

Our thanks go to to the sponsors for making this research possible, and to the project participants for sharing with us their know-how, creativity and talents in what proved to be a most challenging and successful enterprise.

We trust that the work reported here will be of general interest to researchers and developers in the Building Automation sector, and that it will contribute to further improving the efficiency and quality of building control.

The Editors

CONTENTS

Summary **1**

1 Introduction
by Dimitrios Gyalistras, Markus Gwerder and Jürg Tödtli **5**

1.1 The OptiControl Project **6**
1.2 Integrated Room Automation **7**
1.3 Criteria for Non-Standardized Control Solutions **7**
1.4 Assessment of Control Performance **9**
1.5 Selection of Control Approaches **10**
1.6 Overview of Report **11**
1.7 References **12**

2 Control Problem And Experimental Set-Up
by Beat Lehmann, Katharina Wirth, Viktor Dorer, Thomas Frank and Markus Gwerder **15**

2.1 Introduction **16**
2.2 Buildings **16**
2.3 Building Systems **18**
2.3.1 Variants 18
2.3.2 Dimensioning 19
2.3.3 Control Costs 20
2.4 Comfort Requirements **21**
2.4.1 Thermal Comfort 22
2.4.2 Indoor Air Quality 23
2.4.3 Illuminance Comfort 23
2.5 Disturbances **24**
2.5.1 Occupancy and Internal Gains 24
2.5.2 Weather 25
2.6 Technical System Integration **25**
2.7 Discussion **27**
2.8 Conclusions **28**
2.9 References **28**

3 Rule-Based Control Strategies
by Markus Gwerder, Jürg Tödtli and Dimitrios Gyalistras **29**

3.1 Introduction **30**
3.2 High-Level Control **31**
3.2.1 RBC-1 31
3.2.2 RBC-2 32
3.2.3 RBC-3 33
3.2.4 RBC-4 35
3.3 Low-Level Control **36**
3.4 Control Parameters **40**
3.4.1 Basic Parameters 40
3.4.2 Actually Used Parameters 41
3.5 Discussion **42**
3.6 Conclusions **42**
3.7 References **42**

4 Model Predictive Control Strategies
by Frauke Oldewurtel, Colin N. Jones, Alessandra Parisio and Manfred Morari **43**

4.1 Introduction **44**
4.2 General Overview of MPC **45**
4.2.1 Cost Function 46
4.2.2 Current State 47
4.2.3 Dynamics 47
4.2.4 Constraints 48
4.2.5 Certainty Equivalence MPC 48
4.3 Robust/Stochastic MPC **49**
4.3.1 Affine Disturbance Feedback 49
4.3.2 Chance Constraints 50
4.4 Performance Bound **51**
4.5 MPC for OptiControl **51**
4.5.1 Step 1 – Weather Prediction at Building Site 51
4.5.2 Step 2 – Modeling 53
4.5.3 Step 3 – Formulate Constraints 54
4.5.4 Step 4 – Solve Linear Program 56
4.5.5 Step 5 – Apply Control Action 56
4.6 Discussion **56**
4.6.1 Benefits of MPC 56
4.6.2 MPC And Low-Level Control 57
4.6.3 Estimation Of States And Parameters 57
4.7 Conclusions **58**
4.8 References **58**

5 Modeling Of Buildings And Building Systems
by Beat Lehmann, Katharina Wirth, Stephan Carl, Viktor Dorer,
Thomas Frank and Markus Gwerder **59**

5.1 Introduction **60**
5.2 Choice of Building Modeling Approach **60**
5.3 Model Overview **61**
5.4 Description of Subsystems **62**
5.4.1 Mechanical ventilation 62
5.4.2 Hybrid ventilation / natural ventilation 63
5.4.3 Radiator: direct room heating 63
5.4.4 Ceiling slow: heating and cooling 63
5.4.5 TABS: heating and cooling 64
5.4.6 Floor heating: heating and cooling 64
5.4.7 Free cooling with a wet cooling tower 64
5.4.8 Blinds and lighting 65
5.5 Model Validation **65**
5.6 Conclusions **66**
5.7 References **66**

6 Local Weather Forecasts And Observations
by Vanessa Stauch, Francis Schubiger and Philippe Steiner **67**

6.1 Introduction **68**
6.2 The Numerical Weather Prediction Model COSMO **69**
6.3 Data Description **70**
6.3.1 Selected Case Study Sites & Observation Data 70
6.3.2 Derived Weather Variables & Design Reference Years 71
6.3.3 Database for OptiControl 72
6.4 Local forecast correction **72**
6.4.1 State-space formulation for forecast correction 72
6.4.2 Forecast evaluation and discussion 73
6.5 Conclusions **77**
6.6 References **78**
6.7 Acknowledgements **78**

7 Performance Bounds And Potential Assessment
by Dimitrios Gyalistras, Beat Lehmann, Katharina Wirth,
Markus Gwerder, Frauke Oldewurtel and Vanessa Stauch **79**

7.1 Introduction **80**
7.2 Material & Methods **81**
7.2.1 Overview 81
7.2.2 Performance Bound Estimation 81
7.2.3 Factors and Experiments Sets 82
7.2.4 Analysis Procedure 84
7.2.5 Software And Databases 85
7.3 Results **86**
7.3.1 Choice of Building System and Optimization Target 86
7.3.2 Assessment of Low-Cost Energy Saving Measures 89
7.3.3 Electric Lighting And Thermal Comfort Analysis 92
7.3.4 Potential Assessment 96
7.3.5 Comparison 100
7.4 Discussion **101**
7.4.1 Key Assumptions 101
7.4.2 Performance of RBC Strategies 102
7.4.3 Problems And Limitations 103
7.5 Conclusions **103**
7.6 References **105**

8 Analysis Of Savings Potentials And Peak Electricity Demand
by Dimitrios Gyalistras, Katharina Wirth and Beat Lehmann **107**

8.1 Introduction **108**
8.2 Material & Methods **109**
8.2.1 Data 109
8.2.2 Analysis of Variance 109
8.2.3 Analysis of Solar Gains 110
8.2.4 Analysis of Peak Electricity Demand 110
8.3 Results **110**
8.3.1 Overview of Savings Potentials 110
8.3.2 Investigation of Key Factors 113
8.3.3 Analysis of Selected Cases 117
8.3.4 Analysis of Peak Electricity Demand 128
8.4 Discussion **132**
8.5 Conclusions **134**

9 Analysis Of Model Predictive Control Strategies
by Frauke Oldewurtel, Dimitrios Gyalistras, Colin. N. Jones, Alessandra Parisio and Manfred Morari **135**

9.1 Introduction **136**
9.2 Materials and Methods **137**
9.2.1 Simulation Experiments 137
9.2.2 Comparison Procedure 139
9.3 Results **140**
9.3.1 What Is The Added Value of Certainty Equivalence MPC (Q1)? 140
9.3.2 What Is The Added Value of Stochastic MPC (Q2)? 141
9.3.3 How Much Does The Quality Of The Weather Predictions Matter For MPC (Q3)? 143
9.3.4 How Robust Is MPC To Model Parameter Mismatch (Q4)? 146
9.3.5 How Can The Desired Thermal Comfort Level Be Adjusted In MPC (Q5)? 147
9.4 Discussion **148**
9.5 Conclusions **151**

10 Project Status
by Dimitrios Gyalistras and Markus Gwerder **153**

10.1 Overview **154**
10.2 Achievements **156**
10.3 Challenges **158**

Appendix A – Building Model Description

Appendix B – Building Model Validation

Appendix C – Control Costs: Methodology And Factors

Appendix D – Performance Bounds Analyses

Appendix E – Assessment Of Rule Based Control Strategies

SUMMARY

This report presents the work conducted during the first two years of the OptiControl project (www.opticontrol.ethz.ch), an interdisciplinary project dedicated to the development of predictive control technologies for buildings. The overall aim is to minimize the energy usage of buildings whilst maintaining or even improving occupant comfort and reducing peak electricity demand.

Here we report on project Phases I and II that dealt with the development of methods, tools and control strategies, the assessment of the potential of predictive control, and the in-depth analysis of selected cases. This work was based entirely on computer simulations. In Phase III the newly developped control approaches shall be tested in a demonstrator building.

Integrated Room Automation (IRA) for office buildings was identified as a promising candidate for the investigation of predictive control strategies. IRA deals with the automated control of blinds, electric lighting, heating, cooling, and ventilation of an individual building zone or room. Most of the work undertaken within the OptiControl project so far has focused on this application.

A comprehensive set of criteria covering all aspects of IRA control solutions was defined to provide guidance for the research and development work. The criteria ranged from control performance and requirements of different users to marketing potential. Based on these criteria and on further considerations Rule-Based Control (RBC) and Model Predictive Control (MPC) were identified as the most promising control approaches.

A generic framework for the assessment of control performance was developed that uses the so-called Performance Bound (PB) as an absolute benchmark. The PB is a theoretical value and presents the lowest achievable control cost (in terms of energy or money) for a given building, cost function, disturbances (weather, internal gains), and set of comfort requirements. It is estimated by assuming perfect knowledge of the building system and all disturbances acting upon it. The difference in control cost between the best currently known non-predictive controller and the PB presents the theoretical savings potential of predictive control. The realizable potential in practice will always be smaller since every real controller will show higher costs than the PB.

The IRA control task was formally defined in all its facets: Relevant building types, types of heating, cooling, ventilation, blind and lighting subsystems, control operation types, and representative building locations were identified, the subsystems were sized properly, and meaningful energy usages/costs were specified. The hierarchical architecture of modern Building Automation and Control systems was considered from begin on in order to ensure that the solutions developed could be easily integrated therein later on.

Four non-predictive RBC strategies plus associated procedures for the automated tuning of their control parameters were identified or newly designed and implemented for use in simulations: RBC-1, a state-of-the-art strategy; RBC-2: same as RBC-1, but allowing for continuous blind transmission values and for time-continuous (rather than event-triggered) repositioning of blinds; RBC-3: an entirely new strategy that, instead of working with threshold values, uses historical heat and cold demand signals and historical room temperature data, and that also allows for maximum freedom in blind movement; and RBC-4: same as RBC-3, but with blinds repositioning restricted to once per hour.

A new family of Model Predictive Control (MPC) strategies was developed that was tailored to the needs of building control: PB, an algorithm that estimates the PB with the aid of MPC; Certainty Equivalence (CE), a controller that uses imperfect models and/or disturbance predictions but treats them as if they were correct (i.e. equal to certain); and Chance Constrained Stochastic MPC (SMPC), an enhanced approach that may or may not involve perfect models but takes the uncertainty in the disturbances predictions, in particular of weather predictions, into account.

A new model for the coupled thermal, light and air quality dynamics of a single building zone was developed, tested and validated. The model was used to simulate the behavior of real buildings under different control strategies, and to describe the building system's dynamics for MPC. It was a 12th order multiple-input-multiple-output bilinear model with a resistance-capacitance network representation of thermal energy fluxes. Analysis of the approximations employed and a comparison with a detailed radiative-convective model suggested that the model delivers accurate and reliable results.

Hourly weather data from 10 representative European SYNOP measurement sites for the years 2001 (or later) to 2007, predictions by the COSMO-7 numerical weather prediction model for the years 2006 and 2007, and various Design Reference Year datasets (special, representative datasets compiled from long term climate observations) were prepared as an input for building simulations. Algorithms for the disaggregation of hourly global radiation into the direct and diffuse part, and for the derivation of global radiation components on vertical oriented surfaces were implemented. Novel statistical post-processing methods were developed and applied to improve local predictions of the most important weather variables for the building control applications under investigation. In general, forecast biases could be successfully removed on a seasonal basis. The root mean square error of local temperature predictions for the first 24 hours ahead was reduced by 20–30%. For wetbulb temperature the reduction was 35–45%. For the radiation components no reductions or slight increases were obtained for winter and summer, but reductions of 10–60% were achieved for spring and autumn. These improved data sets were made available for building simulations.

The theoretical savings potential of predictive control was assessed by comparing the performance of the controllers RBC-1 to RBC-4 with the PB. The found savings potentials were put into context by comparing them with possible energy savings due to the following low-cost measures related to control: a) a reduction of the thermal comfort when the building is not used, by allowing for room tem-perature set-backs during nights and weekends (base case: no set-backs allowed); b) a general reduction of thermal comfort due to a widening of the room temperature comfort range by ~1.5 ºC (base case: narrow comfort range); c) the use of Indoor Air Quality controlled ventilation (base case: application of a constant minimum fresh air supply rate according to a fixed occupancy schedule); d) the adjustment of the control such that it optimized control actions for energetic rather than monetary cost (base case: optimization of control for money).

Conducted was a large-scale factorial simulation experiment (~23'500 whole-year, hourly time step dynamic simulations) considering 64 building/room types (differing in façade orientation, construction type, building standard etc.), 5 building systems (S1–S5, employing different heating, cooling, and ventilation subsystems), 2 "cost" functions (Non-Renewable Primary Energy [NRPE] usage, and monetary costs), 4 different building sites, 4 thermal comfort definitions, and 2 ventilation strategies. Annual total costs and annual comfort indices were analyzed by building system, building standard (PA–"Passive House", or SA–"Swiss average"), and building class (I–"very frequent", II – "less frequent", III–"exotic" building case).

RBC-3 (time-continuous repositioning of blinds and perfect luminance control via blind operation) proved clearly as the best performing non-predictive controller and in many cases it came very close to the PB. The average absolute (relative) theoretical NRPE savings potential over the building classes I and II was 2.6 kWh/m2/a (9.2%) for the PA building standard and building system variants S1-S5, and 3.8 kWh/m2/a (9.7%) for the SA building standard and building system variants S1-S3. Much larger theoretical savings potentials were obtained for the RBC-1 and RBC-4 controllers that employed much more realistic assumptions on repositioning of blinds as compared to RBC-3: average maximum possible NRPE savings (building classes I and II, building system variants S1–S5) for these two strategies were 34% and 33% for the PA, and 30% and 23% for the SA building standard, respectively.

Generally, all simulation results showed a very high case-to-case variability. For example, for the RBC-3 controller the 10th and 90th percentiles of the theoretical savings potentials straddled the average intervals 0.7–4.7 kWh/m2/a (2%–18%) for PA, and 2.0–5.5 kWh/m2/a (4%–16%) for SA.

From the investigated low-cost energy saving measures related to control the use of Indoor Air Quality controlled ventilation showed the largest effect: ~27% for the PA and ~18% for the SA building standard (average values over building classes I and II and the building system variants S2–S5 that included mechanical ventilation). The assumed widening of the thermal comfort range yielded average savings in the order of 10% (average over building classes I and II and all five building system variants). The use of set-backs resulted to average savings by 3% for PA and 8% for SA, respectively. The choice of cost function (optimization for energy instead of money) was found to be generally of secondary importance.

A closer analysis of the theoretical energy savings potentials showed that they tend to be largest for building zone cases entailing large energy fluxes (high solar heat gains and/or high internal gains). An examination of carefully selected individual building cases showed that the NRPE savings can be traced to the optimized use of the blinds, free cooling and energy recovery. Predictive control of these low-cost devices allows to efficiently pre-heat or pre-cool the building structure. This makes it possible to avoid frequent switching between heating and cooling, and to keep room temperatures as much as possible floating freely within the thermal comfort range.

Comparison of hourly electric power demand values in the PB and the RBC-3 simulations showed that a reduction in energy use does not necessarily imply also a reduction in peak demand. Reduction of peak loads thus makes specific adjustments in the control algorithms necessary. These can be easily accomplished with the developped MPC controllers.

The extent to which the theoretical energy savings potentials can be exploited in practice was explored based on simulation studies with the newly developed MPC strategies and using realistic weather forecasts from the COSMO-7 processing chain. It was found that the SMPC strategy is clearly superior to the CE strategy, and also much better than RBC-4 in terms of NRPE usage, comfort violations and room temperature dynamics. The tunability of the SMPC and CE strategies with regard to thermal comfort was demonstrated, and it was shown that SMPC offers a particularly elegant and plausible tuning procedure. First analyses suggested that the performance of MPC controllers is robust against model parameter mismatch. The use of operational weather forecasts was found to give an improvement as compared to the use of simple persistence forecasts. The uncertainty present in the weather predictions had however a significant effect on CE controller performance, and the use of a low-level controller was identified as a remedy. The use of a Kalman filter for the correction of local weather forecasts at the building site was generally found to be beneficial.

The final section of the report assesses the project's status after the first two years of work. The project's achievements are summarized and discussed, and four important areas for further research are identified: the implementation of improved rule-based reference strategies (support of night/ weekend set-backs, plus adaptations for floor heating and for thermally activated building systems); the enhancement of the comparability of RBC and MPC; the further development of the novel control strategies in order to make them suitable for use in practice; and the integration of MPC in commercial BAC systems.

This page has intentionally been left blank.

Chapter 1

INTRODUCTION

by Dimitrios Gyalistras, Markus Gwerder and Jürg Tödtli

Cite as:

Gyalistras, D., Gwerder, M. & Tödtli, J. (2010). Introduction. In: Gyalistras, D. & Gwerder, M. (eds.): *Use of weather and occupancy forecasts for optimal building climate control (OptiControl): Two years progress report*. Terrestrial Systems Ecology ETH Zurich, Switzerland and Building Technologies Division, Siemens Switzerland Ltd., Zug, Switzerland, pp 5–14. ISBN 978-3-909386-37-6.

1.1 The OptiControl Project

Buildings use ca. 40% of final energy worldwide and account for ca. 33% of global total CO_2 emissions, including emissions from electricity use [1]. Most of the energy is consumed during the use of the buildings [2], and in developed countries roughly half of the energy use goes to the building's heating, ventilation, and air conditioning (HVAC) systems [3]. In the EU a massive growth is predicted in conditioned area and energy consumption in the years to come [4]. At the same time the building sector has a large potential for the cost-effective reduction of CO_2 emissions [1], and most investments in buildings can be expected to pay back through reduced energy bills (e.g.,[5]).

The research project OptiControl (http://www.opticontrol.ethz.ch/) deals with the improvement of the building's automation and control systems as one possibility to reduce energy consumption. The goal is to realize energy savings and reduce peak electricity demand while maintaining high user comfort and work productivity, at modest basic investment and operating costs.

In order to reach this goal the project aims at exploiting newest developments in the areas of building and information technologies, weather forecasting, and Model Predictive Control (MPC) of dynamic systems. The emphasis is on predictive control, for the following reasons:

Firstly, the idea of using load and disturbances forecasts – in particular weather forecasts – for building control is expressed time and again by specialists [12] and laymen alike. It is intuitively appealing, and in many cases it appears also particularly promising. Many studies have dealt with this issue [7]-[26], but to our knowledge the potential and the benefit/costs of the approach have not been investigated systematically so far.

Secondly, the boundary conditions for building control are becoming increasingly dynamic, and this clearly enhances the importance of predictive control. The changes in boundary conditions relate to the increasing use of intermittent, low carbon energy sources, the high solar gains associated with many modern building designs, and the advent of dynamic electricity pricing.

Finally, there are some further developments that may make the use of more sophisticated (e.g., predictive) control approaches necessary in order to get buildings to function efficiently and correctly: increasing comfort requirements, the introduction of new, but in terms of control more demanding building technologies (such as heat pumps, thermally activated building systems, cooling by night-time ventilation etc.), and the need to integrate diverse technologies into overall systems.

The OptiControl project addresses the development of novel building control strategies in three phases that are extending over a period of ca. one year each. The phases are: I. Assessment of potential for improved control; II. In-depth analysis of selected cases; and III. Testing of new control approaches in a demonstrator building. Phases I and II are entirely based on computer simulations.

This report was compiled at the end of Phase II and provides the basis for evaluating a possible continuation of the project by a third year.

At an early stage of the project two major applications were identified as particularly promising for predictive control. They are operating on the level of a single building zone and on the whole-building level, respectively. They are the so-called Integrated Room Automation (IRA), and the generic control of energy fluxes and energy storages related to buildings.

The main focus during the first two project years has been on the IRA application, and this is also the application addressed in the largest part of this report. However, the overall methodology developed for the study of IRA is generic and can be used in the context of other applications as well.

1.2 Integrated Room Automation

The Integrated Room Automation (IRA) application deals with the automated control of blinds, electric lighting, heating, cooling, and ventilation of an individual building zone or room. The control task consists in maintaining occupant comfort at minimum energetic or monetary cost while at the same time rejecting disturbances related to, e.g., weather, internal gains, and occupant behavior.

IRA is a particularly interesting candidate for predictive control studies. The potential benefit of predictive control for IRA lies in optimizing the use of cheap control actions (e.g. blinds positioning, free cooling) and in the exploitation of the building's thermal storage capacity. Also, IRA typically involves very diverse technical equipment. Consequently, the control task is quite complex, and the equipment's energy consumption tends to be higher than in simpler set-ups. This in turn promises higher saving potentials thanks to more sophisticated control.

For several reasons we focused on office buildings. Firstly, office buildings typically employ energy intensive HVAC systems. Within the commercial sector they show together with retail the highest energy consumption, in the order for 2–3% of national total energy use [3]. Secondly, total built area of office buildings has been steadily increasing in the last years. Thirdly, they are the main type of buildings that are equipped with the individual room/zone controllers considered in the IRA application. And finally, offices typically exhibit relatively high internal gains that need to be dealt with in an efficient manner.

1.3 Criteria for Non-Standardized Control Solutions

IRA uses so-called "non-standardized" control solutions. This means that the control has to be tailored to the given building, combination of automated subsystems and user requirements by means of corresponding programs that govern the behavior and interplay of the individual subsystems. Non-standardized control solutions need to be customized, commissioned (engineering) and operated (service). Therefore, building automation systems with programmable controllers are typically used for that purpose.

Research and development efforts within the OptiControl project were guided by a comprehensive set of criteria that were considered important for non-standardized control solutions in the Building Automation (BA) sector (Table 1.1).

The criteria were defined and selected in cooperation with the product marketing section from Siemens Building Technologies (BT). They covered all aspects of a control solution, ranging from performance, requirements of different users, to development and marketing possibilities. Several of the criteria favored simple control solutions, as it is manifested in the current initiative KISS (keep it simple and short) within Siemens BT systems development.

No.	*Criterion*	*Description/Comments*
1	Achievable control performance	Maximum performance that can be attained for a correctly functioning and well-tuned system. The resulting cost/benefit (between different control solutions) can be quantified quite exactly – with considerable effort – by simulation studies. For example, energy/monetary costs as well as comfort indices can be calculated and compared.
2	Robustness on control parameter settings	In practice, the control parameter settings will be far from perfect due to missing information or insufficient understanding of the control system. Therefore, it is essential that the control performance is satisfactory for a broad range of control parameter settings.

No.	*Criterion*	*Description/Comments*
3	Robustness on building system, disturbances, user interactions	A control solution should perform well for all kind of different building systems, disturbances (e.g. weather, internal gains) and user interactions. Typical user interactions are light switching, blind positioning or the shifting of temperature set points. Since the occupant behavior varies considerably, a control solution should be robust also in this regard.
4	Flexibility and tuning effort in the engineering process	In the building automation market exist numerous variants of the here considered applications (besides different locations and building types): Different HVAC, blind and lighting systems, different levels of automation, different control requirements etc. Moreover, a given application can change during the building's lifetime (e.g., due to installation or removal of inner walls). Therefore, there is a need for flexible control solutions that support as many variants as possible with low engineering effort. Tuning effort refers to the effort for determining control parameter values that lead to a good control performance. Tuning can occur in the pre-commissioning, the commissioning, and/or the service phase of a control solution.
5	User acceptance for engineering, commissioning and service	Non-standardized control solutions such as IRA are engineered for each building individually. Engineers must be able to adapt a control solution to a particular case. The solution then needs to be commissioned and – during operation – serviced. In all that, the engineer's skill level has to be considered: the person involved must understand the basic functionality of the control solution. The procedure for adapting and tuning the control solution should be as simple as possible and understandable by engineering, commissioning and service personnel. Training effort to enable an efficient engineering, commissioning and service procedure should be kept as low as possible.
6	User acceptance of the end user	This is an essential prerequisite for the commercial success of a control solution. A study about human-machine interface for building automation can be found in [27]. For the IRA applications investigated therein the following relevant aspects were identified: (i) Desired comfort can be achieved; (ii) Possibility and ease of manual interaction; (iii) Plausibility of automatic control actions – in particular blind movement; disturbances through automatic control actions (e.g. noise of blind movement, automatic light switches).
7	Suitable as extension option	The possibility to use a new control solution as an "add-on" is generally valued as an advantage. The control solution then presents an element in an incrementally extendable solution portfolio. The overall control solution should be based on as many conventional components as possible; the new components can then be introduced selectively to increase performance or provide additional functionality.
8	Investment and maintenance costs	The costs associated with the application of the control solution. Investment costs can be costs for extra needed computing infrastructure, training costs for engineers etc. Maintenance costs include costs for service activities, but also possible costs for purchasing weather forecasts from a meteorological service.
9	Development effort	The smaller this effort is, the higher the chances for a control solution to be developed and applied in the market. A control solution with low development effort can be directly investigated in field tests with low financial risk if the solution fails in these tests. On the contrary, before developing a solution with high development effort, such a solution has to be thoroughly tested in simulations and/or prototypes.
10	Innovativeness and selling arguments	Besides potential benefits in terms of improved comfort and energy efficiency of new control solutions, the offer of an innovative control solution can be exploited for marketing purposes: additional selling arguments are generated.

Table 1.1: Criteria for the assessment of non-standardized control solutions in the Building Automation sector.

1.4 Assessment of Control Performance

The criteria 1–4 from Table 1.1 are accessible to quantitative analysis by means of computer simulations and received particular consideration in the OptiControl project.

The most important criterion was criterion no. 1, the achievable control performance. The conceptual framework used to assess the performance of a specific control strategy (or the comparative performance of several control strategies) is shown in Figure 1.1.

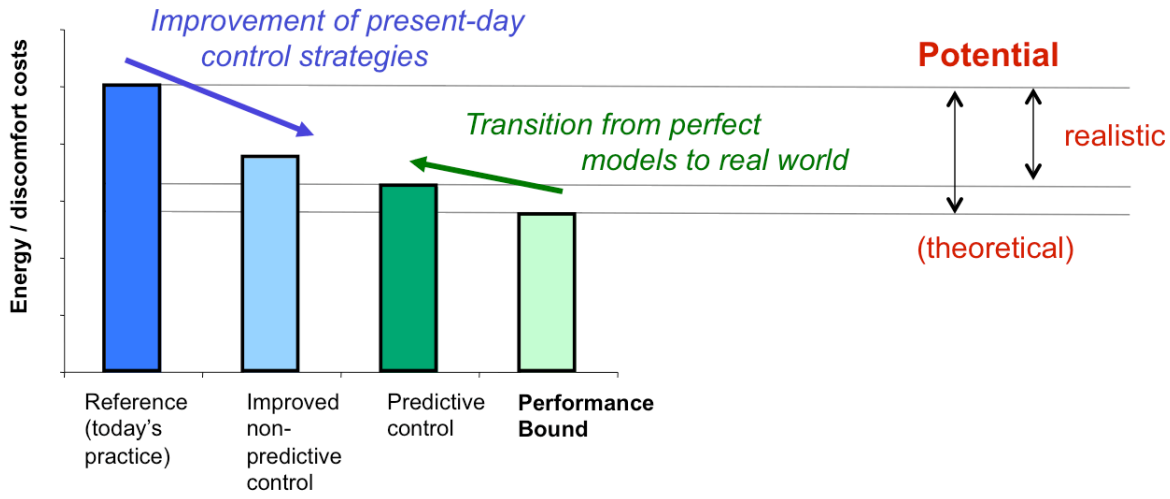

Figure 1.1: Conceptual framework for assessing controller performance.

The key element of the assessment is the so-called Performance Bound (PB). It is a theoretical value that presents the lowest achievable control cost (in terms of energy or money) for a given building, building system, cost function, disturbances (weather, internal gains) and set of comfort requirements.

The PB can be determined by means of mathematical optimization under the assumption that the dynamical behavior of the building and its automated subsystems as well as all (future) weather and internal gains disturbances that are acting upon the system are perfectly known (see also Chapter 4).

Clearly, no real controller will ever reach the PB, but the difference between its performance (e.g. energy usage) and the PB value gives a measure of the maximum achievable improvement. Nothing can be said about to what extent the potential can be exploited by a feasible control. But the sizes of remaining potentials reveal for what applications (building type, HVAC system, location etc.) further control strategy development may be promising.

1.5 Selection of Control Approaches

To date a large variety of control approaches have been proposed for building control (overviews can be found in [28], [29], [13]). These include the usage of neuronal networks (e.g., [30], [17]), fuzzy logic approaches (e.g., [30], [31]), rule-based control (RBC, e.g. [32]), and Model Predictive Control (MPC, e.g. [33], [34], [35], see also predictive heating control in [32]). The OptiControl project focused on the RBC and MPC approaches.

The main reason for selecting RBC was that it is the common solution for non-standardized BA applications. Accordingly, a lot of experience with regard to the engineering, commissioning and servicing of this type of control is available. This is important because in order to profit from the flexibility of the RBC approach a corresponding tuning effort is often needed.

Most RBC solutions currently offered for IRA by Siemens BT are non-predictive. However, the implementation effort for new RBC strategies is relatively low. Given that appropriate rules are being identified the already existing RBC solutions could be extended quite easily to integrate weather forecasts as well as internal gains and occupancy predictions.

The second control approach considered was MPC. It was chosen because it is tailored to predictive control. A major advantage of MPC as compared to all other control approaches is that it employs a mathematical, physically based model of the controlled process, and can thus account for non-linear and complex interactions in multiple-input-multiple-output systems.

A further reason for considering MPC was the large expertise available within the OptiControl project team. Moreover, Siemens BT has just launched an MPC-based predictive heating controller for domestic applications, such that first experience from the usage of MPC in practice is expected to become available in the near future.

According to the experience of the OptiControl team non-specialists are generally able to easily understand both approaches, RBC as well as MPC. This is important for the acceptance of any newly developed control solutions.

A second important element for user acceptance is the plausibility of the control actions. It is well known from practice that the control actions delivered by RBC sometimes appear counter-intuitive and are difficult to understand (e.g., operation of blinds). In contrast, the control actions provided by MPC can be interpreted directly in the context of the underlying model of the physical building system and of the chosen optimization criteria and constraints. This could open up totally new possibilities for improved servicing by engineers, and for making the actions understandable (and thus better acceptable) to the users of a building.

From a methodical point of view the two approaches are to some extent complementary. The individual rules applied in RBC strategies are fairly simple and straightforward to implement, but in order to obtain a good performance a considerable tuning effort may be necessary. Quite differently, MPC involves sophisticated mathematical modeling and optimization techniques that are only accessible to specialists. On the upside, constraints and control targets can easily be specified, such that according changes can be handled well and without new tuning of the control.

Finally, an important synergy of the RBC and MPC approaches should be stated: MPC is mathematically equivalent to a method for finding the globally optimal set of rules and associated parameters in a very large decision space. Hence, careful study of MPC results can be used to derive approximate, reduced sets of relevant rules and parameters for use in RBC controllers.

1.6 Overview of Report

The rest of this report is structured as follows:

Chapter 2 presents the IRA control problem in detail and introduces the various building variants considered for the development and simulation-based assessment of the control strategies.

Chapters 3 and 4 provide an introduction to, and a description of the RBC and MPC control strategies considered, respectively.

Chapter 5 deals with the developed models of buildings and their automated subsystems for use in the simulations and in the MPC controllers.

Chapter 6 discusses the used weather data and the development of local weather forecasts for building applications.

Chapter 7 presents a large-scale simulation study on low-cost energy savings measures related to control, and on the theoretical potential of predictive control for IRA.

Chapter 8 provides a detailed analysis of the found energy savings potentials and of peak electricity demand.

Chapter 9 is dedicated to the analysis of the novel MPC approaches developed for IRA.

Chapter 10 provides an assessment of the current project status and an outlook to future work.

In order to enhance the readability of the Chapters, detailed information is being provided in a series of Appendices. Their contents are as follows:

Appendix A: Description of the building model.

Appendix B: Validation of the building model and the approximations employed.

Appendix C: Methodology and factors for assessing the control costs.

Appendix D: Results from Performance Bound simulations.

Appendix E: Performance assessment of RBC and theoretical potential of predictive control.

1.7 References

[1] Barker, T. et al. (2007): Technical Summary. In: Climate Change 2007: Mitigation. Contribution of Working Group III to the Fourth Assessment Report of the Intergovernmental Panel on Climate Change [B. Metz, O. R. Davidson, P. R. Bosch, R. Dave, L. A. Meyer (eds)], Cambridge University Press, Cambridge, United Kingdom and New York, NY, USA.

[2] Jones, D. Ll. (1998): Architecture and the Environment – Bioclimatic Building Design. Laurence King Publishing, London, 256pp.

[3] Pérez-Lombarda, L., Ortiz, J. & Pout. C. (2008). A review on buildings energy consumption information. Energy and Buildings 40(3): 394-398.

[4] Adnot, J. et al. (2003). EECCAC – Energy Efficiency and Certification of Central Air Conditioners. Study for the D.G. Transportation-Energy (DGTREN) of the Commission of the E.U. Final Report, Volume I, April 2003. ARMINES, Paris, France, 54pp.

[5] Watson, J. (ed.) (2008): Sustainable Urban Infrastructure, London Edition – a view to 2025. Siemens AG, Corporate Communications (CC) Munich, 71pp.

[6] Gwerder, M. (2007). Summary of WS 09: Enhanced Use of Weather Data and Forecasts to Improve the Energy Efficiency and Indoor Environment in Buildings (13th June 2007). Workshop summary, REHVA World Congress Clima 2007 - WellBeing Indoors, 10-14 June 2007, Helsinki, Finland.

[7] Grünenfelder, W.J. & Tödtli, J. (1985). The use of weather predictions and dynamic programming in the control of solar domestic hot water systems. Paper presented at the 3d Mediterranean Electrotechnical Conference (Melecon), 8-10 Oct. 1985, Madrid, Spain, 5pp.

[8] Grünenfelder, W.J. & Tödtli, J. (1988). Vorausschauende Steuerungen für solare Brauchwarmwasseranagen. Paper presented at the 5. Schweizerisches Status-Seminar "Energieforschung im Hochbau", 8-9. Sep. 1988, ETH Zurich, Switzerland, p333-342.

[9] Nygard-Ferguson, M. & Scartezzini, J.-L. (1989). Computer simulation of an optimal stochastic controller applied to passive solar rooms. Energy and Buidings 14(1): 1-7.

[10] Nygard Ferguson, M. & Scartezzini, J.-L. (1992). Evaluation of an optimal stochastic controller in a full-scale experiment. Energy and Buildings, 18(1): 1-10.

[11] Oestreicher, Y., Bauer, M. & Scartezzini, J.-L. (1996). Accounting free gains in a non-residential building by means of an optimal stochastic controller. Energy and Buildings 24(3): 213-221.

[12] Argiriou, A.A., Bellas-Velidis, I. & Balaras, C.A. (2000). Development of a neural network heating controller for solar buildings. Neural Networks 13(7): 811-820.

[13] Gruber, P., Gwerder, M. & Tödtli, J. (2001). Predictive control for heating applications. Paper presented at the 7th REHVA World Congress (Clima 2000/Napoli 2001), 15-18 Sep. 2001, Napoli, Italy, 15pp.

[14] Kummert, M., André, P. & Nicolas, J. (2001). Optimal heating control in a passive solar commercial building. Solar Energy 69(Suppl. 6): 103-116.

[15] Prud'homme, T. & Gillet, D. (2001). Advanced control strategy of a solar domestic hot water system with a segmented auxiliary heater. Energy and Buildings 33(5): 463-475.

[16] Guillemin, A. & Morel, N. (2002). Experimental results of a self-adaptive integrated control system in buildings: a pilot study. Solar Energy 72(5): 397-403.

[17] Argiriou, A.A., Bellas-Velidis, I., Kummert, M. & André, P. (2004). A neural network controller for hydronic heating systems of solar buildings. Neural Networks 17(3): 427-440.

[18] Henze, G.P., Felsmann, C. & Knabe, G. (2004a). Evaluation of optimal control for active and passive building thermal storage. International Journal of Thermal Sciences 43(2): 173-183.

[19] Gwerder, M. & Tödtli, J, (2005). Predictive control for integrated room automation. Paper presented at the 8th REHVA World Congress (Clima 2005), 9-12 Oct. 2005, Lausanne, Switzerland, 6pp.

[20] Henze, G.P., Kalz, D., Liu, S. & Felsmann, C. (2005). Experimental analysis of model-based predictive optimal control for active and passive building thermal storage inventory. International Journal of HVAC&R Research, 11(2): 189-214.

[21] Bianchi, M.A. (2006). Adaptive modellbasierte prädiktive Regelung einer Kleinwärmepumpenanlage. PhD Thesis No. 16892, ETH Zurich, Switzerland, 167pp.

[22] Himmler R., Peter, M., Sasse, C., Fisch, N.M. & Cerny, R. (2006). WPR - Wetterprognosegeführte Regelung von thermisch aktivierten Decken. In: Proceedings of the First German-Austrian IBPSA Conference, October 9-11, 2006, Technische Universität München, Germany, p172-173.

[23] Liu, S. & Henze, G.P. (2006). Experimental analysis of simulated reinforcement learning control for active and passive building thermal storage inventory. Part 1: Theoretical foundation. Energy and Buildings 38(2): 142-147.

[24] Gähler, C., Gwerder, M., Lamon, R. & Tödtli, J. (2007). Optimal control of cogeneration building energy systems. In: Seppänen, O. & Säteri, J. (eds): Proceedings of REHVA World Congress Clima 2007 - WellBeing Indoors, FINVAC ry, Helsinki, Finland, Session B05, paper no. 1148.

[25] Werner, M. & Hardt, S. (2007). Betriebsoptimierung mit Wettervorhersage-Steuerung. Technik am Bau 5/2007: 58-61.

[26] SMHI (2008). SMHI WeatherSync - Forecast control for heating in buildings. Swedish Meteorological and Hydrological Institute (SMHI), Norrköping, Sweden, 10pp.

[27] Hausladen, G., Frieling, E., Frenkler, F. (2008). Schnittstelle Mensch- Gebäudetechnik, Abschlussbericht. TU-München, Universität Kassel.

[28] Dounis, A.I., Lefas, C.C. & Argiriou A. (1995). Knowledge-based versus classical control for solar-building designs. Applied Energy 50(4): 281-292.

[29] Tödtli, J. (1997). Overview on Technical Session 5 (Control). Invited paper, presented at the 6th REHVA World Congress (Clima 2000), 30 Aug.-2 Sep. 1997, Brussels, Belgium, 34pp.

[30] NEUROBAT Final Report (1998). Predictive Neuro-fuzzy Building Control System. CSEM Neuchâtel, EPF Lausanne.

[31] Bauer, M., Geiginger, J., Hegetschweiler, W. et al (1996). Delta: A Blind Controller using Fuzzy Logic, Swiss Federal Institute of Technology Lausanne.

[32] Siemens Building Technologies building automation system DESIGO™ V2.37: System documentation (2007), expert edition.

[33] Kallina, G. (1987). Erfahrungen mit einem Optimierungsrechner für Heizungsanlagen in einem grossen Wohngebäude. Automatisierungstechnische Praxis atp, 29. Jahrgang, Heft 1/1987.

[34] Munack, A. (1984). Zur Optimalregelung einer Warmwasser-Fussbodenheizung. HLH Bd. 35, 1984.

[35] Hücker, J., Rake, H. (2000). Prädiktiver Kompaktregler für Heizen-/Kühlen-Prozesse mit schaltenden Stellgliedern. Automatisierungstechnische Praxis atp, 42. Jahrgang, Heft 5/2000.

This page has intentionally been left blank.

Chapter 2

CONTROL PROBLEM AND EXPERIMENTAL SET-UP

by Beat Lehmann, Katharina Wirth, Viktor Dorer,
Thomas Frank and Markus Gwerder

Cite as:

Lehmann, B., Wirth, K., Dorer, V., Frank, Th. & Gwerder, M. (2010). Control problem and experimental set-up. In: Gyalistras, D. & Gwerder, M. (eds.): *Use of weather and occupancy forecasts for optimal building climate control (OptiControl): Two years progress report*. Terrestrial Systems Ecology ETH Zurich, Switzerland and Building Technologies Division, Siemens Switzerland Ltd., Zug, Switzerland, pp 15–28. *ISBN 978-3-909386-37-6.*

2.1 Introduction

The purpose of this section is twofold: Firstly, to present all facets of the control problem posed by the Integrated Room Automation (IRA) application. Secondly, to describe – and give the rationale for – the experimental set up that we have chosen for the simulation-based analysis, development and testing of the various IRA control strategies that are described later in Chapters 3 and 4.

2.2 Buildings

By definition, IRA deals with the control of individual building zones or rooms. These are to some extent interconnected, e.g. by the exchange of energy and air, the centralized heat/cold generation and distribution, the use of centralized air handling units, the presence of building usage schedules, the grouping of zones/rooms into groups with common schedules for comfort, or light etc. However the presence of individual room/zone control is the dominating factor.

Accordingly, in the present work we studied the individual building zones/rooms in isolation from each other, deliberately neglecting any coordination and control issues on the so-called automation (whole building) level. This corresponds to the practice employed in design tools such as SIA 382 [1], where dynamical calculations are used to determine heat, cold and air conditioning demand.

In terms of the building construction we considered different types of zones/rooms that were defined by the following set of attributes: façade orientation, construction type, building standard, and window area fraction of the façade.

Figure 2.1 shows two selected configurations as an example, and Table 2.1 gives an overview of the attribute values considered.

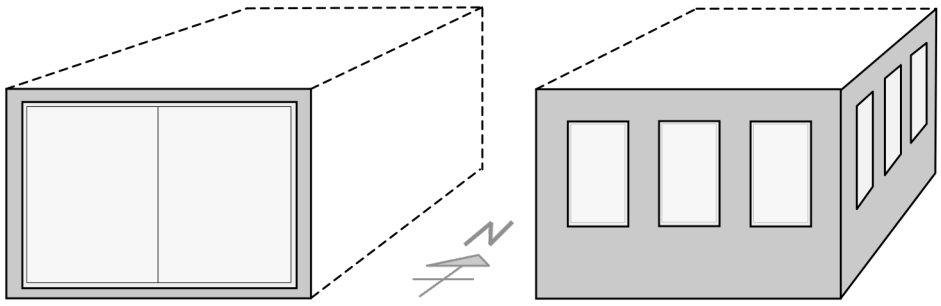

Figure 2.1: Schematic representation of two building zones. Left: normal office, façade orientation "South" (S), window area fraction "high" (80%); right: corner office, façade orientations South+East (SE), window area fraction "low" (30%).

The choice of values sets for the various attributes (Table 2.1) presented a compromise between two conflicting objectives: on the one hand we aimed at covering as many realistic situations as possible, on the other hand we had to keep the total number of cases (as given by all possible combinations of attribute values) sufficiently small in order to restrict the needed overall computational effort for a systematic investigation.

Attribute	*Value*	*Identifier*	*Remarks*
Façade Orientation	North	N	Normal office
	South	S	–¨–
	South+East	SE	Corner office
	South+West	SW	–¨–
Construction Type	Heavyweight	h	$c_{dyn} \approx 80$ Wh/m^{2}K
	Lightweight	l	$c_{dyn} \approx 36$ Wh/m^{2}K
Building Standard	Swiss Average	sa	$U_{op} \approx 0.6$ W/m^{2}K $U_{win} = 2.8$ W/m^{2}K
	Passive House	pa	$U_{op} \approx 0.1$ W/m^{2}K $U_{win} = 0.7$ W/m^{2}K
Window Area Fraction	Low	wl	30% window area per façade
	High	wh	80% –¨–

Table 2.1: Considered building attributes and associated sets of attribute values. c_{dyn}: internal dynamic heat capacity of the room; U_{op}: overall heat transfer coefficient of opaque façade parts; U_{win}: overall heat transfer coefficient of windows including frame. Reference for c_{dyn} and U-values is the floor area.

Clearly, the 32 possible combinations of building attributes according to Table 2.1 are not all of equal interest, and one can expect that the buildings they stand for are very unevenly distributed within the building stock of a given nation or market. Table 2.2 presents our subjective ranking of the 32 building types according to their importance for Switzerland.

Building Standard	*pa*				*sa*			
Window Area Fraction	*wh*		*wl*		*wh*		*wl*	
Construction Type	*h*	*l*	*h*	*l*	*h*	*l*	*h*	*l*
Façade Orientation								
N	I	II	II	II	III	III	I	II
S	I	II	II	II	III	III	I	II
SE	II	II	II	II	III	III	II	II
SW	II	II	II	II	III	III	II	II

Table 2.2: Classification of building cases according to four key attributes. I: Common and widespread configurations; II: Less common configurations; III: Exotic cases. For abbreviations see Table 2.1.

The classification was based on the following considerations: usually the "sa" buildings have low, the "pa" buildings high window area fractions on one façade. When combined with the most widespread construction type, "h", the resulting building types were defined to belong to the most important class, Class I. Combinations with very high energy consumption ("sa" + "wh") that are rare in practice – at least in Switzerland – were assigned to Class III. All remaining cases were defined to belong to Class II.

Note that the overall thermal building envelope loss factor as a function of window type, window area fraction and number of facades is varying in a very broad range, even if only one particular building standard is considered. A comprehensive compilation of overall loss factors can be found in Appendix A (Table A-3).

2.3 Building Systems

2.3.1 Variants

The solution to the IRA control task clearly depends strongly on the building system at disposal. Many such systems occur in practice. Figure 2.2 illustrates as an example the technical set up associated with a particular building system variant (S1, see below).

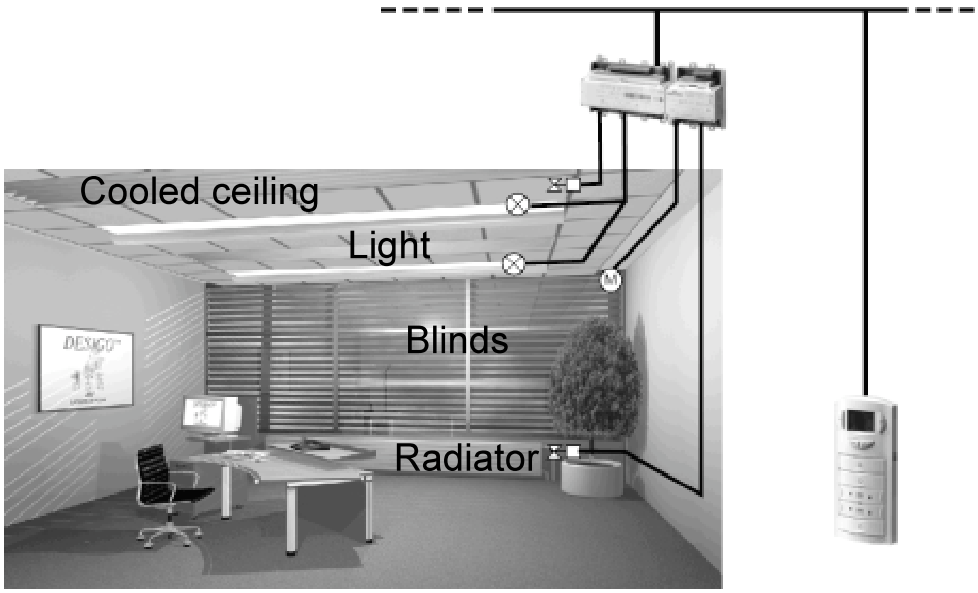

Figure 2.2: Example for an IRA technical set up.

For this study we considered five typical variants of building systems that employed different combinations of automated subsystems (Table 2.3).

	Building System				
Automated Subsystems	*S1*	*S2*	*S3*	*S4*	*S5*
Blinds	x	x	x	x	x
Electric lighting	x	x	x	x	x
Mechanical ventilation flow, heating, cooling	–	x	x	x	x
Mechanical ventilation energy recovery	–	x	x	x	x
Natural ventilation heating/cooling (night-time only)	–	–	–	x	–
Cooled ceiling (capillary tube system)	x	x	–	–	–
Free cooling with wet cooling tower	x	x	–	–	x
Radiator heating	x	x	–	–	–
Floor heating	–	–	–	x	–
Thermally activated building systems for heating/cooling	–	–	–	–	x

Table 2.3: Building systems considered. "x" denotes the presence of a subsystem.

As can be seen from Table 2.3 all five systems include automated blinds and light control. For system variants S2-S5, that all involve mechanical ventilation, we also assume the presence of a subsystem for energy recovery from the facility's exhaust air stream.

System variant S1 is the only one with no ventilation subsystem present. System variant S2 has the same heating and cooling subsystems as variant S1, but in addition also a mechanical ventilation subsystem. Variant S3 is defined to have only a ventilation subsystem, i.e. no other subsystems are assumed to be at disposal for heating and cooling. Finally, system variants S4 and S5 are used to investigate hybrid (mechanical + natural) ventilation schemes, and the use of Thermally Activated Building Systems (TABS), respectively.

A more detailed description of the individual subsystems is given in Chapter 5.

2.3.2 Dimensioning

The dimensioning of the building system components determines the maximum available control power and thus presents an important boundary condition for the control. On the one hand, too little power may lead to unacceptable discomfort and/or it may jeopardize options for more efficient control (e.g., if there is not enough power available for reheating after night set-back). On the other hand, assuming too much power may favor unrealistic control solutions.

In order to enable studies of the sensitivity of control solutions to the dimensioning of subsystem components we defined two dimensioning strategies, a scant and an ample one (Table 2.4).

	Dimensioning Strategy	
Parameters used to calculate design power values for heating and cooling depending on building and building systems	*scant* (D_s)	*ample* (D_a)
Design outside air temperature for transmission through building envelope	4-d-rm	4-d-rm
Design outside air temperature for infiltration	4-d-rm	hr-min-max
Reference room temperature mechanical ventilation heating	TrMin	TrMin
Reference room temperature mechanical ventilation cooling	TrMax	TrMax
Assumed room temperature for heat recovery mechanical ventilation heating	TrMax	TrMin
Assumed room temperature for heat recovery mechanical ventilation cooling	TrMin	TrMax
Design air change rate mechanical ventilation	n_Min	n_Max
Power allowance for heating/cooling after periods with reduced comfort requirements (e.g. night set back).	none	up to + 30% of design power

Table 2.4: Overview of used dimensioning strategies. 4-d-rm: 4 day running mean; hr-min-max: hourly minimum/maximum values; n_Min: air change rate for minimum fresh air supply at maximum occupancy; n_Ma: maximum allowed air change rate; TrMin/TrMax: lower/upper room temperature setpoints.

The scant dimensioning variant was chosen to explore how the investigated control strategies behave when they are pushed to their limits. The variant used scant dimensioning parameters and no additional heating or cooling power was granted.

The ample dimensioning variant was chosen to account for the fact that in practice systems are generally over-dimensioned. Here we considered conservative dimensioning parameters and an over-dimensioning of the systems up to the maximum allowable values stated in the standards.

For both variants the calculation of maximum heating power was based on Swiss dimensioning standards for heating subsystems ([2], [3]). For the dimensioning of the cooling systems the underlying method for heating systems was adapted. Design values for heating and cooling power depended in our study solely on losses/gains by transmission over the building envelope and of the mechanical ventilation system. Details on the calculations can be found in Appendix A.4.

Under both dimensioning variants, when several heating or cooling subsystems were available (Building System variants S1, S2, S4, S5) the total available heating or cooling power was distributed among the subsystems as follows: the transmission and infiltration heat gains/losses were considered for the slab system or radiator heating, the power needed for conditioning of ventilation air was attributed to the mechanical ventilation system. In Building System Variant 3 (mechanical ventilation only) all heating/cooling power was assigned to the mechanical ventilation.

The heating/cooling power of the mechanical ventilation subsystem was assumed to be limited such that the inlet air was tempered within the thermal comfort range of 16–40 °C. To prevent violation of these limits the maximum increase/decrease of if inlet air temperature by heating/cooling was limited. In extreme cases this can imply a power limitation to actual values below the design values (see Chapter 5.4.1).

Standard design outside air temperatures for the Swiss sites and for the heating case were obtained from [4]. Values for all considered non-Swiss sites and for the cooling case in general were calculated using the standard procedure, but based on all whole-year, hourly temperature datasets in our database (see Chapter 6). Details on the used design outside air temperature are given in Appendix A (Table A.2).

2.3.3 Control Costs

The minimization of control costs under comfort maintenance presents the primary objective of the IRA control task. Two kinds of control costs were assessed: Non-Renewable Primary Energy (NRPE) usage, and Monetary Cost (MC).

The cost of a given control action was determined as follows:

In a first step, the delivered energy (DE, electricity) was calculated. The DE depends on the efficiency of the activated distribution subsystem and on the building's energy generation/conversion system (Table 2.5).

In a second step a conversion factor (NRPE- or MC-Factor; Table 2.6) was applied to determine the primary energy amount or monetary cost required in order to obtain the given amount of DE.

Note that the only kind of energy used in the present study was electrical energy. A full description of the calculation of the control costs is given in Appendix C.

Delivered Energy	*Generation/ conversion system*	*Distribution subsystem*	*Annual Average Efficiency (η_{system})*
Heat	Earth coupled heat pump	Floor heating, TABS Mechanical ventilation Radiators	340% 310% 300%
Cold	Mechanical chiller	Ventilation (fan coil) TABS Cooled ceiling	350% 345% 340%
Electricity (for aux. drives)	Wet cooling tower (free cooling)	TABS Cooled ceiling	2.0 W/m2 2.25 W/m2
Electricity (for fan operation)	Ventilation	Mechanical ventilation	0.34 W/(m3/h)

Table 2.5: Kinds of delivered energies considered, associated generation/conversion and distribution subsystems, and their average efficiencies or specific power demand.

	NRPE-Factor [kWh PE/kWh DE]		*MC-Factor [CHF/kWh DE]*		
	UCTE	CH		UCTE	CH
Electricity	<u>3.32</u>	2.5	HT LT	<u>0.30</u> <u>0.11</u>	0.27 0.14

Table 2.6: Conversion factors assumed for primary energy production. NRPE: Non-Renewable Primary Energy usage; MC: Monetary Cost; PE: Primary Energy; DE: Delivered Energy; UCTE: generation mix by the Union for the Co-ordination of Transmission of Electricity; CH: Swiss generation mix; HT: high tariff; LT: low tariff . HT was assumed to hold from 7:00-20:00 local time for all days of the year. Costs used in the present study are underlined.

2.4 Comfort Requirements

The focus of the present study is on the thermal comfort, the visual comfort, and the CO_2 concentration within a given zone/room. Further aspects of indoor environmental quality such as airflow rates, humidity, and other air pollutants besides CO_2 were not considered. Humidity was not considered because it is normally controlled via the central air handling unit. CO_2 can serve as an indicator for other relevant pollutants.

The physical variables of interest were thus the room temperature as perceived by human occupants (typically calculated as a combination of the room's air temperature and the surface temperature of the enclosing surfaces), the illuminance (light level), and the average CO_2 concentration within the room. The used comfort definitions for these variables are presented below.

2.4.1 Thermal Comfort

The choice of thermal comfort criteria is not straightforward because a variety of definitions exists in the literature that employ different assumptions for the clothing factor. Also, the width of the thermal comfort range is known to have a significant effect on the control costs.

In order to account for this we considered four different thermal comfort definitions. Each definition actually corresponds to a different procedure to define the thermal comfort range at a given point in time, as summarized in Table 2.7.

Calculation Procedure	*Comfort Range Width*	
	Working hours	*Non-working hours*
A_n	Narrow	Narrow
A_w	Wide	Wide
B_n	Narrow	12°C - 35°C
B_w	Wide	12°C - 35°C

Table 2.7: Calculation procedures used to determine the thermal comfort range at a given point in time. For the definitions of "Narrow" and "Wide" see Figure 2.3.

The minimum and maximum room temperature set points for heating and cooling that were used to delineate the "Narrow" and "Wide" comfort ranges were chosen to be similar to the definitions in SIA 382/1 [5]. The actual range at a given point in time was determined as a function of the exponentially weighted running mean of the past measured outside air temperature values (Figure 2.3).

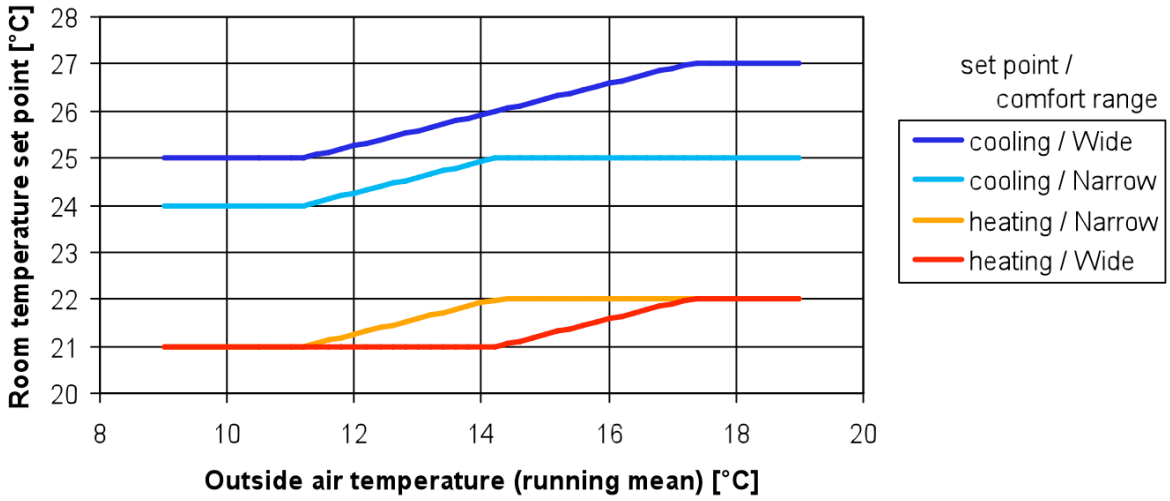

Figure 2.3: Room temperature set points for heating and cooling, and for the temperature comfort ranges "Narrow" and "Wide".

The running mean was calculated in a similar manner as described in EN 15251 [6]. Our calculation differed from the EN standard because the latter relies upon daily mean values, whereas we used *hourly* mean temperatures. The reason was that the hourly time step guaranteed a smooth comfort range devolution, whereas the daily time step resulted into large discontinuities that implied unrealistically large heat/cold pulses for control. (The standards are used for design, they are not made for control purposes). As shown in Appendix A-3.7 the set point progressions calculated with

the hourly values are much smoother than those obtained with the standard method. Note that the running mean values can differ considerably from the current outside air temperature.

In variants A_n and A_w the comfort settings from Figure 2.3 were applied 24 hours a day and 7 days a week, whereas in variants B_n and B_w they were applied only during working hours. The working hours were determined from the occupancy schedule (see Section 2.5.1) as being all hours with an occupancy density different from zero.

2.4.2 Indoor Air Quality

To achieve an acceptable indoor air quality in non-smoking offices, different methods are possible. Standard [7] stipulates a minimum fresh air supply rate of at least 36 m^3/h per person. Another possibility is the CO_2 control of the ventilation. In this case air supply is controlled continuously such that the CO_2-concentration remains below specific design values. According to EN15251 [6], and assuming an outside air concentration of 400 ppm, the recommended upper concentration limits for the comfort categories "I" and "II" are 750 ppm and 900 ppm, respectively.

In this study both ventilation methods were considered (Table 2.8).

Ventilation Strategy	*Description*
V	Non-air quality controlled ventilation. Ventilation is operated based on a time schedule.
W	CO_2-controlled ventilation (approximated). The air change rate is adapted dynamically depending on occupancy density.

Table 2.8: Ventilation strategies considered.

As indicated in Table 2.8 the CO_2-based control was not modeled directly, but was instead approximated by assuming an occupancy-dependent air change rate. This was done because the CO_2-concentration shows in reality very fast dynamics that would have made it necessary to employ a time step of 5 min or less in the simulations. Given that the used time horizon for predictive control was typically at least one day this very small time step would have resulted into a prohibitive increase of the needed computation time.

The achieved indoor air quality (category I or II) in our simulations thus depended on the chosen strategy and the air supply parameters. Further information on the ventilation strategies is given in Section 5.4.1 and Appendix B.4.

2.4.3 Illuminance Comfort

For the illuminance comfort we applied a standard lower illuminance setpoint value for occupied offices of 500 lux. No upper limit was defined assuming that in case of excess incoming solar radiation the user would be able to obtain glare protection by manual adjustment of an internal blind.

2.5 Disturbances

The state of a single room or building zone is continuously perturbed by a variety of factors that cannot be controlled by an individual room/zone controller, or not at all. These include the state of neighboring building zones or spaces, the weather, the internal gains due to equipment; energy, moisture and CO_2 fluxes by the occupants, and occupant behavior. To the extent that these influences cannot be predicted they present from a control point of view "disturbances" that need to be rejected in order to keep the controlled system's state within the desired bounds.

As already discussed in Section 2.2 the effect of neighboring building zones or spaces was considered as secondary and was thus neglected.

Inopportune occupant behavior can clearly thwart the success of even the best control strategy. However, particularly in the case of IRA it seemed appropriate to assume that the user does not act directly on the subsystems (e.g., manipulate radiator valves), but instead communicate his or her wishes (such as changes in comfort parameters) to the control system via a corresponding interface. The IRA controller should then carry out the corresponding actions and adjust its strategy accordingly. Hence disturbances due to occupant behavior were not further considered in this study.

Thus we focused on the disturbances related to the internal gains and the weather. Below we describe our approach for both in more detail.

2.5.1 Occupancy and Internal Gains

The occupancy density of the building (a number ranging from 0-100%) was used as the key quantity to determine the internal heat gains from persons and equipment, plus CO_2 production.

We considered two internal gains levels that were based on the Swiss standard SIA 2024 [7] for cellular offices (Table 2.9).

Parameter	*Unit*	*Internal gains level*	
		low	*high*
Floor area per person	m^2	14	7.8
Internal gains due to persons	W/m^2	5	9
Internal gains due to equipment	W/m^2	7	15
CO_2 – production	$m^3/(h\ m^2)$	1.1e-3	1.9e-3

Table 2.9: Definition of internal gains levels.

Presence of persons and usage of equipment typically show a pronounced diurnal and weekly variation. We used hourly profiles from the Swiss standard SIA 2024 [7] for cellular offices.

The assumed weekdays profiles are shown in Figure 2.4.

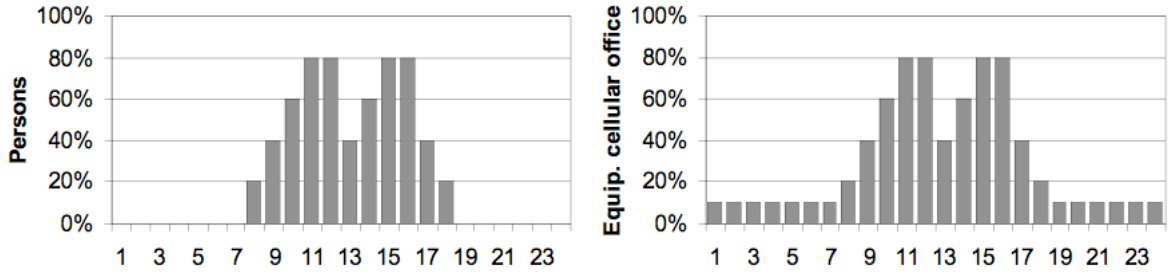

Figure 2.4: Diurnal occupancy profiles for weekdays. Data are mean values over the hour indicated. Time labeling is for local wintertime.

During weekends (not shown) no persons were assumed to be present and the person gains were set to zero. The equipment gains were set to the weekdays' night-time value.

A switch to Daylight Savings Time (DST) was always considered by assuming a shift in all profiles to one hour earlier during the period March 20th until October 31st.

2.5.2 Weather

Weather variations affect a building, its thermal dynamics, and its technical systems in a variety of ways. In this study we focused on the effects of the following weather variables: global irradiation, air temperature and wet bulb temperature.

Other variables that may affect building energy performance and occupant comfort are for example wind, longwave radiation and humidity. We discarded them because they were considered to be of secondary importance for the present study.

In order to account for a range of outdoor climatic conditions we considered weather data from several European locations. For further information on the criteria used to select these locations and on the used meteorological data sets see Chapter 6.

2.6 Technical System Integration

IRA controllers are integrated into larger Building Automation and Control (BAC) systems. The integration normally involves a hierarchical control structure that is typically realized in both, the hard- and the software.

Figure 2.5 shows the system topology of the Siemens building automation system Desigo V2.37 [8] as an example. In this system the control is structured in field level, automation level and management level. The field level includes individual room control. Primary plant control (e.g. control of air handling units) and room control integration are done at the automation level. The management level is mainly used for operation and monitoring.

Automation level control programs typically are customized solutions. They combine locally developed solutions with proven solutions from the head quarter. The relevant tasks of automation level control for IRA are:

- Building usage and occupancy schedule
- Room group definition (and schedule) for lights, blinds, room set points etc.
- High-level control of lights, blinds
- Control of primary plants (e.g. air handling units, heat/cold generation and distribution)

Field level control programs are typically standardized. They are written by headquarter engineers, and only parameter values are changed by regional companies or value added partners. Relevant tasks with regard to IRA are:

- Room temperature control by valve/damper operation to given set point
- Room ventilation control by damper operation (heating/cooling, poss. air quality control)
- Room luminance control (presence dependent, poss. to given luminance set point)
- Interaction to room control human-machine interfaces (room device, light/blind switches etc.)

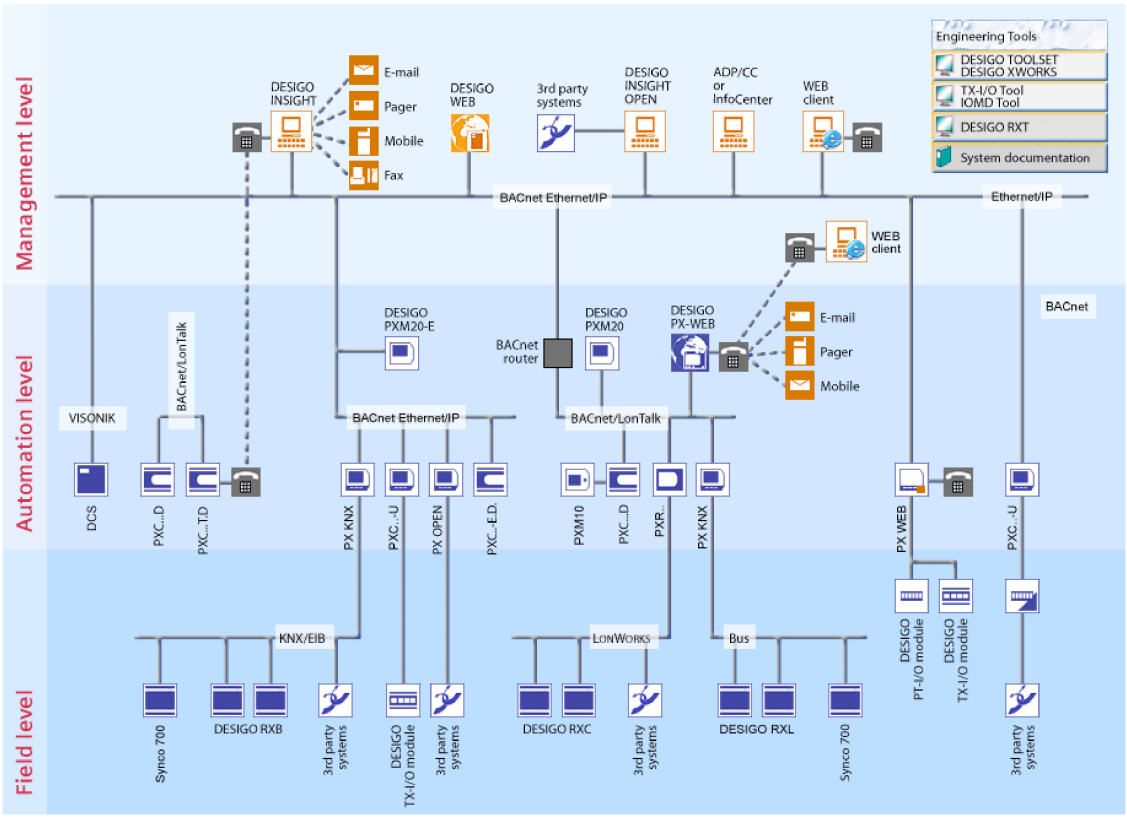

Figure 2.5: Topology of the Siemens building automation system Desigo V2.37 [8].

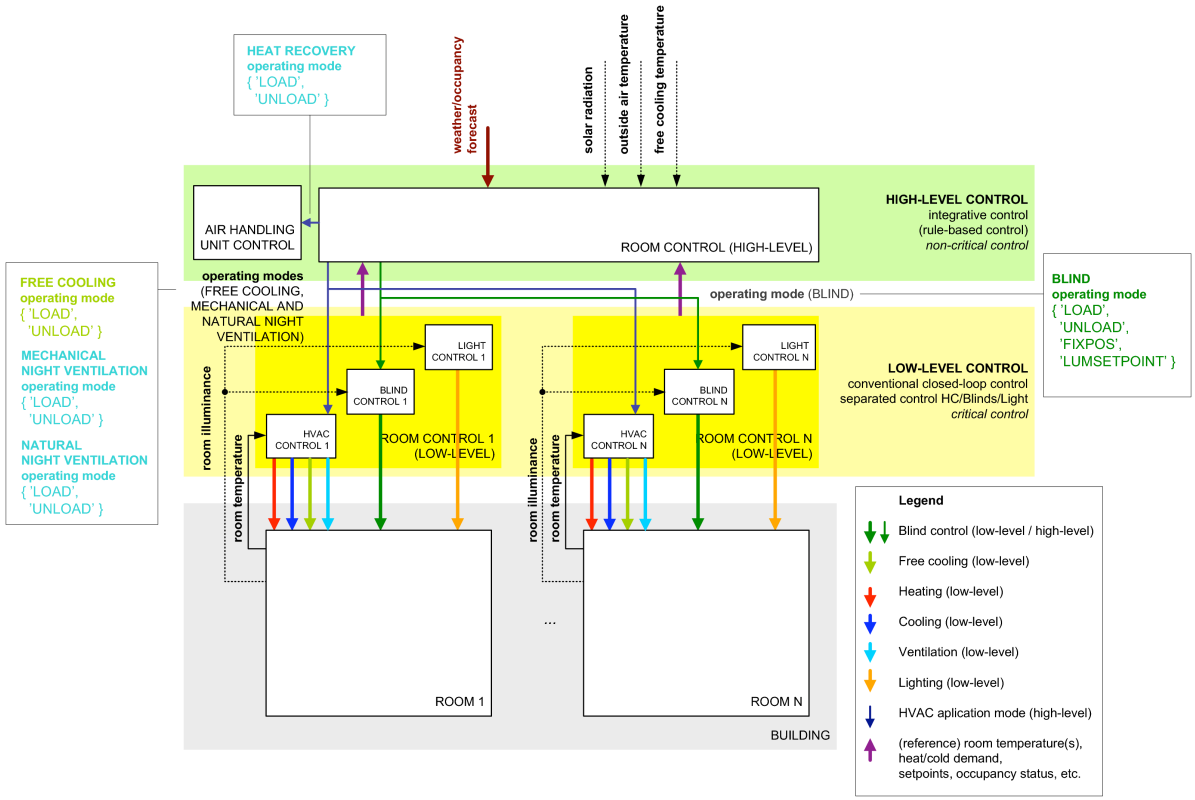

Figure 2.6: Schematic representation of present-day IRA control solutions. Note, only a subset of all signals is displayed.

Figure 2.6 shows how IRA can be realized in present-day BAC systems. It can be seen that the approach involves a hierarchical control structure with so-called high-level and low-level controllers. The task of the high-level controller is to determine a set of so-called operating modes that are sent to the low-level controller. In the opposite direction, the low-level controller delivers measurements (e.g. room temperatures), heat/cold demand, setpoints etc. to the high-level controller.

The definition of appropriate operating modes is crucial. In commercial BAC systems such as [8], such modes have been defined in particular for "low cost" control actions (compare Chapter 3): blind movement, free cooling usage, mechanical night-time ventilation, natural night-time ventilation and energy recovery operation.

2.7 Discussion

The chosen focus on a single building zone/room corresponded to a well-established practice. We assume that the overall energy performance of a given building can still be estimated at reasonable precision, by scaling up the results obtained from a series of individual single zone/room calculations. Our single zone approach contains, however, a slight inconsistency because we consider energy recovery as part of the IRA problem, whereas this function can only be applied centralized for the air handling unit that supplies the considered single zone/room.

Finding the optimal dimensioning of a building system's components proved to be a demanding task. In reality, the solution will also depend on the chosen control strategy. This requires an iterative procedure that is not feasible for the large number of cases considered in the present study. Instead we chose to consider the two extreme variants of scant and ample dimensioning, assuming that in reality the optimal dimensioning for a particular system would lie somewhere in-between.

2.8 Conclusions

The chosen experimental set-up considers (i) all relevant dimensions of the IRA control task (building, building system, comfort, disturbances) and (ii) a plausible, well-chosen set of variants for each dimension. This work presents a prerequisite for the derivation of appropriate models, the formal specification of modeling and simulation software, and the design of systematic simulation studies.

By taking into consideration the interfaces and hierarchical structure of present-day BAC systems we could ensure that the control algorithms developed in the course of the project can be smoothly integrated in existing buildings or new BAC products later on.

2.9 References

[1] SIA Design Tool „Klimatisierung“ based on SIA standards 380/4 and 382/1

[2] SIA 384/1 (2009): Heizungsanlagen in Gebäuden – Grundlagen und Anforderungen

[3] SIA 384.201 (2005): Heizungsanlagen in Gebäuden – Berechnung der Normheizlast

[4] SIA 2028 (2008): Klimadaten für Bauphysik, Energie- und Gebäudetechnik

[5] SIA 382/1 (2007): Lüftungs- und Klimaanlagen – Allgemeine Grundlagen und Anforderungen

[6] Standard EN 15251:2007: Eingangsparameter für das Raumklima zur Auslegung und Bewertung der Energieeffizienz von Gebäuden - Raumluftqualität, Temperatur, Licht und Akustik.

[7] SIA 2024 (2006): Standard-Nutzungsbedingungen für die Energie- und Gebäudetechnik, Raumnutzungen „Einzel-, Gruppenbüro“ und „Grossraumbüro“, pp. 34-37

[8] Siemens Building Technologies building automation system DESIGO™ V2.37: System documentation (2007), expert edition.

Chapter 3

RULE-BASED CONTROL STRATEGIES

by Markus Gwerder, Jürg Tödtli and Dimitrios Gyalistras

Cite as:

Gwerder, M., Tödtli, J. & Gyalistras, D. (2010). Rule-based control strategies. In: Gyalistras, D. & Gwerder, M. (eds.): *Use of weather and occupancy forecasts for optimal building climate control (OptiControl): Two years progress report*. Terrestrial Systems Ecology ETH Zurich, Switzerland and Building Technologies Division, Siemens Switzerland Ltd., Zug, Switzerland, pp 29–42. ISBN 978-3-909386-37-6.

3.1 Introduction

The state-of-the-art of Integrated Room Automation is rule-based control (RBC). Since RBC is likely to remain the most frequently used control approach in the years to come, a series of RBC strategies were considered in order to (i) explore their performance, and (ii) use them as a benchmark for comparison with the model predictive control (MPC) strategies.

As the naming indicates, an RBC based controller determines all control inputs based on a series of rules of the kind "if *condition* then *action*". The conditions and actions typically involve numerical parameters (e.g., threshold values), the so-called control parameters. Determining both, a good set of rules, as well as the associated parameters is decisive for good RBC performance.

An overview of the RBC strategies considered is given in Table 3.1.

Strategy	*Description*	*Main Input Data High-level Control*	*Blind Transmission Values*	*Blind Repositioning*
RBC-1	Typical, broadly applied strategy.	Current measurements of room temperature, outside air temperature, external heat gains, occupancy state.	Three transmission values: fully open, fully closed and shading transmission.	In real application: event driven (threshold crossings). In simulations: once per hour (decision based on hourly mean data).
RBC-2	As RBC-1, but more freedom in blind movement.	– ¨ –	Continuous blind transmission values.	Continuous.
RBC-3	Novel strategy (newly elaborated within the OptiControl project).	As RBC-1/2, in addition: historical heat and cold demand signals, historical room temperature data.	– ¨ –	– ¨ –
RBC-4	As RBC-3, but with restricted blind repositioning.	– ¨ –	– ¨ –	Once per hour.

Table 3.1: Overview of investigated rule-based control strategies.

All four RBC strategies are non-predictive. i.e. they do not accommodate rules to consider any predictions related to weather or internal gains. Also, all strategies adhere to the hierarchical control scheme described earlier in Section 2.6, i.e. they consist of a high- and a low-level control part. However, they differ only in their high-level control parts.

The high-level controllers were defined to drive one or several of the following "low-cost" actions: Blind positioning, free cooling operation, mechanical night-time ventilation operation, natural night-time ventilation operation, and energy recovery (ERC) operation.

In Section 3.2 we first describe the four RBC strategies' high-level control parts. Section 3.3 gives a description of the common low-level controller. The control parameters (printed bold in Sections 3.2 and 3.3) and their calculation procedures are presented in Section 3.4. A short discussion and concluding remarks are finally given in Sections 3.5 and 3.6.

3.2 High-Level Control

3.2.1 RBC-1

Control strategy RBC-1 reflects a broadly applied strategy (see for example [1]). Cooling by free cooling, mechanical and natural night-time ventilation were realized as defined in [2].

Blind Positioning

The high-level controller only uses the operating mode FIXPOS for blinds. In addition, three specified blind transmission values are communicated to the low-level control: Fully closed, fully opened and a defined shading transmission value.

```
If (total solar gains > solar gains threshold value[1])
    // high external gains
    if (room is occupied)
        blind transmission = shading transmission;
    else
        blind transmission = fully closed transmission;
    end
else
    // low external gains
    blind transmission = fully open transmission;
end
blind operating mode = FIXPOS
```

Free Cooling Operation

```
If (mean outside air temperature of last 24 hours > ...
    free cooling limit) & (room is unoccupied)
    // high outside air temperature and room not occupied
    if (room temperature > free cooling target room temp. setpoint)
        free cooling operating mode = UNLOAD;
    else
        free cooling operating mode = LOAD;
    end
else
    // low external gains
    free cooling operating mode = LOAD;
end
```

Mechanical Night-Time Ventilation Operation

```
If (mean outside air temperature of last 24 hours > mechanical...
...night-time ventilation limit) & (room is unoccupied) & (night)
    // high outside air temp. and room not occupied and night-time
    if (room temp. > mech. night-time target room temp. setpoint)
        mechanical night-time ventilation operating mode = UNLOAD;
    else
        mechanical night-time ventilation operating mode = LOAD;
    end
else
    // low external gains
    mechanical night-time ventilation operating mode = LOAD;
end
```

[1] Control parameters are printed in bold.

Natural Night-Time Ventilation Operation

```
If (mean outside air temperature of last 24 hours > natural ...
...night-time ventilation limit) & (room is unoccupied) & (night)
    // high outside air temp. and room not occupied and night-time
    if (room temp. > natural night-time target room temp. setpoint)
        natural night-time ventilation operating mode = UNLOAD;
    else
        natural night-time ventilation operating mode = LOAD;
    end
else
    // low external gains
    natural night-time ventilation operating mode = LOAD;
end
```

Energy Recovery (ERC) Operation

```
If (room temp. below center of room temp. comfort range)
    // room temp. lower than center of room temp. comfort range
    energy recovery operating mode = LOAD;
else
    // room temp. higher than center of room temp. comfort range
    energy recovery operating mode = UNLOAD;
end
```

3.2.2 RBC-2

Blind Positioning

This strategy deviates from the first only in one respect: When the room is occupied and high solar gains are present, the blind operating mode is set to LUMSETPOINT which means that the blinds are used to control the (lower) luminance set point.

In practice, this strategy is not applied. We considered it for comparison with the MPC controllers (see Chapter 4) that were allowed to control the room luminance by the blinds.

```
If (total solar gains > solar gains threshold value)
    // high external gains
    if (room is occupied)
        blind operating mode = LUMSETPOINT;
    else
        blind operating mode = FIXPOS;
        blind transmission = fully closed transmission;
    end
else
    // low external gains
    blind operating mode = FIXPOS;
    blind transmission = fully open transmission;
end
```

The rules employed for all other high-level control inputs are identical to those given for RBC-1.

3.2.3 RBC-3

Control strategy RBC-3 was newly developed within the OptiControl project and presents one of the most advanced RBC approaches known to us. It was designed such that it requires less control parameters than RBC-1 and RBC-2, and that the parameter's values can be determined more easily.

Note that so far, RBC-3 has only been used in simulations. It may be necessary to modify the control strategy for practical use.

Blind Positioning

The rules for determining the blind operating mode are shown in Figure 3.1. Instead of working with threshold values, the strategy works with historical heat and cold demand signals and historical room temperature data. Primarily, heating and cooling demands of the last 24 hours are evaluated; if there was no heating and cooling demand during the last 24 hours, the strategy attempts to shift the room temperature towards the middle of the room temperature comfort range.

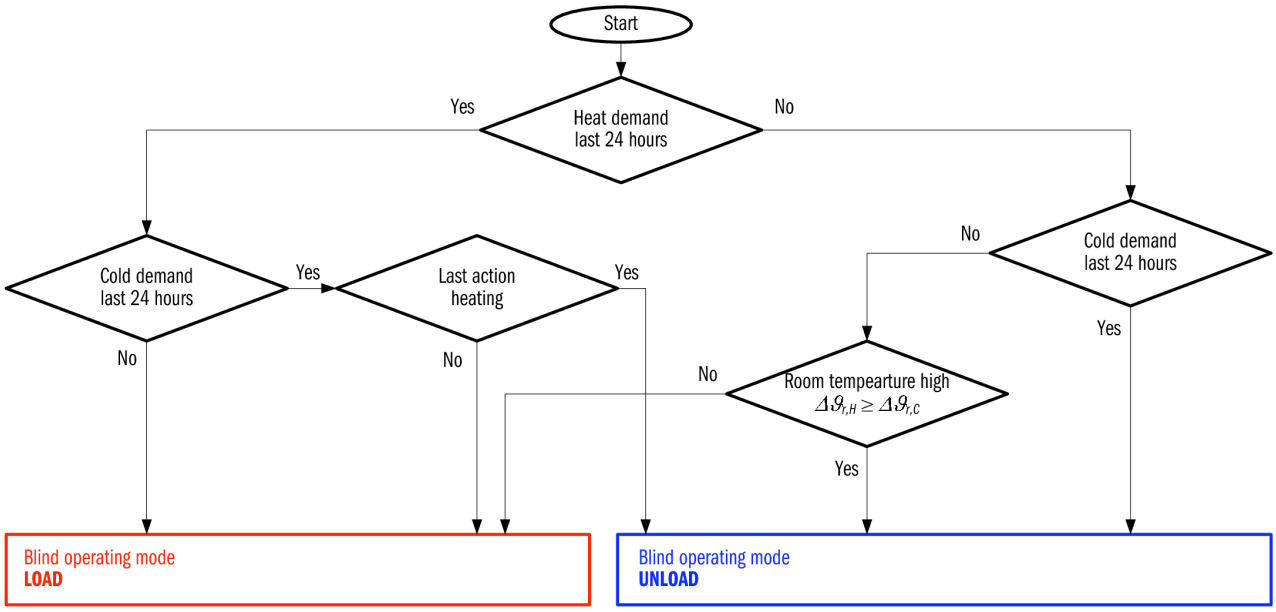

Figure 3.1: Determination of blind operating mode for control strategy RBC-3.

Free Cooling Operation

The rules for determining the free cooling operating mode are shown in Figure 3.2. Similar to the approach taken for blind positioning the control is based on the heating and cooling demands of the last 24 hours. If there was no such demand during the last 24 hours, free cooling is forced (operating mode UNLOAD), however only if there is some probability that the room temperature will be exceeded during the next control step. To this end the controller evaluates the sum of the maximal room temperature rise and of the minimal room temperature encountered during the last 24 hours. If the resulting value exceeds the comfort range, the operating mode is set to UNLOAD.

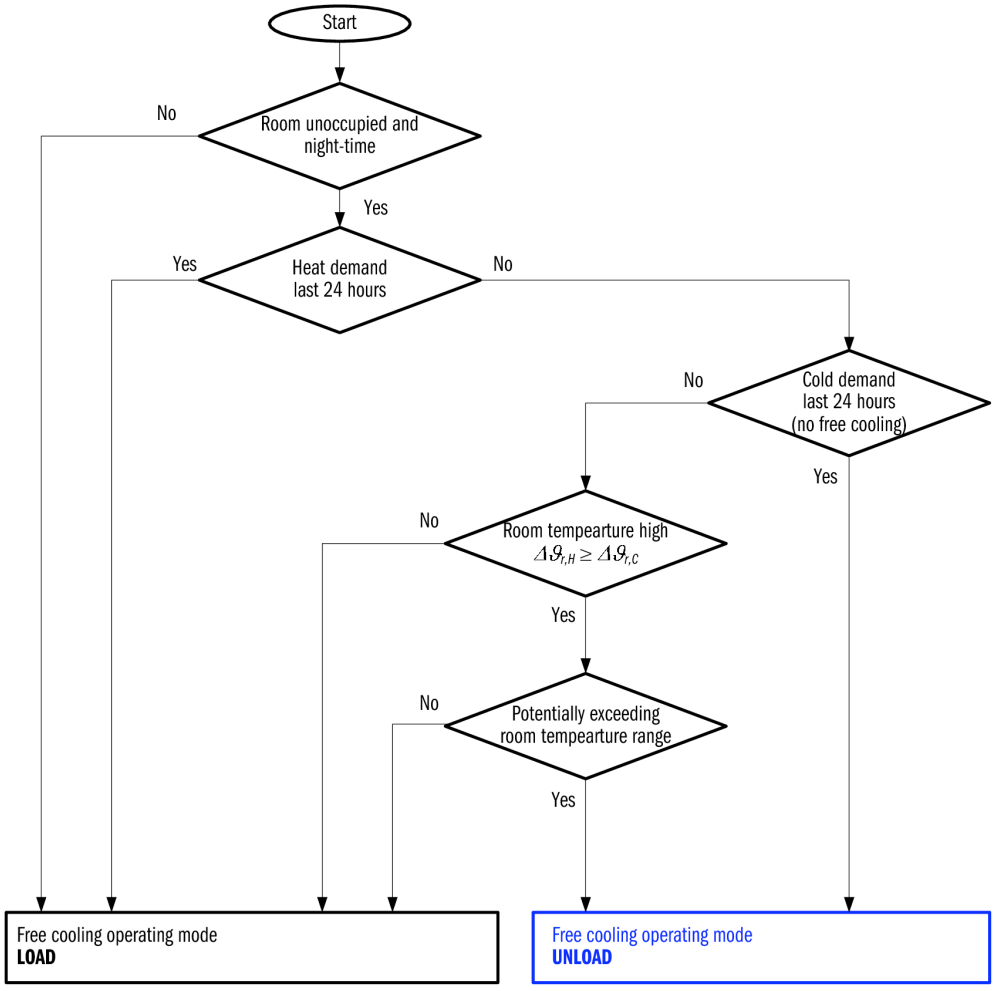

Figure 3.2: Determination of free cooling operating mode for control strategy RBC-3.

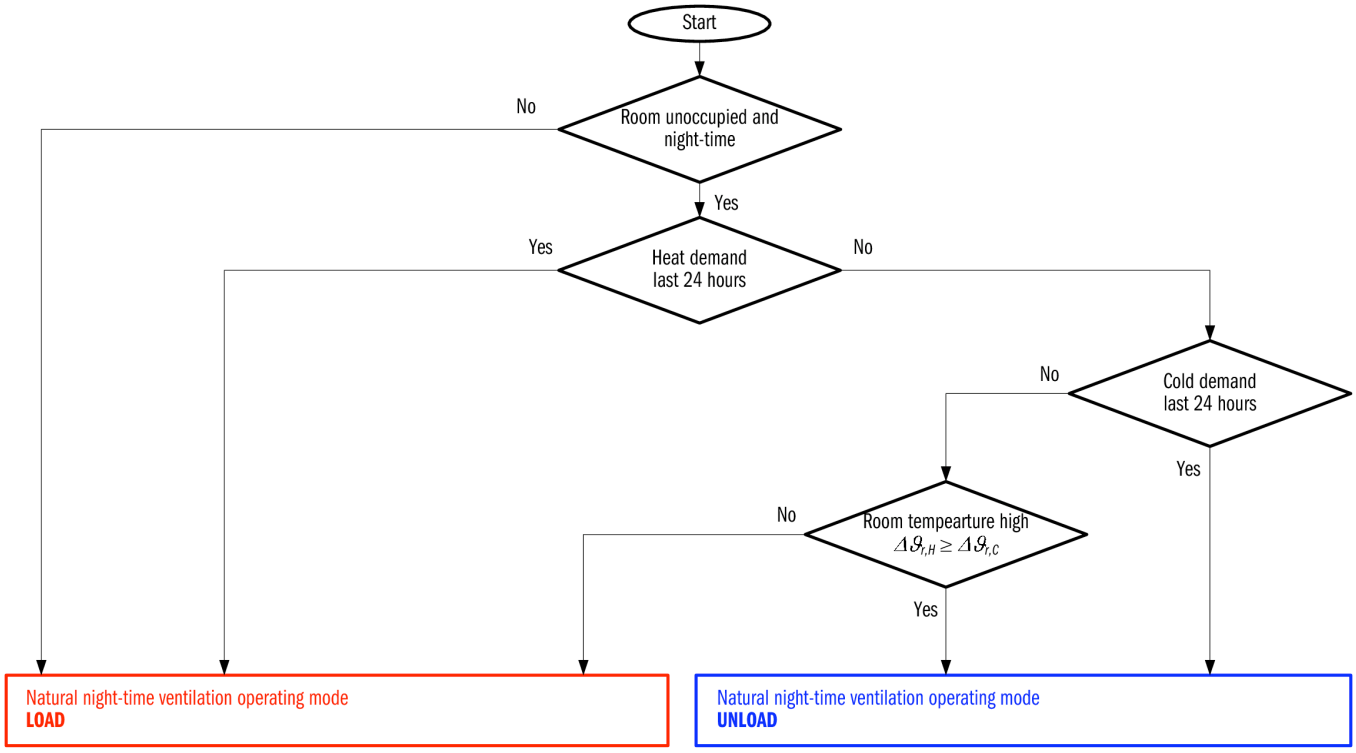

Figure 3.3: Determination of natural night-time ventilation operating mode for control strategy RBC-3.

Mechanical Night-Time Ventilation Operation

The rules used to determine the mechanical night-time ventilation operating mode are identical as for free cooling.

Natural Night-Time Ventilation Operation

The rules used to determine the natural night-time ventilation operating mode are similar to the ones for blind operation. In addition, there is a rule accounting for the occupancy status and the time of day (Figure 3.3).

Energy Recovery (ERC) Operation

The rules used to determine the Energy Recovery operating mode are identical as for blind operation.

3.2.4 RBC-4

Blind Positioning

This strategy deviates from RBC-3 only in one respect: Whereas RBC-3 allows for continuous blind transmissions during a control step (see next Section), the blind transmission in RBC-4 is restricted to one transmission value per control step, as determined at the beginning of that step.

This was accomplished as follows: First, the blind operating mode for the time step ahead is determined as for RBC-3. Then the blind transmission value is determined based on the operating mode. And finally, the blind operating mode is set to FIXPOS.

- Operating mode LOAD

```
If (night)
    // night-time
    blind transmission = fully closed transmission;
else
    // day-time
    blind transmission = fully open transmission;
end
blind operating mode = FIXPOS
```

- Operating mode UNLOAD

```
If (night)
    // night-time
    blind transmission = fully open transmission;
else
    // day-time
    if (room occupied)
        blind transmission is set so that lower luminance setpoint is
        reached based on last luminance measurement
        (not changed/controlled in the next sampling time);
    else
        blind transmission = fully closed transmission;
    end
end
blind operating mode = FIXPOS
```

For all other control inputs, RBC-4 uses the same rules as RBC-3.

3.3 Low-Level Control

The used low-level controller operates in two steps. In the first step, the operating modes and signals as obtained from the respective high-level controller are used to determine corresponding control actions for the “low-cost” action aggregates. In a second step, the remaining control outputs are calculated. These are the control outputs involving “high-cost” actions such as active heating or cooling, and ventilation.

Blind Positioning

- Operating mode FIXPOS

```
Blind transmission value set as specified by the high-level control-
ler.
```

- Operating mode LOAD

```
If (night)
    // night-time
    blind transmission = fully closed transmission;
else
    // day-time
    blind transmission = fully open transmission;
end
```

- Operating mode UNLOAD

```
If (night)
```

```
    // night-time
    blind transmission = fully open transmission;
else
    // day-time
    If (room occupied)
        maintain lower luminance set point (if possible);
    else
        blind transmission = fully closed transmission;
    end
end
```

- Operating mode LUMSETPOINT

```
maintain lower luminance set point (if possible);
```

Free Cooling Operation

- Operating mode LOAD

```
Do not force free cooling.
```

- Operating mode UNLOAD

```
If (free cooling temperature < room temperature - minimal...
...required temperature diff. room – free cooling temperature)
    // force free cooling
    free cooling usage  = full;
else
    // do not force free cooling
end
```

Mechanical Night-Time Ventilation Operation

- Operating mode LOAD

```
Do not force Mechanical night-time ventilation.
```

- Operating mode UNLOAD

```
If (outside air temperature < room temperature - minimal...
...required temperature diff. room – outside)
    // force mechanical night-time ventilation
    mech. vent. air change rate = mech. vent. air change rate;
else
    // do no mechanical night-time ventilation
end
```

Natural Night-Time Ventilation Operation

- Operating mode LOAD

```
Do not force natural night-time ventilation.
```

- Operating mode UNLOAD

```
If (outside air temperature < room temperature)
    // perform natural night-time ventilation
    automated window position = open;
```

```
else
    // do no mechanical night-time ventilation
    automated window position = closed;
end
```

Energy Recovery (ERC) Operation

- Operating mode LOAD

```
If (room temperature > outside air temperature)
    // heating potential: force energy recovery usage
    if (mechanical ventilation air change rate > 0)
        energy recovery usage = full;
    else
        energy recovery usage = none;
    end
else
    // cooling potential: do not force energy recovery usage
end
```

- Operating mode UNLOAD

```
If (room temperature < outside air temperature)
    // cooling potential: force energy recovery usage
    if (mechanical ventilation air change rate > 0)
        energy recovery usage = full;
    else
        energy recovery usage = none;
    end
else
    // heating potential: do not force energy recovery usage
end
```

Active Heating and Cooling Operation

Depending on the Building System variant considered (see Section 2.3.1) the low-level controller had to provide one or several of the following control inputs: heating or cooling power for mechanical ventilation; heating or cooling power for the slab subsystem (e.g. cooled ceiling, TABS); heating power for the radiators.

In a conventional low-level control solution the heating aggregates (e.g. floor heating, radiators, heating by mechanical ventilation) are used in a predefined sequence to "lift" the room temperature to its lower set point. Similarly, the cooling aggregates (e.g. chilled ceiling, cooling by mechanical ventilation) are used in a predefined sequence to "bring down" the room temperature to its higher set point. If all heating or cooling aggregates are fully deployed, the air change rate will be increased as a further heating or cooling measure. Typically, the low-level temperature control is based on (sequenced) PI-controllers [3].

Conventionally, the mechanical ventilation air change rate (or volumetric flow rate) is controlled to a minimal set point. The mechanical ventilation air change rate is increased – from its minimal set point – either as a heating or cooling measure (as stated above), or as a measure to meet air quality requirements (e.g. CO_2 concentration control).

In the simulation studies all needed signals for active heating and cooling operation as well as the mechanical air change rate were computed with the aid of a perfect MPC controller (see next Chapter) that was operated with a one-step optimization horizon. When a high-level control input implied a fix value (e.g. for blind positioning) this was passed on as a constraint to the MPC optimization problem. All other, "free" low-level control actions where then optimally determined by MPC.

For RBC-1 to RBC-3 the perfect MPC control was based on perfect knowledge of all disturbances (weather, internal gains) for the time step ahead. This procedure approximated an ideal, continuous time, closed-loop low-level control for all "free" control actions over the entire next time step of the discrete time simulation.

For RBC-4 the assumption of a perfect MPC control was relaxed as follows: the fix blind positioning was determined using solar gains from the *previous* time step. This was done in order to simulate the situation that the low-level controller was not allowed to continuously adjust the blinds *during* the current time step, i.e. that the blinds were allowed to move only once at begin of every time step (hour), based on the solar gains measurements available up to the begin of that time step.

Electrical Lighting Operation

For the electrical lighting we assumed presence of a constant light level controller. Further we assumed that the luminance was measured (by a photometer) and that it was always controlled to the luminance setpoint. This control was assumed to be ideal.

3.4 Control Parameters

3.4.1 Basic Parameters

Table 3.2 lists all basic control parameters and their values employed in the four RBC strategies. The basic parameters were used to derive all further control parameters (see next Section) for all building and Building System variants considered. The values shown in Table 3.2 were universally used. They were determined by experience, rules of the thumb, and systematic simulation studies.

	Parameter	*Unit*	*RBC-1*	*RBC-2*	*RBC-3*	*RBC-4*
Blinds	*Solar gains threshold value (for setting the blinds to shading transmission)*	W/m^2	15	15	–	–
	Illuminance on reference plane with blinds set to shading transmission at threshold	lux	300	–	–	–
Free cooling	*Min. required temperature difference room – free cooling temperature*	K	5	5	5	5
	Target room temperature setpoint offset	K	1	1	–	–
Mechanical night-time ventilation	*Air change rate*	1/h	3	3	3	3
	Min. required temperature difference room – outside	K	7	7	7	7
	Target room temperature setpoint offset	K	1	1	–	–
Natural night-time ventilation	*Target room temperature setpoint offset*	K	1	1	–	–

Table 3.2: Overview of basic control parameters for rule-based control.

Several remarks apply to Table 3.2:

In practice, the solar gains threshold value is typically specified as a threshold for the measured solar radiation on a vertical surface with the orientation of the room. This value depends strongly on the window area fraction, window properties etc. For our simulations we defined as a basic – and universally applied – control parameter a threshold value for the solar gains per floor area inside the room.

In order to calculate the shading transmission of the blinds for control strategy RBC-1 was used a value of 300 lux for the illuminance on reference plane with blinds set to the shading transmission at the solar gains threshold value.

The "minimal required temperatures differences" for free cooling and mechanical night-time ventilation were specified as follows: for values exceeding these differences, the costs for free cooling or mechanical night-time ventilation became lower than he cooling costs with active cooling measures. Guideline values have been reported in [4].

Reasonable air change rates for mechanical night-time ventilation are around 2 to 4 h^{-1} (see [4]).

The target room temperature setpoints for free cooling, mechanical and natural night-time ventilation were set to 1 K above the lower temperature setpoints of the thermal comfort range (see Section 3.4.1).

3.4.2 Actually Used Parameters

Table 3.3 shows the RBC control parameters actually used in the simulations. It can be seen that several of the parameters were derived from the basic control parameters discussed above.

	Parameter	*Unit*	*RBC-1*	*RBC-2*	*RBC-3*	*RBC-4*
Blinds	*Solar gains threshold value (for setting the blinds to shading transmission)*	W/m^2	15	15	–	–
	Transmission value when occupied and high solar gains (shading transmission)	-	*calc 1)*	–	–	–
Free cooling	*Min. required temperature difference room – free cooling temperature*	K	5	5	5	5
	Target room temperature setpoint	K	*calc 4)*	*calc 4)*	–	–
	Free cooling limit	°C	*calc 2)*	*calc 2)*	–	–
Mechanical night-time ventilation	*Air change rate*	1/h	3	3	3	3
	Min. required temperature difference room – outside	K	7	7	7	7
	Target room temperature setpoint	K	*calc 4)*	*calc 4)*		
	Mechanical night-time ventilation limit	°C	*calc 3)*	*calc 3)*	–	–
Natural night-time ventilation	*Target room temperature setpoint*	K	*calc 4)*	*calc 4)*	–	–
	Natural night-time ventilation limit	°C	*calc 3)*	*calc 3)*		

Table 3.3: Overview of actually used parameters for rule-based control. "calc x" denotes calculation of the parameter value based on procedure x (see text for details).

The used calculation procedures were as follows:

1) Blind transmission value when occupied and high solar gains (RBC-1)

   This blind transmission value was calculated such that at the given threshold value (15 W/m^2), the specified illuminance (300 Lux, Table 3.2) on the reference plane was obtained.

2) Free cooling limit (RBC-1 and RBC-2)

   The free cooling limit (outside air temperature threshold) was calculated such, that at this temperature the average internal heat gains occurring during a workday stationary compensated the heat loss through the façade. For the calculation, it was assumed that the room temperature is in the middle of the comfort range.

3) Mechanical and natural night-time ventilation limit (RBC-1 and RBC-2)

   The calculation was the same as for the free cooling limit.

4) Free cooling, mechanical and natural night-time ventilation target room temperature setpoint (RBC-1 and RBC-2)

   The target room temperature setpoint was set to 1 K above the lower temperature setpoint of the thermal comfort range. Example: If the lower comfort temperature was 22 °C the used target room temperature setpoint was 23 °C.

3.5 Discussion

The control strategies presented here were designed for simulations only. In real operation, additional features (e.g. hysteresis functions) are necessary to prevent undesired control behavior such as frequent switching, or to cope with restrictions for blind control in case of rain or strong winds.

The novel strategy RBC-3 has only been used in simulations so far. It is possible that it has to be modified for robust and trouble-free usage in practice.

The continuous blind control assumed in strategies RBC-2 and RBC-3 is typically not feasible in real buildings since it would not be accepted by the occupants. The reason why we considered these strategies was for better comparison with the MPC controllers (that are using continuous blind transmission values), and because we wanted to investigate how far one can push non-predictive control. In the future RBC-2 and RBC-3 could however gain practical importance for electrochromic windows control.

As stated in Chapter 1 (Table 1.1), the achievable control performance is only one of several criteria that determine the market potential of a given control strategy. The robustness on control parameter settings and the availability of procedures for tuning of the control parameters can be as important.

In practice RBC control parameter values are typically determined by tuning rules, or by rules of thumb. Due to the very large number of cases considered in our simulation studies (see Chapter 8) manual tuning was neither possible, nor desirable (in order to ensure strict comparability of the results). Instead automated calculation procedures were developed. These can also be applied in reality, provided that the needed building parameters are known at sufficient accuracy.

3.6 Conclusions

A range of rule-based control strategies with different properties is available:

- RBC-1 is a typical, state-of-the-art control strategy.
- The enhanced strategy RBC-2 differs only in blind control from RBC-1; it allows the effect of adding maximum freedom in blind control to be evaluated.
- The newly designed strategy RBC-3 is an advanced, but still non-predictive strategy that is therefore particularly suitable for exploring the potential of predictive control.
- The control strategy RBC-4 is based on RBC-3, but restricts blind transmission setting to once per hour. Comparison with RBC-1 thus allows to assess the novel rules developed in RBC-3.

All RBC strategies come with a generic procedure that allows their control parameters to be determined from a small set of generally valid, basic parameters plus selected building parameters.

3.7 References

[1] e.control™ - Systeme für die Raumautomation. Spega, Spelsberg gebäudeautomation gmbh + co kg. Produktkatalog 2008/2009.

[2] Siemens Building Technologies: control standard night cooling, EPS-I-054-0-2, Rev. 0.2 (2003), Siemens internal document.

[3] Siemens Building Technologies building automation system DESIGO™ V2.37, application library RXC V2 (2007).

[4] Zimmermann, M. et al (1999). Handbuch der passiven Kühlung. Rationelle Energienutzung in Gebäuden. EMPA ZEN. ISBN 3-905594-06-4.

Chapter 4

MODEL PREDICTIVE CONTROL STRATEGIES

by Frauke Oldewurtel, Colin N. Jones, Alessandra Parisio and Manfred Morari

Cite as:

Oldewurtel, F., Jones, C.N., Parisio, A. & Morari, M. (2010). Model predictive control strategies. In: Gyalistras, D. & Gwerder, M. (eds.): *Use of weather and occupancy forecasts for optimal building climate control (OptiControl): Two years progress report*. Terrestrial Systems Ecology ETH Zurich, Switzerland and Building Technologies Division, Siemens Switzerland Ltd., Zug, Switzerland, pp 43–58. ISBN 978-3-909386-37-6.

4.1 Introduction

In this chapter we describe the developed predictive control strategies. They are all based on the so-called Model Predictive Control (MPC) approach. MPC uses a model of the building and its automated subsystems plus predictions of relevant disturbances (e.g., related to weather) over a given prediction horizon to define an optimization problem. Its solution yields the control actions.

Table 4.1 gives an overview of the MPC strategies investigated.

Strategy	*Description*
PB	Performance Bound: Ideal MPC with perfect information (including weather predictions)
CE	Certainty Equivalence MPC: MPC with realistic weather predictions
SMPC	Chance Constrained Stochastic MPC: MPC with realistic weather predictions and uncertainty taken into account

Table 4.1: Overview of investigated Model Predictive Control strategies.

The *Performance Bound* (PB) controller is the control performance of an ideal controller that has perfect knowledge of the controlled systems' dynamics as well as perfect knowledge of all future disturbances acting upon the system. This controller has perfect information and it uses this information to gain the optimal control performance regarding a specified optimization target. The PB defines an absolute benchmark, all performances of other controllers will be worse.

Certainty Equivalence MPC (CE) is the standard MPC approach that is used in virtually all commercial MPC applications. It takes the imperfect/uncertain weather predictions and makes its control decision by assuming that the predictions are correct (i.e. equal to certain).

The *Chance Constrained Stochastic MPC* (SMPC) is a newly developed strategy that can account directly for the uncertainty in the weather predictions, and in principle also in the prediction of any other disturbances.

Note that both CE and SMPC do not take uncertainties in the building model into account.

The Chapter is organized as follows: In Section 4.2 a general overview of MPC is given, including a detailed description of CE. Section 4.3 introduces both Robust and Stochastic MPC and explains all ingredients of the newly developed SMPC approach. Section 4.4 addresses the PB. Section 4.5 explains the specific adaptations of MPC for building control and describes the overall resulting algorithm in detail. The Chapter concludes with a discussion and some conclusions (Sections 4.6 and 4.7).

4.2 General Overview of MPC

Model Predictive Control (MPC) is a very simple and satisfyingly intuitive approach to constrained control. During each sampling interval, a finite horizon optimal control problem is formulated and solved over a finite future window. The result is a trajectory of inputs and states into the future that satisfy the dynamics and constraints of the building while optimizing some given criteria.

In terms of building control, this means that at the current point in time, a heating/cooling etc. plan is formulated for the next several hours to days, based on predictions of the upcoming weather conditions. Predictions of any other disturbances (e.g., internal gains), time-dependencies of the control costs (e.g., dynamic electricity prices), or of the constraints (e.g., thermal comfort range) can be readily included in the optimization.

The first step of the control plan is applied to the building, setting all the heating, cooling and ventilation elements, before the window is shifted backwards by one step (and a further time step is added at the end of the window), and the process is repeated at the next sample. This *receding horizon* approach is what introduces feedback into the system, since the new optimal control problem solved at begin of the next time interval will be a function of the new state at that point in time and hence of any disturbances that have meanwhile acted on the building.

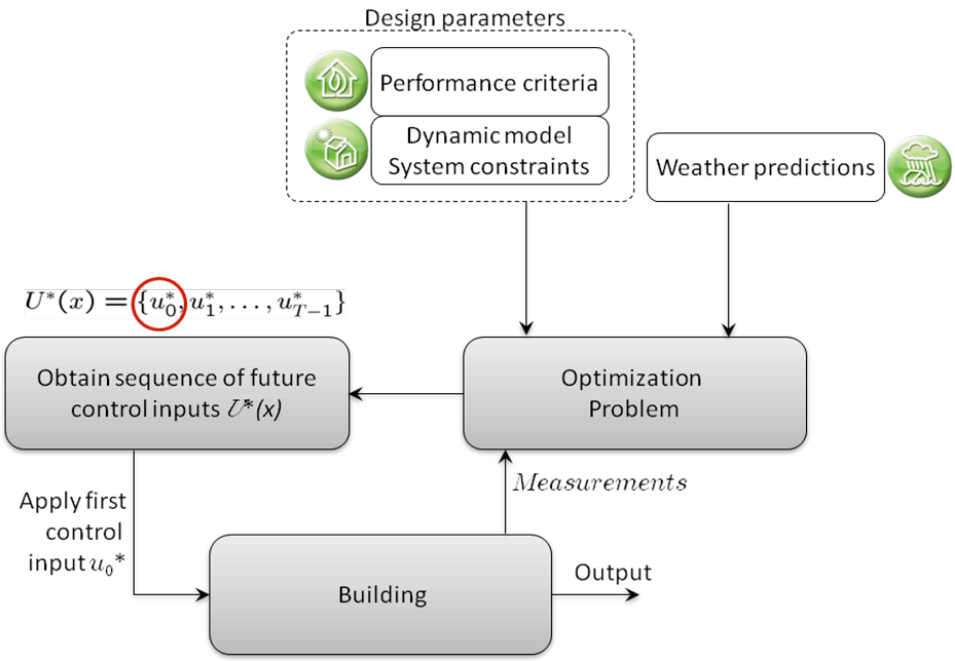

Figure 4.1: Basic principle of Model Predictive Control.

Figure 4.1 summarizes the basic MPC control scheme. One can see that the modeling and design effort consists of specifying a dynamic model (Chapter 5), as well as constraints of the control problem and a cost function that encapsulates the desired behavior (Chapter 2). In each sampling interval, these components are combined and converted into an optimization problem depending on the MPC framework chosen. A generic framework is given by the following finite-horizon optimization problem:

$$\begin{aligned} \min_{u_0,\dots,u_{N-1}} \; & V_N(x_N) + \sum_{i=0}^{N-1} l(x_i, u_i, r_i) && \text{(1) Cost function} \\ \text{subject to} \quad & x_0 = x && \text{(2) Current state} \\ & x_{i+1} = f(x_i, u_i) && \text{(3) Dynamics} \\ & (x_i, u_i) \in \mathbb{X}_i \times \mathbb{U}_i && \text{(4) Constraints} \end{aligned}$$

We now detail each of the four components in the above MPC formulation and discuss how they affect the system and the resulting optimization problem.

4.2.1 Cost Function

The cost function generally serves two purposes:

- *Stability.* It is common to choose the structure of the cost function such that the optimal cost forms a Lyapunov function for the closed loop system, and hence will guarantee stability. In practice, this requirement is generally relaxed for stable systems with slow dynamics, such as buildings, which leaves the designer free to select the cost strictly on a performance basis.
- *Performance target.* The cost is generally, but not always, used to specify a preference for one closed-loop behavior over another, e.g., minimum energy or maximum comfort.

Several common cost functions are in use, the majority of which are *convex*, which results in simple optimization problems to solve. Some common choices are shown in Table 4.2.

Cost Function	*Mathematical Description*
Quadratic regulation	$l(x_i, u_i) = x_i' Q x_i + u_i' R u_i$
Integral cost	$l(x_i, u_i) = \|u_i\|_1$
Probabilistic cost	$l(x_i, u_i) = \mathbb{E}(g(x_i, u_i))$

Table 4.2: Some common cost functions.

Quadratic regulation / tracking. The relative weighting between the states and the inputs provide a trade-off between regulation quality and input energy. If the system has no constraints, or the constraints are not active, then such a cost will be equivalent to the classic Linear Quadratic Regulator / Linear Quadratic Gaussian controller.

In the context of building control, such a cost would generally only be used at the lowest level to replace, for example, existing PI or rule-based controllers.

Integral cost. The cost represents the total amount of product used, which would be a common choice for minimizing energy.

Probabilistic cost. If the system is subject to random disturbances, then one may choose to minimize the expected value of an event occurring, or the probability of some condition being violated, such as room comfort bounds.

4.2.2 Current State

The system model is initialized to the measured/estimated current state of the building and all future (control) predictions begin from a building in this initial state. Exceptions to this are certain robust MPC strategies in which the current state is not assumed to be known exactly, but only to be within a bounded set.

4.2.3 Dynamics

The system model is a critical piece of the MPC controller. Several types of models have been considered in MPC schemes. A summary is given in Table 4.3.

System Model Type	*Mathematical Description*
Linear	$x_{i+1} = Ax_i + Bu_i$
Input-affine	$x_{i+1} = f(x_i) + g(x_i)u_i$
Hybrid / piecewise affine	$x_{i+1} = \begin{cases} A_1 x_i + B_1 u_i, & \text{if } x_i \in P_1 \\ \vdots & \\ A_n x_i + B_n u_i, & \text{if } x_i \in P_n \end{cases}$
Non-linear	$x_{i+1} = f(x_i, u_i)$

Table 4.3: Common system model types.

Linear. This is the most common model type and the only one that will result in a convex and easily solvable optimization problem.

Input-affine. This model-type can cover a large number of very complex systems and is in general very difficult to handle. However, there are recent theories that can in some circumstances provide very simple and stabilizing MPC controllers for this class of system.

The building model discussed later and in Chapter 5 is of this class, since it contains a bilinear term between states and inputs. In practice, such a model can either be approximated as a hybrid system, linearized and treated as a linear system, or considered as a nonlinear system. In the OptiControl project, we repetitively linearized the system around the current operating condition, which simplifies computation while maintaining the benefits of considering the full nonlinear model.

Hybrid or piecewise affine (PWA). A hybrid system is one that contains a mixture of discrete and continuous components, such as switches or valves in combination with continuous systems. This class of models is extremely general and can be used to approximate any smooth system to an arbitrary degree of accuracy. The optimization problems that result involve mixed-integer values and are theoretically very difficult to solve, although many well-tested methods are available.

Non-linear. Systems that cannot be classified into one of the above categories are significantly more difficult to handle. If no special structure can be exploited, then there are still methods to control them in an MPC framework, although confidence in the resulting scheme is diminished and a much larger certification/ validation phase would be called for.

4.2.4 Constraints

The ability to specify constraints in the MPC formulation and have the optimization routine handle them directly is the key strength of the MPC approach. Many different types of constraints are used in practice, a few of which are listed in Table 4.4.

Constraints Type	*Mathematical Description*
Linear	$Ax_i \leq b$
Convex quadratic	$(x_i - \bar{x})^T P(x_i - \bar{x}) \leq 1$
Chance constraints	$P(Ax_i \leq b) \leq \alpha$, $E(Ax_i) \leq b$
Second order constraint	$\|Ax_i + b\|_2 \leq c$
Switched constraints	if $x_i \in P$ then $A_1 x_i \leq b_1$ else $A_2 x_i \leq b_2$
Non-linear	$h(x_i, u_i) \leq 0$

Table 4.4: Common types of constraints.

Linear/polyhedral. The most common type of constraint, which is generally used to place upper/lower bounds on system variables. This class of constraints can also be used to approximate any convex constraint to an arbitrary degree of accuracy. Linear constraints also result in the simplest optimization problems.

Convex quadratic. Bound the state or input to be within an ellipse. Arises, for example, when bounding total input energy amongst several actuators, or in certain formulations of robust MPC.

Chance constraints. Bound the probability of a bound being violated.

Second order cone. Bound the 2-norm of a linear function of the state or input. Arises in several forms of stochastic MPC.

Switched constraints. Set constraints if a given condition is met. Common in many types of hybrid or switched systems.

Non-linear. Any form of constraint that doesn't fit into the above categories. Is generally very difficult to incorporate into a solver.

4.2.5 Certainty Equivalence MPC

The MPC formulation dubbed Certainty Equivalence MPC in the remainder of this report is exactly the MPC formulation given above in which the cost function was taken to be the integral cost (Section 2.3.3) of all control actions applied to the building zone investigated. All constraints were linear and represented the upper and lower bounds on input energy (Section 2.3.2), possible actuator ranges (e.g., blind positioning was restricted from 0 [fully closed] to 100% [fully opened]), or the various comfort requirements for the room temperature, the indoor air quality, and the illumination (Section 2.4).

4.3 Robust/Stochastic MPC

The above MPC framework implicitly assumes that the provided dynamic model is able to perfectly predict the future behavior of the building over the desired control window, or prediction horizon. This assumption is clearly not reasonable because there will be both modeling errors and disturbances (weather, occupants, etc.) acting on the system over this period. Robust or stochastic MPC schemes work with a model of these disturbances and attempt to compensate for these future unknown inputs in the formulated plan.

The basic principle for all of these schemes is that there is no longer a single unique future trajectory of the system, but rather there is a whole set of possible outcomes for each input that might be applied. Handling this set of future possible trajectories modifies how one deals with the cost function and constraints in the above MPC framework.

- *Cost*. One can now minimize a function of the most likely future trajectory (expected value), the worst-case against some metric (min-max), or some representative trajectory (nominal).
- *Constraints*. The key additional feature of robust MPC is that the constraints must be satisfied for *all* possible disturbances that may occur in the future, or a pre-specified set of the most probable ones. This always has the effect of reducing the size of the constraint sets, or of moving the system away from its constraints. Depending on the system type and formulation chosen, this can be very conservative, or not at all.

Robust and stochastic MPC techniques are still very much under development and new techniques have been created specifically for the OptiControl project [2]. The following two sections detail the stochastic MPC formulation used in the OptiControl project.

4.3.1 Affine Disturbance Feedback

An MPC controller formulates a plan regarding what inputs will be applied to the building over a given time horizon into the future. If we consider a robust or stochastic formulation in which it is possible for different disturbances to affect the system in the future, then a single plan will no longer do – we must have a plan for each possible disturbance that might occur. We break our decisions into two parts: those which must be made *now* and those that do not have to be made until the future, at which point we will have more information about disturbances, the 'wait and see' inputs.

This is a classic control setting and can be formulated and solved using *dynamic programming* (DP). However, solving a DP is computationally intractable except for very special cases, and most forms of control (including MPC) are simply computationally tractable approximates of dynamic programming. One such approximation that has been shown to be extremely close to optimal in recent years is called the *affine disturbance feedback* formulation.

Consider the following linear model

$$x_{i+1} = Ax_i + Bu_i + w_i$$

in which x_i is the state at time i, u_i is the input and w_i is an unknown disturbance acting on the system. We choose the input that we will plan to apply at time i in the future to be an affine function of the as yet unknown disturbances that will act on the system between now (time 0) and time i:

$$u_i = \sum_{j=0}^{i-1} M_{ij} w_j + h_j$$

Instead of optimizing over the inputs u_i as in standard MPC, we optimize over the matrices M_{ij} and hence make the future planned inputs responsive to the as yet unknown disturbances. It should be emphasized that since the MPC controller is still applied in a receding-horizon fashion that these

future plans are never actually applied to the system, but are only used as a computational procedure in order to make good decisions now.

There are several benefits to using this affine disturbance feedback formulation:

- The added conservatism that is present in all robust/stochastic MPC approaches is significantly reduced from current state-of-the-art methods.
- The resulting dynamic plan over the future prediction horizon is generally very close to the optimal one generated by dynamic programming and hence the performance of the system is very good.
- The resulting optimization problem can be formulated as a convex problem by using a robust programming approach. This is a critical property since it makes computation rapid and simple using common commercial codes.

The main limitation of this formulation is the added computational complexity of optimizing over the matrices M_{ij} rather than just the inputs u_i. This can however be mitigated by, for example, restricting the degrees of freedom of the matrices M_{ij}, or by optimizing over weighted sums of a small number of pre-computed matrices. These techniques have been shown to be effective in building control while significantly reducing the computational effort.

4.3.2 Chance Constraints

The disturbances acting on the building are primarily in the form of uncertainty in the weather prediction. The distribution of error in the prediction can be well modeled as a Gaussian. Since Gaussian distributions have infinite support, it is no longer possible to guarantee that all possible states in the future will satisfy the constraints, since it will always be possible for an arbitrarily large disturbance to impact the system (at least in terms of the mathematical formulation).

In order to cope with this form of uncertainty, we utilized a *chance-constrained* formulation in which we required that the future state of the building satisfies the constraints only with a given probability:

$$P(Ax_i \leq b) \geq 1 - \alpha$$

This formulation has significant benefits for building control

- The European standards specify comfort bounds in this manner, so it is now possible to directly encode the desired specifications into the controller without the need of additional tuning.
- When combined with the affine disturbance feedback discussed in the previous section, it is still possible to formulate the resulting optimization as a second order cone problem. Such problems are convex and can be readily solved by existing commercial codes, although they can be fairly compute-intensive at larger scales.

The remainder of this document will refer to the stochastic MPC approach in which comfort bounds are expressed as chance constraints and future control input signals are parameterized in terms of an affine disturbance feedback as SMPC. A more detailed description of the SMPC approach can be found in [2].

4.4 Performance Bound

The fundamental challenge in control is to make an optimal decision about an action to take now, given that information about the future is not yet available, such as tomorrow's weather. If, however, all future information (including the exact dynamic behavior of the controlled system) were to be known, then a perfect decision can be made. For analysis purposes, it is possible to formulate such a *non-causal* problem for a given building and a given year after the weather has been recorded and is therefore known.

The resulting amount of primary energy (assumed that primary energy use is minimized by the ideal control) required to maintain the comfort bounds within the building is truly optimal and cannot be beaten by any scheme which has less (i.e. causal) information available. For this reason, we dub the resulting amount of primary energy used the *Performance Bound* (PB).

The procedure for computing the PB is exactly the same as that for certainty equivalence MPC, with two critical differences: First, instead of using weather predictions in the formulation, the real weather measurements are used. Second, the plan must not be computed in a receding horizon fashion, since no feedback is required, but the optimal sequence for the entire interval considered (e.g., one year) can in principle be computed in one shot. However, due to the presence of a bilinear model this was actually found to be impracticable, such that a somewhat modified procedure had to be employed (see Section 8.3.1).

4.5 MPC for OptiControl

In this section we detail the specific type of MPC formulation that has been used in the OptiControl project. Specifically, we outline how one translates from the various inputs to the controller (MeteoSwiss weather predictions, local weather and building measurements, as well as building model data) to a mathematical structure that can be processed by standard optimization software.

An overview of the developed MPC controller is given in Figure 4.2. In the following sections we detail the individual steps.

4.5.1 Step 1 – Weather Prediction at Building Site

The output of this block is a prediction of the weather over the future horizon that the controller is considering and consists of a time-varying linear model of weather parameters (temperature, radiation, etc) driven by Gaussian disturbances. The resulting model consists of a series of dynamic update matrices and the covariance matrices of the disturbances.

a) Local measured weather: Measurements of the current temperature, radiation, etc.
b) Error model for weather forecast: Historical weather predictions and corresponding measurements are used to derive a model of how the uncertainty in the forecasts evolves as a function of time. See Chapter 7 for details.
c) Weather forecast: Weather forecasts are available from weather services at regular time intervals and for a given number of hours ahead. In this study we use the 72 hour predictions as delivered every 12 hours by the MeteoSwiss COSMO-7 numerical weather prediction model. The predictions used are those from the model gridpoint found closest to the building site.
d) Kalman predictor (local Kalman filter): Since the weather forecast is not updated continuously (e.g., only each 12^{th} hour in case of the COSMO-7 model) it is out of date for the majority of the time given the regular measurements at the building. In addition, the weather forecast is typically not available for the exact location of the building. In order to improve the forecast on an hourly basis, we fuse it with those measurements. This is done using a standard Kalman predictor, which uses a linear/Gaussian forecast error model in order to make an optimal update of the prediction based on the newly measured local weather conditions.

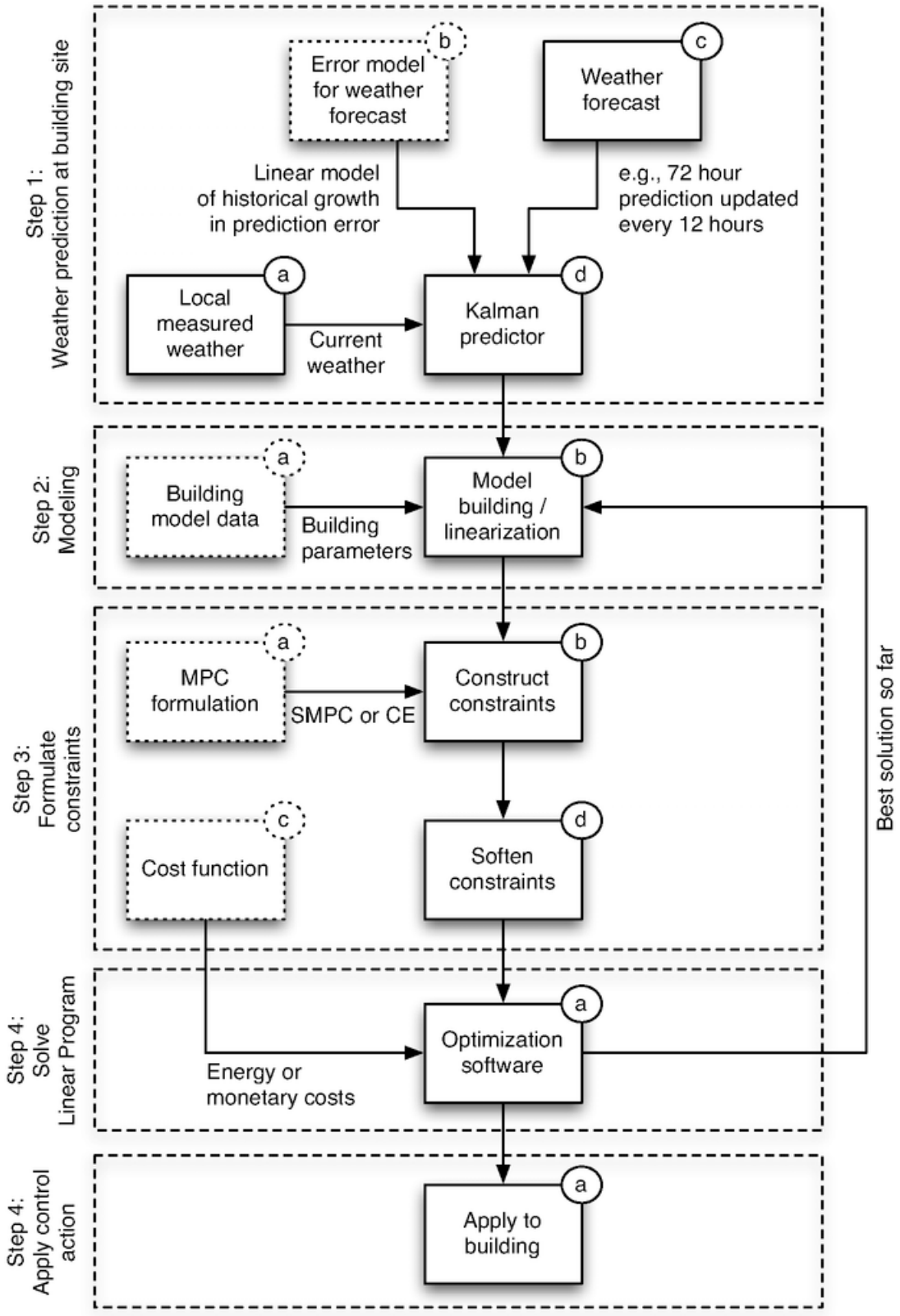

Figure 4.2: Decision flow of the Model Predictive Control strategy developed for the OptiControl project.

4.5.2 Step 2 – Modeling

This block combines the weather prediction model with the dynamic model of the building and linearizes the result.

The principle of the modeling can easily be described with a small example as given in Figure 4.3. The model is based on an RC network, where the nodes are the states and these are representing the room temperature or the temperatures in the wall, floor or ceiling. Then the heat transfer rate is given by

$$\frac{dQ}{dt} = U \cdot A \cdot (\vartheta_e - \vartheta_i)$$
$$\Rightarrow \underbrace{\frac{dQ}{d\vartheta_i}}_{C_i} \cdot \frac{d\vartheta_i}{dt} = \underbrace{U \cdot A}_{K_{ie}} \cdot (\vartheta_e - \vartheta_i)$$

where A is the area, U is depending on the material and describes the heat transmission, and ϑ_i and ϑ_e are the temperatures at node i and e respectively.

The heat transmission coefficient is computed as

$$1/K_{ie} = 1/K_i + 1/K_e$$

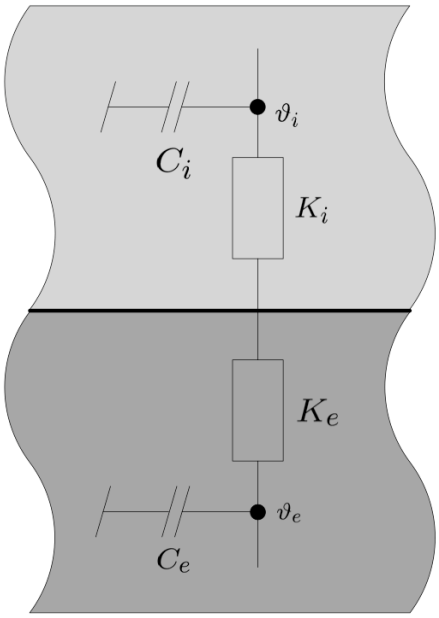

Figure 4.3: Heat transmission between two nodes.

This yields

$$C_i \cdot \frac{d\vartheta_i}{dt} = K_{ie} \cdot (\vartheta_e - \vartheta_i)$$

where Ci is the capacity. For each node, i.e. state, such a differential equation is formulated.

Some of the resistances are however not constant but can be varied, for example the heat transmission through the windows is not constant but can be varied by opening and closing the blinds. This is modeled by splitting the heat transmission into two parts, the first one describing the heat transmission with closed blinds which is again constant, and a second part describing the heat transmission with partially or fully opened blinds. For the latter the right-hand side of the last equation is multiplied with an input u that is between 1 and 0. Please note that the outside air temperature, the outside wetbulb temperature and the neighboring room temperature are also nodes in this model but are taken as fixed sources. With these assumptions the building can be described with a bilinear model of the following form

$$x_{k+1} = Ax_k + B_u u_k + B_v v_k + \sum_{i=1}^{n_u} [(B_{vu,i} v_k + B_{xu,i} x_k) u_i]$$
$$y_{k+1} = Cx_k + D_u u_k + D_v v_k + \sum_{i=1}^{n_u} [(D_{vu,i} v_k) u_i]$$

Thus, the dynamic behavior of the building is nonlinear, in this case bilinear between inputs, states and weather parameters. Non-linearities in the dynamic equations of an MPC problem will always result in a non-convex optimization, which can be extremely difficult to solve. The approach that we take here is a form of Sequential Quadratic Programming (SQP) for solving non-linear problems in which we iteratively linearize the non-convex constraints around the current solution, solve the optimization problem and repeat until a convergence condition is met. This standard procedure is

simplified here because the non-linearites are mild and since the cost is linear, rather than quadratic, we have only to solve a series of linear programs, instead of the standard quadratic ones.

4.5.3 Step 3 – Formulate Constraints

This block constructs the data required to solve an optimization problem from the incoming time-varying linear model of the building dynamics and the constraints that the future state should satisfy.

a) MPC Formulation
b) Construct Constraints

Two types constraints are to be enforced: input power limits and room temperature comfort bounds (as well as some other output bounds). Since the model has been linearized, the predicted room temperature at *t* time steps in the future is a linear function of the state now (time *t* = 0) and the intervening inputs u_i and weather w_i acting on the building. As a result, we can write the room temperature y_t at time *t* in the future as

$$y_t = Fx_0 + \sum_{i=0}^{t-1} (G_i u_i + H_i w_i)$$

for appropriate vectors *F*, G_i and H_i, which are computed directly from the output of Step 2.

The critical issue is that the disturbances w_i are not known exactly, but they are only known to be normally distributed with mean $\overline{w}_i$ and covariance Σ_i. We have considered three methods for enforcing bounds on the temperature despite this disturbance:

i) Certainty Equivalence (CE)

This is the standard approach. The idea is to assume that the weather disturbance simply takes its mean value. The result is a simple linear constraint of the form

$$\underline{y} \le y_t = Fx_0 + \sum_{i=0}^{t-1} (F_i u_i + H_i \overline{w}_i) \le \overline{y}$$

where $\overline{y}$ and $\underline{y}$ are the desired upper and lower comfort bounds.

The primary limitation of certainty equivalence is, of course, the fact that if the weather does not actually equal the expected value, then the bound may be violated. This is most often dealt with by artificially tightening the upper and lower bounds, which provides a buffer zone and can be effective for small variances. The cost to be paid is the additional energy required to be conservative and hold the temperature further away from the bounds than is strictly required. See Chapter 10 for an analysis of this tuning procedure.

ii) Chance Constraints

One method of automatically determining an appropriate amount to tighten the constraints is to formulate them as chance constraints as discussed above.

$$P\left(y_t = Fx_0 + \sum_{i=0}^{t-1} (G_i u_i + H_i w_i) \le \overline{y} \right) \ge 1 - \alpha$$

where α is the desired probability of constraint satisfaction. A classic result by Prékopa [3] allows us to re-write this difficult probabilistic constraint as a linear condition

$$\beta + \underline{y} \leq y_t = Fx_0 + \sum_{i=0}^{t-1} (G_i u_i + H_i \overline{w}_i) \leq \overline{y} - \beta$$

where β is a constant defined as

$$\beta = \Phi^{-1}(1-\alpha)\|[H_0 \cdots H_{t-1}]\|_2$$

Despite the complex look of the above equation, it is in fact identical to the tuning of certainty equivalence discussed above, where the tightening is set in order to achieve a particular probability of constraint violation. While this procedure is conceptually appealing, the value β can be unnecessarily large and grows quickly with the length of the prediction horizon, which is why the procedure discussed in the next section was introduced.

iii) Chance constraints with affine disturbance feedback (SMPC)

A less conservative approach that has been developed for the OptiControl project is a chance constraint formulation combined with affine disturbance feedback, as discussed above in Section 4.3.1. In this approach, we set the input equal to an affine function of the as yet unknown weather conditions, which changes the probabilistic constraint to

$$P\left(y_t = Fx_0 + \sum_{i=0}^{t-1} \left(G_i \hat{u}_i + (H_i + \hat{M}_i) w_i\right) \leq \overline{y}\right) \geq 1 - \alpha$$

where one can see that we have added the new optimization variable $\hat{M}_i$. This procedure theoretically allows us to mitigate the effect of the disturbance to any desired level (note that for simplicity we have neglected the fact that $\hat{M}_{i-1}$ is always zero and so we cannot completely compensate for the disturbance). This mitigation is, however, bounded by the amount of input energy available to the controller, since the approach requires that we allocate some input energy to compensating for the disturbance ($\hat{M}_i$), and some for steering the system to a desired state ($\hat{u}_i$).

The above equation can be converted into a set of linear inequalities that are appropriate for an optimization routine by using a robust programming approach, which we do not detail here. The added complexity arises from the fact that the variable β introduced in the previous section is now a nonlinear function of the new optimization variable $\hat{M}_i$. The resulting optimization problem is a second order cone problem, which is convex and therefore theoretically simple to solve. However, due to the large number of variables involved, it can be very time consuming and as a result somewhat impractical (see Chapter 10 for a detailed analysis). For this reason, we choose these matrices during a pre-processing step and fix them for the entire year, which returns the constraints to simple linear inequalities.

c) Cost function: The cost functions considered are either Non-Renewable Primary Energy usage or the Monetary Cost of energy over the prediction horizon (Section 2.3.3). Because the weather is not known exactly over this period, it is not possible to know exactly what cost will be incurred, but only a probability distribution over possible costs. We here choose to minimize the expected value of this distribution, although it would also be possible to minimize the variance if desired. Since the cost is linear and the distribution Gaussian, the expected value is simple a linear function of the mean values and is therefore simple to formulate.

d) Soften constraints: It is not always possible to satisfy all constraints of the building and so a relaxation-procedure is required that chooses automatically which constraints are to be violated first. This is achieved by adding variables to the optimization routine that allow every constraint to be violated. We then penalize these variables very heavily, which forces them to zero, and the satisfaction of all constraints, if at all possible. If this is not possible, then these additional vari-

ables give the optimizer sufficient flexibility to always find a solution that can be applied to the building. One can define the relative importance of each constraint by tuning the relevant weighting matrices and thereby have the system violate the least important first.

4.5.4 Step 4 – Solve Linear Program

Once the constraints and cost have been formulated, the resulting problem can be passed to a standard optimization routine. In OptiControl, we have generally made use of the standard commercial package CPLEX, since it is extremely effective for the large-scale and sparse problems that result.

As discussed above, we apply an SQP approach to solving the non-convex optimization problem, which requires that we successively re-linearize around the current problem solution until convergence. The convergence condition is to test when two successive iterations do not change the solution to the linear program, at which point further iterations would not change the solution and we have reached a locally optimal solution (see also Section 8.2.2).

4.5.5 Step 5 – Apply Control Action

The optimal solution of the linear program consists of a sequence of planned inputs over a time horizon into the future. We apply only the first of these inputs to the building, before re-solving the entire problem at the next point in time.

4.6 Discussion

4.6.1 Benefits of MPC

Model Predictive Control provides a simple and direct method of describing 'what' a controller is trying to achieve (minimize energy without loss of comfort), without the requirement of specifying 'how' this is to be done, as is the case with rule-based approaches. MPC can be interpreted as a complex set of rules mapping weather predictions, building knowledge and measurements to optimal control decisions for heating, cooling etc.

The first key benefit is that these rules do not need to be explicitly enumerated by an expert and experience has shown that MPC is generally most effective in situations in which good rules are too complicated for such an expert to determine.

Second, the ability to directly describe 'what' a controller is trying to achieve makes tuning rules more obvious to the user and easier to manipulate. For example, the user could easily set a single parameter on the fly that adjusts the system between 100% energy minimization and 100% comfort maximization.

To judge the performance of a specific control strategy, a comparison to the corresponding PB simulation can be done, which will show the remaining potential of better control strategies. Nothing can be said about to what extent the potential can be exploited by a feasible control, but the sizes of remaining potentials reveal for what applications (building type, HVAC/light/blind system, location etc.) further control strategy development may be promising.

4.6.2 MPC And Low-Level Control

The PB assumes perfect knowledge of all disturbances, such that the resulting control actions approximate an ideal, continuous time, closed-loop low-level control. This is similar to the low-level control employed in the context of strategies RBC-1 to RBC-3 (Section 3.3).

Differently from the PB, the CE and SMPC strategies are fed with imperfect weather predictions. Since they are run without a low-level controller any control actions taken for the time step ahead cannot be corrected any more during this time step.

Due to the suboptimal blind control, the CE and SMPC strategies cannot be meaningfully compared against the strategies RBC-2 or RBC-3. A comparison is, however, possible with strategies RBC-1 and RBC-4 because for these strategies the adjustment of the blinds is restricted in a similar manner as for CE and SMPC.

Three lines of work are currently pursued in order to augment the CE and SMPC strategies such that they can be made to function together with a low-level controller:

The first approach consists in deriving the needed low-level control inputs (Section 3.3) based on a rule-based interpretation of the CE or SMPC solutions.

The second approach is to use the next predicted room temperature by the MPC procedure as a set-point for the low-level controller.

The third approach incorporates a model of the low-level controller in the overall MPC model, and has the MPC controller generating all needed low-level control inputs directly.

4.6.3 Estimation Of States And Parameters

MPC controllers rely on a state-estimator in order to determine the temperature of all building elements (walls etc.). The effect of such an estimator has been neglected the OptiControl project so far such that the reported results for MPC will be degraded somewhat in a more realistic setting.

MPC controllers do not generally involve a large number of ‘tuning’ parameters per se. However, there are many parameters that must be set, most of which will have physical meaning. These consist of the building model, the disturbance model used in the Kalman filter, the energy cost of each actuator and the desired probability of constraint violation. All of these have physical meaning and can reasonably be determined from building data, save for the constraint violation probability. While this term has physical and mathematical meaning, it is more likely to be used as a direct and simple tuning knob by the user to adjust the system between ‘high comfort/high energy’ mode to ‘low comfort/low energy’ mode.

4.7 Conclusions

MPC can be adapted for building control, and extensions of the approach are possible in order to account for uncertainty in weather predictions (and other disturbances) in a mathematically rigorous and physically consistent way.

As a side-product, MPC can also be used to estimate a given building system's energetic or monetary Performance Bound. The latter provides an absolute benchmark for assessing the performance of any controller.

The control strategies specifically developed for the OptiControl project share all typical benefits of the MPC approach: intuitive appeal, high flexibility, possibility to relate control actions to a physically based model of the building, and optimality of solutions (at least at a good approximation) even for complex control problems that involve a bilinear building model, time-dependent constraints and many actuators.

These advantages are obtained at the cost of having to determine a sufficiently accurate and realistic model of the building and its automated subsystems.

An additional effort needed in the practical application of MPC is that the model parameters and the system's current state must be estimated by means of appropriate procedures.

In summary, MPC is a promising approach for building control. Its performance in real applications can be expected to vary with the quality of the model and the available input data (model parameters, system states, weather predictions etc.) to an extent that remains to be investigated.

4.8 References

[1] Peter Kall, Janos Mayer, "Stochastic Linear Programming: Models, Theory, and Computation", Springer-Verlag, Berlin, 2005.

[2] F. Oldewurtel, C. N. Jones, M. Morari, "A Tractable Approximation of Chance Constrained Stochastic MPC based on Affine Disturbance Feedback", *in Proc. 47th IEEE Conf. on Decision and Control*, Cancun, Mexico, 2008.

[3] A. Prékopa, "Stochastic programming", Kluwer Academic Publishers, Dordrecht, The Netherlands, 1995.

Chapter 5

MODELING OF BUILDINGS AND BUILDING SYSTEMS

by Beat Lehmann, Katharina Wirth, Stephan Carl, Viktor Dorer,
Thomas Frank and Markus Gwerder

Cite as:

Lehmann, B., Wirth, K., Carl, S., Dorer, V., Frank, Th. & Gwerder, M. (2010). Modeling of buildings and building systems. In: Gyalistras, D. & Gwerder, M. (eds.): *Use of weather and occupancy forecasts for optimal building climate control (OptiControl): Two years progress report*. Terrestrial Systems Ecology ETH Zurich, Switzerland and Building Technologies Division, Siemens Switzerland Ltd., Zug, Switzerland, pp 59–66. ISBN 978-3-909386-37-6.

5.1 Introduction

The application Integrated Room Automation (IRA) deals with the simultaneous control of common HVAC and building systems like heating, cooling, ventilation, blinds and lighting.

In order to be able to assess different control strategies by simulation – but also for the development of Model Predictive Controllers (MPC) – the building's thermal dynamics and its technical installations need to be incorporated into a corresponding simulation model.

Here we report on the selection of a suitable modeling approach, and on the derivation and testing of a corresponding model of a single building zone or room that was specifically developed for the OptiControl project.

The accuracy of the used approximations and linearizations, the computing requirements as well as maintenance effort and versatility of the model are also discussed.

5.2 Choice of Building Modeling Approach

Our choice of modeling approach was based on the following requirements:

- The model should be detailed enough to provide a reliable simulation of the building's dynamics and all control relevant processes. To this end a temporal resolution of one hour or less was considered necessary.
- The model should be simple enough to be incorporated in an MPC controller. As described in Section 4.5 the MPC approach imposed the restriction of a bilinear model.
- The model should be usable for large-scale simulation studies, i.e. have reasonable input data needs and be computationally efficient.

Many different building models of varying complexity are available to date that were evaluated for the task at hand. It is in this context that we developed a classification of building models that is reported in Table 5.1.

Modeling Level	*Characteristics and (example)*	*Characteristics – Scope*
L1	Verbal model	Easily understandable characterization of a building – communication with non-specialists.
L2	Correlation model (Energy signature, [1])	Linear correlation between average power use and external temperature – design and rough energy demand calculations.
L3	Linear dynamical model (Simple 3-node thermal RC network, [2])	Simplest possible representation of a building's thermal dynamics – design and energy demand calculations of buildings
L4	Bilinear dynamical model (Detailed multi-node thermal RC-network)	Representation of building physical processes at intermediate precision and detail – reliable energy and comfort simulations.
L5	Detailed model based on building simulation software libraries (e.g. TRNSYS)	Best possible representation and detailed simulation of building physical processes.

Table 5.1: Hierarchy of building models. RC = Resistance-Capacitance.

The newly derived model was the one defined on the level L4. It is described below.

5.3 Model Overview

Figures 5.1 and 5.2 give an overview of the model's components and of the chosen thermal Resistance-Capacitance (RC) network, respectively.

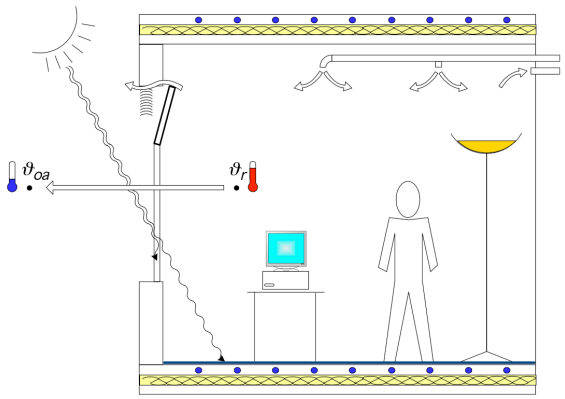

- Floor heating (*hPowSlab*)
- TABS: Thermally activated building system for heating (*hPowSlab*) and cooling (*cPowSlab*)
- Slow ceiling for cooling (*cPowSlab*)
- Free cooling with wet cooling tower (*fcUsgFact*) acting through cooled ceiling or TABS
- Radiator (hPowRad)
- Mechanical ventilation with energy recovery (*nMevE*, *nMev0*), heating (*hPowMev*) and cooling (*cPowMev*)
- Hybrid ventilation: working hours (*nMevE, nMev0*) - non working hours (*nNav*)
- Blinds (*bPos*)
- Artificial lighting (*eLighting*)
- Indoor air quality (CO_2)

Figure 5.1: Overview and abbreviations of subsystems considered for modeling.

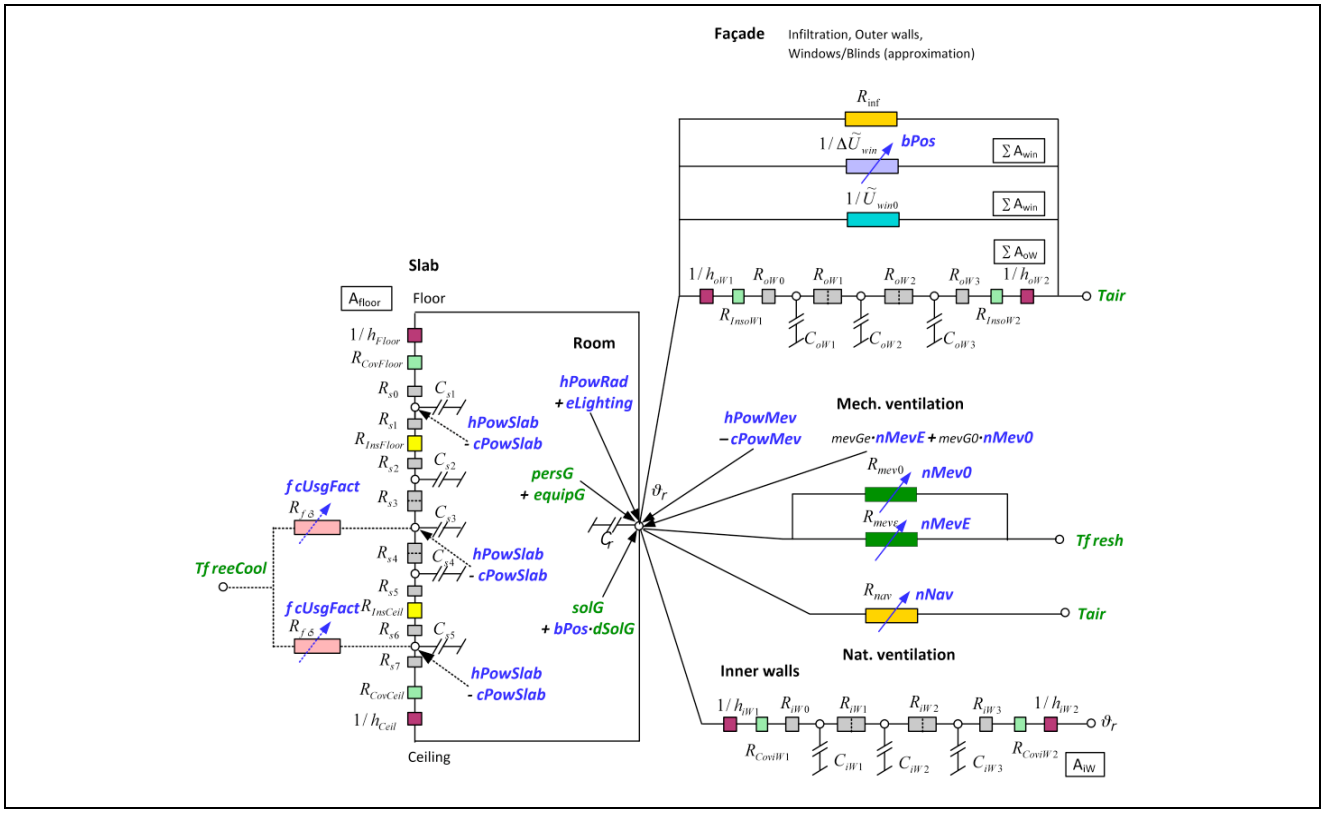

Figure 5.2: Thermal Resistance-Capacitance (RC) network model. Note, for illustration all supported subsystems are shown simultaneously.

Note, for illustration both Figures contain all subsystems that occur in Building System variants S1 to S5 (see Section 2.3). A separate representation for each of the 5 subsystem variants considered in this study can be found in the Appendix A.

The model of the building is constructed around the central room node ϑ_r. Thereby the massive structure of the building consists of a combined floor/ceiling slab, a façade wall with integrated windows and an internal wall representing all walls to neighbouring rooms. These rooms are assumed to have identical boundary conditions which in turn means that there is no influence of neighbouring rooms to the modelled room.

The different heating and cooling systems are acting either on the room node or – depending on the chosen slab system – on one of the slab nodes (floor heating: node 1, TABS: node 3, cooled ceiling: node 5). Internal gains from persons, equipment and lighting as well as solar gains are also transferred to the room node.

5.4 Description of Subsystems

This section contains the most important information concerning modeling, restrictions, approximations and parameters of HVAC and other system parts of the model. The mathematical formulation and analysis of approximations can be found in Appendix A.

5.4.1 Mechanical ventilation

Mechanical ventilation systems provide the room with fresh air to guarantee indoor air quality. Two operation modes of ventilation are implemented: a) non-air quality controlled ventilation with constant minimal airflow rate and b) CO_2-controlled ventilation with variable minimal airflow rate (CO_2-sensor).

In the case of **non-air quality controlled ventilation** (ntbW1; Variant V in Table 2.8) the system is operated based on a working hour time schedule. Ventilation starts 1 h before the beginning of work and runs until 1 h after the end of work: 06:00 - 19:00 local time [3]. The minimal air change rate during on-times is kept constant and set to the design value for maximum occupancy.

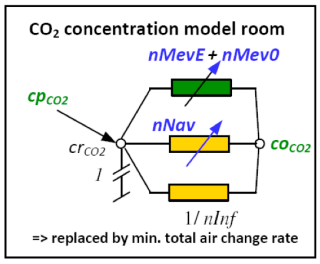

In the **CO_2-controlled ventilation** (ntbOccup; Variant W in Table 2.8) the minimal air change rate is adapted so that the indoor air quality requirements are met. CO_2 production is proportional to the presence of persons (15 l/hP). The amount of CO_2 exchange through ventilation depends on the CO_2 concentration gradient to outside air and on the air change rate. As CO_2 exchange processes run much faster than heat transfer, the CO_2 calculations would need a much smaller time step than used for the thermal model. As an approximation we use the occupancy profile (Section 2.5) to calculate a minimum air change rate. The resulting CO_2-concentration in the room is then calculated only in a separate post processing step. Tests showed that this is a conservative approach.

The analysis of simulation results has shown that most cases fulfil class I comfort requirements in the case of non-air quality controlled ventilation whereas with CO_2-control typically only class II is reached (Appendix B.4).

In order to prevent draught risk the maximum air change rate is limited to n = 4.0 h^{-1}.

Mechanical ventilation can also be used for **heating**, **cooling** and for cooling by **mechanical night-time ventilation**. The thermal energy of the exhaust air can be recovered by an air to air heat exchanger (efficiency ε = 0.8), e.g. with a rotary heat exchanger or a counter current heat exchanger with bypass. With heating and cooling registers the supply air can be further warmed up or cooled down to reach the required inlet temperature. The power demand of the ventilator (mevGe+mevG0) is accounted for in the thermal balance. In order to maintain thermal comfort upper and lower bounds for room inlet air temperature (ϑ_{mev}) are limited to 16°C and 40°C. As the thermal balance for the supply air temperature is not a bilinear function, the heating and cooling power reserves (for which the temperature bounds are reached) are calculated and limited instead of the temperature itself. Tests showed that this is a conservative approach (Appendix B.3).

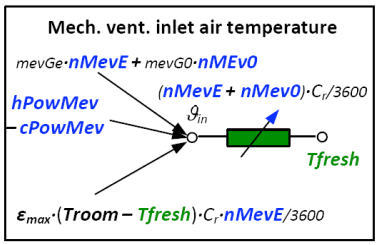

5.4.2 Hybrid ventilation / natural ventilation

Hybrid ventilation is the combination of mechanical ventilation during occupancy hours and natural ventilation (through window opening, thermally driven) for night-time cooling. **Natural ventilation** by single sided window opening can be modeled with a physical correlation in which the air change rate is proportional to the square root of the difference between room and outside air temperature [4]. We can not use this model in the controller, because the model for heat flow has to be linear or bilinear in room temperature and outside air temperature. Instead we limit the maximum air change rate to 3 h^{-1} and the controller chooses a value below this limit. Within post processing we check if the required air change rate can be supplied. Tests showed that at low temperature differences (especially during summer periods) heat transfer is modelled with reasonable accuracy, but at high temperature differences heat flux is highly underestimated. As this shortcoming can be compensated by a prolongation of the operating hours during such high cooling potential periods the approximated model can nevertheless be used for the purposes of the potential assessment simulations. If controlling a real building, undercooling of the building has to be prevented by a low level controller (Appendix B.2).

5.4.3 Radiator: direct room heating

The radiator heating system is modeled as direct power input to the room node ϑ_r. As in the room model combined heat transfer coefficients for convection and radiation are used, this modeling approach corresponds quite well to a real situation with typical radiator devices (fractions of approximately 35% and 65% of convective and radiant dissipation of heat). As the losses of a distribution system would also be dissipated within the building, it is acceptable that no distribution system is considered.

5.4.4 Ceiling slow: heating and cooling

“Slow ceilings” are cooling ceilings which are directly mounted to the ceiling surface, e.g. capillary tube systems embedded in a gypsum layer. Because of their thermal connection to the building structure a considerable part of the system power is transferred directly to the building mass and therefore is released only with delay to the room. Compared to suspended chilled ceilings such systems react “slowly” concerning the power release to the room.

As it can be assumed that for heating and for mechanical cooling the necessary temperatures can be achieved by the respective generation systems at any time, the corresponding heating and cooling powers (hPowSlab, cPowSlab) can directly be fed into the slab node where the piping system is located. As the energy consumption for the distribution pumps is typically small compared to the transferred thermal energy in these cases this energy consumption is accounted for in the definition of the overall system efficiencies.

Free cooling with a wet cooling tower is modeled using the free-cooling link (cf. Section 5.4.7). The resistance describing the system characteristics for "ceiling slow" is chosen according to a typical system layout of a capillary tube system with a wet cooling tower. The corresponding value of R_{fc5} is 0.29 [m^2K/W]. As described in Section 5.4.7 the representation of the system with only one system value is a rather rough approximation. Nevertheless the most important influences are considered.

5.4.5 TABS: heating and cooling

Thermally activated building systems (TABS) is the generic term for systems for heating and cooling of buildings which incorporate the building mass as thermal energy storage ([5], [6]). In a classical TABS-setup the tube system – by which the storage is activated with – is located near the center of the slabs. In the building model the TABS is therefore connected to the slab node number 3. As the system "ceiling slow" is just a sub-variant of TABS, the same statements concerning modeling, approximations and usability are valid also for the classical TABS.

In the free-cooling case the overall system efficiency of a typical layout of a TABS combined with a wet cooling tower is R_{fc3} = 0.33 [m^2K/W].

5.4.6 Floor heating: heating and cooling

Floor heating and cooling are modeled as direct power input to the slab node number 1 of the building model. As it can be assumed that the generation systems are dimensioned well and therefore the required system temperatures can be hold this is an acceptable assumption to represent the real behavior of this system.

5.4.7 Free cooling with a wet cooling tower

Free cooling with a wet cooling tower is modeled using a correlation developed in the framework of the TABS-project [5]. The corresponding formula (8-14) out of this handbook reads as follows:

$$\dot{q} = \frac{\dot{m}_{sp,p}\, c_p}{\frac{\dot{m}_p\, c_p}{\dot{m}_s\, c_s}\left(\frac{1}{\varepsilon_s - 1}\right) + \left(\frac{1}{\varepsilon_p - 1}\right) + \frac{\dot{m}_{sp,p}\, c_p}{U_t}} \left(\overline{\vartheta}_k - \vartheta\right)$$

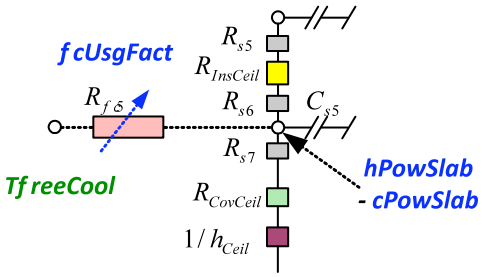

The fraction in this equation describes the heat transfer between the free cooling temperature ϑ (*TfreeCool*) and the medium core temperature of the slab $\overline{\vartheta}_k$ where the piping system is located (e.g. temperature of slab node number 5 in the case of the slow ceiling system). The following system parts are contained in this correlation:

$U_t, \dot{m}_{sp,p}, c_p$ System characteristics, mass flow and fluid properties of the slab piping system

$\varepsilon_s, \dot{m}_s, c_s$ System characteristics, mass flow and fluid properties of the wet cooling tower

$\varepsilon_p, \dot{m}_p$ System characteristics of the heat exchanger between cooling tower and piping system

The system characteristic U_t of the slab piping system has thoroughly been tested within the TABS-project and was proofed to be reliable for typical TABS and TABS-kind applications.

Also the description of the system characteristics of heat exchangers by the means of their temperature efficiency ε is common and reliable for this type of unit.

In contrast to this, the system characteristic ε_s of the wet cooling tower in reality is nonlinear and had to be linearized for its use within the model. Whereas the errors of this linearization are small within a large region around the dimensioning point of the cooling tower, the power output of the system is overestimated by up to around 15% when operated in conditions far away from the dimensioning point (e.g. at low wet bulb temperatures). In addition the influence of part load operation on the system efficiency is neglected.

Nevertheless it can be stated that with this mathematically simple approach the overall behavior of the free cooling system can be represented quite well, as the most important influencing factors are considered. Moreover the individual dimensioning of each system part – narrow or rather broad layout – in total can be much more decisive concerning energy consumption than the errors through model approximations.

The latter is also the reason, why for each system (slow ceiling, TABS) and dimensioning variant (cf. chapter 3.3.2) only one typical dimensioning has been chosen independently of other experiment boundaries like internal gains level, window area fraction or site.

5.4.8 Blinds and lighting

Blind position can be set between fully closed and fully opened by pulling up and down or rotating the slats (bPos between 0 and 1). In corner offices both expositions have identical blind positions.

Room illuminance implies heat gain to the room trough solar gains and artificial lighting (eLighting) [7]. Solar gains and illuminance are separated into two parts: through closed blinds (SolG, illum) and difference to fully open blinds (dSolG, dIllum).

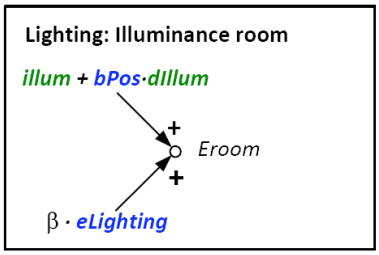

Room illuminance is composed of natural lighting and artificial lighting. The artificial part is proportional to power demand of artificial lighting (β = 70 lm/W).

5.5 Model Validation

The validation of the developed models against detailed building and system simulators such as TRNSYS was to some extent hampered by the fact that an implementation of the used control strategies in these programs would have been necessary.

However, based on ample experience gathered in other projects (e.g. TABS-Control) we could reasonably assume that the chosen L4-model contained the most important characteristics of a building and that therefore the dynamic behavior of the building is well represented.

A quantitative check was performed with the aid of the "L5" (cf. Table 5.1) Helios validated building simulation program for selected cases. The results showed good consistency of the calculated room temperatures when the same model parameters and input data were used. We concluded that the new building model is implemented correctly (Appendix B.1).

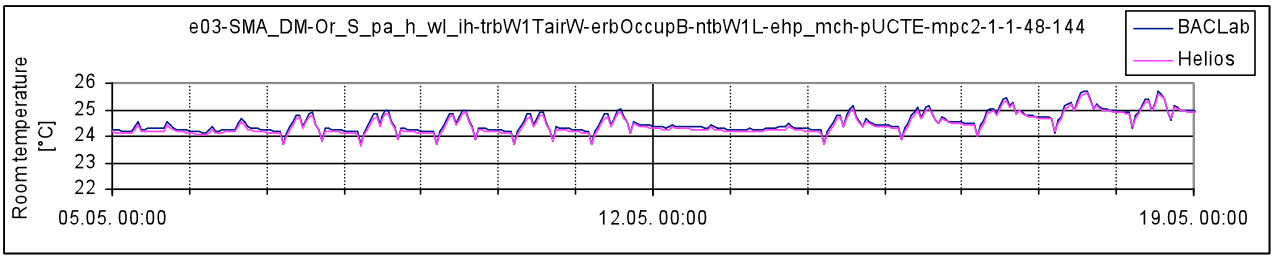

Figure 5.3: Validation of room temperature by comparison with the HELIOS model.

Error analysis for natural ventilation (which is crucial in terms of modeling) showed only small deviations in transferred cooling energy even if the temporal ventilation pattern in part differed significantly from achievable air change rates in reality.

Consistency of the numerous and interdependent parameters of site, building and HVAC model was assured by thorough cross check of the inputs and the generation of the parameter sets through an automated procedure (BuSy Server/OCBDB).

5.6 Conclusions

A bilinear dynamical model for a single building zone has been newly developed. The model is based on a detailed multi-node RC network. It is suitable to simulate the building zone's dynamical behavior, in particular the joint dynamics of room temperature, illumination and CO_2-concentration. The model also supports several technical systems typically present in modern office buildings.

In order to achieve an acceptable computational performance a reduction of complexity and some bilinear approximations had to be made. Based on experience and validation exercises it has been shown that the model nevertheless delivers accurate and reliable results.

Thanks to its computational efficiency and bilinear structure the newly derived model is suitable as a plant system model for large-scale simulation studies and in particular also as a controller model for Model Predictive Control.

5.7 References

[1] EN 15603:2009: Energy performance of buildings – Overall energy use and definition of energy ratings

[2] EN 13790:2009: Energy perfomance of buildings – Calculation of energy use for space heating and cooling

[3] SIA 382/1 (2007): Lüftungs- und Klimaanlagen – Allgemeine Grundlagen und Anforderungen

[4] SIA 2023 (2004): Lüftung in Wohnbauten, Anhang C (Fensterlüftung)

[5] M. Koschenz, B. Lehmann: Thermoaktive Bauteilsysteme tabs, Empa Dübendorf, 2000

[6] J. Tödtli et al: TABS- Control, Steuerung und Regelung von thermoaktiven Bauteilsystemen. Faktor Verlag Zurich (Switzerland); 2009. ISBN: 978-3-905711-05-9

[7] M. Bauer, J. Geiginger, W. Hegetschweiler et al: Delta: A Blind Controller using Fuzzy Logic, Swiss Federal Institute of Technology Lausanne, 1996

Chapter 6

LOCAL WEATHER FORECASTS AND OBSERVATIONS

by Vanessa Stauch, Francis Schubiger and Philippe Steiner

Cite as:

Stauch, V., Schubiger, F. & Steiner, P. (2010). Local weather forecasts and observations. In: Gyalistras, D. & Gwerder, M. (eds.): *Use of weather and occupancy forecasts for optimal building climate control (OptiControl): Two years progress report*. Terrestrial Systems Ecology ETH Zurich, Switzerland and Building Technologies Division, Siemens Switzerland Ltd., Zug, Switzerland, pp 67–78. ISBN 978-3-909386-37-6.

6.1 Introduction

A benefit from the use of weather forecasts in building automation applications may be taken for granted by an interested user of building climate control solutions. However, as will be shown in this report, its ultimate value is highly dependent on the nature of the building, the building automation system, the ambient weather and climate, and the control strategy applied.

One prerequisite common to all predictive control applications is a high quality local weather forecast, particularly of the outside air temperature, the incoming solar radiation and some measure of humidity as an indicator of the intrinsic energy potential in the surrounding air. Therefore, the main focus of this chapter is devoted to providing the best available local predictions of the weather variables in question.

Numerical weather prediction (NWP) models are particularly appealing for this application as they can deliver regularly updated time series of near surface weather variables. High performance computers solve fundamental nonlinear partial differential equations describing the dynamic of the atmosphere numerically on a finite three-dimensional grid with a certain spatial and temporal resolution. Typical sub-grid scale processes such as convection or turbulence need to be represented by suitable parameterizations being inevitably simplifications of the underlying physics. Limited area models nested within global NWP models allow for increasing the spatial resolution and hence the finer simulation of the atmospheric evolution and its interaction with the earths' surface. However, small scale processes that are triggered and controlled by certain local conditions might still not be represented sufficiently on the model grid or by the implemented parameterizations. In addition, each grid point of the model is to be interpreted as the spatial average over the entire grid cell. As a result, the comparison of surface point measurements with model predictions at a neighboring grid point may reveal undesired discrepancies that, depending on the requirements of the application, may possibly compromise the use of NWP models for local weather predictions.

One way to further improve local numerical predictions is based on modeling the difference between the predicted values at one (or more) suitable grid point of the model grid and the local measurements *a posteriori* (e.g. Glahn & Lowry 1972). For this, past model forecasts and observations are analyzed statistically in order to identify an appropriate error model that can be used to correct the future predictions. Most of these post-processing approaches use regression techniques in the widest sense and they mainly differ in the complexity of the respect models, and in the extend of the underlying database used for identification and calibration. Here, we will make use of a linear error model that will be updated recursively as soon as new observations become available (Persson 1989, Cattani 1994). This approach based on a linear Kalman filter has been successfully implemented at MeteoSwiss several years ago and has been permanently extended and improved in the course of the OptiControl project.

In the following sections, we present the NWP model COSMO that operationally computes weather forecasts for Switzerland and a large part of Europe. We have selected ten case study sites that serve as climatological representations of typical European areas of high population densities that are particularly interesting for office buildings with indoor climate control. Several years of meteorological observations and corresponding COSMO predictions furnish the database compiled for a large simulation study to investigate the use of weather forecasts in building climate control. A second part of this chapter is devoted to the statistical post-processing method and its beneficial effect on the performance of the weather predictions.

6.2 The Numerical Weather Prediction Model COSMO

Highly resolved limited area NWP models are seen to be the superior choice for the prediction of near surface local weather variables in particular in complex topography. MeteoSwiss runs a pair of NWP models COSMO (COnsortium of Small scale Modelling, www.cosmo-model.org) that is driven by the global NWP model IFS (Integrated Forecasting System) of the European Centre of Medium Range Weather Forecasting (ECMWF). The current setup includes two models with a horizontal grid size of 6.6 km (COSMO-7) and of 2.2 km (COSMO-2) and 60 vertical levels describing the atmospheric states and their temporal evolution. The respect subdomains of the two COSMO models are shown in Figure 6.1. Several sub-models and parameterization schemes describing turbulence, cloud formation, moist convection, radiation and soil-to-surface interactions complement the numerical core of the model. The derivation of near surface weather parameters such as temperature in 2m height or wind speed in 10m height above ground is based on interpolation algorithms between the lowest atmospheric level and the surface (for further information on the COSMO model see Steppeler et al. 2003 and the documentation on www.cosmo-model.org). The sub-models and parameterization schemes are subject to constant further developments and improvements. For instance, the 2m temperature diagnostic has been substantially improved and implemented in June 2008 (Buzzi 2008).

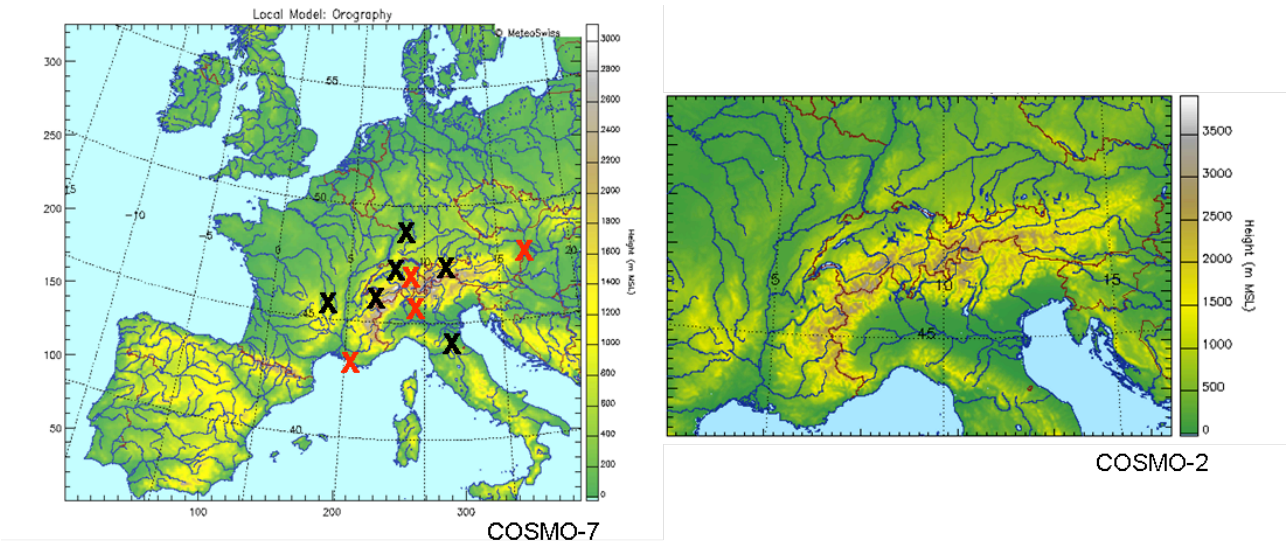

Figure 6.1: Subdomains of the two deterministic COSMO models (COSMO-7 on the left, COSMO-2 on the right) run operationally by MeteoSwiss. The boundary conditions for the COSMO-7 forecasts are provided by the global NWP model Integrated Forecasting System (IFS) of the European Centre for Medium Range Weather Forecasting (ECMWF) in Reading, UK. The crosses on the left indicate the location of the selected case study sites for the OptiControl project (see later).

COSMO-7 is issued twice a day at 00UTC and at 12UTC and runs integrations for 72 hours into the future. Simultaneously, atmospheric and soil surface observations are permanently assimilated in order to somewhat synchronize model states with observed states. Every three hours, a 24-hour forecast is issued with COSMO-2 that is nested within the COSMO-7 grid. All model forecasts are computed on high performance computer at the Swiss National Supercomputing Centre at Manno, Switzerland (www.cscs.ch). For a particular local forecast, a special algorithm identifies the best suited model grid point within a certain search radius around the station in question. In brief, the height difference between measurement site and model topography is given the highest weight followed by the spatial distance.

In addition to the two deterministic COSMO schemes operated by MeteoSwiss, the COSMO consortium also runs a limited area ensemble prediction system (COSMO-LEPS, Marsigli et al. 2005). The objective of global ensemble prediction systems is to account for the uncertainties in our knowledge about the true states of the atmosphere and errors in NWP model formulations by running a forecast model with varying initial conditions and perturbed physics. The resulting ensemble provides a measure for the predictability of the future weather evolution given our limited knowledge and allows for a probabilistic approach to weather forecasts. COSMO-LEPS as a high resolution counterpart (horizontal grid mesh of 10km) is nested within the IFS ensemble and therefore combines the probabilistic approach and high resolution NWP. As will be discussed later, probabilistic COSMO-LEPS products particularly of global radiation forecasts might provide an appealing alternative to deterministic forecasts for the OptiControl application.

6.3 Data Description

For the various simulation studies performed in this project, local forecasts and observations of the relevant weather variables were required for a number of locations that can be seen to represent the climate conditions in Switzerland and the European subdomain covered by the COSMO models.

6.3.1 Selected Case Study Sites & Observation Data

In addition to the overall aim to represent the European climate, the choice of the case study sites mainly depended on the availability of high quality long-term hourly observations of the most important weather variables for building control applications. Also, sites being located well within the COSMO-7 and COSMO-2 domain have been preferably chosen. Given these requirements and recommendations of the National Weather Services in charge, ten meteorological measurement sites in five different European countries have been selected for OptiControl investigations (Table 6.1, see black and red crosses in Figure 6.1 for their geographical distribution).

Country	Site Name	Site abbrev.	Weather & Climate	Height (masl)
Switzerland	**Zürich-Fluntern**	**SMA**	**Swiss plateau climate with characteristic inversion conditions**	**556**
	Genève-Cointrin	GVE	typical Swiss station for inflow conditions from south-west	420
	Basel-Binningen	BAS	representative for the climate north of the Jura mountains	316
	Lugano	**LUG**	**representative for the Swiss climate south of the Alps**	**273**
France	**Marseille-Marignane**	**MSM**	**Mediterranean climate with total inflow from the Mediterranean Sea**	**5**
	Clermont-Ferrand	CLF	Typical station with high precipitation in autumn	330
Germany	Mannheim	MHM	Transition zone between maritime and continental climate	96
	Hohenpeissen-berg	HPB	Typical mountainous temperate climate, above the inversion layer	989
Austria	**Wien Hohe Warte**	**WHW**	**Austrian plain with continental climate**	**209**
Italy	Modena	MOD	typical for the Po plain, persistent inversion conditions in autumn and winter	77

Table 6.1: Overview of the case study sites selected for the simulation study in OptiControl along with a short description of the ambient weather and climate and their geographical heights. Selected sites for the buildings simulations (see later) in bold.

Figure 6.2 shows the seasonal climate characteristics of the ten case study sites as temperature-radiation diagrams compared to long-term seasonal means at 17 European capital cities (Meteonorm, version 6.0.2.4). The range of possible European temperature-radiation relations is largely covered by the case study sites missing only the area of cold temperatures and low radiation input. However, the associated cities are located outside the COSMO domains (capitals of Scandinavian countries and Moscow) and therefore cannot be included in this study. For this report, again four representative sites (Zurich, Lugano, Marseille, Vienna, see also red crosses in Figure 6.1 and bold sites in Table 6.1) from the 10 presented locations were selected (green markers in Fig 6.2) in order to accomplish the numerous aspects of the control problem under investigation.

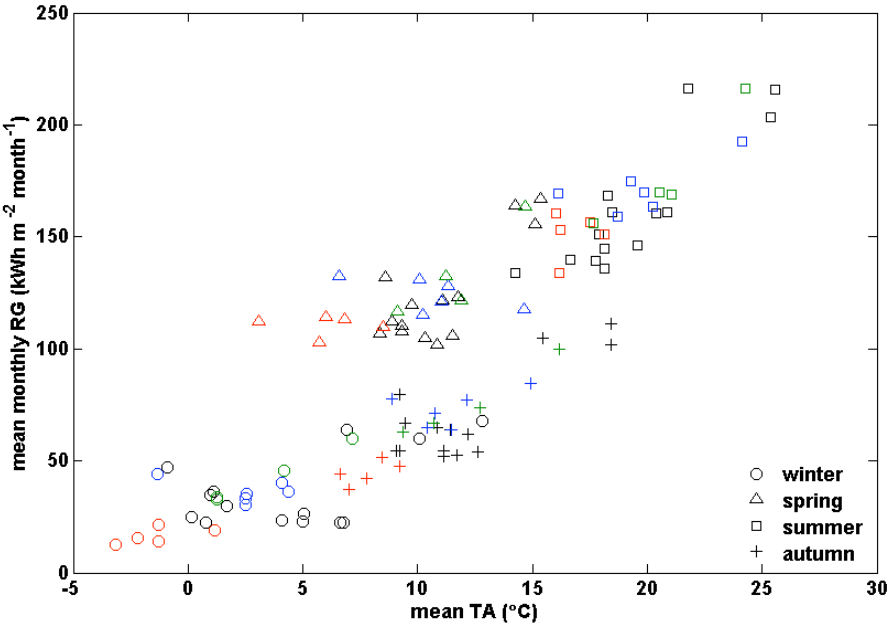

Figure 6.2: Pairs of seasonal mean temperature and seasonal mean global radiation for the selected case study sites (blue and green markers) compared to long-term averaged values of 17 capital cities of Europe (black and red markers). Green markers highlight the climate of the four sites out of the 10 OptiControl sites selected for the building control simulations. Red markers denote locations outside the COSMO-7 domain. European capitals shown: Amsterdam, Berlin, Bern, Brussels, Dublin, Helsinki, Copenhagen, Lisbon, Ljubljana, London, Madrid, Oslo, Rome, Sarajevo, Stockholm, Warsaw, Vienna.

6.3.2 Derived Weather Variables & Design Reference Years

The radiation budget and its impact on the indoor climate of buildings are particularly sensitive to the orientation of the windows in the building. Therefore, radiation conversion models have been applied to the observations as well as the COSMO models' forecasts that first disaggregate the global radiation into a direct and a diffuse component (Perez et al. 1992) and second that derive the incident radiation on vertical surfaces with orientation (Perez et al. 1987, Zelenka 1988).

For the potential assessment of the predictive building climate control, representative annual data sets of the weather variables of interest and case study sites (design reference year, DRY) have been provided. Their compilations follow the standards of the SIA Merkblatt 2028 (2008) that has been particularly designed for building physics, energy and building technology.

6.3.3 Database for OptiControl

An OptiControl Weather and occupancy DataBase (OCWDB) has been developed in order to facilitate an automatic and targeted access to the data required for the specific simulation in question. It contains all available hourly observation datasets as well as COSMO-7 predictions for the relevant weather variables, for the years 2006 and 2007 and all sites. For the COSMO-7 predictions, the direct model output (prior to any statistical correction) and results of several correction algorithms are stored in order to be in the position to analyze the sensitivity of the control solution to variations in the weather predictions' accuracy (see Stauch et al. 2008). In total, 474 data files in the OCWDB version 1.7 (release date, 09.02.2009) were made available for building control simulations.

6.4 Local forecast correction

Statistical adaptation of NWP model outputs to local conditions of a location of interest has been successfully established in the meteorological community as an efficient top down solution to model the systematic differences between model predictions, Z_{DMO} and observations, Z_{OBS} (termed forecast error in the following). Given the various sources and complex composition of these forecast errors, flexible post processing methods are required that constantly adapt to new conditions. To accommodate this, a recursive estimation procedure is applied using a suitable linear error model and a Kalman filter (Kalman 1960) to update the coefficients dynamically once new observations become available. While the forecast error of temperature predictions has been intensely studied in the past, local radiation forecasts have experienced less attention. Therefore, we will first focus on the characterization of the different forecast errors and then discuss their improvement of statistical post-processing.

6.4.1 State-space formulation for forecast correction

The correction model applied here assumes a forecast error, $err_Z = Z_{DMO} - Z_{OBS}$, that is linearly dependent on the predicted variable, Z_{DMO}, itself. The linear coefficients, $x_i(t)$, are assumed to evolve with time following a random walk process:

$$\hat{err}_Z(t) = x_1(t) + x_2(t) \cdot Z_{DMO}(t) + \eta_Z(t) \text{ with } \eta_Z(t) \sim N(0, R(t)), \qquad [1]$$

$$x_i(t+1) = x_i(t) + \xi_i(t) \text{ with } \xi_i(t) \sim N(0, Q(t)). \qquad [2]$$

[1] and [2] are the observation equation and the system equation of the implemented Kalman filter and $\eta_Z(t)$ and $\xi_i(t)$ are the zero mean serially uncorrelated observation and system noise with the time dependent variances $R(t)$ and $Q(t)$ to account for changes in err_Z and the resulting dynamics of the changes in the coefficients x_i. The temporal evolution of the observation variance R predominantly originated by the changing error structure depending on the current weather situation is integrated within the prediction-correction algorithm proposed by Smith (1967). This adaptation is mapped onto Q via a fixed noise variance ratio, NVR, that has been optimized for each variable over the entire year in order to avoid filter divergence.

$$NVR = \left(\frac{Q(t)}{R(t)} \right)$$

The latest update of model [1] and [2] is then used to predict the expected error for the entire forecast horizon (72 hours for COSMO-7), i.e. the coefficients x_i are held constant for the prediction. Obviously, this assumption becomes less likely to be true with lead time. The COSMO-7 forecast correction implemented here includes 24 separate daily prediction-correction schemes for each weather variable to account for the pronounced daily cycle of the errors. This way, each hourly prediction step is taken only three times in order to make a robust 72-hour weather forecast correction.

6.4.2 Forecast evaluation and discussion

This forecast error correction has been applied to all available data sets and weather variables in the database. However, its effect on the forecast performance will be different for the air temperature and wetbulb temperature on the one hand and for the radiation variables on the other hand, due to their very different error characteristics. While the temperature forecasts are mainly biased with a reasonably small variability (the magnitude of the standard deviation of the error is very similar to the bias), the radiation forecast errors are particularly characterized by a high variability and a comparably small systematic component.

Figure 6.3 illustrates the two forecast error structures for three-days ahead predictions with a subsample of the Zurich data for 2007. The forecast correction has - by design - the largest positive effect on biased forecasts. As a result, the temperature predictions are substantially improved after the correction leading to unbiased forecasts even with a slightly reduced variability. In contrast, although the correction on the radiation components again reduces the bias in the prediction, the effect is somewhat blurred by the large variability of the error. For comparison, a persistence forecast is also shown as it will be used later in the simulation studies. The variability of the persistence errors increases more with forecast time than the NWP predictions as expected.

To elaborate the impact of the correction on the DMO for all selected locations, Figure 6.4 shows the relationship between the seasonal bias and the standard deviation of the errors for all available predictions averaged over the first 24 hours (all sites, variables, years) before (left panels) and after the correction (right panels). As expected, the correction affects most notably the bias while the standard deviation remains nearly unchanged. The figure also illustrates a major difference in the error characteristics of the temperature variables compared to the radiation components (two left panels). The magnitudes of the standard deviation and the bias for the temperature variables are very similar whereas the standard deviations to bias ratios of the radiation components range to up to 100.

The overall effect of the correction on the forecast performance for the first 24 hours is discussed by means of the improvement expressed by the relative differences in the root mean square errors ($\Delta RMSE$) of the direct model output forecasts and the corrected forecasts. This normalization allows to intercomparing the different variables. The *RMSE* for a certain variable evaluates both, the bias and the variability of the prediction error. For an unbiased forecast, *RMSE* equals the standard deviation of the error.

$$RMSE_Z = \sqrt{\frac{\sum_{i=1}^{n} \left(Z_{MOD,i} - Z_{OBS,i}\right)^2}{n}},$$

with the subscript 'MOD' being either *DMO* or the correction, *KF1*. The $\Delta RMSE$ for the evaluation of the post-processing scheme is then calculated as follows,

$$\Delta RMSE = \frac{RMSE_{DMO} - RMSE_{KF1}}{RMSE_{DMO}} \cdot 100\%.$$

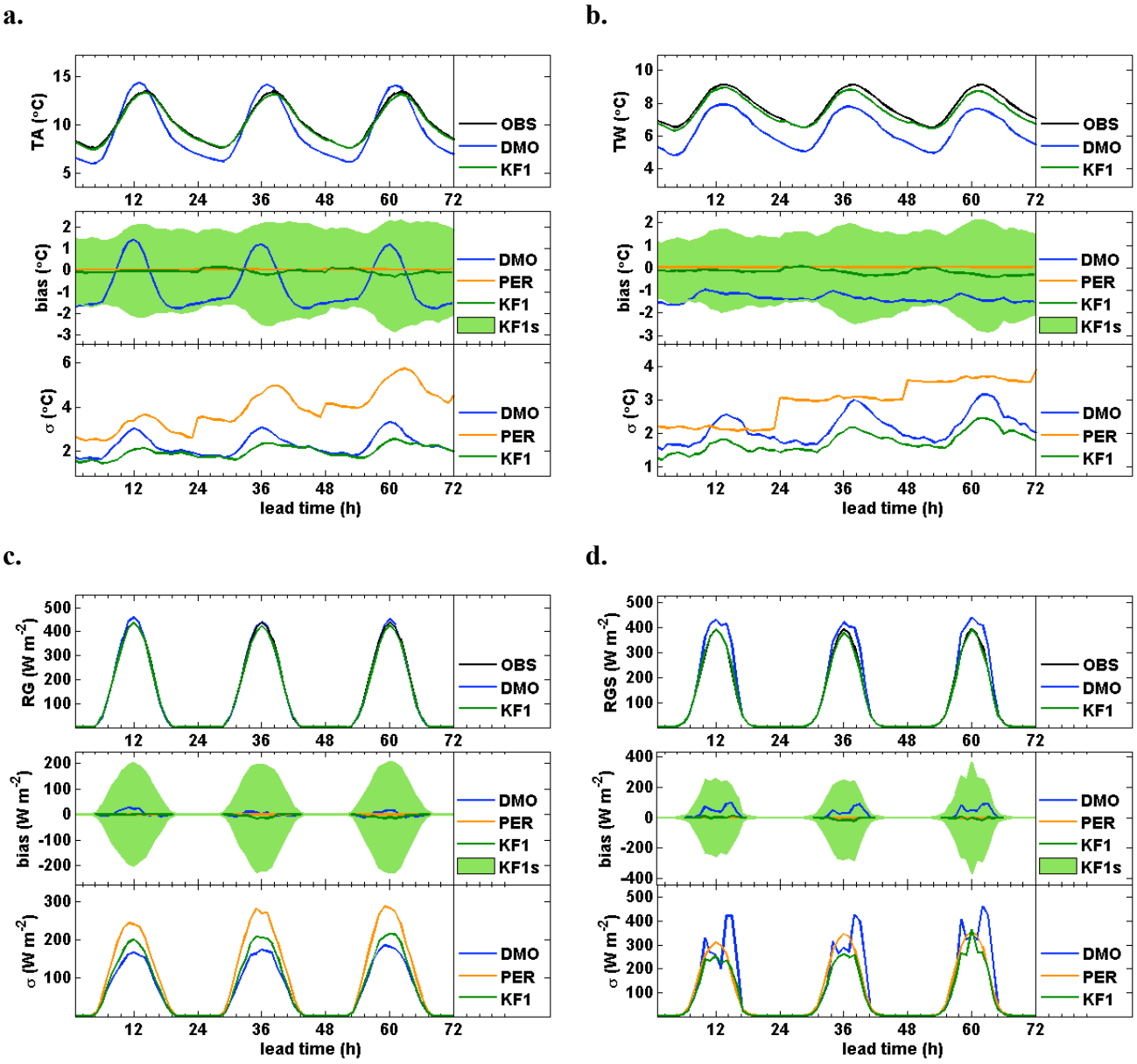

Figure 6.3 Summary verification results for the four weather variables temperature, TA (a.), wetbulb temperature, TW (b.), global radiation, RG (c.), global radiation south orientation, RGS (d.) for the entire year 2007 at Zurich. OBS are the mean observations, DMO is the direct COSMO-7 model output, PER shows the persistence forecast taking the latest measurements available and project them into the future, KF1 is the Kalman filter correction and KF1s is the standard deviation of the forecast error of KF1. σ in the bottom panels denotes the standard deviation of the forecast error.

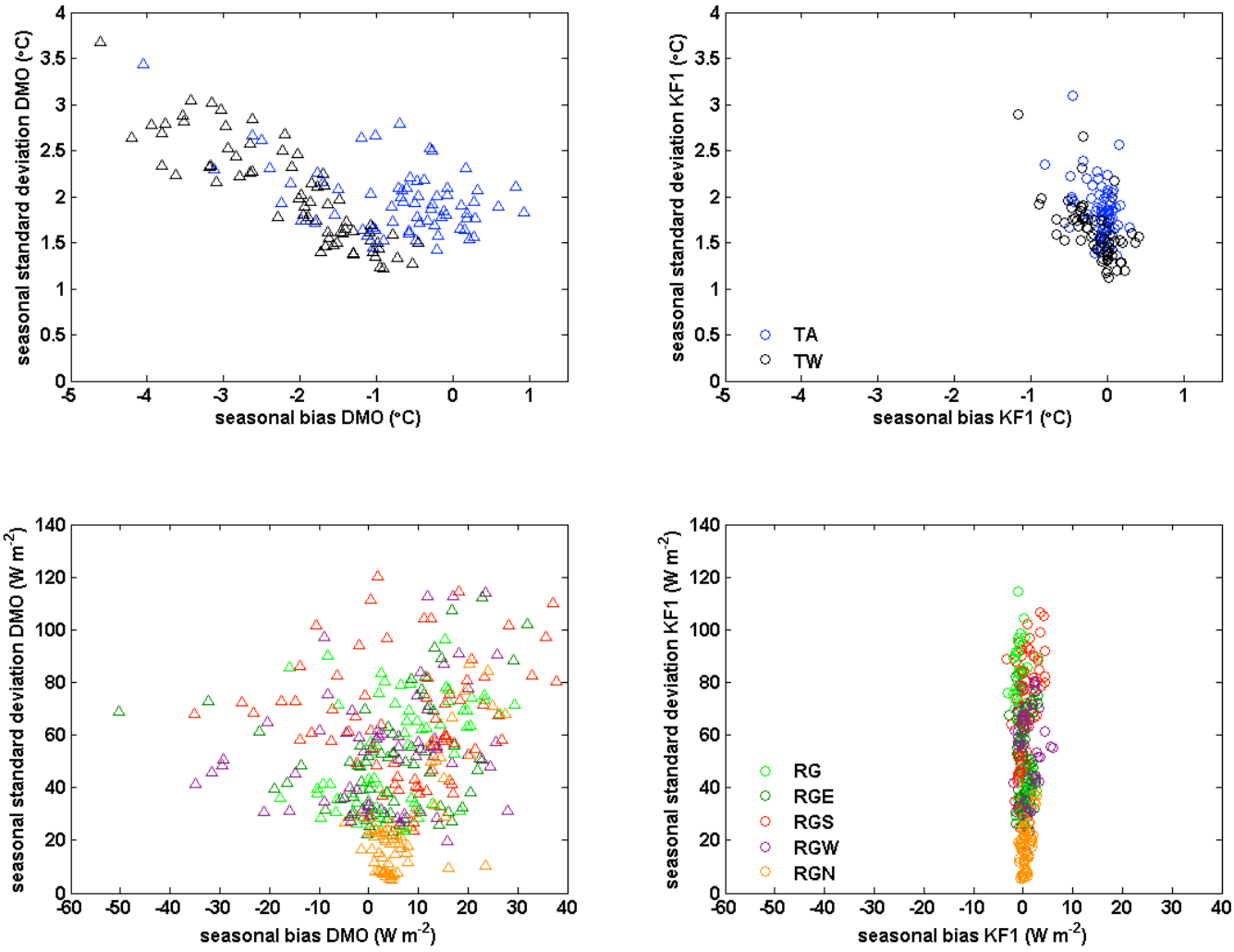

Figure 6.4 Summary verification results for all seasons, sites and years available for the air temperature and wetbulb temperature (top panels) and all radiation components (bottom panels) for the first 24 hours of predictions. Shown is the relationship between the mean absolute bias and the mean standard deviation of the error (predictions – observations) for the direct model output (DMO, left panels) and after correction (KF1, right panels). The color code for DMO is the same as for KF1. TA, 2m temperature; TW, wetbulb temperature; RG, global radiation; RGE, global radiation east orientation; RGS, global radiation south orientation; RGW, global radiation west orientation; RGN, global radiation north orientation.

As the controllers' actions are derived from the optimization of a temporally integrated cost function, the quality of the weather forecasts integrated over the entire prediction horizon used for this optimization is also investigated. For this, temperature variables are averaged and radiation variables are summed over the first 24 hours. Figure 6.5 compares the distribution of $\Delta RMSE$ values of all sites and seasons of 2007 for the different weather variables. Not surprisingly, the effect of the correction is different for the variables of interest being highest for air and wetbulb temperature (*TA*: 20-30%, *TW*: 35-45%). Given the correction algorithm removes the systematic biases, negative values of the $\Delta RMSE$ indicate that this correction has been done at the cost of an increased variability. The effect of the correction highly varies with season and site. The global radiation with north orientation shows the largest benefit from the correction because the standard deviation of the fore-

cast error prior to the correction is already small. On the contrary, the mean effect of the correction on the radiation with south orientation is even negative. The differences in the relative improvements between hourly and daily averaged data are small. However, the daily forecast performance improvement is derived from hourly values and only reflects the effect of averaging/summation. Further improvement should be achieved if a correction is applied directly on the daily values.

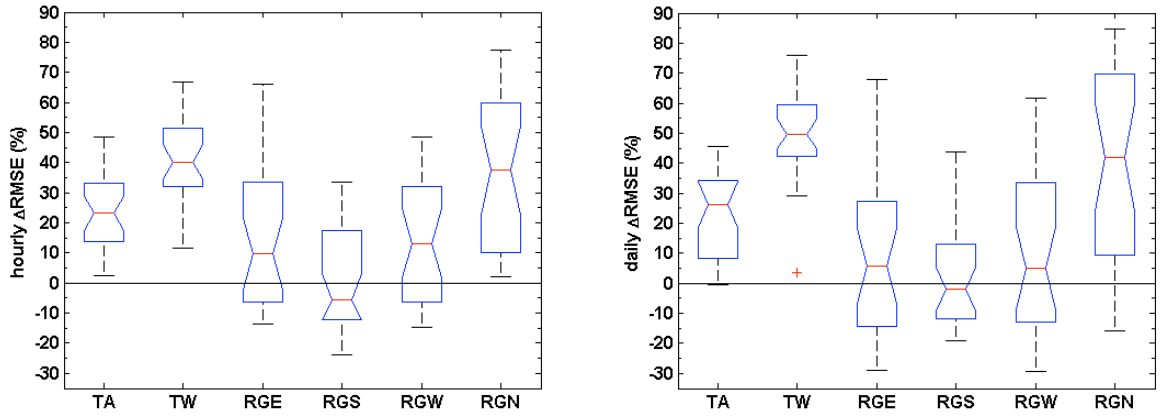

Figure 6.5: Distribution of the relative improvement of KF1 correction over the direct model output for all weather variables based on hourly data (left panel) and daily integrated data (right panel). Shown are the ΔRMSE values for all seasons and sites in 2007. TA, 2m air temperature; TW, 2m wetbulb temperature; RGE, global radiation east orientation; RGS, global radiation south orientation; RGW, global radiation west orientation; RGN, global radiation north orientation.

Interestingly, the distribution of the $\Delta RMSE$ is highly stratified by season. Figure 6.6 reveals that the correction for summer and winter has negative effects on the radiation components and large positive effects in spring and autumn. This result might suggest that the assumption of a fixed noise variance ratio (*NVR*) does not apply to the filter problem at hand. Instead, further investigation is focused on how to better constrain the estimation with non-constant *NVR*s.

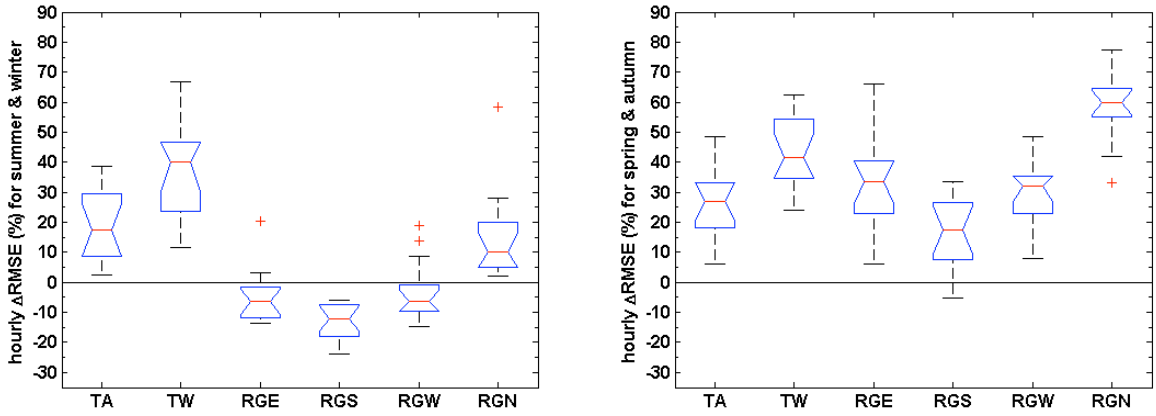

Figure 6.6: Distribution of the relative improvement of KF1 correction over the direct model output for all weather variables in summer and winter (left panel) and in spring and autumn (right panel).

The high variability in the radiation forecasts will very likely cause problems for the predictive control of indoor building climate. One possibility to handle this might offer the use of COSMO-LEPS predictions with their instantaneous probabilistic information. On the other hand, if forecasts with only a short prediction horizon are required (system variants 1 and 2 in particular), the building simulations might benefit from the 3hour update cycle and the higher horizontal resolution of the COSMO-2 model. A study for air temperature forecasts showed that the local predictions could be further improved by more than 5% for 60 Swiss locations.

6.5 Conclusions

The performance of COSMO-7 predictions is dependent on site, season, weather situation and weather variable in question. The forecast error can be divided into a systematic component (bias) and a random component (uncertainty). We have shown that the systematic errors in the COSMO-7 predictions can be successfully removed on a seasonal basis by the application of an appropriate statistical post-processing procedure.

The weather variables of interest as well as the associated COSMO-7 forecast errors have very different statistical properties. While the temperature and wetbulb temperature evolve relatively smoothly in space and time on an hourly basis, the radiation variables are characterized by a particularly pronounced temporal and spatial variability. This variability is originated from the naturally high variability of cloud cover and their formation and distribution within the vertical atmospheric layers above the surface. Therefore, overall improvements of the DMO are largest for the temperature predictions (~20-30%) and wetbulb temperature predictions (~35-45%) for the first 24 hours of the prediction. On the contrary, the success of the statistical correction of the radiation components as it is implemented to date is highly dependent on the season. Improvements range between 10 and 60% for spring and autumn and are even negative (~ -10%) in winter and summer. This discrepancy might originate from a constant noise variance ratio assumed for the Kalman filter and could be tackled with a seasonally varying *NVR* currently under investigation.

From these results, we have composed a database containing local observations and best available weather predictions as input for a comprehensive simulation study that evaluates the potential benefit of using weather forecasts in predictive control of indoor building climate. Further investigations will analyze the potential of the high resolution COSMO-2 predictions with a three hourly update on the one hand, and the possible advantages of the probabilistic information in COSMO-LEPS on the other hand at the cost of the spatial resolution.

6.6 References

[1] Steppeler, J., G. Doms, U. Schättler, H. Bitzer, A. Gassmann, U. Damrath, and G. Gregoric (2003) *Meso-gamma scale forecasts using the non-hydrostatic model LM*. Meteorology and Atmospheric Physics, 82, 75-96.

[2] Glahn HR, Lowry DA (1972) The use of model output statistics (MOS) in objective weather forecasting. Journal of applied Meteorology, 11, 1203-1211.

[3] Persson AO (1989) Kalman filtering, a new approach to adaptive statistical interpretation of numerical meteorological forecasts. ECMWF Newsletter no 46, 16-20.

[4] Cattani D (1994) Application d'un filtre de Kalman pour adapter les températures à 2 mètres fournies par le modèle ECMWF aux stations météorologiques de la Suisse. Rapports de travail de l'Institut Suisse de Météorologie, no 175.

[5] Stauch V, Gwerder M, Gyalistras D., Schubiger F. (2008). Statistical adaptation of mesoscale numerical weather forecasts for designing predictive control of indoor building climates. Proc. 8th Annual Meeting of the EMS and 7th European Conference on Applied Climatology, 29 September - 3 October 2008, Amsterdam, The Netherlands, Vol. 5, EMS2008-A-00545

[6] Merkblatt SIA 2028 *Klimadaten für Bauphysik, Energie- und Gebäudetechnik* (2008)

[7] Buzzi, M., 2008, *Challenges in Operational Numerical Weather Prediction at High Resolution in Complex Terrain*, Ph. D. thesis, Swiss Federal Institute of Technology (ETH).

[8] Marsigli, C., F. Boccanera, A. Montani, and T. Paccagnella (2005) *The COSMO-LEPS mesoscale ensemble system: validation of the methodology and verification*. Nonlinear Processes in Geophysics, 12, 527-536.

[9] Meteonorm, Version 6.0.2.4, METEOTEST, Fabrikstrasse 14, CH-3012 Bern.

[10] Smith GL (1967) *Sequential estimation of observation error variances in a trajectory estimation problem.* AIAA Journal, Vol 5 (11), 1964-1970.

[11] Kalman RE (1960) *A New Approach to Linear Filtering and Prediction Problems*, Transactions of the ASME–Journal of Basic Engineering, Vol 82.

[12] Perez R, Ineichen P, Maxwell E, Seals R, Zelenka A (1992) Synamic global to direct conversion models. ASHRAE transactions, Research Series 1992, 354-369.

[13] Zelenka A (1988) Asymmetrical analytically weighted R_b factors. Solar energy, 41, 405-415

[14] Perez R, Seals P, Ineuche P, Steward R, Menicucci D (1987) A new simplfied version of the Perez diffuse irradiance model for tilted surfaces, description, performance validation. Solar Energy 39, 221-231.

6.7 Acknowledgements

Meteorological observations have been provided by various national weather services. We are particularly grateful to:

- French Weather Service (MeteoFrance) for providing us with the observations at the measurement sites Marseille-Marignane and Clermont-Ferrand
- German Weather Service (DWD) for providing us with the observations at the measurement sites Mannheim and Hohenpeissenberg
- Austrian Weather Service (ZAMG) for providing us with the observations at the measurement site Wien Hohe Warte
- Italian Weather Service for Emilia-Romagna (ARPA-SIM) for providing us with the observations at the measurement site Modena

Chapter 7

PERFORMANCE BOUNDS AND POTENTIAL ASSESSMENT

by Dimitrios Gyalistras, Beat Lehmann, Katharina Wirth,
Markus Gwerder, Frauke Oldewurtel and Vanessa Stauch

Cite as:

Gyalistras, D., Lehmann, B., Wirth, K., Gwerder, M., Oldewurtel, F. & Stauch, V. (2010). Performance bounds and potential assessment. In: Gyalistras, D. & Gwerder, M. (eds.): *Use of weather and occupancy forecasts for optimal building climate control (OptiControl): Two years progress report*. Terrestrial Systems Ecology ETH Zurich, Switzerland and Building Technologies Division, Siemens Switzerland Ltd., Zug, Switzerland, pp 79–106. ISBN 978-3-909386-37-6.

7.1 Introduction

The present Chapter pursues two interrelated goals:

The first goal is to assess the sensitivity of control costs for Integrated Room Automation (IRA) to the following variations in the boundary conditions for control:

(1) the choice of the building system and of the optimization target (money vs. energy);

(2) the introduction of night/weekend set-backs (a reduction of the thermal comfort when the building is not used);

(3) a widening of the thermal comfort range width (a general reduction of thermal comfort); and

(4) the introduction of CO_2-controlled ventilation (use of CO_2-sensors).

The decisions (1) are typically taken by architects and HVAC designers at an early building design phase. We do this investigation because to our knowledge not much work has been published on this issue so far. The variations (2)–(4) correspond to advanced control functionalities that are of interest because they can contribute to reducing building energy demand at relatively low investment cost; this is because they do not require major construction work, or any major retrofitting or changes in the installed energy systems.

The effects (1)-(4) are studied with the aid of Performance Bound calculations (PB, Section 4.4). By relying on the PB we ensure that any found differences in the control costs (energy or money) reflect but the effect of the prescribed variations in the boundary conditions and are not distorted by the shortcomings of a particular control algorithm.

The second goal is to explore the theoretical energy savings potentials of the rule-based, non-predictive control algorithms RBC-1 to RBC-4 (Chapter 3), and to compare them to the energy savings obtained from (1)–(4).

The savings potentials are determined based on the approach outlined earlier (Section 1.4): first the Performance Bound (PB) is calculated as an absolute benchmark, and then the control costs as obtained from a given RBC algorithm are compared to the PB. The difference to the PB presents a theoretical number that indicates the savings that could be achieved if that algorithm were replaced with optimal control and perfect disturbance predictions.

Initial studies indicated that the absolute and comparative performance of control algorithms varied drastically with several factors such as the building standard, construction type, location etc. To deal with this issue we conducted a large-scale factorial simulation study that investigated a large number of building cases.

A second problem was that the quality of control can not be readily assessed by the cost criterion alone since a given algorithm may save costs at the expense of comfort. Therefore, selected thermal (dis)comfort statistics were also considered.

In Section 7.2 we first describe the design, set-up, and analysis of our simulations. Section 7.3 provides: (i) the PB simulation results from investigations (1)-(4); (ii) the performance of the four RBC algorithms as compared to the PB and with each other; and (iii) an overall comparison of the results from (i) and (ii). Our findings are discussed in Section 7.4. Our conclusions are given in Section 7.5.

7.2 Material & Methods

7.2.1 Overview

For our study we considered a large number of individual simulation runs that differed systematically in one or several "factors" (or key assumptions) from each other, as explained later. Each simulation run was done for the length of one year.

The simulated plant model (a model of the building plus its heating, cooling, ventilation etc. subsystems) was the continuous-time, bilinear model described earlier in Chapters 4 and 5. The model was transformed to a discrete time model using a sampling time of 1 h. This was also the time step used for computation of the control inputs, the updating of the model's state, and the monitoring of the simulation results.

In the PB simulations the plant model was driven with control inputs that were determined from a Model Predictive Control (MPC) procedure (see below). In all other simulations the control inputs were derived by a low-level control algorithm that was based on the modes delivered by one of the rule-based controllers RBC-1 to RBC-4 (see Chapter 3).

Below we first provide details on the procedure used to estimate the PB. Then we proceed with the description of the simulation experiments, analysis procedure, and used software.

7.2.2 Performance Bound Estimation

By definition, for the estimation of the PB it was assumed that the plant's dynamical behavior is perfectly known, i.e. the model used for MPC was identical to the model that was used to simulate the plant behavior. The same also applied to the used weather and internal gains predictions – the used predictions at any given point in time were identical to the data that was used to drive the plant model in the time steps ahead.

The standard application of MPC employs a receding horizon procedure (see Chapter 3). In our case this would have involved 8760 optimizations (one per hour of the year). Moreover, in order to account for the availability of perfect knowledge on the future weather and internal gains, each such optimization would have needed to consider a "sufficiently" long prediction horizon of length T_H.

Since this procedure is computationally very expensive an alternative approach was considered that exploits the fact that in the PB simulations the plant model and the plant system's state at begin of each optimization step are also perfectly known. This makes it in principle possible to determine the optimal sequence of control inputs and the associated system states all at once, by solving a single optimization problem over a prediction horizon T_H = 8760 hours.

Unfortunately, this approach proved impractical due to the presence of the bilinearities in the model used for MPC. The bilinearities make it necessary that the optimal solution is determined by means of an iterative procedure (see Chapter 4.5), and for the "single optimization" approach the iteration procedure was found to converge only very slowly. As a result, the original gain in efficiency was jeopardized by the need to solve a large number of very large (entire year) optimization problems.

Therefore the following intermediate solution was adopted: the MPC algorithm was run once every T_{OL} = 48 h (2 d), with a prediction horizon of T_H = 144 h (6 d). The subscript "OL" stands for "open loop" and this refers to the fact that the control inputs during the 48 hours following an optimization were precisely the ones delivered by this optimization, i.e. during these 48 hours the control inputs were directly applied to the plant model without any feedback to the controller.

The numerical values for T_{OL} and T_H were chosen according to the following procedure: First, we performed PB simulations for a large number of building cases using a receding horizon strategy with T_H = 6, 12, …72 h. Then the annual total Non-Renewable Primary Energy (NRPE) usage was evaluated as a function of T_H. It was found that – even for the most extreme cases – an increase in T_H beyond 60–70 h did not affect the NRPE value by more than 1% (some of these results are reported in [1]). From this investigation it was concluded that when using $T_H > T_{Hmin}$ = 72 h (3 d) the optimal control inputs for the first $T_{OL} = T_H - T_{Hmin}$ time steps can be used without the need to conduct a new optimization within that time interval.

However, the simulated cases that were used to obtain this result did not assume the presence of night/weekend set-backs. Allowance for weekend set-backs introduces a strong change in the constraints for the room temperature for a duration of 48 h (2 d). To account for this effect we finally chose T_H = 144 h (6 d) and increased T_{Hmin} to 96 h (4 d), i.e. T_{OL} = 48 h (2 d).

The iterative procedure for solving the bilinear optimization problem was terminated when the following condition was met: $(MAX(X_i - X_{i-1}) \leq 0.1$ ºC) OR $(|(c_i - c_{i-1})/c_{i-1}| \leq 1.0e^{-3})$, $i > 1$. Here, i denotes the iteration number, X_i denotes the matrix containing the controlled system's predicted states over the entire optimization horizon from the i-th iteration, MAX(M) is the maximum of all elements of matrix M, and c_i is a scalar denoting the total cost of all control actions over the entire optimization horizon from the i-th iteration. The maximum allowed number of iterations was set to 10. If this number was reached the found optimal solution from the very last iteration was used.

7.2.3 Factors and Experiments Sets

Table 7.1 summarizes the factors that were varied in our simulation experiments. There was a total of fourteen different factors that fell into the following groups: definition of building technical system and cost function (factors no. 1–4); boundary conditions for control (no. 5–7); weather conditions (no. 8–9); and general building characteristics (no. 10–14). Further information on the individual factors can be found in Chapters 2 and 6.

The simulation experiments conducted for a given control strategy (PB or RBC-1 to RBC-4) and particular combination of factors 1–7 (in particular the Building System variant, Cost Function variant, Thermal Comfort variant and Ventilation Strategy) were grouped into so-called "Experiments Sets". Each Experiments Set covered all possible combinations in the factors no. 8–14.

Table 7.2 summarizes the Experiments Sets considered, and Table 7.3 shows the numbers of simulations present in an Experiments Set per Buildings Class (Table 2.2) and Building Standard.

Performance Bound simulations were conducted for both Cost Function variants, and for all Experiments Sets (E1–E10), i.e. there were 7'168 simulations per Cost Function variant.

Simulations with the rule-based controllers RBC-1 to RBC-4 were conducted only for the Cost Function variant NRPE, and only for the Experiments Sets E1–E3. This corresponded to 2'304 simulated cases per controller.

No	*Factor*	*Variants Considered*	*# Variants*	*Further Information*
1	Building System	S1, S2, S3, S4, S5	5	Table 2.3
2	Energy System	Heat: earth coupled heat pump Cold: mechanical (compression) chiller	1	Table 2.5
3	Dimensioning Strategy	D_s – Scant	1	Table 2.4
4	Cost Function	NRPE – Non-Renewable Primary Energy usage MC – Monetary Cost (diurnally varying tariff)	2	Table 2.4
5	Thermal Comfort	A_w – No set-back, wide comfort range B_w – Set-back allowed, wide comfort range A_n – No set-back, narrow comfort range B_n – Set-back allowed, narrow comf. range	4	Table 2.4
6	Ventilation Strategy	none – No ventilation (S1) V – non-air quality controlled ventil. (S2–S5) W – CO_2-based control (S2–S5)	1 * 2	Table 2.5
7	Illuminance Comfort	Occupancy dependent, bright	1	Section 2.4.3
8	Site	SMA – Zürich-Fluntern LUG – Lugano WHW – Wien Hohe Warte MSM – Marseille-Marignane	4	Chapter 6
9	Weather Data Set	DM – Average Design Reference Year	1	Chapter 6
10	Façade Orientation	N, S, SW (corner room), SE (corner room)	4	Table 2.1
11	Construction Type	h – heavyweight l – lightweight	2	-"-
12	Building Standard	sa – Swiss average ph – Passive house	2	-"-
13	Window Area Fraction	wl – low wh – high	2	-"-
14	Internal Gains Level	il – low ih – high	2	Table 2.6

Table 7.1: Overview of factors varied in the simulations experiments. *: Building System variant S1 has no ventilation subsystem , Ventil. Strategies V and W apply to variants S2–S5 only.

Experiments Set Identifier	*Building System Variant*	*Thermal Comfort*	*Ventilation Strategy*
E1	S1	A_w	-
E2	One of S2–S5	A_w	V
E3	One of S2–S5	A_w	W
E4	S1	B_w	-
E5	One of S2–S5	B_w	V
E6	One of S2–S5	B_w	W
E7	S1	A_n	-
E8	One of S2–S5	A_n	V
E9	S1	B_n	-
E10	One of S2–S5	B_n	V

Table 7.2: Overview of Experiments Sets.

Buildings Class	*Passive House*	*Swiss Average*
I	16	16
II	112	48
III	–	64
Total	128	128

Table 7.3: Numbers of simulation experiments per Experiments Set.

7.2.4 Analysis Procedure

7.2.4.1 Standard Procedure

The following data were archived for each individual simulation run: (i) all parameter values and settings determining the run's execution and results; (ii) the hourly values of the plant model's state (x), input (u), output (y), and diagnostic output (z) vectors (cf. Appendix A); (iii) the hourly values of the control costs (c) and cumulative control costs (cc) vectors; (iv) the hourly values of the system outputs' upper and lower constraints vectors (ymin, ymax); and (v) the number of bilinearity iterations employed for each optimization within the simulation run.

From the hourly cost data of each simulation run were computed the monthly, seasonal and annual total cost of all control actions and of each individual control action (e.g. radiator heating, free cooling etc.). In order to assess the sensitivity of the control costs to the Cost Function definition the following additional analyses were done for various PB simulations: the hourly control outputs obtained when optimizing for NRPE usage (respectively MC) were re-evaluated to compute the associated MC (respectively NRPE usage). For these alternative costs again corresponding monthly, seasonal and annual totals were computed.

The simulated hourly system output values were post-processed in two steps, as follows:

First, from the hourly y, ymin and ymax data were calculated the following annual, seasonal, and monthly indices related to comfort and the simulated systems' behavior: a) Room temperature: cumulative sum of deviations below (above) the lower (upper) comfort range bound (in K·h), and numbers of violations of the upper and lower bound, respectively, by at least 0.0, 0.1, 0.5 and 1 ºC; b) Room illuminance: cumulative sum of deviations below (above) the lower (upper) comfort range bound (in lux·h), and numbers of violations of the upper and lower bound, respectively, by at least 10, 50, and 100 lux; c) Ceiling surface temperature (condensation control, only for systems with cooled ceiling present): cumulative sum of deviations below lower prescribed bound (in K·h), and numbers of violations of the lower bound by at least 0.0, 0.1, 0.5 and 1 ºC; and d) Total air change rate (only for systems with ventilation system present): cumulative sum of deviations below (above) the lower (upper) comfort range bound (in h^{-1}·h), and numbers of violations of the upper and lower bound, respectively, by at least 0.0, 0.01, 0.1 and 0.25 h^{-1}; e) various statistics for the mechanical ventilation air change rate plus the mechanical ventilation's heating and cooling reserve.

The second post-processing step was as follows: all annual statistics from one or several Experiments Sets were collected into a so-called "data collection". Depending on the question investigated for the further analysis considered were either all data points from this data collection or their pairwise differences to the corresponding data points from a second data collection reflecting a variation in a specific factor (e.g., narrow vs. wide thermal comfort range width).

The resulting data points were then stratified by the following factors: Control Costs variant (NRPE usage or MC), Building System variant (S1–S5), Building Standard (Passive House or Swiss Average), and Building Class (I–III). Finally, for each factor combination corresponding summary statistics (e.g. boxplots) were derived.

In this Chapter we focus but on annual results: annual costs (NRPE usage or MC) and selected annual comfort and electrical lighting (see below) statistics. More detailed analyses considering some of the monthly and hourly results are reported in Chapter 8.

7.2.4.2 Electric Lighting Analysis

After performing a large number of PB simulations was detected that for electrical lighting no upper bound had been specified. Given that the room illuminance level was also unlimited (Section 2.4.3) this had the following consequence: whenever there was a limitation in "normal" heating power the MPC optimization algorithm employed electrical lighting for heating. This occurred in several instances because maximum non-electrical heating power had been specified based on a scant dimensioning procedure (Table 2.4).

In order to ensure comparability of the PB results we decided to allow for this extra electrical lighting in all PB simulations. (Note, this problem did not occur in the simulations with the rule-based controllers, because in these cases electrical lighting was always limited correctly). The extra electrical lighting power and costs were evaluated for each individual PB simulation as follows:

In a first step were detected all hours with extra lighting present as the hours for which held the condition (E_r-E_{rMin} > 0.1) AND (u_{EL} > 0.01), where E_r is the current and E_{rMin} is the minimum required room illuminance level (both given in lux), and u_{EL} is the electrical lighting power (in W/m^2).

In a second step was evaluated the condition $\eta \cdot u_{EL} \leq E_{rMin}$, where η is the luminosity efficacy of electrical lighting. If this condition was found to be true the power for extra lighting was estimated to be equal to u_{EL}, i.e. it was assumed that E_{rMin} had been reached thanks to illuminance input through the windows, such that all lighting power was assumed to be extra power. Otherwise the extra power was set to the power needed to reach the current illuminance level above the minimum level, i.e. u_{EL}-E_{rMin}/η.

In a third step, the cost of the extra electrical lighting power was evaluated for all found cases using the current Cost Function. At last, the annual total extra electrical lighting cost and further annual statistics were calculated.

7.2.5 Software And Databases

All simulations were done with the BACLab software, a specialized building modeling and simulation software that was developped within the OptiControl project. The software version used for the PB simulations was BACLab v1.1. For the simulations with the rule-based controllers we used BACLab v1.2 (extra electrical lighting bug fixed). The post-processing was done with BACLab v1.8pre to v1.91pre (versions with enhanced post-processing functionality).

The weather and occupancy data were those from the OptiControl occupancy and weather database OCWDB v1.7. The building and building systems parameters were accessed via the server software BuSyServer v1.1 from the database BuSyDB v2.4.

7.3 Results

7.3.1 Choice of Building System and Optimization Target

Here we investigate what are the savings in control costs when there is no ventilation system (building system variant S1), and in as far buildings systems that serve the same purpose (variants S2–S5) result into different control costs. We also investigate the use of different optimization targets (monetary vs. energetic cost), an issue of interest to energy planners and energy providers.

Figure 7.1 juxtaposes the annual NRPE usage and MC for the five Building System variants S1–S5 and Buildings Class I. Summary statistics for Buildings Classes I–III are given in Table 7.4. Graphical results for Buildings Classes II and III and further statistics are reported in Appendix D.1.

Building Standard: From Figure 7.1 can be seen that median values (red lines) for NRPE usage or MC were always lower for the Passive House Building Standard (left panels) as compared to the Swiss Average standard (right panels). The same was found to hold also for Buildings Class II (Table 7.4). On average over the Classes I and II NRPE usage between the two Building Standards differed by a factor of two, whereas for annual MC was obtained a factor of 1.6 (Table 7.4).

Building System variant: As expected, for both Cost Functions and all Building Classes the variant S1 yielded on average the lowest cost. Variant S3 (heating/cooling with ventilation only) yielded the highest costs. Variants S2, S4 and S5 generally showed intermediate and generally very similar average costs (Figure 7.1, Table 7.4).

Buildings Class: Both, average NRPE usage and MC showed a clear dependence on Buildings Class: Class I always had the lowest average costs, followed by Class II and then by Class III (Table 7.4).

Figure 7.2 reports the found absolute differences in PB annual total costs for Buildings Class I when different optimization targets/Cost Functions were used for control cost optimization and evaluation. Average relative differences for all Buildings Classes are reported in Table 7.5. Further graphical representations and statistics can be found in Appendix D.2.

Building Standard: The choice of alternative Cost Functions was found to matter less for the Passive Houses as compared to the Swiss Average cases: the found overall average relative differences for NRPE usage amounted for Passive Houses to 2.4% and for the Swiss Average cases to 5.4%; for MC the corresponding values were 3.1% and 8.4%, respectively (Table 7.5).

Building System variant: Variant S3 showed the highest average absolute and relative sensitivities to the choice of Cost Function. However, in two cases the most sensitive variant in both, absolute and relative terms, was found to be variant S5 (for MC, Swiss Average Building Standard, Buildings Classes II and III): the obtained average MC-increases when the control was optimized for NRPE were no less than 13.6% and 20.2%, respectively. The lowest average absolute and relative sensitivities were always found for Building System variant S4 (Table 7.5, Appendix D.2).

Buildings Class: There was a clear dependency on Buildings Class, with increasing average absolute and relative differences through Classes I to III.

Cost Function: From Table 7.5 can be seen that MC responded for Buildings Class I in 9 out of 10 cases more sensitively to the use of an alternative Cost Function than NRPE usage. For Class II the average relative differences were highest for MC and NRPE usage in 5 cases each.

Note, the relative differences for the individual building cases showed large deviations from the average values reported in Table 7.5 (cf. Figure 7.2). The most extreme relative differences obtained amounted to 31% for NRPE usage and 46% for MC (Appendix D.2).

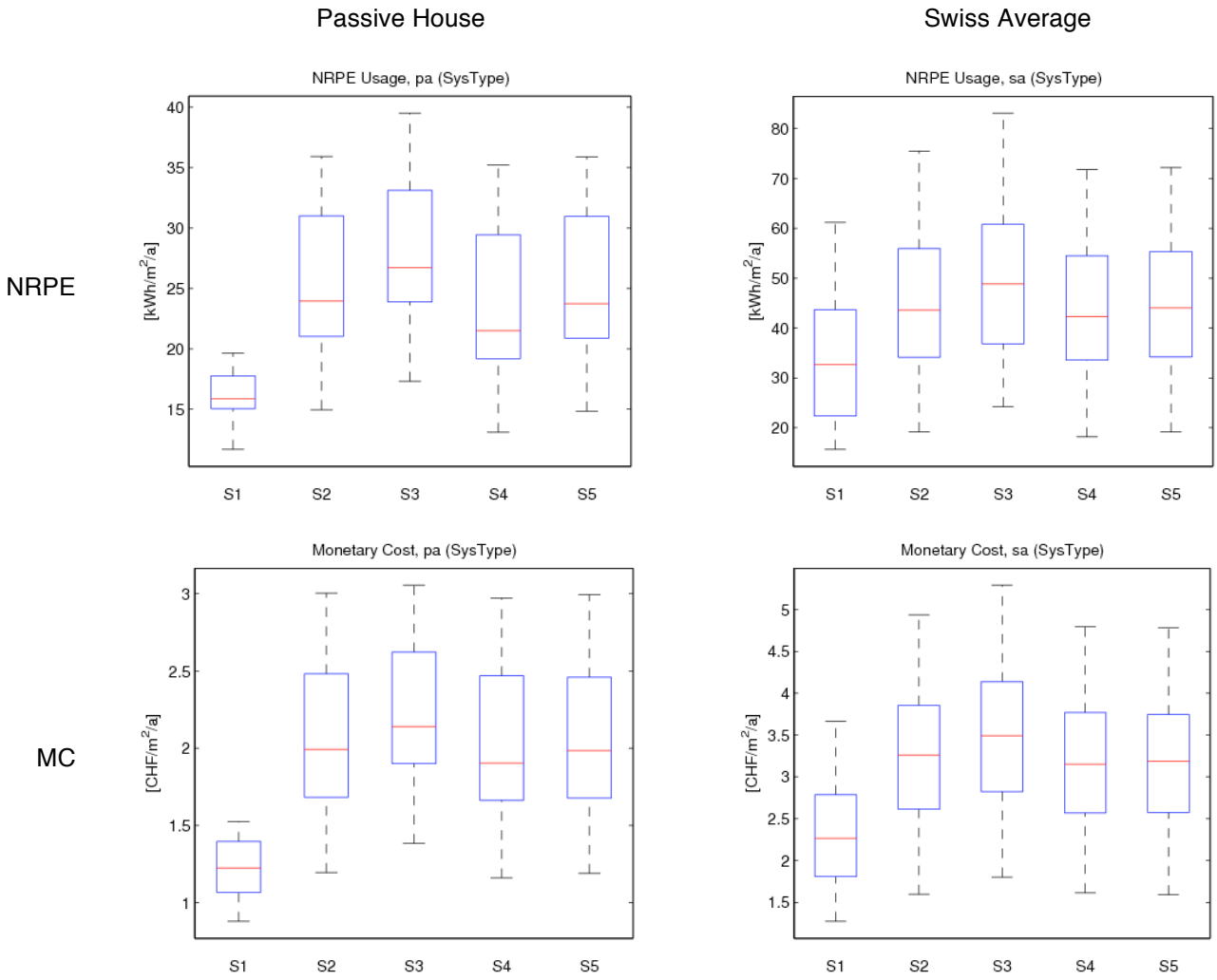

***Figure 7.1:** Overview of Performance Bound results for annual total costs and Buildings Class I. NRPE: Non-Renewable Primary Energy usage; MC: Monetary Cost; S1–S5: Building System variants. For each Cost Function were considered Experiments Sets E1–E6, respectively. On each box, the central mark is the median, the edges of the box are the 25th and 75th percentiles, and the whisker covers ca. 99% of the simulated cases for the particular Cost Function, Building Standard, and Building System variant. Outliers are drawn as single points. Note the different y-axis ranges.*

Cost Function	*Buildings Class*	*Passive House*						*Swiss Average*					
		S1	*S2*	*S3*	*S4*	*S5*	*Mean*	*S1*	*S2*	*S3*	*S4*	*S5*	*Mean*
NRPE	*I*	15.8	24.7	28.2	23.3	24.7	***23.3***	33.7	44.9	50.3	43.7	44.6	***43.4***
[kWh/m²/a]	*II*	19.8	28.5	32.8	27.6	28.9	***27.5***	45.0	55.6	66.3	58.6	59.2	***56.9***
	III	–	–	–	–	–	–	63.9	74.8	93.7	84.2	85.1	***80.3***
	Mean I+II	**17.8**	**26.6**	**30.5**	**25.4**	**26.8**	***25.4***	**39.3**	**50.3**	**58.3**	**51.1**	**51.9**	***50.2***
MC	*I*	1.22	2.04	2.19	2.01	2.03	***1.90***	2.31	3.22	3.50	3.16	3.15	***3.07***
[CHF/m²/a]	*II*	1.49	2.29	2.52	2.30	2.28	***2.18***	2.63	3.53	4.12	3.53	3.43	***3.45***
	III	–	–	–	–	–	–	3.38	4.30	5.34	4.37	4.17	***4.31***
	Mean I+II	**1.35**	**2.16**	**2.36**	**2.16**	**2.16**	***2.04***	**2.47**	**3.37**	**3.81**	**3.35**	**3.29**	***3.26***

***Table 7.4:** Mean Perfomance Bound results for annual total costs. NRPE: Non-Renewable Primary Energy usage. MC: Monetary Cost. S1–S5: Building System variants. For each Cost Function were considered Experiments Sets E1–E6, respectively. Shown are average values from all simulated cases for the respective Cost Function, Buildings Class, Building Standard, and Building System variant.*

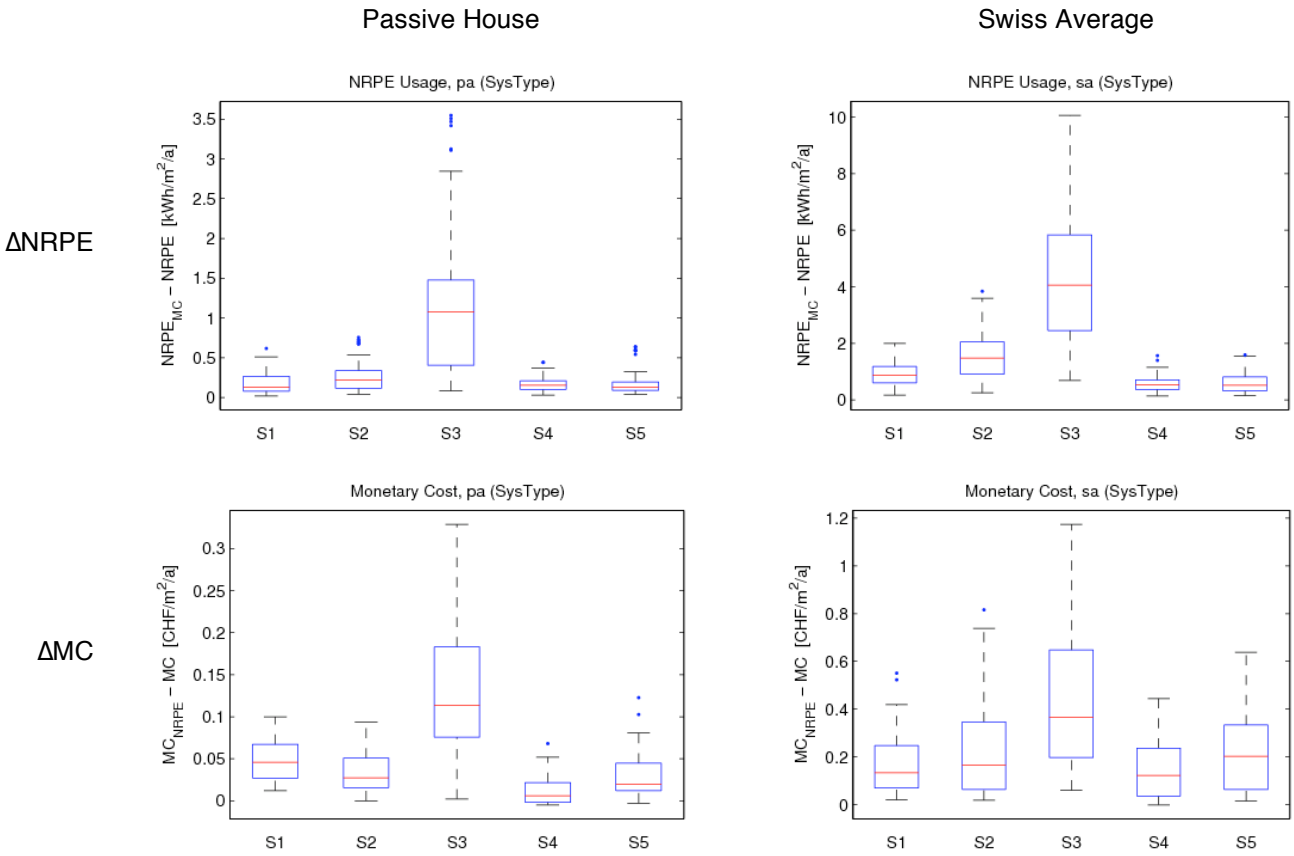

***Figure 7.2:** Overview of absolute differences in annual total Performance Bound costs for Buildings Class I when using different Cost Functions for control cost optimization and evaluation. ΔNRPE: difference in Non-Renewable Primary Energy (NRPE) usage when control was optimized for Monetary Cost (MC); ΔMC: difference for MC when control was optimized for NRPE usage; $NRPE_{MC}$: NRPE usage obtained after optimization for MC; MC_{NRPE}: MC obtained after optimization for NRPE; S1–S5: Building System variants. For each Cost Function were considered Experiments Sets E1–E6, respectively. Each box was derived from all simulated cases for the respective Cost Function, Buildings Class, Building Standard, and Building System variant.*

Cost Function	*Buildings Class*	*Passive House*						*Swiss Average*					
		S1	*S2*	*S3*	*S4*	*S5*	*Mean*	*S1*	*S2*	*S3*	*S4*	*S5*	*Mean*
ΔNRPE%	*I*	1.2	1.1	4.0	0.8	0.8	***1.6***	2.7	3.2	8.1	1.2	1.3	***3.3***
	II	3.1	2.6	8.0	1.2	1.5	***3.3***	8.3	8.7	13.7	2.8	3.5	***7.4***
	III	–	–	–	–	–	–	11.1	11.2	13.0	4.5	5.3	***9.0***
	Mean I+II	**2.2**	**1.9**	**6.0**	**1.0**	**1.1**	***2.4***	**5.5**	**6.0**	**10.9**	**2.0**	**2.4**	***5.4***
ΔMC%	*I*	4.1	1.7	6.2	0.6	1.5	***2.8***	6.7	6.3	12.0	4.2	6.6	***7.2***
	II	4.5	2.1	6.1	1.1	2.8	***3.3***	9.4	8.1	10.6	6.9	13.6	***9.7***
	III	–	–	–	–	–	–	10.6	9.0	9.7	8.9	20.2	***11.7***
	Mean I+II	**4.3**	**1.9**	**6.2**	**0.9**	**2.1**	***3.1***	**8.1**	**7.2**	**11.3**	**5.5**	**10.1**	***8.4***

***Table 7.5:** Mean relative differences in annual total Performance Bound costs when using different Cost Functions for control cost optimization and evaluation. ΔNRPE%: rel. difference for Non-Renewable Primary Energy (NRPE) usage when control was optimized for Monetary Cost (MC); ΔMC%: rel. difference for MC when control was optimized for NRPE usage; S1–S5: Building System variants. For each Cost Function were considered Experiments Sets E1–E6, respectively. Shown are percentage values averaged over all simulated cases for the respective Cost Function, Buildings Class, Building Standard, and Building System variant.*

7.3.2 Assessment of Low-Cost Energy Saving Measures

7.3.2.1 Effect of Night/Weekend Set-Back

This investigation is of interest to control equipment suppliers and energy performance contractors. It shows the savings potential of an ideal Optimal Start/Stop Control (OSSC) function.

Figure 7.3 shows boxplots of absolute differences in annual total PB costs for Buildings Class I from the pair-wise comparison of cases with (thermal comfort variant B_w) and without (variant A_w) set-back. The average relative differences in NRPE usage and MC are given in Table 7.6. Further graphical results and more detailed statistics are reported in Appendix D.3.

Building Standard: The Swiss Average cases always yielded larger average absolute (Figure 7.3) and relative (Table 7.6) differences than their Passive House counterparts.

Building System variant: For both Building Standards the largest average absolute differences were obtained for variant S3 (Figure 7.3, Appendix D.3), and the largest average relative differences for variants S3 and S1. The least sensitive Building System variants were S5 and S4 (Table 7.6).

Buildings Class: The set-back effect for the Passive Houses of Buildings Class I (Figure 7.3, left panels) was generally small (at most a few percent) and showed a skewed distribution, i.e. there were many cases with practically no effect present. Buildings Class II yielded similarly skewed distributions as Class I (Appendix D.3), but the differences obtained were generally much larger than for Class I (Table 7.6, Appendix D.3). For the Swiss Average Building Standard average relative differences were again small for Buildings Class I (Figure 7.3, right panels) and increasingly larger for Classes II+III (Table 7.6).

Cost Function: In all cases MC yielded the smallest, and NRPE usage the largest average relative differences (Table 7.6).

7.3.2.2 Effect of Thermal Comfort Range Width

This investigation is of interest to building users/owners, operators/facility managers, and also performance contractors. It shows the control costs savings potential of reduced thermal comfort.

The found effects due to the change in comfort range width from “narrow” to “wide” are illustrated for Buildings Class I in Figure 7.4. Average relative effects for all Buildings Classes are reported in Table 7.7. Further results on the thermal comfort range width effect can be found in Appendix D.4.

Building Standard: The average absolute effects were always larger for the Swiss Average cases as compared to their Passive House counterparts (Figure 7.4, Appendix D.4). The average relative effects were also larger for the Swiss Average Building Standard in 3 out of 10 cases for Buildings Class I, and in 9 out of 10 cases for Class II (Table 7.7).

Building System variant: Variant S3 gave for Buildings Class I throughout the largest average absolute and relative effects (Figure 7.4, Appendix D.4), the only exception being a slightly larger average relative MC effect by variant S4 (Table 7.7). For Classes II and III the largest average absolute effects were obtained for variants S3 or S4 (Appendix D.4), and the largest average relative effects for variants S1 or S4 (Table 7.7). The smallest average absolute effects were obtained for variants S1, S2 or S5 (Figure 7.4, Appendix D.4), and the smallest average relative effects for variants S2 or S5 (Table 7.7).

Buildings Class: The average absolute and relative effects showed a clear dependence on Building Class, with increasing values from Class I through Class III (Appendix D.4, Table 7.7).

Cost Function: In most cases MC was found to yield smaller average relative effects than NRPE usage. The only two exceptions occurred for the Swiss Average Building Standard, variant S5, Buildings Classes II and III (Table 7.7).

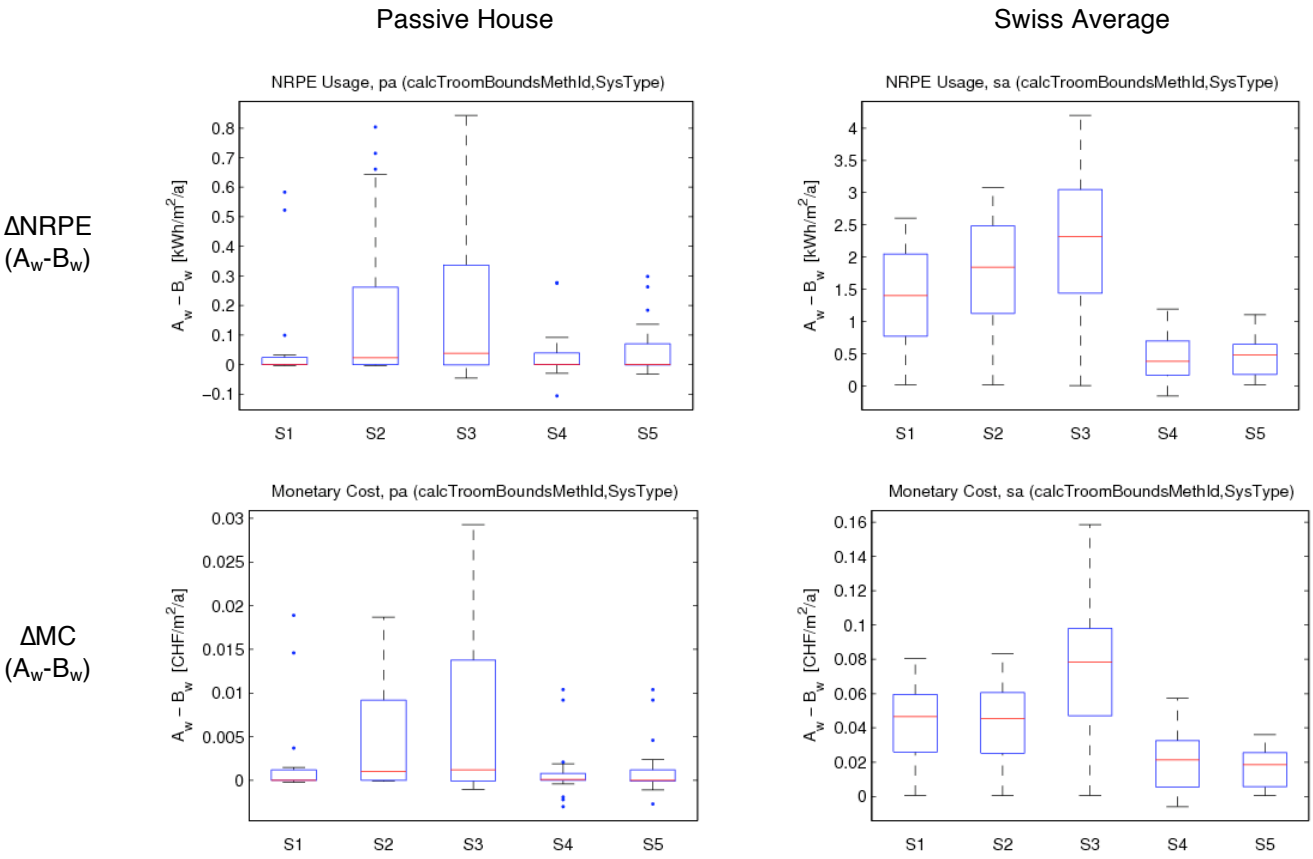

Figure 7.3: Overview of absolute differences in annual total Performance Bound costs for Buildings Class I due to allowance of night/weekend set-back. ΔNRPE: difference in Non-Renewable Primary Energy usage; ΔMC: difference in Monetary Cost; A_w: no night/weekend set-back allowed, wide comfort range; B_w: set-back allowed, wide comfort range; S1–S5: Building System variants. Each box was derived based on the pair-wise comparison of individual simulations from Experiments Sets pairs E1-E4, E2-E5, and E3-E6 for the respective Cost Function.

Cost Function	*Buildings Class*	*Passive House*						*Swiss Average*					
		S1	*S2*	*S3*	*S4*	*S5*	*Mean*	*S1*	*S2*	*S3*	*S4*	*S5*	*Mean*
ΔNRPE%	*I*	0.4	0.7	0.7	0.1	0.2	***0.4***	3.7	3.5	4.0	1.0	1.0	***2.6***
	II	5.7	4.7	5.5	4.6	3.9	***4.9***	17.5	15.4	17.8	10.2	9.2	***14.0***
	III	–	–	–	–	–	–	30.6	27.6	29.3	20.2	19.1	***25.4***
	Mean I+II	**3.1**	**2.7**	**3.1**	**2.4**	**2.0**	***2.7***	**10.6**	**9.4**	**10.9**	**5.6**	**5.1**	***8.3***
ΔMC%	*I*	0.2	0.2	0.3	0.0	0.1	***0.2***	1.7	1.3	2.0	0.7	0.5	***1.2***
	II	3.4	2.4	2.9	2.5	2.0	***2.6***	11.5	8.9	10.9	8.5	6.5	***9.3***
	III	–	–	–	–	–	–	23.1	18.9	21.2	19.0	15.8	***19.6***
	Mean I+II	**1.8**	**1.3**	**1.6**	**1.3**	**1.0**	***1.4***	**6.6**	**5.1**	**6.4**	**4.6**	**3.5**	***5.2***

Table 7.6: Mean relative differences in annual total Performance Bound costs due to allowance of night/weekend set-back. ΔNRPE%: rel. difference in Non-Renewable Primary Energy usage; ΔMC%: rel. difference in Monetary Cost; S1–S5: Building System variants. For each Cost Function were considered pair-wise comparisons of individual simulations from Experiments Sets pairs E1-E4, E2-E5, and E3-E6, respectively. Shown are percentage values averaged over all comparisons for the respective Cost Function, Buildings Class, Building Standard, and Building System variant.

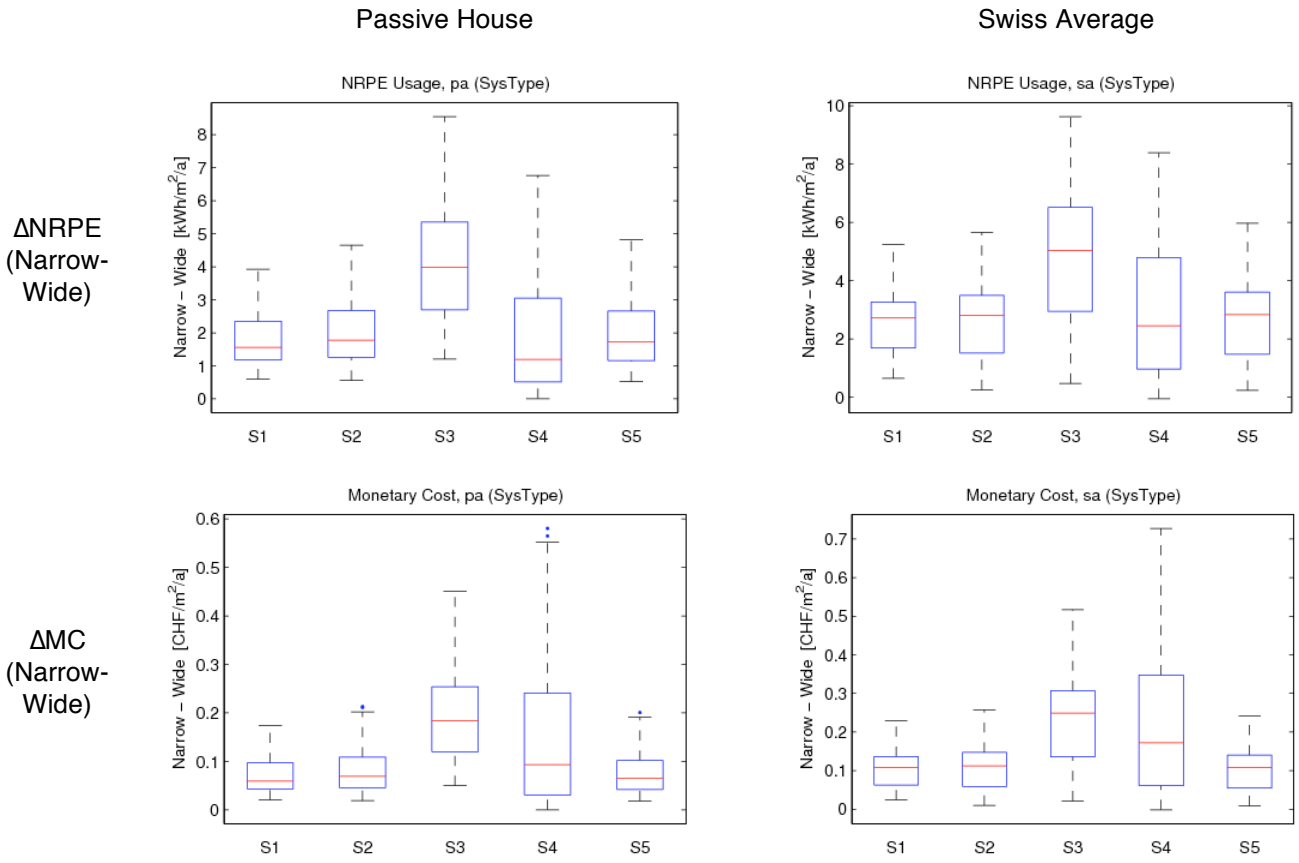

Figure 7.4: Overview of absolute differences in annual total Performance Bound costs for Buildings Class I due to change in comfort range width. ΔNRPE: difference in Non-Renewable Primary Energy usage; ΔMC: difference in Monetary Cost; Narrow: Thermal Comfort variant A_n or B_n; Wide: Thermal Comfort variant A_w or B_w; S1–S5: Building System variants. Each box was based on the pairwise comparison of individual simulations from Experiments Sets pairs E1-E7, E2-E8, E4-E9, and E5-E10 for the corresponding Cost Function.

Cost Function	*Buildings Class*	*Passive House*						*Swiss Average*					
		S1	*S2*	*S3*	*S4*	*S5*	*Mean*	*S1*	*S2*	*S3*	*S4*	*S5*	*Mean*
ΔNRPE%	*I*	10.4	6.6	11.5	6.6	6.6	***8.3***	8.9	5.9	9.1	6.8	6.1	***7.3***
	II	15.2	9.4	13.2	10.9	9.9	***11.7***	16.1	11.2	13.0	13.6	12.5	***13.3***
	III	–	–	–	–	–	–	16.9	12.9	14.1	14.7	14.0	***14.5***
	Mean I+II	**12.8**	**8.0**	**12.4**	**8.7**	**8.2**	***10.0***	**12.5**	**8.6**	**11.1**	**10.2**	**9.3**	***10.3***
ΔMC%	*I*	5.9	3.4	7.2	6.1	3.2	***5.2***	5.3	3.4	6.2	6.4	3.3	***4.9***
	II	13.0	6.8	9.9	10.0	6.0	***9.1***	15.3	9.8	11.5	14.1	9.7	***12.1***
	III	–	–	–	–	–	–	16.7	11.9	13.5	17.0	12.9	***14.4***
	Mean I+II	**9.5**	**5.1**	**8.6**	**8.1**	**4.6**	***7.2***	**10.3**	**6.6**	**8.9**	**10.3**	**6.5**	***8.5***

Table 7.7: Mean relative differences in annual total Performance Bound costs between comfort range widths "Narrow" and "Wide". ΔNRPE%: rel. difference in Non-Renewable Primary Energy usage; ΔMC%: rel. difference in Monetary Cost; S1–S5: Building System variants. For each Cost Function were considered pairwise comparisons of individual simulations from Experiments Sets pairs E1-E7, E2-E8, E4-E9, and E5-E10, respectively. Shown are the values "100(Narrow-Wide)/Narrow" averaged over all comparisons for the respective Cost Function, Buildings Class, Building Standard, and Building System variant.

7.3.2.3 Effect of Ventilation Strategy

This analysis is of interest to control suppliers, ventilation equipment suppliers and energy performance contractors. It shows the benefit of introducing air quality controlled ventilation.

Figure 7.5 shows for Buildings Class I boxplots of differences in NRPE usage (top panels) and MC (bottom panels) due to the use of alternative Ventilation Strategies. Average relative effects are reported in Table 7.8. Further results are documented in Appendix D.5.

Building Standard: Average absolute differences were found to be always slightly smaller for the Passive House cases as compared to the Swiss Average cases (Figure 7.5, Appendix D.5). Average relative differences where however always larger for the Passive House standard (Table 7.8).

Building System variant: Average absolute differences generally did not differ very much between Building System variants (e.g., Figure 7.5 bottom). Nevertheless, for the Passive House Building Standard the largest absolute differences were always obtained for variant S4, and for the Swiss Average Building Standard always for variant S2; the smallest average absolute differences were obtained almost always for variant S3 (Appendix D.5). Average relative differences were largest for variants S4 (mainly for the Passive Houses) or S2 (mainly for the Swiss Average cases). The average relative differences were always smallest for variant S3.

Buildings Class: Average absolute differences were found to increase slightly from Class I through to Class III (Appendix D.5). On the contrary, average relative differences tended to decrease with increasing class number (Table 7.8).

Cost Function: Average relative differences generally did not vary much between Cost Functions. However, NRPE showed in almost all cases smaller differences than MC. The only exceptions occurred for the case Passive House/S4 where MC yielded clearly larger values (Table 7.8).

7.3.3 Electric Lighting And Thermal Comfort Analysis

7.3.3.1 Usage of Extra Electric Lighting For Heating

As already stated in Section 7.2.4.2 electric lighting was unintendendly made available for heating in the PB simulations. Here we report on the extra electric lighting control costs.

Table 7.9 gives for the two Cost Function variants considered the found numbers of cases where the ratio of annual total extra electric lighting costs to annual total costs in the Performance Bound simulations exceeded a given percentage value (N>x%). Further results related to the usage of electric lighting for heating can be found in Appendix D.6.

Building Standard: Extra electric lighting was used much less in the Passive House simulations as compared to the Swiss Average simulations. From a total of 2304 cases analyzed for each Cost Function and Building Standard extra electric lighting exceeded 1% of annual total NRPE usage in 16% of all Passive House cases, as opposed to 50% of all Swiss Average cases. For MC the corresponding numbers were 6% and 36%, respectively (Table 7.9).

Building System variant: Extra electric lighting occurred most frequently for variant S4, with N>1% being the case in 27% of all Passive House and in 77% of all Swiss Average simulations. Variants S5, S3 and S1 showed intermediate extra lighting usage. The least extra electric lighting usage occurred for variant S2, with N>1% in 0.5% of all Passive House and in 9% of all Swiss Average simulations.

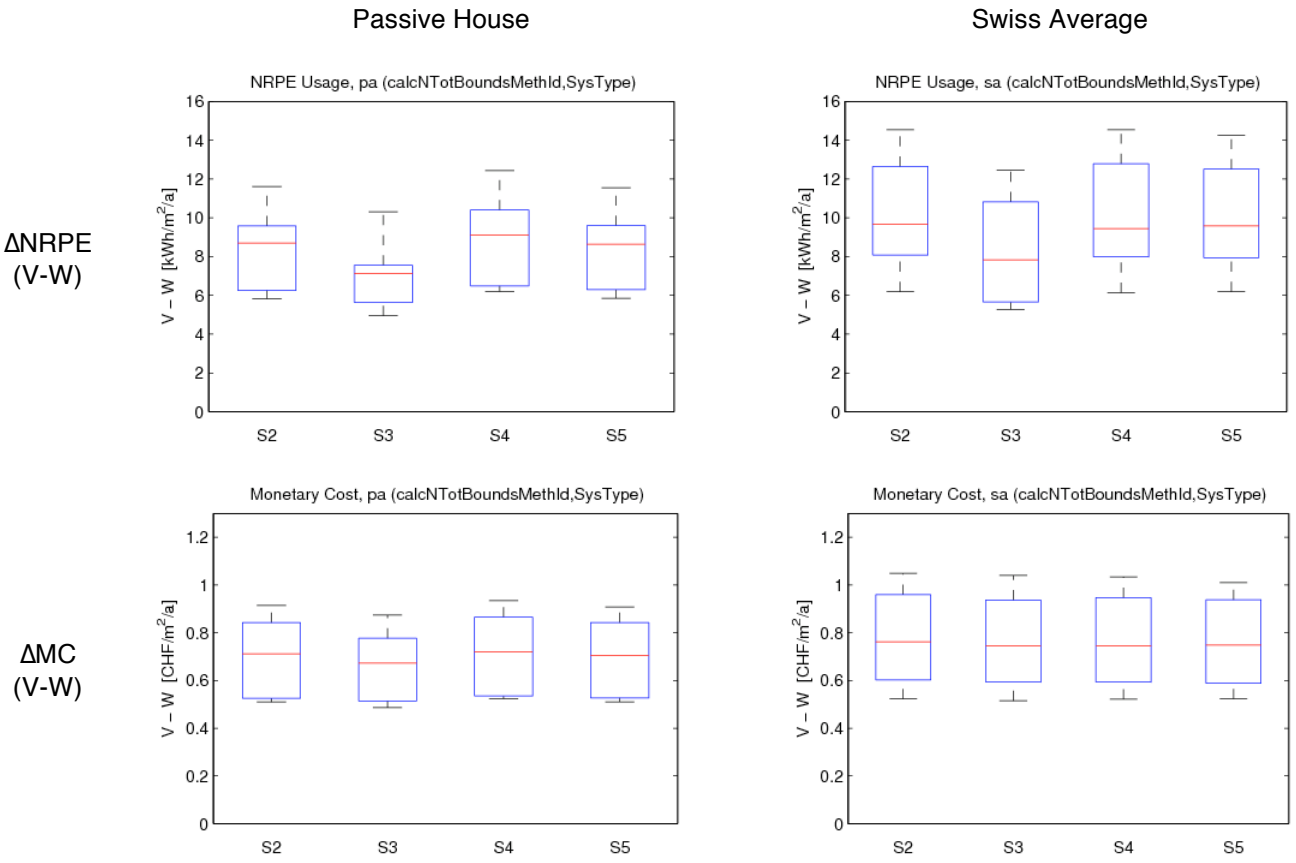

Figure 7.5: Overview of absolute differences in annual total Performance Bound costs for Buildings Class I due to use of different Ventilation Strategies. ΔNRPE: difference in Non-Renewable Primary Energy usage; ΔMC: difference in Monetary Cost; V: two-stage ventilation control; W: CO_2-based control; S1–S5: Building System variants. Each box was based on the pairwise comparison of individual simulations from Experiments Sets pairs E2-E3, and E5-E6 for the corresponding Cost Function.

Cost Function	*Buildings Class*	*Passive House*					*Swiss Average*				
		S2	*S3*	*S4*	*S5*	*Mean*	*S2*	*S3*	*S4*	*S5*	*Mean*
ΔNRPE%	*I*	28.5	22.1	31.7	28.6	***27.7***	21.0	16.1	21.5	20.9	***19.9***
	II	27.8	20.2	29.5	27.5	***26.2***	19.5	13.0	17.9	18.2	***17.1***
	III	–	–	–	–	–	16.0	9.8	13.8	14.3	***13.5***
	Mean I+II	**28.2**	**21.1**	**30.6**	**28.1**	***27.0***	**20.3**	**14.5**	**19.7**	**19.6**	***18.5***
ΔMC%	*I*	29.1	26.0	29.9	29.1	***28.5***	21.8	19.9	21.7	21.8	***21.3***
	II	29.2	25.0	28.9	29.1	***28.1***	22.8	18.4	21.3	22.5	***21.2***
	III	–	–	–	–	–	20.2	14.7	18.6	19.9	***18.3***
	Mean I+II	**29.1**	**25.5**	**29.4**	**29.1**	***28.3***	**22.3**	**19.2**	**21.5**	**22.1**	***21.3***

Table 7.8: Mean relative differences in annual total Performance Bound costs between Ventilation Strategies "V" (two-stage ventilation control) and "W" (CO_2-based control). ΔNRPE%: rel. difference in Non-Renewable Primary Energy usage; ΔMC%: rel. difference in Monetary Cost; S1–S5: Building System variants. For each Cost Function were considered pairwise comparisons of individual simulations from Experiments Sets pairs E2-E3, and E5-E6, respectively. Shown are the values "100(V-W)/V" averaged over all comparisons for the respective Cost Function, Buildings Class, Building Standard, and Building System variant.

Cost Function	*Buildings Class*	*Statistic*	*Passive House*					*Swiss Average*				
			S1	*S2*	*S3*	*S4*	*S5*	*S1*	*S2*	*S3*	*S4*	*S5*
NRPE	*I*	*N*	32	64	64	64	64	32	64	64	64	64
		N>1%	0	0	3	6	0	3	0	21	22	18
		N>2.5%	0	0	0	0	0	0	0	5	2	2
		N>5%	0	0	0	0	0	0	0	0	0	0
	II	*N*	224	448	448	448	448	96	192	192	192	192
		N>1%	23	5	39	184	99	35	25	82	156	115
		N>2.5%	3	0	10	73	38	8	1	54	106	78
		N>5%	0	0	0	32	11	0	0	8	62	55
	III	*N*	–	–	–	–	–	128	256	256	256	256
		N>1%	–	–	–	–	–	50	62	140	219	203
		N>2.5%	–	–	–	–	–	29	26	103	146	141
		N>5%	–	–	–	–	–	9	1	64	99	85
MC	*I*	*N*	32	64	64	64	64	32	64	64	64	64
		N>1%	0	0	0	0	0	0	0	0	16	0
		N>2.5%	0	0	0	0	0	0	0	0	0	0
		N>5%	0	0	0	0	0	0	0	0	0	0
	II	*N*	224	448	448	448	448	96	192	192	192	192
		N>1%	0	0	0	89	38	0	0	25	151	113
		N>2.5%	0	0	0	16	2	0	0	4	81	51
		N>5%	0	0	0	3	0	0	0	0	22	5
	III	*N*	–	–	–	–	–	128	256	256	256	256
		N>1%	–	–	–	–	–	7	3	94	225	196
		N>2.5%	–	–	–	–	–	0	0	53	163	138
		N>5%	–	–	–	–	–	0	0	7	89	79

Table 7.9: Numbers of simulated cases (N) and numbers of cases where the ratio of annual total extra electric lighting costs to annual total costs in the Performance Bound simulations exceeded a given percentage value (N>x%). NRPE: optimization was done for Non-Renewable Primary Energy usage; ΔMC: optimization was done for Monetary Cost; S1–S5: Building System variants. For each Cost Function were considered Experiments Sets E1–E6, respectively.

Buildings Class: Extra electric lighting usage increased with Buildings Class. For Passive Houses N>1% was obtained in 2% and 12% of all Class I and Class II simulations, respectively. For the Swiss Average Building Standard and Classes I-III the corresponding numbers were 14%, 41% and 52%, respectively.

Cost Function: MC clearly showed the smaller number of simulations with extra electric lighting present (Table 7.9).

7.3.3.2 Thermal Comfort Violations

Figure 7.6 reports annual sums of Kelvin-hours (Kh) where the room temperature exceeded (S_U) or fell below (S_L) the prescribed thermal comfort range in the PB simulations. Further statistics related to thermal comfort violations are reported in Appendix D.7.

From Figure 7.6 can be seen that the obtained S_U values were generally below 30 Kh, and the S_L values generally above -30 Kh, respectively.

Building Standard: Altogether, comfort violations were smaller for the Passive House (left panels) as compared to the Swiss Average (right panels) Building Standard.

Building System variant: Violations were on average largest for Building System variants S3 and S4 and smallest for variants S1 or S5.

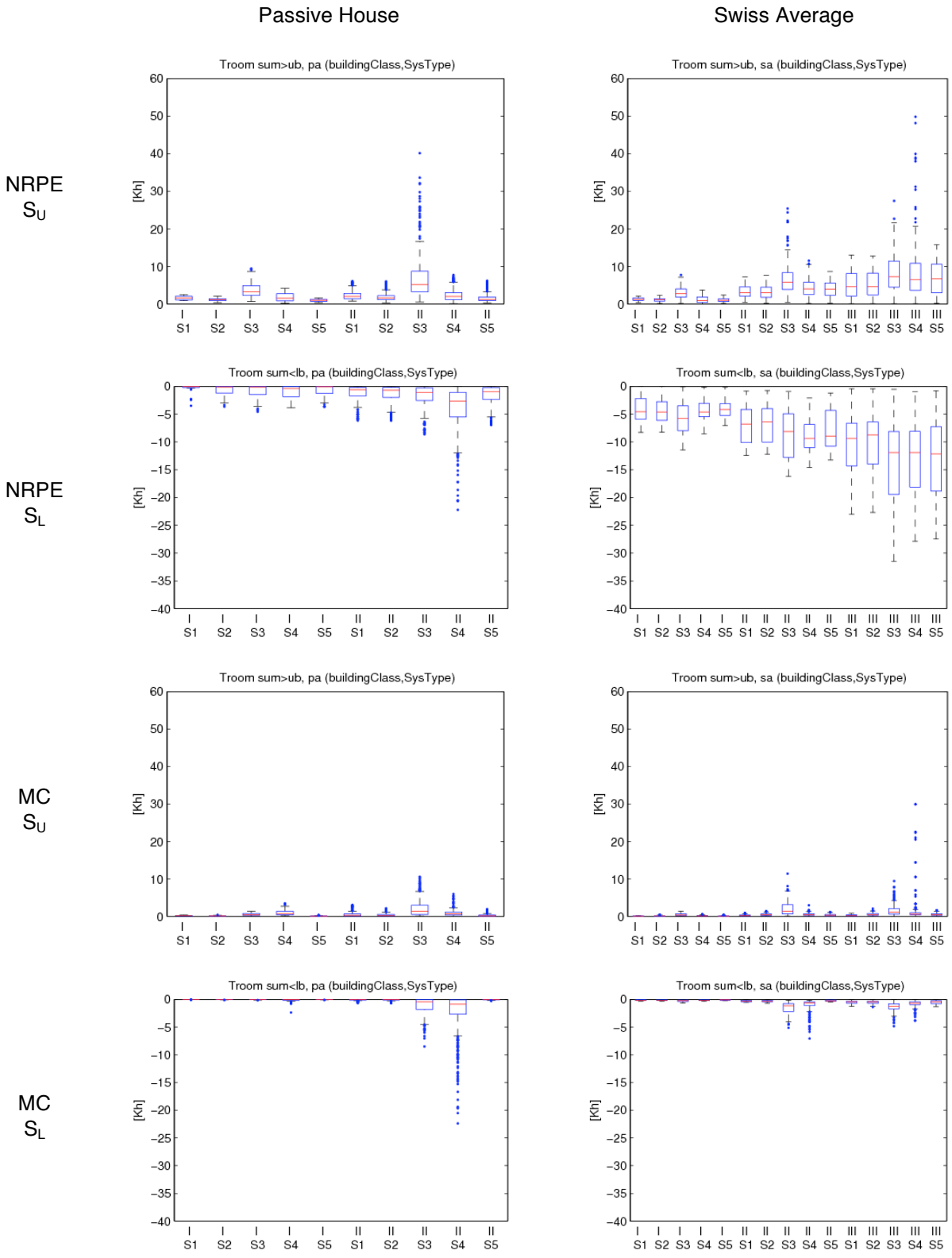

Figure 7.6: Overview of thermal comfort violations in the Performance Bound simulations. NRPE: Optimization was done for Non-Renewable Primary Energy usage; MC: optimization was done for Monetary Cost; S_U, S_L: annual sums of Kelvin-hours (Kh), measuring deviations of the room temperature above the comfort range's upper bound, respectively below its lower bound; I-III: Buildings Classes; S1–S5: Building System variants. For each Cost Function were considered Experiments Sets E1–E6, respectively. Each box shows statistics from all simulated cases for the respective Cost Function, Buildings Class, Building Standard, and Building System variant.

Buildings Class: The violations increased through Buildings Classes I to III.

Cost Function: Both S_U and S_L were smaller in the MC as compared to the NRPE simulations

A closer analysis showed that the found S_U and S_L values were typically caused by many small deviations < 0.1 K rather than a few large ones (Appendix D.7).

7.3.4 Potential Assessment

Table 7.10 summarizes the results from the savings potentials analysis of the four rule-based control algorithms RBC-1 to RBC-4. Shown are the average theoretical relative savings potentials (ATRSP) for annual total NRPE usage, plus median values of the annual S_U and S_L thermal comfort statistics. Each data point was computed from all simulated cases for the respective Building Standard, Building System variant, and Buildings Class.

From Table 7.10 can be seen that the ATRSP values varied widely. For the Passive House Building Standard the found range was 1%–45%. For the Swiss Average Building Standard and the Building System variants S1–S3 was obtained a range of 4% to 47%; for variants S4 and S5, where all four RBC algorithms showed large thermal comfort violations, the range was -7% to +33%.

The largest ATRSP were obtained for the Passive House Building Standard for RBC-1 (in 6 out of 10 cases = five Building System variants × two Buildings Classes) and RBC-4 (4 cases). For the Swiss Average Building Standard the largest ATRSP were obtained for RBC-1 (in 10 out of 15 cases), RBC-2 (4 cases) and RBC-4 (1 case). The smallest ATRSP were always obtained for RBC-3.

The smallest S_U median values were obtained generally for RBC-2 and RBC-3, and the largest ones for RBC-4. Only in one case (Passive House, Building System variant S3, Buildings Class I) the largest S_U median value was found to occur for RBC-1.

The least negative S_L median values were obtained for the Passive Houses for RBC-3, RBC-1 or RBC-4, and for the Swiss Average cases for RBC-3 or RBC-4. The most negative S_L median values were mostly obtained for RBC-2.

Building Standard: For RBC-1, RBC-3 and RBC-4 the ATRSP were generally larger for the Passive House as compared to the Swiss Average cases. For RBC-2 the opposite was generally found to be the case, except for Building System variant S5 and Buildings Class II. The S_U median values were in general smaller for the Passive Houses as compared to the Swiss Average cases; exceptions occurred for the RBC-4 algorithm and Buildings Class I for all Building System variants, and in several cases for variant S3. The S_L statistics were in all cases more favorable for the Passive House as compared to the Swiss Average Building Standard.

Building System variant: For the Passive House Building Standard the smallest ATRSP were always obtained for variant S4. The largest ones were obtained for RBC-1, RBC-2 and RBC-4 always for variants S1, and for RBC-3 always for variant S5. Forthe Swiss Average Building Standard we compare only the variants S1–S3 that showed comparable levels of thermal comfort violations: the smallest ATRSP were obtained for variant S2 (Buildings Classes I and II), or for variant S3 (Classes II+III); the largest ASRP were always found for variant S1. All in all, thermal comfort violation levels were comparable for variants S1–S3, but clearly larger for variants S4 and S5.

Buildings Class: For the Passive House Building Standard and Class I were always obtained smaller ATRSP values as compared to Class II. For the Swiss Average Building Standard and algorithms RBC-1, RBC-2, and RBC-4 the ATRSP generally increased through Classes I to III (the only exceptions occurred for RBC-2 and Building System variant S5, and RBC-4 and Building System variant S1, where the largest ATRSP were obtained for Class II, respectively). Ranking by

Building System	*Statistic*	*Buildings Class*	*Passive House*				*Swiss Average*			
			RBC1	*RBC2*	*RBC3*	*RBC4*	*RBC1*	*RBC2*	*RBC3*	*RBC4*
S1	*(X-PB)/X*	*I*	40	29	12	39	30	30	9	21
	[%]	*II*	42	35	16	45	39	38	10	40
		III	–	–	–	–	47	42	7	39
	S_U	*I*	1	0	2	70	1	0	3	4
	[Kh]	*II*	6	1	3	87	19	3	5	255
		III	–	–	–	–	574	4	8	3980
	S_L	*I*	-2	-5	-2	-8	-54	-57	-39	-42
	[Kh]	*II*	-19	-20	-11	-17	-61	-65	-44	-64
		III	–	–	–	–	-86	-92	-56	-61
S2	*(X-PB)/X*	*I*	32	25	9	29	26	26	7	16
	[%]	*II*	35	31	12	36	34	35	8	34
		III	–	–	–	–	41	39	6	39
	S_U	*I*	0	0	2	15	1	0	2	4
	[Kh]	*II*	3	1	2	12	17	2	4	30
		III	–	–	–	–	252	4	7	1181
	S_L	*I*	-7	-15	-7	-13	-59	-64	-44	-46
	[Kh]	*II*	-20	-27	-12	-21	-61	-68	-46	-57
		III	–	–	–	–	-77	-90	-57	-72
S3	*(X-PB)/X*	*I*	32	22	6	29	28	28	7	16
	[%]	*II*	35	30	8	31	34	35	5	26
		III	–	–	–	–	37	38	4	27
	S_U	*I*	20	10	8	107	12	11	6	8
	[Kh]	*II*	24	10	9	52	22	8	7	81
		III	–	–	–	–	335	6	7	1624
	S_L	*I*	-7	-17	-3	-1	-75	-80	-53	-56
	[Kh]	*II*	-23	-30	-8	-7	-75	-94	-56	-60
		III	–	–	–	–	-107	-140	-72	-80
S4	*(X-PB)/X*	*I*	21	10	1	26	19	18	1	12
	[%]	*II*	28	22	5	28	27	27	2	19
		III	–	–	–	–	31	28	1	14
	S_U	*I*	4	1	1	140	6	4	1	7
	[Kh]	*II*	15	5	3	220	28	7	4	394
		III	–	–	–	–	346	6	5	3229
	S_L	*I*	-66	-140	-13	-17	-517	-569	-338	-343
	[Kh]	*II*	-162	-228	-46	-44	-674	-875	-455	-497
		III	–	–	–	–	-925	-1157	-651	-618
S5	*(X-PB)/X*	*I*	34	27	15	31	28	28	12	19
	[%]	*II*	36	34	18	38	31	32	6	27
		III	–	–	–	–	33	30	-7	29
	S_U	*I*	1	0	6	68	2	0	9	15
	[Kh]	*II*	19	2	15	69	78	15	25	108
		III	–	–	–	–	550	23	42	1366
	S_L	*I*	-12	-29	-23	-26	-1101	-1855	-610	-643
	[Kh]	*II*	-70	-120	-48	-63	-1624	-1808	-1090	-1560
		III	–	–	–	–	-3351	-3460	-1948	-2918

Table 7.10: Overview of average theoretical relative savings potentials ([X-PB]/X) and of median values of two thermal comfort indicators (S_U, S_L) as obtained for the rule-based control algorithms RBC1–RBC4. Savings potentials refer to the annual total Non-Renewable Primary Energy (NRPE) usage. X: NRPE usage by a given RBC algorithm; PB: Performance Bound. S_U and S_L give annual sums of Kelvin-hours (Kh) and measure deviations of the room temperature above the comfort range's upper bound, respectively below its lower bound. For each controller were considered Experiments Sets E1–E3, respectively. Individual numbers were derived from all simulated cases for the respective Building System variant, Buildings Class, Building Standard, and control algorithm.

Buildings Class showed a less clear pattern for RBC-3 where ATRSP values did not differ much between Classes. In almost all cases and independently of Building Standard the S_U and S_L median values indicated increasing levels of thermal comfort violations with increasing Class number.

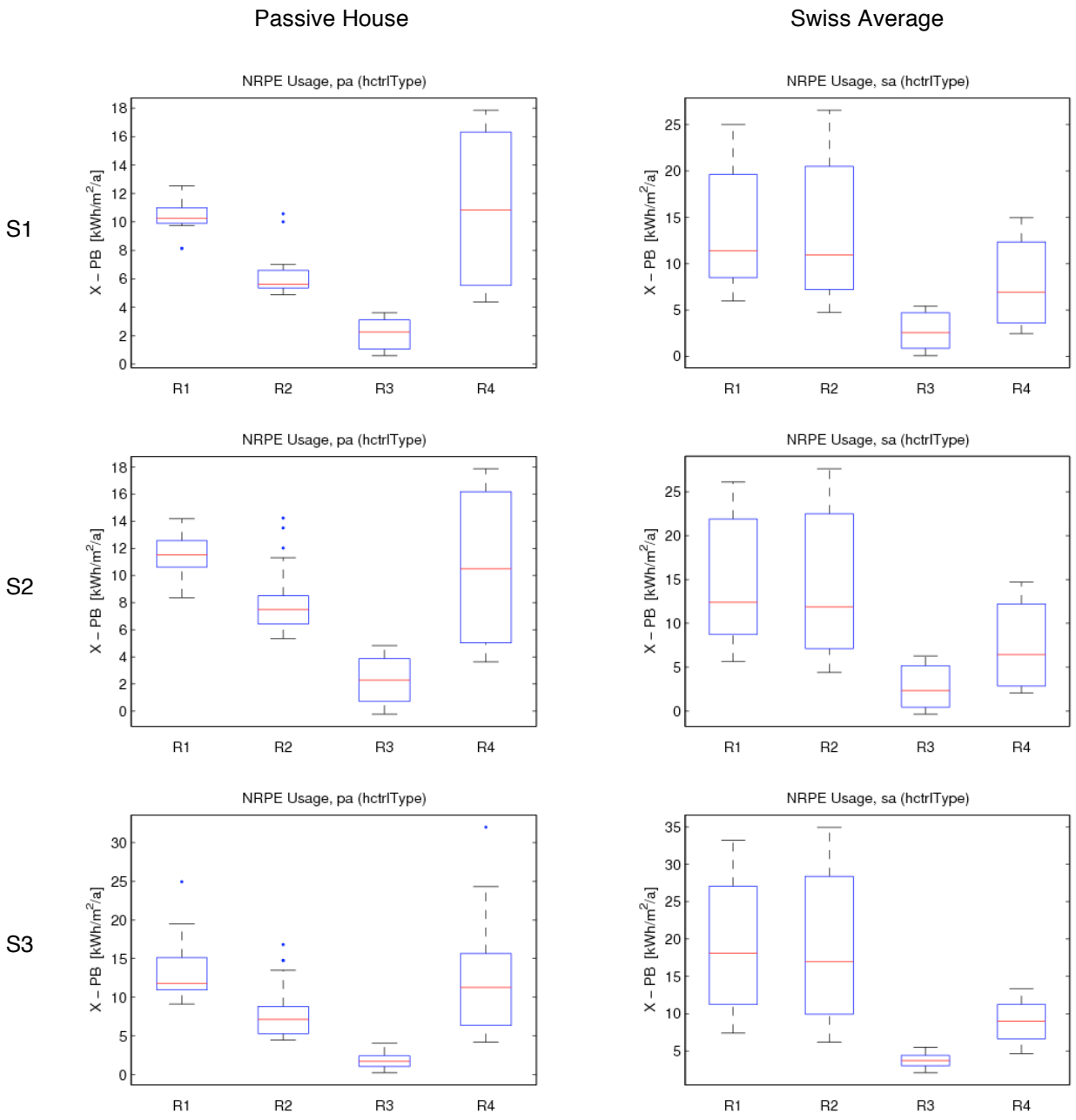

Figure 7.7: Overview of absolute theoretical savings potentials (X-PB) for the rule-based control algorithms RBC1–RBC4 (abbreviated as R1–R4) for Building System variants S1–S3 and Buildings Class I. The savings potentials refer to Non-Renewable Primary Energy (NRPE) usage. X: NRPE usage by RBC algorithm; PB: Performance Bound. For each control algorithm were considered Experiments Sets E1–E3, respectively. Shown are statistics from all simulated cases for the respective Building System variant, Building Standard and control algorithm. Note the different y-axis scalings.

The found absolute savings potentials for Building System variants S1–S3 and Buildings Class I are summarized in Figure 7.7. It can be seen that for both Building Standards the smallest absolute savings potentials were always obtained for RBC-3, followed by RBC-2 for the Passive House and RBC-4 for the Swiss Average cases. The potentials were always higher for the Swiss Average as compared to the Passive House Building Standard. The data also showed a high case-to-case variability, in particular for RBC-4 for the Passive House and for RBC-1 and RBC-2 for the Swiss Average cases. Further results on absolute and relative theoretical savings potentials can be found in Appendix E.

Building System	*Buildings Class*	*Passive House*			*Swiss Average*		
		N	*RBC3-PB [kWh/m²/a]*	*(RBC3-PB)/RBC3 [%]*	*N*	*RBC3-PB [kWh/m²/a]*	*(RBC3-PB)/RBC3 [%]*
S1	*I*	16 (16)	0.8–3.3	5–22	12 (16)	1.1–5.3	3–19
	II	112 (112)	1.6–5.6	6–29	31 (48)	2.6–6.3	5–21
	III	–	–	–	24 (64)	3.0–7.8	5–28
S2	*I*	32 (32)	0.4–4.5	1–17	20 (32)	0.6–6.1	1–17
	II	224 (224)	1.2–6.6	4–22	59 (96)	2.2–6.2	3–17
	III	–	–	–	45 (128)	3.0–7.6	4–19
S3	*I*	32 (32)	0.8–2.7	2–11	15 (32)	2.9–4.6	6–12
	II	223 (224)	1.0–4.4	2–14	40 (96)	2.7–4.4	4–11
	III	–	–	–	18 (128)	2.1–5.9	3–16
S4	*I*	23 (32)	-0.1–1.0	-1–4	4 (32)	0.5–1.2	2–5
	II	117 (224)	-0.1–2.5	0–9	0 (96)	–	–
	III	–	–	–	0 (128)	–	–
S5	*I*	20 (32)	0.6–8.2	3–27	0 (32)	–	–
	II	90 (224)	0.9–8.1	2–23	0 (96)	–	–
	III	–	–	–	0 (128)	–	–

Table 7.11: Ranges (10^{th}–90^{th} percentile) of absolute and relative theoretical savings potentials for the rule-based controller RBC3. All numbers refer to annual total Non-Renewable Primary Energy (NRPE) usage. Statistics refer to the subsets of cases from Experiments Sets E1–E3 for which the RBC3 simulations satisfied the condition "S_U < 50 Kh and S_L > -50 Kh" for the respective Building System variant, Buildings Class, and Building Standard. S_U and S_L are annual sums measuring deviations of the room temperature above the comfort range's upper bound, respectively below its lower bound. N: sample size (numbers in brackets give the number of all simulated cases from Experiments Sets E1–E3, cf. Table 7.3). PB: Performance Bound.

Table 7.11 summarizes the obtained ranges for the absolute and relative savings potentials of the best performing RBC algorithm, RBC-3. Note the results shown refer to the subset of cases where violations for both, the upper and lower thermal comfort bound amounted to less than 50 Kh.

It can be seen that the smallest 10^{th} percentile values for the absolute and relative savings potentials were around zero. The highest 90^{th} percentiles were around 8 kWh/m²/a and 28%, respectively. For Building System variants S4 and S5 and the Swiss Average Building Standard there were practically no cases available that satisfied the thermal comfort requirements.

Building Standard: The 90^{th} percentiles for the absolute (respectively relative) savings potentials were for the Passive House cases mostly below (respectively above) those for the Swiss Average Building Standard.

Building System variant: The highest 90^{th} percentile values for the absolute savings potentials were obtained for the Passive House Building Standard for variant S5 followed by variant S2, and for the Swiss Average Building Standard for variant S2 or S1. The highest 90^{th} percentiles for the relative savings potentials occurred for variants S1 or S5 (Passive House) and S1 (Swiss Average).

Buildings Class: In almost all cases the 90^{th} percentiles for the absolute and relative savings potentials increased with Buildings Class number.

The average absolute (respectively relative) savings potentials for the Passive House Building Standard, Buildings Classes I+II and Building System variants S1–S5 for the cases shown in Table 7.11 were 2.6 kWh/m²/a (respectively 9.2%). The average 10^{th}–90^{th} percentile intervals resulting from Table 7.11 were 0.7–4.7 kWh/m²/a (respectively 2–18%).

For the Swiss Average Building Standard, Classes I+II and variants S1–S3 the average savings potentials for the cases shown in Table 7.11 were 3.8 kWh/m²/a (9.7%). The average intervals were 2.0–5.5 kWh/m²/a (4–16%).

7.3.5 Comparison

Figure 7.8 draws together the results from the previous Sections by juxtaposing the average relative effects due to the various changes in boundary conditions for control with the RBC-3 average relative savings potentials.

It can be seen that generally the variations in the Ventilation Strategy showed the largest effect. On average over Buildings Classes I+II and Building System variants S2–S4 the found relative changes amounted to ~27% for the Passive House and ~18% for the Swiss Average Building Standard, respectively.

The second and third most important effects for Buildings Class I (top panels in Figure 7.8) were obtained for the RBC-3 savings potentials (~9% on average over variants S1–S5) and the variations in the thermal Comfort Range width (~8%), respectively .

Figure 7.8: Comparison of average relative changes in annual total Non-Renewable Primary Energy (NRPE) usage due to variation in different factors (1–4) with average relative savings potentials for the rule-based control algorithm RBC-3 (cf. Table 7.11). I, II: Buildings Class; S1–S5: Building System variant; 1 – Effect of using alternative Cost Functions for control cost optimization and evaluation (cf. Table 7.5); 2 – Effect of allowance for night/weekend set-back (cf. Table 7.6); 3 – Effect of change in Thermal Comfort range width (cf. Table 7.7); 4 – Effect of different Ventilation Strategies (cf. Table 7.8). *: Value not available (Building System variant S1) or intentionally omitted (excessive thermal comfort violations, variants S4 and S5).

For Buildings Class II and the Passive House Building Standard (bottom left panel in Figure 7.8) the second most important effect after the choice of Ventilation Strategy was given by the thermal Comfort Range width variations (~12%). The third largest relative deviations were obtained for the RBC-3 savings potentials (10%).

For Buildings Class II and the Swiss Average Building Standard (bottom right panel) second came the set-back effect (~14%), followed by the thermal Comfort Range width variations (13%) and the RBC-3 savings potentials (~9%).

7.4 Discussion

7.4.1 Key Assumptions

The results presented here depended on a series of key assumptions (Table 7.1) whose variation could affect the found sensitivities (Section 7.3.1–2) and savings potentials (Section 7.3.4), as well as the quantitative ranking of all results (Section 7.3.5). Here we comment on four selected issues:

A first key factor that determined our results was the dimensioning of the building system components. It can be expected that the used scant dimensioning procedure (Section 2.3.2) lead to rather conservative estimates of the cost savings due to night/weekend set-backs (Figure 7.3, Table 7.6). This is because the smaller is the maximum available heating power the slower can the system recover the room temperature from a set-back without thermal comfort violations, i.e. the smaller becomes the possible set-back amplitude and the associated cost savings.

Secondly, our comparison of different thermal comfort requirements assumed a difference of 1 ºC in comfort range width during winter and of up to 2 ºC during summer (Figure 2.3). The magnitude of the found effects (Figure 7.4, Table 7.7) clearly depended directly on this particular assumption.

Thirdly, the found large differences in costs when using alternative ventilation strategies (Figure 7.5, Table 7.8) depended strongly on the chosen (in the case of CO_2-based control: occupancy dependent) air change rates. This was because the latter determine the costs for fan operation. A closer analysis showed that in particular for the CO_2-based control the assumed air change rate for unoccupied rooms was probably too small to guarantee proper mixing of the air (s.a. Section 5.4.1). Moreover, the CO_2-based control yielded generally higher CO_2-concentrations than the non-air quality controlled ventilation (Appendix B.4) such that, again, higher air change rates would have been required to obtain a comparable air quality for the two ventilation strategies.

One could therefore argue that the obtained cost savings are probably larger than what could be attained in practice. However, our simulations also assumed a simplified linear (instead of quadratic or cubic) increase of energy usage with ventilation rate. This probably lead to a counteracting effect, an underestimation of the energy usage by the non-air quality dependent control and thus also of the energy savings due to its replacement by CO_2-based control.

Finally, in all our simulations the maximum room illuminance levels were not restricted, assuming that occupants could obtain glare protection through manual adjustment of an internal blind. For all control algorithms this translated into the possibility of keeping the blinds at any time fully open in order to make maximum use of solar gains. Quite differently, if we had assumed a need for glare protection this would have made it necessary for the controllers to use the blinds for blocking of direct solar irradiation in case of a room being occupied, with corresponding limitations in maximum possible solar gains. The overall effect on the sensitivities and savings potentials considered here is far from obvious and can probably only be estimated with the aid of further simulations.

Note that all relative savings potentials reported here refer to annual *total* NRPE usage, i.e they included energy usage for heating, cooling, ventilation and lighting. Higher relative savings would have been obtained if we had excluded the lighting costs from our calculations, as this has often been the case in other studies.

7.4.2 Performance of RBC Strategies

The performance of the four RCB algorithms differed largely in terms of both, NRPE usage and comfort violations (Table 7.10, Figure 7.7).

The amount of comfort violations in the RBC simulations provided a measure of the algorithm's (in)adequacy for the control task at hand. The fact that the PB showed throughout small amounts of comfort violations (Figure 7.6) suggests that in spite of the used scant dimensioning procedure the available control power was in principle sufficient to achieve the required thermal comfort, at least for the cases wher no extra lighting was used for heating.

All four RBC algorithms considered in this study were actually tailored to the comparatively fast reacting Building System variants S1–S3. It was thus no surprise that the largest comfort violations were found to occur for Building System variants S4 and S5 (Table 7.10) that involved two very slow components in the form of floor heating and TABS, respectively. Specialized control algorithms for these systems are available (e.g., [2]) and should be used in future work.

The differences in savings potentials between the RBC algorithms were mainly due to the use of different approaches for blinds control (cf. Chapter 3). The particularly good performance of the RBC-3 algorithm as compared to the other three algorithms was due to both, ideal luminance control with the aid of the blinds, and the allowance for time-continuous as well as unrestricted (no fixed blind positions) variation of the blind transmission value.

The importance of the time-continuous adjustment becomes apparent in the comparison with algorithm RBC-4 (e.g., Figure 7.7) that was identical to RBC-3, except that in RBC-4 the blind movement was restricted to once per hour.

In practice, occupants will not accept a time-continuous adjustment of the blinds as it was assumed in the RBC-3 algorithm. Also, the assumed luminance control by blinds is typically not feasible in practice. RBC-3 was considered in this study mainly because it had exactly the same freedom in blind movement as the PB calculations, such that its savings potentials provided a very conservative measure of the utility of predictive control. The RBC-3 results indicate substantial energy savings potential thanks to the use of electrochromic windows that one day might enable more or less continuous control of solar gains in a manner that could be accepted by most users.

An alternative to the usage of the RBC-3 algorithm for assessing the potential of predictive control would have been to compare the PB with instantaneous optimal control. The latter uses the currently cheapest control action to keep the room temperature, illuminance and air quality within the prescribed comfort range, without using any information on past control actions, disturbances or states. This control strategy was investigated in [1] and was found to perform clearly worse then RBC-3. Indeed, we are not aware of any other non-predictive control algorithm that performs better than RBC-3. Again, this suggests that our RBC-3 results give a conservative estimate of the potential of predictive control.

The practical feasibility of all investigated measures for reducing NRPE usage (Figure 7.8) can be expected to vary strongly from case to case. For instance, energy savings due to a wider thermal comfort range imply a reduction in thermal comfort that may not be readily accepted by all occupants, or the introduction of air-quality control for ventilation makes additional sensors and control equipment necessary. For the many found cases with substantial savings potentials (Figure 7.7, Table 7.11) the use of predictive control could present a comparatively cost-effective option to reduce control costs, given that appropriate (cf. Section 1.3) control algorithms to exploit these potentials become available.

7.4.3 Problems And Limitations

Our assessment of RBC savings potentials was to some extent distorted by the thermal comfort violations in the RBC simulations and by the use of electrical lighting for heating in the PB simulations. However, there are two reasons why we believe that the savings potentials were in general under- rather than overestimated:

Firstly, if we had assumed a more ample dimensioning of the building energy systems the RBC-3 algorithm would have used the additionally available heating and cooling power to avoid the thermal comfort violations at the expense of additional energy usage. Indeed, the RBC-3 average savings potentials for the sub-sample of cases with small comfort violations (Table 7.11) were found to be as large as, or slightly larger than, the whole-sample average values reported in Table 7.10 (analyses not shown).

Secondly, the use of electrical lighting for heating in the PB simulations generally tended to inflate the total cost since light is the most expensive heating source. If additional heating power for the cheaper heating sources would have been available, the PB optimization procedure would have recognized that and would have yielded lower costs than reported here.

However, an interesting exception should be noted that was detected in some cases for the Building System variant S4: the PB calculations were found to use electric lighting simultaneously with floor heating while the latter was not fully turned on. The reason related to the delayed response of the floor heating system and the associated slow increase of room temperature. The longer warming-up phase resulted into higher transmission losses through the building envelope and thus proved overall less economic than the more rapid heating with the aid of electric lighting in the PB calculations. This result suggests that in some instances the installation of fast auxiliary devices (e.g., electrical heating) can be appropriate to improve the overall efficiency of slow heating systems.

A distinctive feature of our results was that the effects of varying boundary conditions for control (Section 7.3.1) were investigated using strictly the PB. Accordingly, our results only state what differences could be expected to occur if perfect control would apply, whereas the results obtained in practice will also depend on the properties of the particular control algorithm employed. It can be expected that the more the control costs of a given algorithm deviate from the PB (cf. Figure 7.7) the less representative will be the theoretical estimates reported in this work.

Finally note that our study did not consider entire buildings, but only isolated building zones. Following a commonly used procedure [3] the whole-building control costs can be estimated as a weighted average of the individual zone costs. Since Buildings Class I represents zones with Façade Orientations N and S, and Buildings Class II stands for Façade Orientations SE and SW our results can be used to estimate sensitivities or savings potentials for the quite frequent case of buildings with a rectangular ground plan and large N- and S-facing facades: depending on the building's exact geometry (number of corner vs. number of non-corner offices) the whole-building values should lie somewhere between the Class I and Class II results.

7.5 Conclusions

From our investigation of the four rule-based, non-predictive control algorithms RBC-1 to RBC-4 we conclude that the largest savings potentials for annual total Non-Renewable Primary Energy (NRPE) usage occur, in descending order, for the algorithms RBC-1, RBC-4 and RBC-2. The algorithm RBC-3 shows the best energetic performance and yields the smallest NRPE savings potentials. Average differences between different control strategies are large, clearly showing that control is essential in energy efficient building operation.

Relative savings potentials for RBC-3 are generally higher for the Passive House as compared to the Swiss Average Building Standard, and they are on average smallest for Buildings Class I (most frequent buildings cases), larger for buildings Class II (less frequent cases) and largest for Buildings Class III (exotic cases).

Average absolute and relative savings potentials for the Passive House Building Standard, the Buildings Classes I+II, and the Building System variants S1–S5 amount to 2.6 kWh/m^2/a or 9.2%, respectively. For the Swiss Average Building Standard, Classes I+II and variants S1–S3 the average savings potentials are 3.8 kWh/m^2/a (9.7%). Savings potentials are highly case-dependent. In 10% of the cases investigated the absolute (relative) savings potentials exceed 4.7 kWh/m^2/a (18%) for the Passive House and 5.5 kWh/m^2/a (16%) for the Swiss Average Building Standard.

Theoretical average relative savings potentials for the RBC-1 and RBC-4 controllers (building classes I and II, building system variants S1–S5) are 34% and 33% for the PA, and 30% and 23% for the SA building standard, respectively.

The found average relative savings potentials for RBC-3 were typically smaller than the effect obtained due to the introduction of (i) ventilation with air quality control. The RBC-3 average relative savings potentials were comparable to the effects of (in descending order of importance): (ii) a widening of the thermal comfort range by ~1.5 ºC, (iii) the allowance for night/weekend room temperature set-backs, and (iv) the choice of alternative cost functions for optimization of control costs.

Sensitivity to (i) is smaller for the Swiss Average as compared to the Passive House Building Standard; smallest for the Building System variant S3 (ventilation-only system); and it decreases with Buildings Class number. For the sensitivities to factors (ii)–(iv) hold exactly the opposite trends, with Building System variant S3 showing the highest sensitivity from all five Building System variants investigated.

Clearly, somewhat different results could have been obtained under other assumptions than the specific ones adopted in the present study. The relevance of our findings draws from the high quality of the used models and algorithms, the careful selection of building cases, technical systems and operation types that defined our experimental set-up, and the wide range of situations covered in our large-scale, systematic simulation study.

Some problems occurred due to (i) the unintended usage of electrical lighting for heating in the Performance Bound simulations, (ii) partially large thermal comfort violations by the rule-based control algorithms due to scant dimensioning of the building technical systems, and (iii) the restricted applicability of the rule-based algorithms for Building System variants S4 and S5, in particular for the Swiss Average Building Standard. Nevertheless, our estimates of NRPE savings potentials are in general on the conservative side.

Our analysis was restricted to investigating the influence of but three selected out of several factors that defined the individual buildings cases' responses: Building Standard, Building System variant, and Buildings Class. A more detailed analysis considering the effect of all factors involved could provide a better insight into the mechanisms responsible for the encountered, wide range of sensitivities and potentials. Such work, centered on the savings potentials of the RBC-3 algorithm, is reported in the following Chapter.

7.6 References

[1] Gyalistras, D. (2009). Gyalistras, D., & Fischlin, A., Morari, M., Jones, C.N., Oldewurtel, F., Parisio. A., Frank, T., Carl, S., Dorer, V., Lehmann, B., Wirth, K., Steiner, P., Schubiger, F., Stauch, V., Tödtli, J., Gähler, C. & Gwerder, M. (2009). Saving energy by improved building control. Poster presentation, Annual Meeting of The Alliance for Global Sustainability: Urban Futures: the Challenge of Sustainability, 26-29 January 2009, ETH Zurich, Switzerland. See also http://www.opticontrol.ethz.ch/Lit/Gyal_09_Poster-AGSAM09.pdf.

[2] J. Tödtli et al.: TABS- Control, Steuerung und Regelung von thermoaktiven Bauteilsystemen. Faktor Verlag Zurich (Switzerland); 2009. ISBN: 978-3-905711-05-9.

[3] SIA Design Tool „Klimatisierung“ based on SIA standards 380/4 and 382/1.

This page has intentionally been left blank.

Chapter 8

ANALYSIS OF SAVINGS POTENTIALS AND PEAK ELECTRICITY DEMAND

by Dimitrios Gyalistras, Katharina Wirth and Beat Lehmann

Cite as:

Gyalistras, D., Wirth, K. & Lehmann, B. (2010). Analysis of savings potentials and peak electricity demand. In: Gyalistras, D. & Gwerder, M. (eds.): *Use of weather and occupancy forecasts for optimal building climate control (OptiControl): Two years progress report*. Terrestrial Systems Ecology ETH Zurich, Switzerland and Building Technologies Division, Siemens Switzerland Ltd., Zug, Switzerland, pp 107–134. ISBN 978-3-909386-37-6.

8.1 Introduction

In the previous chapter the performances of the four rule-based control strategies RBC-1 to RBC-4 were compared among each other and with the Performance Bound (PB). RBC-3 turned out to be the best performing strategy that generally showed the lowest annual total Non-Renewable Primary Energy (NRPE) usage and the best thermal comfort statistics (Table 7.10).

In the present Chapter we analyze in more detail the differences in NRPE usage between the RBC-3 results and the PB. We focus on Buildings Classes I and II of Building System variants S1 to S3 because for these cases thermal comfort violations with the RBC-3 strategy stayed within a reasonable range (Table 7.10, Appendix E).

The differences or "savings potentials" represent the *maximum possible* (i.e., theoretical) savings that could be achieved by some better strategy than RBC-3. Since RBC-3 is the best performing non-predictive control strategy known to us any cases with large savings potentials indicate situations were major improvements might be only possible with the aid of predictive control.

The aims of the present Chapter are

(i) to identify key factors associated with large savings potentials for the strategy RBC-3,
(ii) to provide some insight on the mechanisms responsible for these potentials, and
(iii) to investigate the effect of control strategy choice on peak electricity demand.

The analyses (i) and (ii) are done with the following hypotheses on the possible added value of advanced/predictive control in mind:

- "The importance of advanced control increases with the complexity of the building technical system under consideration"
- "Intelligent control is particularly favorable in the presence of high energy fluxes"
- "Predictive control is more useful for 'heavy' as opposed to 'light' buildings"
- "Predictive control is particularly advantageous during the transition seasons"

With analysis (iii) we introduce peak electricity demand as an additional quantitative criterion for the assessment of controller performance next to the two dimensions NRPE usage and comfort. Peak electricity demand can be expected to become increasingly important for electricity companies and building owners with increasing use of electrical energy for heat/cold generation (e.g. heat pumps), of co- or polygeneration in buildings, and of renewable energy sources.

In all our simulations we have been considering an energy system that uses electricity for heat/cold production, ventilation and lighting (Table 2.5). Here we aim at providing a first insight on the behavior of the PB and of the RBC-3 controllers with regard to electric power consumption based on the analysis of selected cases. Note that peak electricity demand has not been considered in the formulation of the control strategies so far.

The chapter is structured as follows: In Section 8.2 we describe the data used and the analysis procedures employed. Section 8.3 first gives an overview of the database and then proceeds with a statistical analysis of the found savings potentials, with the aim of answering (i). Then we identify representative cases that are subsequently analyzed in more detail in order to shed light on (ii) and (iii). Section 8.4 discusses the results, followed by the conclusions in Section 8.5.

8.2 Material & Methods

8.2.1 Data

All analyses were based on the annual PB and RBC-3 simulations described earlier in Chapter 7. As shown in Chapter 7, due to the used scant dimensioning procedure the strategy RBC-3 was found to perform only poorly in terms of comfort for Buildings Class III and Building System variants S4 and S5 (see Table 7.11. Therefore these cases were excluded from the analysis.

The simulations analyzed were defined by the following settings/factors (cf. Table 7.1): Energy System: earth coupled heat pump plus mechanical (compression) chiller; Dimensioning Strategy: Scant; Cost Function: NRPE; Thermal Comfort: A_w (no set-back, wide comfort range); Ventilation Strategy: none for S1, V (non-air quality controlled ventilation) or W () for S2 and S3; Illuminance Comfort: Occupancy dependent, bright.

For the Passive House Building Standard the Buildings Classes I+II covered 128 cases: 4 Building Sites, 4 Façade Orientations, 2 Construction Types, 2 Window Area Fractions, and 2 Internal Gains Levels (see Table 7.1). For the Swiss Average Building Standard there were only 64 cases since with Buildings Classes I+II only one type of Window Area Fraction (low, "wl") was considered.

8.2.2 Analysis of Variance

Analysis of variance (ANOVA) is a statistical procedure to partition an observation into components due to explanatory variables or "factors". The latter are categorical variables that are used to distinguish a series of characteristics or "levels". We used ANOVA to analyze sources of variation in the savings potentials as follows:

The observations (Y) were given by the NRPE savings potentials, $Y_i = RBC3_i - PB_i$ $[kWh/(m^2a)]$, where the subscript i denotes the i-th case entering the analysis, $RBC3_i$ denotes the annual NRPE usage of the RBC-3 strategy for case i, and PB_i is the corresponding Performance Bound value.

The factors and factor levels considered for Building System variant S1 and the Swiss Average Building Standard were as follows: Building Site, S ∈ {LUG, MSM, SMA, WHW}; Façade Orientation, FO ∈ {N, S, SE, SW}; Construction Type, CT ∈ {h, l}; and Internal Gains Level, IGL ∈ {ih, il} (cf. Table 7.1). For Building System variant S1 and the Passive House Building Standard was considered in addition the factor Window Area Fraction, WAF ∈ {wh, wl}. For Building System variants S2 and S3 the above sets of factors were enhanced by the factor Ventilation Strategy, VS ∈ {V, W}.

We used ANOVA to establish one statistical model per Building Standard and Building System variant that estimated the Y_i as a function of the factor levels. As one example below is shown the model for the Passive House Building Standard and Building System variants S2 or S3:

$$Y_i = \mu + a_{(S_{(i)})} + b_{(FO_{(i)})} + c_{(CT_{(i)})} + d_{(IGL_{(i)})} + e_{(VS_{(i)})} + \varepsilon_i \qquad \text{Eq. 1}$$

Here, μ is the average of all cases considered in the analysis, $a_{(\cdot)}$–$e_{(\cdot)}$ are coefficient vectors denoting factor- and level-specific deviations (Δ) from μ, and ε denotes a residual term that accounts for unexplained variability.

The significance of a given factor was measured by the p-value of the null hypothesis that the factor has no effect, i.e. that the found differences between the coefficient vector elements for that particular factor were only due to a chance event. Large coefficient values in combination with a small p-value for a given factor suggest that variations in that factor are important in explaining deviations from the sample mean μ.

8.2.3 Analysis of Solar Gains

The savings potentials were also investigated as a function of solar gains and further variables by means of multiple linear regression.

The solar gain potential of each case entering the analysis was first estimated by means of the specific (with reference to floor area) solar gain area, defined as

$$S = \frac{gA_{win}}{A_{floor}} \qquad \text{Eq. 2}$$

where g is the window's solar gain factor (total solar heat transmittance), A_{win} is the total area of all transparent window parts, A_{floor} denotes the building zone's floor area.

For the absolute savings potentials, Y, was firstly considered a linear model of the form

$$Y_i = \alpha + \beta \cdot (S_i R_i) + \varepsilon_i \qquad \text{Eq. 3}$$

where α and β are the regression coefficients, R denotes the annual average of the hourly means of all relevant vertical global radiation components (up to two components for corner offices), and ε is the regression's error term.

Note that the term $S_i \cdot R_i$ accounts for the joint effect of the factors Building Site, Façade Orientation, and Window Area Fraction.

The above regression model (Eq. 3) was then stepwise enhanced by two binary explanatory variables, the Construction Type (light = 0, heavy = 1) and the Internal Gains Level (low = 0, high = 1).

8.2.4 Analysis of Peak Electricity Demand

Peak electricity demand is usually considered for a whole building but such values were not readily available from our simulations. In this study we therefore considered the electricity demand of the simulated individual rooms or building zones.

Our analysis was based on hourly mean electric power demand (EPD) values that were estimated from the hourly total delivered energy (DE) as follows:

$$DE_{(h)} = \sum_{i=1}^{nDevices} (NRPE_{i(h)} / f_{NRPE}) \; + \; DE_{Equip(h)} \qquad [Wh/m^2] \qquad \text{Eq. 4}$$

$$\overline{EPD}_{(h)} = DE_{(h)} / \Delta t \qquad [W/m^2], \;\; \Delta t = 1 \; [h] \qquad \text{Eq. 5}$$

According to Equation 4 the hourly DE for each device (index *i*; heat pump, chiller etc.) was calculated by dividing the device's hourly total NRPE usage with the conversion factor f_{NRPE} (see Table 2.6). The power demand of the office equipment (DE_{Equip}, see Figure 2.4, right) was also considered. EPD (Equation 5) was finally obtained by dividing DE by the length of the discrete time step used in the simulations, in this case one hour.

8.3 Results

8.3.1 Overview of Savings Potentials

Figure 8.1 shows the absolute savings potentials as a function of the corresponding PB values, separately for the Passive House (left, 128 cases) and the Swiss Average (right, 64 cases) Building

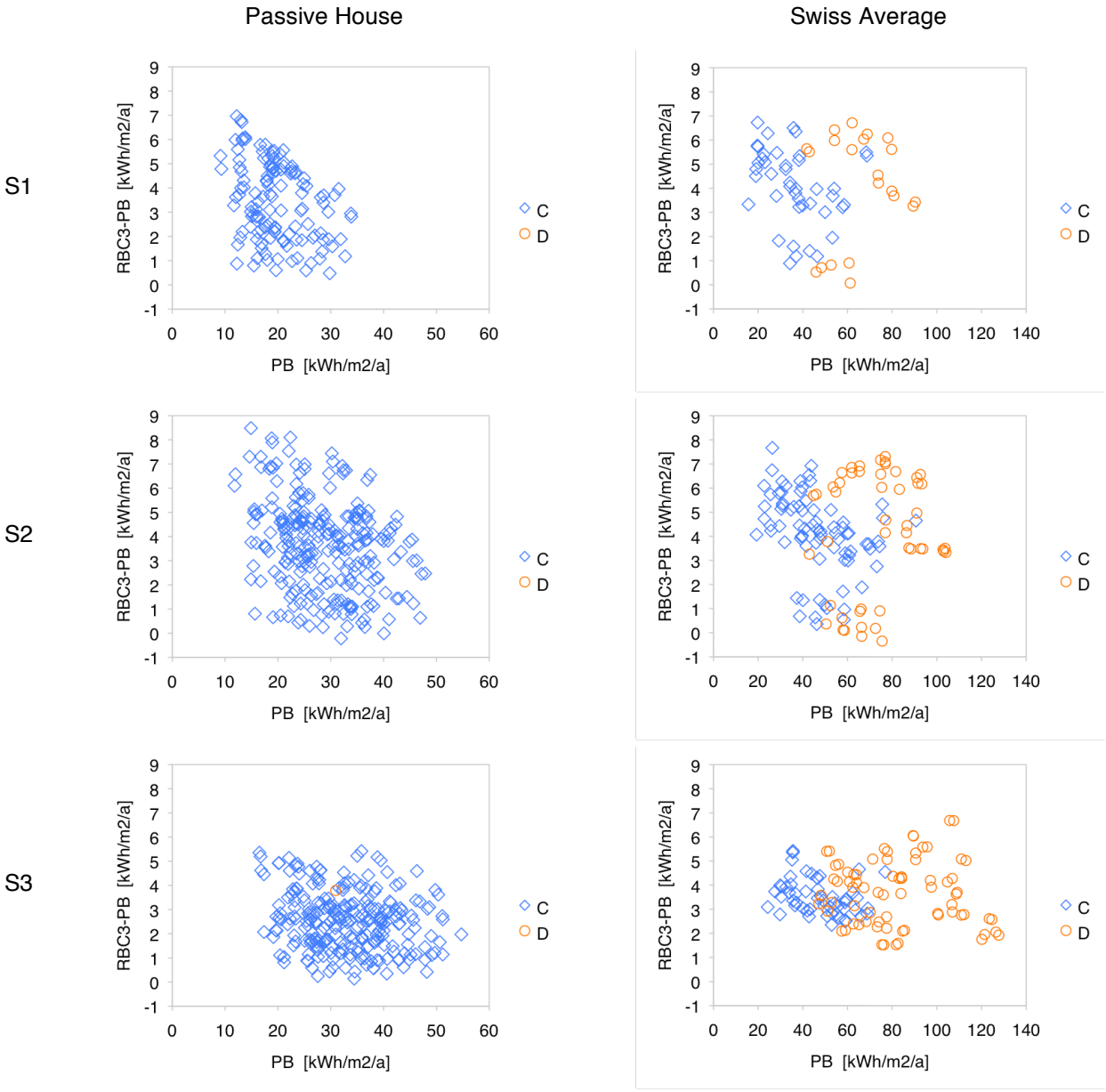

Figure 8.1: Comparison of Performance Bound (PB) values and absolute savings potentials for the Passive House (left) and the Swiss Average (right) Building Standards. S1–S3: Building System variant. C: RBC-3 simulations satisfying the thermal comfort requirement "S_U < 50 Kh and S_L > -50 Kh", where S_U and S_L are annual sums measuring deviations of the room temperature above the comfort range's upper bound, respectively below its lower bound; D: RBC-3 simulations with thermal discomfort (above requirement not satisfied).

Standards and for each of the Building System variants S1–S3. Data points involving RBC-3 simulations that did not satisfy the thermal comfort requirements (cases with amount of violations of the upper and lower comfort bound exceeding 50 Kh/a and/or falling below -50 Kh/a, respectively) are shown in orange.

It can be seen that in general a wide range of theoretical savings potentials was obtained for any given PB value.

Some systematic variation was found for the PB as a function of Building System variant: average PB values for the Passive House Building Standard and for the Building System variants S1, S2 and S3 amounted to 19.8, 28.7 and 33.1 kWh/(m^2a), respectively. For the Swiss Average Building Standard the corresponding numbers were 45.7, 56.8 and 67.7 kWh/(m^2a), respectively.

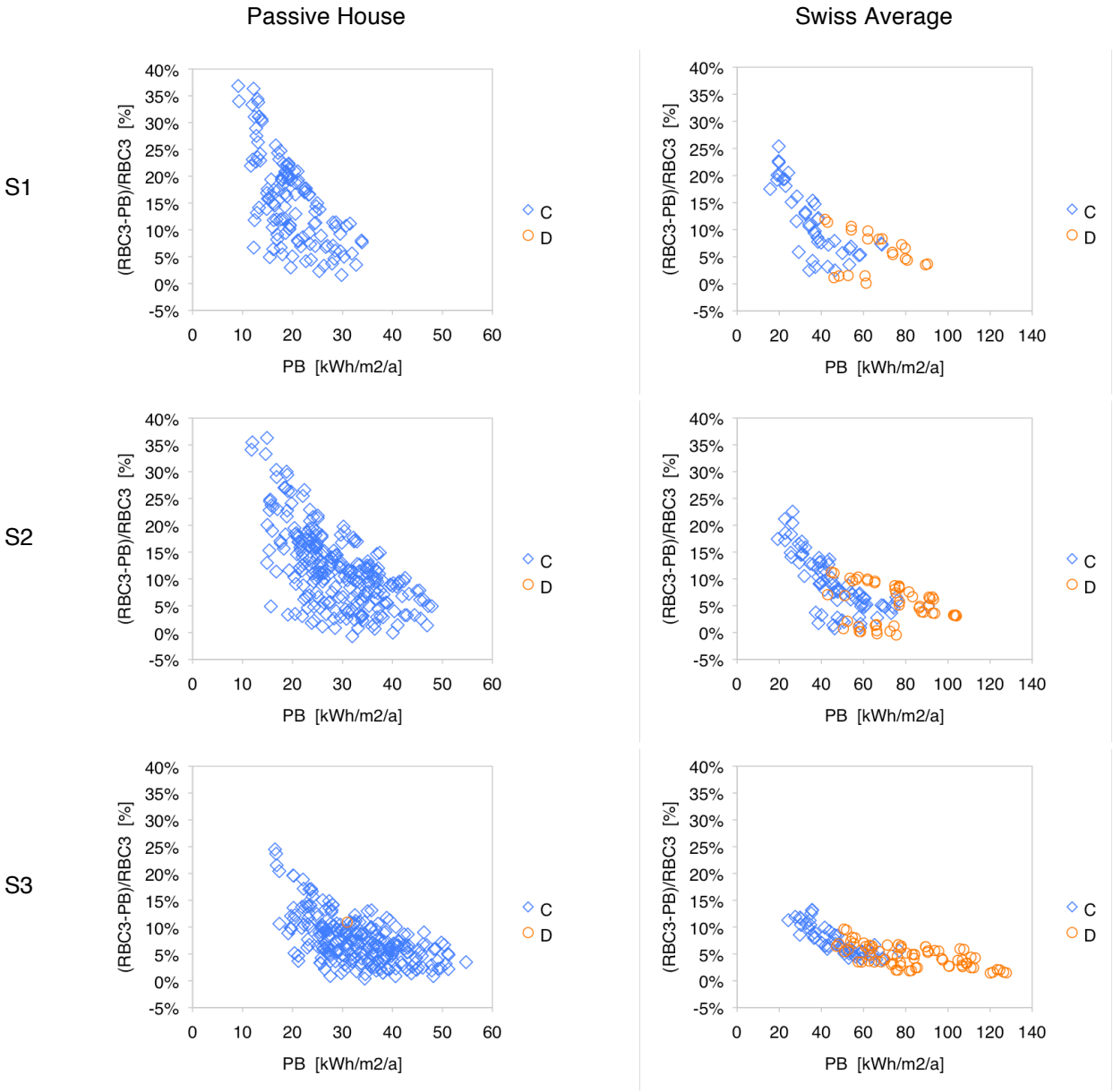

Figure 8.2: Same as Figure 8.1, but for relative savings potentials.

With regard to the savings potentials the largest values were found on average for variant S2, followed by S1 and then by S3: the mean potentials amounted to 3.6, 3.4 and 2.5 kWh/(m^{2}a) for the Passive Houses, and 4.1, 4.1 and 3.6 kWh/(m^{2}a) for the Swiss Average houses, respectively.

The largest found absolute savings potentials for the two Building Standards were 8.5 kWh/(m^{2}a) and 7.7 kWh/(m^{2}a), respectively. They both occurred for Building System variant S2 (Figure 8.1).

Figure 8.2 gives an overview of the relative savings potentials. It can be seen that they were generally larger for the Passive Houses than for the Swiss Average houses. The average relative savings potentials for Building System variants S1–S3 amounted for Passive Houses to 16%, 12% and 8%, and for Swiss Average houses to 10%, 8%, and 6% respectively. The largest relative savings potentials for the two Building Standards were found for Building System variant S2 and they amounted to 37% and 25%, respectively.

Since the absolute and relative saving potentials were positively correlated (not shown), and because in the end the absolute potentials are probably the most important ones, for all subsequent analyses we focused on the absolute figures.

8.3.2 Investigation of Key Factors

Figure 8.3 summarizes the coefficient vectors from the ANOVA for the two Building Standards and the three Building System variants considered. Several features can be discerned:

The factor Façade Orientation yielded in general the largest coefficient values. The only exception was the Swiss Average/S3 case (bottom right panel in Figure 8.3), where the orientation effect was found to be small and insignificant ($p = 0.19$). In all other cases strongly reduced savings potentials were obtained for the offices with N-orientated facades, whereas above-average potentials were obtained for the SW and SE corner offices.

The Building Site factor was less important, and its influence varied with Building System variant. For variants S1 and S2 and both Building Standards average savings potentials were found to be smallest for site SMA and largest for site WHW. For variant S3 the smallest average potential was obtained for site LUG, and the largest one for sites MSM (Passive House) and, again, WHW (Swiss Average).

The factor Construction Type showed opposite responses depending on Building Standard. In the Passive House cases heavy buildings showed a below-average, and light ones an above-average savings potential. For the Swiss Average cases exactly the opposite was found to be the case.

The factor Window Area Fraction was only relevant for the Passive House Building Standard (note, all Swiss Average cases entering the analysis had a low Window Area Fraction). A high Window Area Fraction was found to lead to above-average savings potentials.

With regard to the factor Internal Gains Level all statistical models showed enhanced savings potentials under high internal gains. The only exception was the Passive House/S3 case where this factor's influence was negligible and insignificant ($p = 0.76$).

The factor Ventilation Strategy was generally found to have small and/or insignificant effects. The only exception was the Passive House/S3 case, where the use of CO_2-controlled ventilation lead to slightly higher savings potentials as opposed to non-air quality controlled ventilation.

The total proportion of variance explained by the ANOVA models was 70–75% for Building System variants S1 and S2 and ca. 60% for variant S3.

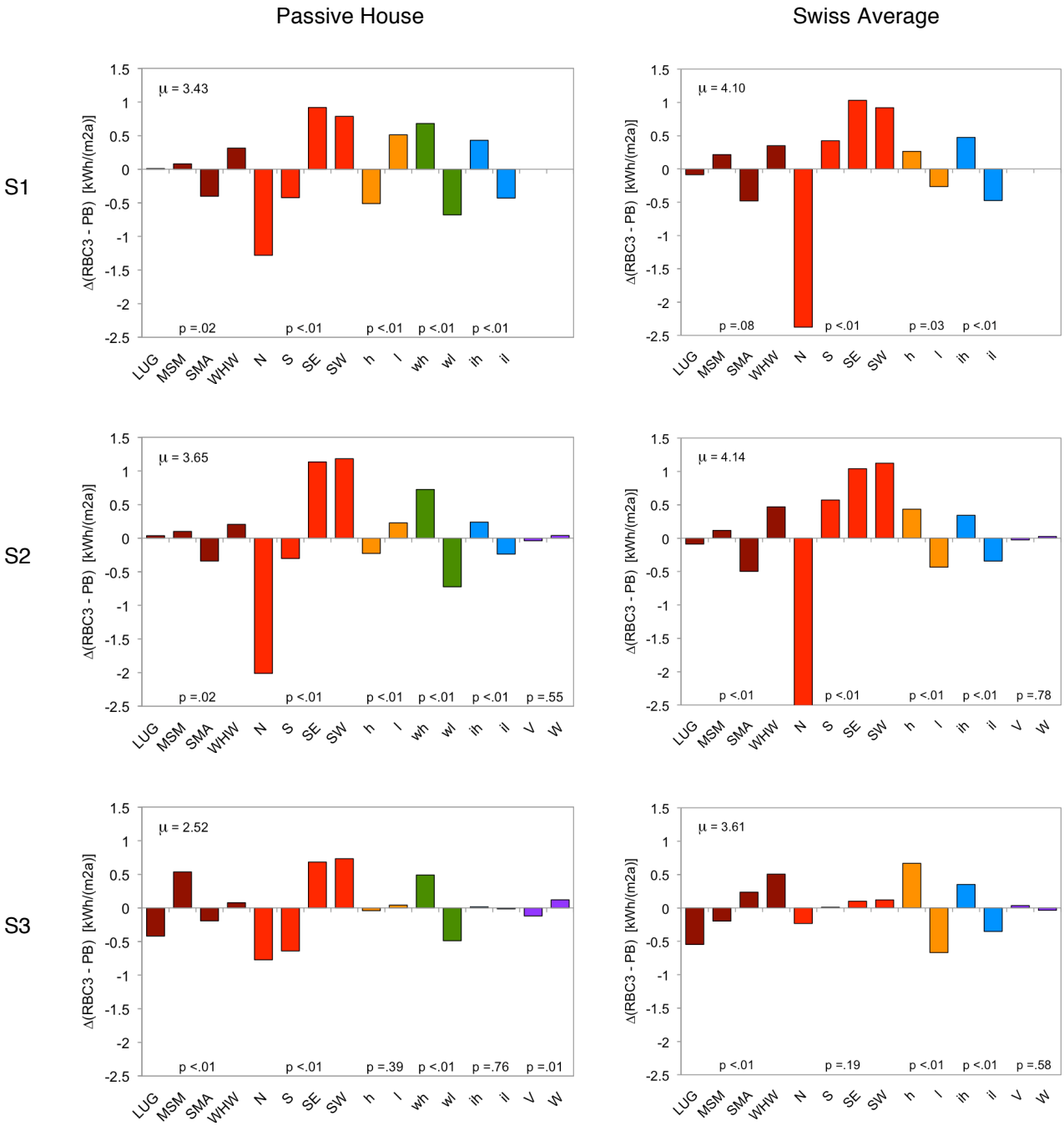

***Figure 8.3:** ANOVA results for absolute savings potentials. ANOVA was performed separately for Building System variants S1–S3 (from top to bottom) and for the Passive House (left) and the Swiss Average (right) Building Standards. Analyses were done for Thermal Comfort definition A_w (no set-back, wide comfort range) and Buildings Classes I+II (see Table 2.2). The μ values in the top left of each panel denote the average savings potential (in kWh/m²/a) of all cases entering the respective analysis. Bars show ANOVA factor level coefficients (deviations Δ from μ) for the following factors: Building Site (levels: LUG, MSM, SMA, WHW); Façade Orientation (N, S, SE, SW); Construction Type (h, l); Window Area Fraction (wl, wh); Internal Gains Level (il, ih); Ventilation Strategy (V, W) (see also Table 7.1). The p-values quantify the statistical significance of the found differences between levels for a given factor; $p < 0.01$ denotes that the found factor level coefficients would occur by chance less than once in 100 times if the saving potentials were equal across all factor levels.*

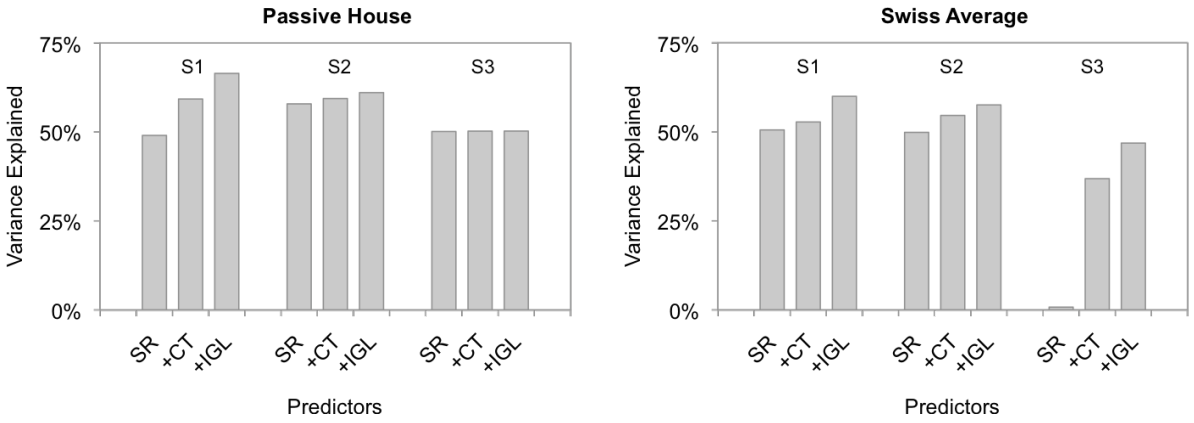

Figure 8.4: Goodness-of-fit statistics for the prediction of absolute savings potentials from selected variables. Shown are the proportions of variances explained ($100 \cdot r^2$) by different linear regression models for Building System variants S1–S3 and for the Passive House (left) and the Swiss Average (right) Building Standards. Each group of three bars refers to models using the following predictor variables: SR: product of specific solar gain area and of the annual average of the mean of the relevant vertical global radiation components; +CT: Construction Type added as a second explanatory variable; +IGL: Internal Gains Level added as a third explanatory variable.

The goodness-of-fit statistics from the second statistical analysis performed, the multiple linear regression analysis, are shown in Figure 8.4. It can be seen that in general the variable S·R explained around 50% of the variance in savings potentials. A notable exception was, however, the case Swiss Average/S3 where S·R showed no explanatory power at all.

Figure 8.4 further illustrates that when the linear regression models were enhanced by both variables Construction Type (CT) and Internal Gains Levels (IGL) the proportions of explained variances for Building System variant S1 increased by totally 17% (Passive Houses) and 13% (Swiss Average houses). For variant S2 the overall increases in explained variance were smaller and amounted to 3% and 10%, respectively. For variant S3 and for the Passive House case it was found that inclusion of CT and IGL did not contribute anything to the explanation of the savings potentials. Very differently, for the Swiss Average case the proportion of explained variance by the two variables was 34%.

Figure 8.5 shows the absolute savings potentials as a function of S·R and CT. It can be seen that the savings potentials tended to increase with increasing S·R. The only exception was again the case Swiss Average/S3 (bottom right panel in Figure 8.5).

From Figure 8.5 can further be seen that the effect of varying CT depended on S·R: Under low S·R values heavy buildings showed generally lower savings potentials as compared to light buildings. For large solar gains the opposite was found to be the case.

Note that the analysis for the Passive Houses included many cases with high S·R values, but that no such cases were available for the Swiss Average Building Standard where all considered buildings had a low Window Area Fraction.

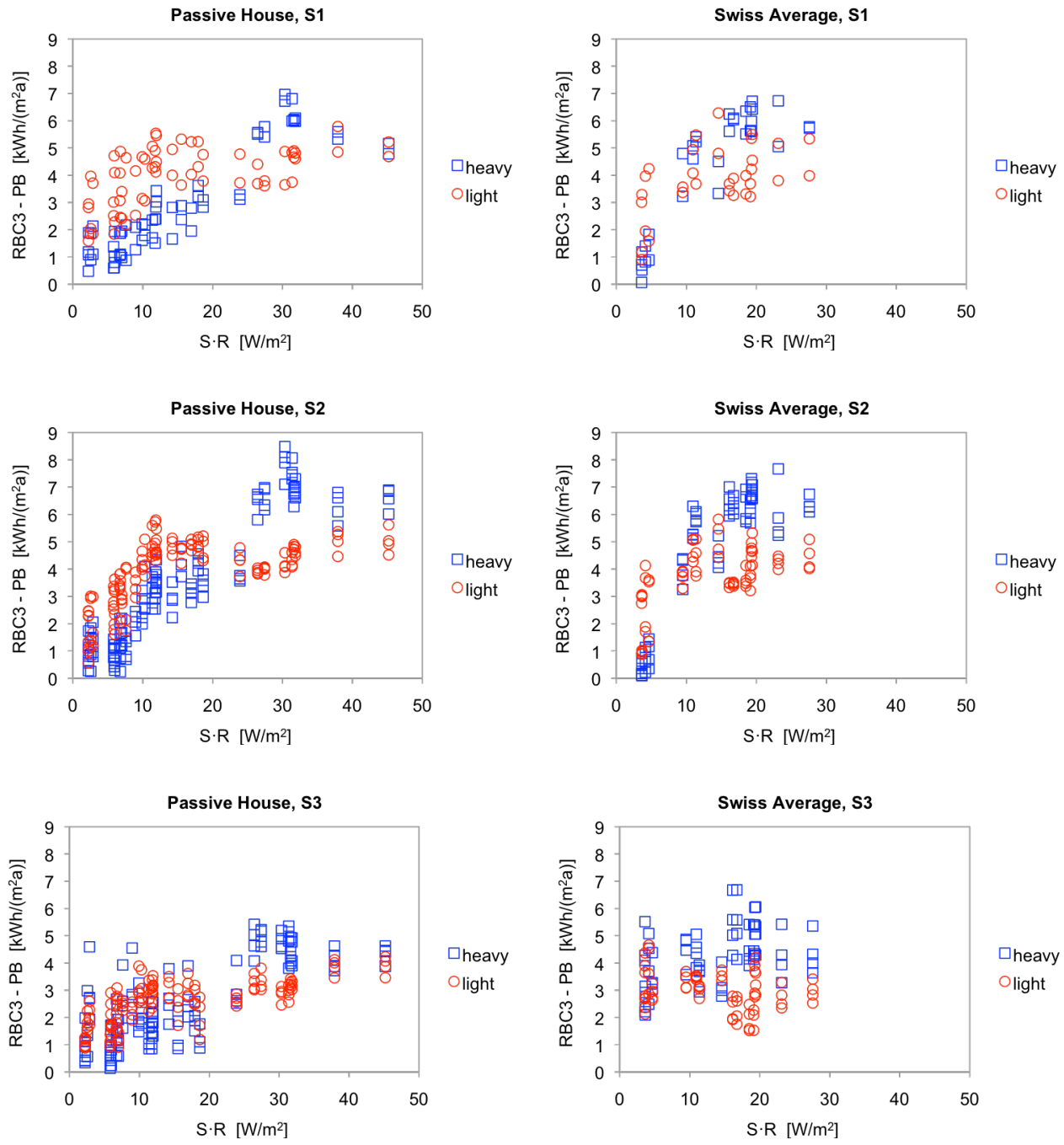

Figure 8.5: Absolute savings potentials as a function of S·R and Construction Type (heavy/light). S: specific solar gain area; R: annual average of the mean of the relevant vertical global radiation components; Passive House, Swiss Average: Building Standards; S1–S3: Building System variant.

8.3.3 Analysis of Selected Cases

8.3.3.1 Case Selection

The selection of representative cases for more detailed analyses was based on the following considerations: Firstly, the cases should be relevant in practice, i.e. they should represent widespread situations in the present building stock. Secondly, in order to facilitate the study of the underlying mechanisms they should show substantial (but not necessarily extreme) savings potentials. And thirdly, they should include variations in all major factors that are influencing the savings potentials, in order to enable the analysis of factor-specific effects.

These considerations lead to the selection of the 18 cases summarized in Table 8.1 (sorted by Building System Variant [BSV] and Building Site). The reasoning behind this selection is explained with the aid of Figures 8.6 to 8.9.

Figures 8.6 and 8.7 show the absolute and relative savings potentials, respectively, of all investigated cases for Buildings Class I and Building System variants S1–S3. The numbers at the top of the panels indicate the cases selected.

The two cases labeled no. 7 and no. 9 in Figures 8.6 and 8.7 were chosen as the "base cases" for the Passive House and the Swiss Average Building Standards, respectively. Both cases represent Building System variant S2, Ventilation Strategy "CO_2-controlled ventilation", Building Site "SMA/Zurich-Fluntern", Façade Orientation "South", Construction Type "heavy", and Internal Gains Level "high". The only difference between the two cases – next to the Building Standard – was the use of a "high" Window Area Fraction for the Passive House case and a "low" one for the Swiss Average case.

Cases 1, 3, and 12 (also shown in Figures 8.6 and 8.7) resulted from Case 9 by varying the Building Site SMA/Zurich-Fluntern to LUG/Lugano, MSM/Marseille-Marignane and WHW/Wien Hohe Warte, respectively.

Cases 2 and 10 resulted from Cases 1 ("warm" site) and 9 ("cool" site), respectively, by using instead of ventilation strategy W (CO_2-controlled ventilation) the strategy V (non-air quality controlled ventilation).

Case 13 was derived from Case 9 by modifying the Building System Variant from S2 to S3.

The derivation of some further cases is illustrated with the aid of Figures 8.8 and 8.9 that show the found absolute and relative savings potentials, respectively, for Buildings Class II and Building System variant S2.

Cases 4 and 8 were derived from Cases 3 ("warm" site) and 7 ("cool" site), respectively, by varying the construction type from "heavy" to "light".

Cases 5 and 6 resulted from Cases 7 and 9, respectively, by changing the façade orientation from "South" to "Southwest" (corner room).

No	*Site*	*BSV*	*BS*	*FO*	*CT*	*WAF*	*IGL*	*VS*	*Savings Potential*		*PB*		*RBC-3*	
									kWh/m²/a	*%*	S_U	S_L	S_U	S_L
1	LUG	S2	sa	S	h	wl	ih	W	5.8	17	1	-1	2	-20
2	LUG	S2	sa	S	h	wl	ih	V	6.0	13	2	-2	1	-19
3	MSM	S2	sa	S	h	wl	ih	W	4.2	14	2	0	8	-10
4	MSM	S2	sa	S	l	wl	ih	W	5.8	16	4	-2	15	-13
5	SMA	S2	pa	SW	h	wh	ih	W	6.2	21	2	-4	0	-29
6	SMA	S2	sa	SW	h	wl	ih	W	6.0	7	3	-11	0	-73
7	SMA	S2	pa	S	h	wh	ih	W	3.7	14	1	0	1	-8
8	SMA	S2	pa	S	l	wh	ih	W	4.8	16	2	-1	1	-14
9	SMA	S2	sa	S	h	wl	ih	W	4.3	10	1	-4	1	-41
10	SMA	S2	sa	S	h	wl	ih	V	4.4	8	1	-4	0	-44
11	WHW	S2	pa	SW	h	wh	ih	W	6.3	24	3	-2	7	-21
12	WHW	S2	sa	S	h	wl	ih	W	5.3	15	2	-3	7	-27
13	SMA	S3	sa	S	h	wl	ih	W	4.5	9	2	-5	1	-46
14	WHW	S3	pa	SW	h	wh	il	W	4.9	20	4	-5	5	-32
15	LUG	S4	sa	S	h	wl	ih	W	1.8	6	1	-2	2	-85
16	SMA	S4	pa	S	h	wh	ih	W	0.1	0	1	0	0	-10
17	SMA	S5	pa	S	h	wh	ih	W	7.6	25	1	0	2	-24
18	WHW	S5	pa	S	h	wh	ih	W	8.3	28	2	0	49	-24

Table 8.1: Selected cases for detailed analyses. The "base cases" no. 7 and 9 are highlighted. BSV: Building System variant; BS: Building Standard; FO: Façade Orientation; CT: Construction Type; WAF: Window Area Fraction; IGL: Internal Gains Level; VS: Ventilation Strategy; PB: Performance Bound; RBC-3: Rule-based control strategy no. 3; S_U, S_L: Annual sums of Kelvin-hours (Kh), measuring deviations of the room temperature above the comfort range's upper bound, respectively below its lower bound. For further abbreviations see Table 7.1. Absolute and relative (%) savings potentials refer to annual total Non-Renewable Primary Energy (NRPE) usage and were calculated as RBC3-PB and 100·(RBC3-PB)/RBC3, respectively, where PB and RBC3 denote the annual Performance Bound and the annual total NRPE usage by the RBC-3 control strategy, respectively.

Case 11 was selected as a high savings potential case for Buildings Class II.

Finally, the Cases 14–18 (Table 8.1) were selected according to the following criteria:

Case 14: a further high potential case for Buildings Class II (similar to Case 11, but representing Building System variant S3 and Internal Gains level "low");

Cases 15 and 16: same as Cases 1 ("warm" site) and 7 ("cool" site), respectively, but employing Building System variant S4 (natural ventilation) instead of S2.

Case 17: same as Case 7, but using Building System variant S5 (TABS) instead of S2.

Case 18: same as Case 17, but for a further "cool" site, WHW/Wien Hohe Warte, instead of SMA/Zurich-Fluntern.

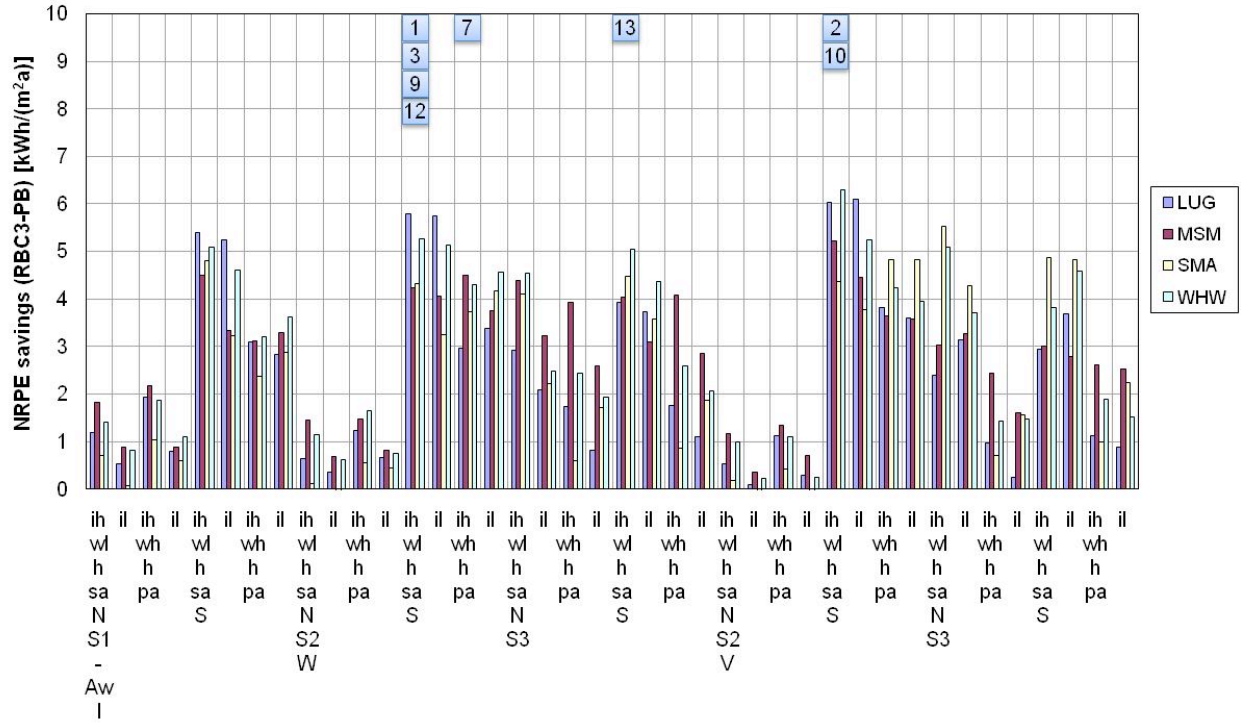

Figure 8.6: Absolute savings potentials for control strategy RBC-3, Thermal Comfort definition A_w (no set-back, wide comfort range), and Buildings Class I. S1, S2, S3: Building System variant; -, W, V: Ventilation Strategy; N, S, SE, SW: Façade Orientation; sa, pa: Building Standard; l, h: Construction Type; wl, wh: Window Area Fraction; il, ih: Internal Gains Level; LUG, MSM, SMA, WHW: Building Site (see also Table 7.1). Blue boxes indicate cases selected for more detailed analyses (cf. Table 8.1).

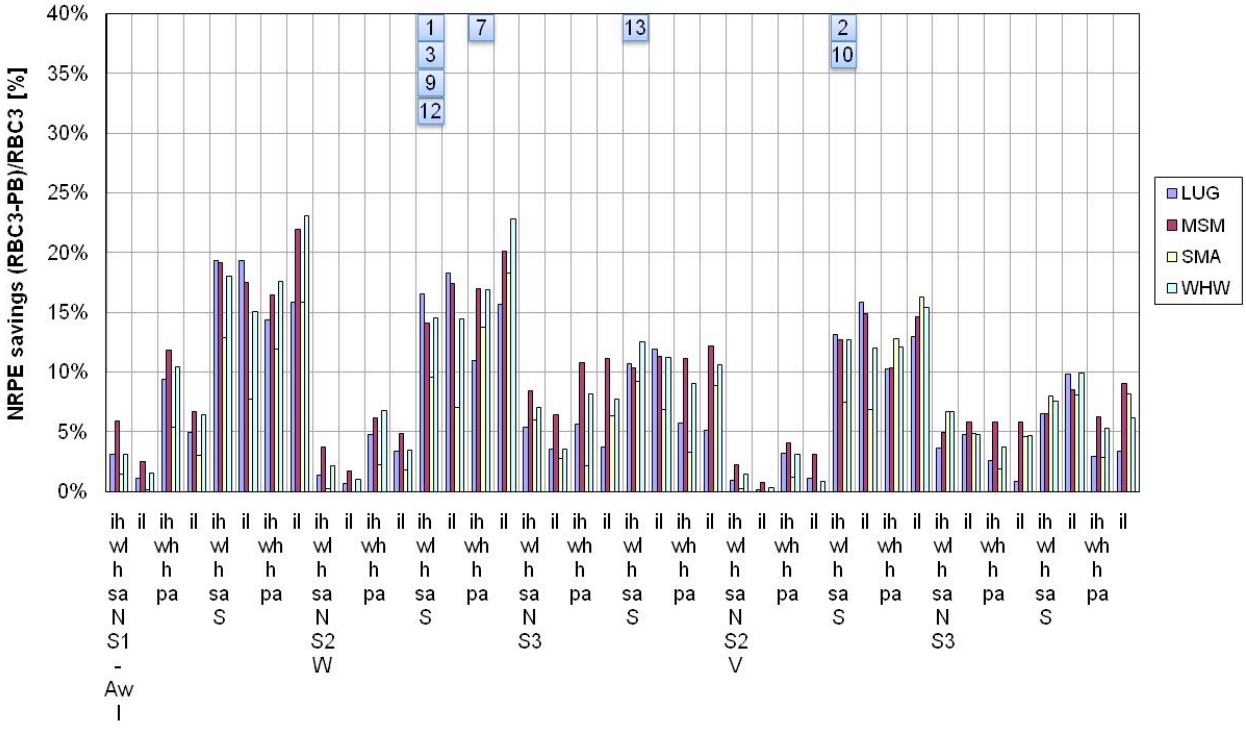

Figure 8.7: Same as Figure 8.6, but for relative savings potentials.

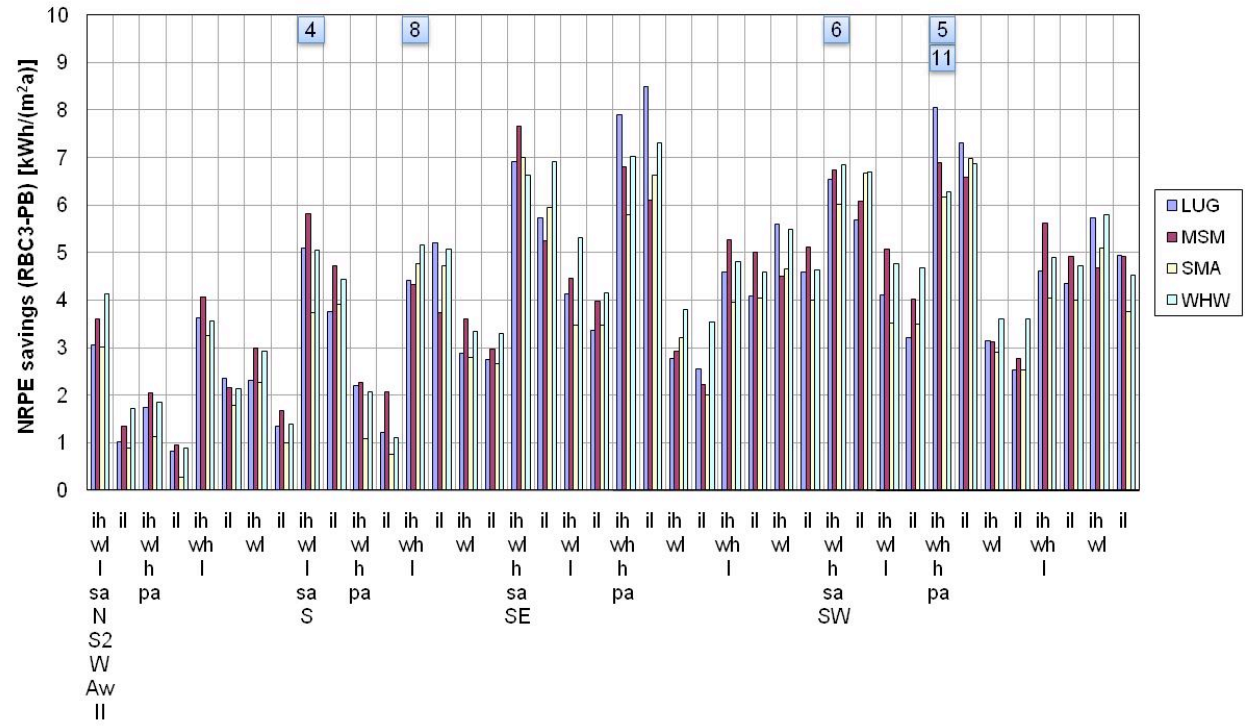

Figure 8.8: Absolute savings potentials for control strategy RBC-3, Building System variant S2, Thermal Comfort definition A_w (no set-back, wide comfort range), Buildings Class II, and Ventilation Strategy W (CO_2-controlled ventilation). N, S, SE, SW: Façade Orientation; sa, pa: Building Standard; l, h: Construction Type; wl, wh: Window Area Fraction; il, ih: Internal Gains Level; LUG, MSM, SMA, WHW: Building Site (see also Table 7.1). Blue boxes indicate cases selected for more detailed analyses (cf. Table 8.1).

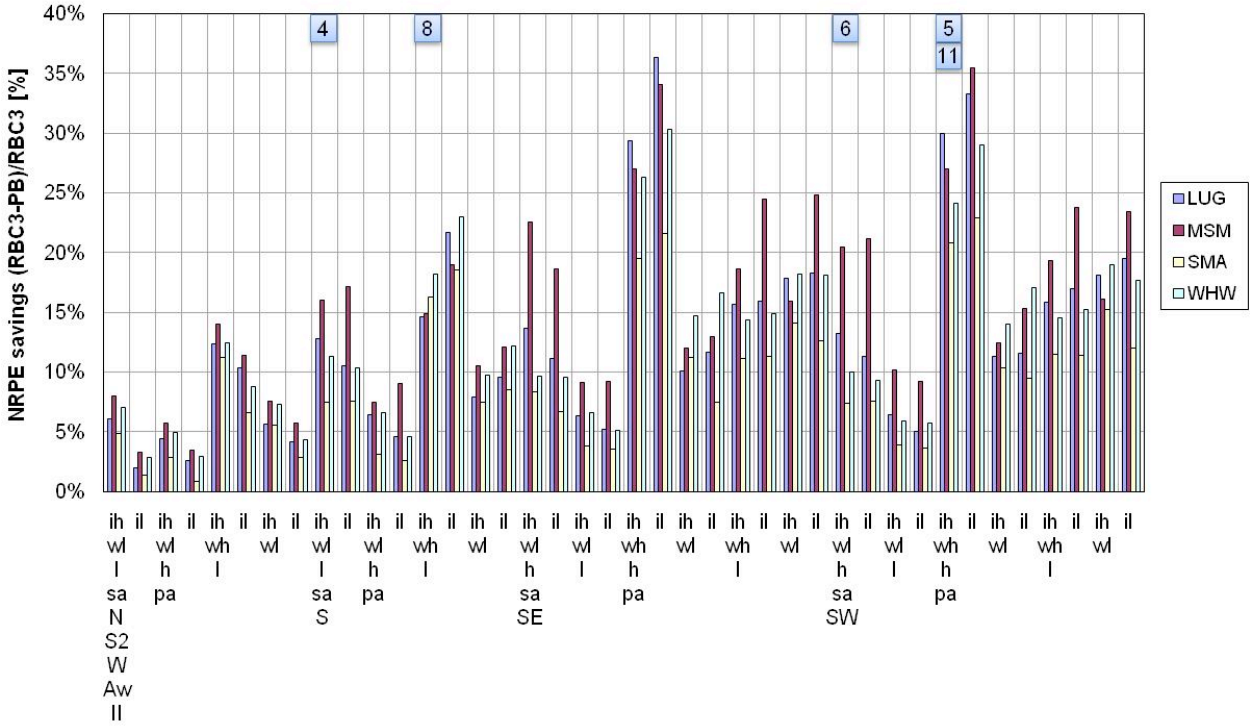

Figure 8.9: Same as Figure 8.8, but for relative savings potentials.

8.3.3.2 Annual Cycles of Savings Potentials

Figures 8.10 and 8.11 compare monthly PB values and absolute savings potentials for a subset of eight selected cases that all refer to Building System variant S2. Displayed is the total NRPE usage by all subsystems (left panels), as well as the NRPE usage associated with heating only (middle panels) or cooling only (right panels).

According to the definition of Building System variant S2 the heating NRPE usage was given by the sum of heating energy consumed by the mechanical ventilation and by the radiators. The cooling NRPE usage consisted of the energy used for cooling by mechanical ventilation plus the energy usage by a mechanical chiller or a wet cooling tower for operation of the cooled ceiling.

Note, total NRPE usage by all subsystems (left panels in Figures 8.10 and 8.11) included the energy usage by electric lighting and fan operation. These subsystems are however not detailed in Figures 8.10 and 8.11 because they showed practically no savings potentials for the cases considered here. The NRPE usage by the lighting and fans is examined in the next Section in more detail.

Figure 8.10 displays results for the Passive House Building Standard. It can be seen that the total NRPE usage by the PB (left panels, dark grey portion of the bars) showed for all cases a distinct annual cycle. The total usage reflected a larger NRPE demand for heating during the winter half year (middle panels, brown portion of the bars) as opposed to a generally smaller NRPE demand for cooling during the summer half year (right panels, dark blue portion of the bars). Note the different y-axis ranges between panels on the same row.

The PB for heating NRPE usage was found to be highest for the corner offices (Cases 5 and 11), whereas for the other two cases (Cases 7 and 8) there was hardly any heating demand in the PB calculations. Cooling NRPE usage occurred for the PB in all cases.

Quite differently from the total NRPE usage in the PB calculations the total NRPE savings potentials (left panels, light grey portion of the bars) showed very jagged annual cycles. They resulted from the superposition of heating savings potentials for the period October through April (middle panels, orange portion of the bars), and cooling savings potentials throughout the year with generally higher values during summertime (right panels, light blue portion of the bars).

Figure 8.11 presents a similar analysis as is shown in Figure 8.10, but for the Swiss Average Building Standard, and with emphasis on the variation between sites.

From Figure 8.11 (left panels) can be seen that the total NRPE usage of the two warmer sites (Cases 1 and 3) showed a less pronounced annual cycle as compared to the two cooler sites (Cases 9 and 12). This behavior was due to the combination of a modest heating demand (middle panels) with an elevated cooling demand (right panels) at the warmer sites, while at the cooler sites there was generally a much stronger, seasonally varying heating demand.

The total NRPE savings potentials shown in Figure 8.11 (left panels, light grey portion of the bars) again exhibited irregular annual cycles, as this was the case for the results reported in Figure 8.10.

A further common result that can be discerned from Figures 8.10 and 8.11 is that the control strategy RBC-3 was always found to lead to longer heating (middle panels) and cooling seasons (left panels) as compared to the PB.

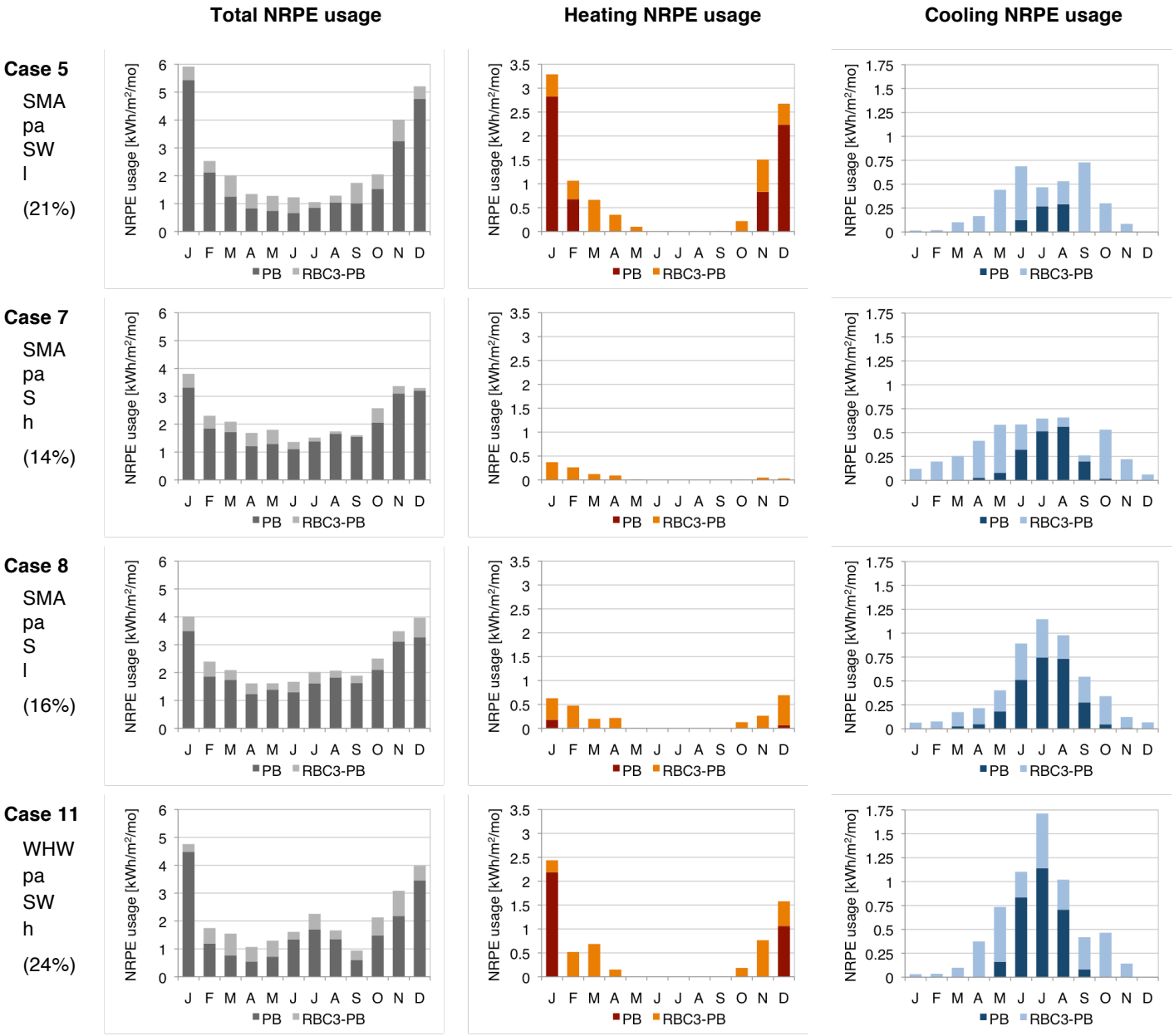

Figure 8.10: Comparison of monthly Performance Bound values (PB, dark portions of bars) and of monthly savings potentials (RBC3-PB, light portions of bars) for selected cases representing Building System variant S2 and the Passive House (pa) Building Standard. NRPE: Non-Renewable Primary Energy; SMA, WHW: Building Sites; S, SW: Façade Orientations; h, l: Construction Types. Numbers in brackets at the left hand side give annual total relative savings potentials 100·(RBC3-PB)/RBC3, where RBC3 and PB denote the annual Performance Bound and the annual total NRPE usage for the RBC-3 control strategy, respectively.

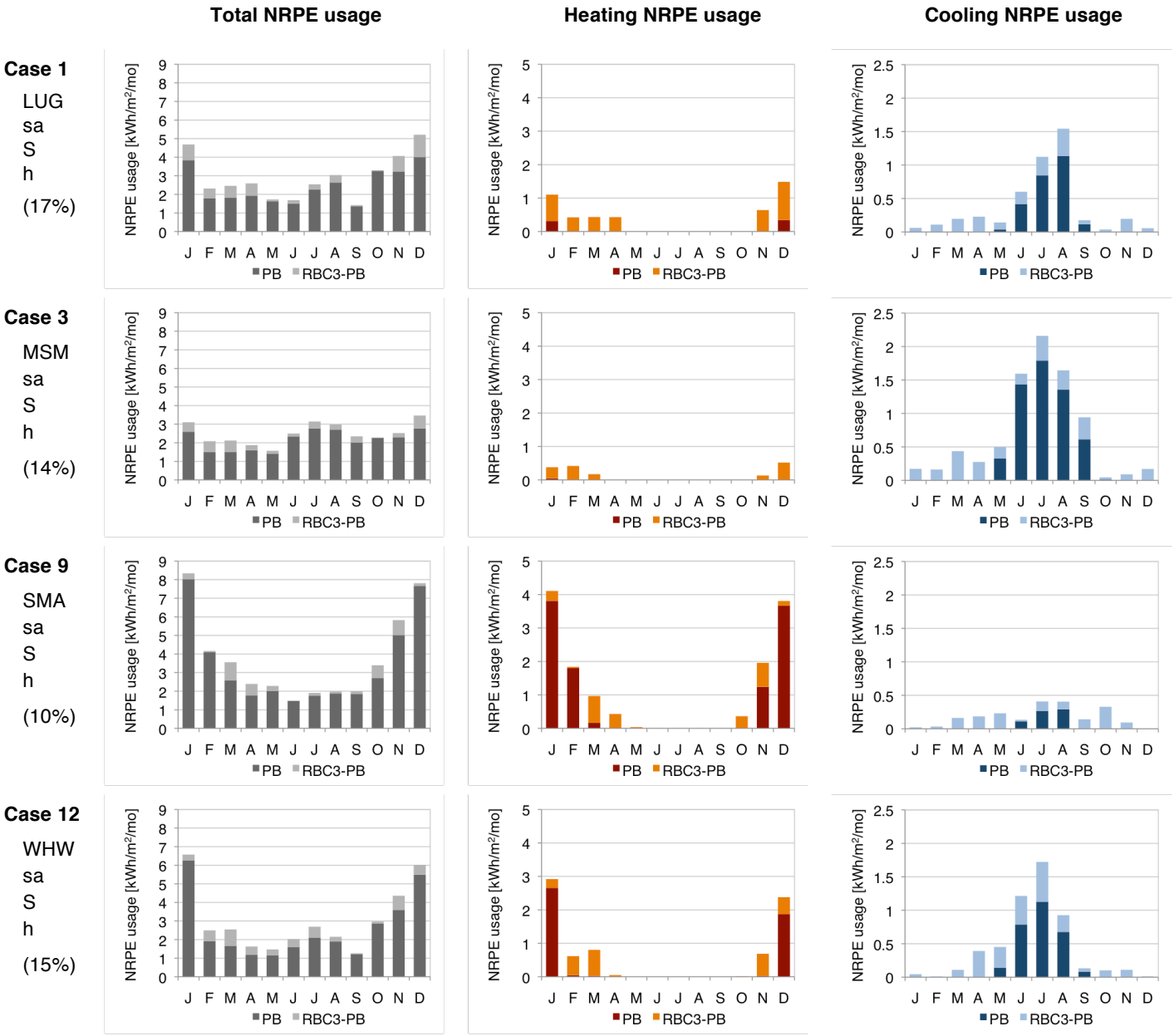

Figure 8.11: Comparison of monthly Performance Bound values (PB, dark portions of bars) and of monthly savings potentials (RBC3-PB, light portions of bars) for selected cases representing Building System variant S2 and the Swiss Average (sa) Building Standard. NRPE: Non-Renewable Primary Energy; LUG, MSM, SMA, WHW: Building Sites; S: Façade Orientation; h: Construction Type. Numbers in brackets at the left hand side give annual total relative savings potentials 100·(RBC3-PB)/RBC3, where RBC3 and PB denote the annual Performance Bound and the annual total NRPE usage for the RBC-3 control strategy, respectively.

8.3.3.3 Allocation to Subsystems

Figure 8.12 illustrates for all 18 cases from Table 8.1 how the NRPE savings potentials were distributed across the various technical subsystems. Note, the energy demand associated with the operation of blinds was neglected in all cases. Cases 15 and 16 involved energy usage for the operation of the night-time natural ventilation subsystem, and this contribution to the total NRPE usage was also neglected.

It can be observed that for Cases 1–12, i.e. all cases related to Building System variant S2, the largest savings potentials were always associated with radiator heating (rH) and free cooling (fC) usage. The only exception was Case 4 where a substantial savings potential was found for the cooling of the ceiling through a mechanical chiller (cC). Case 4 was the only one that represented the Construction Type "light" at a "warm" site. Some savings potentials for the cC subsystem were also found for the Cases 3, 11 and 12.

Cases 13 and 14 represented the Building System variant S3 (ventilation-only system). Here, significant savings potentials were found for the NRPE usage associated with fan operation (v) and with the heating via the ventilation subsystem (vH).

Cases 15 and 16 referred to Building System variant S4 that involved floor heating (fH). For Case 15 the fH subsystem was identified as the only relevant source of possible NRPE savings. For Case 16 the RBC-3 strategy was in terms of NRPE usage very close to the PB such that there were no savings potentials present.

The last two cases reported in Figure 8.12, Cases 17 and 18, related to the Building System variant S5 that employed TABS. In both cases substantial savings potentials were detected for the ventilation (vH) and free cooling (fC) subsystems. Some potential was also found with regard to fan operation (v).

Cases 1–2 and 9–10 enable a comparison of the role of ventilation strategies W (CO_2-controlled ventilation) and V (non-air quality controlled ventilation) at a warm (LUG/Lugano) and a cool site (SMA/Zurich Fluntern), respectively. From both comparisons can be seen that strategy W (Cases 1 and 9) required much less energy for fan operation (v) than strategy V (Cases 2 and 10). Also, the found total savings potentials were somewhat larger for strategy W (17% for site LUG, and 10% for site SMA) as compared to strategy V (13% and 8%, respectively). However, for all cases the largest savings potentials were found for the radiator (rH) and free cooling (fC) subsystems.

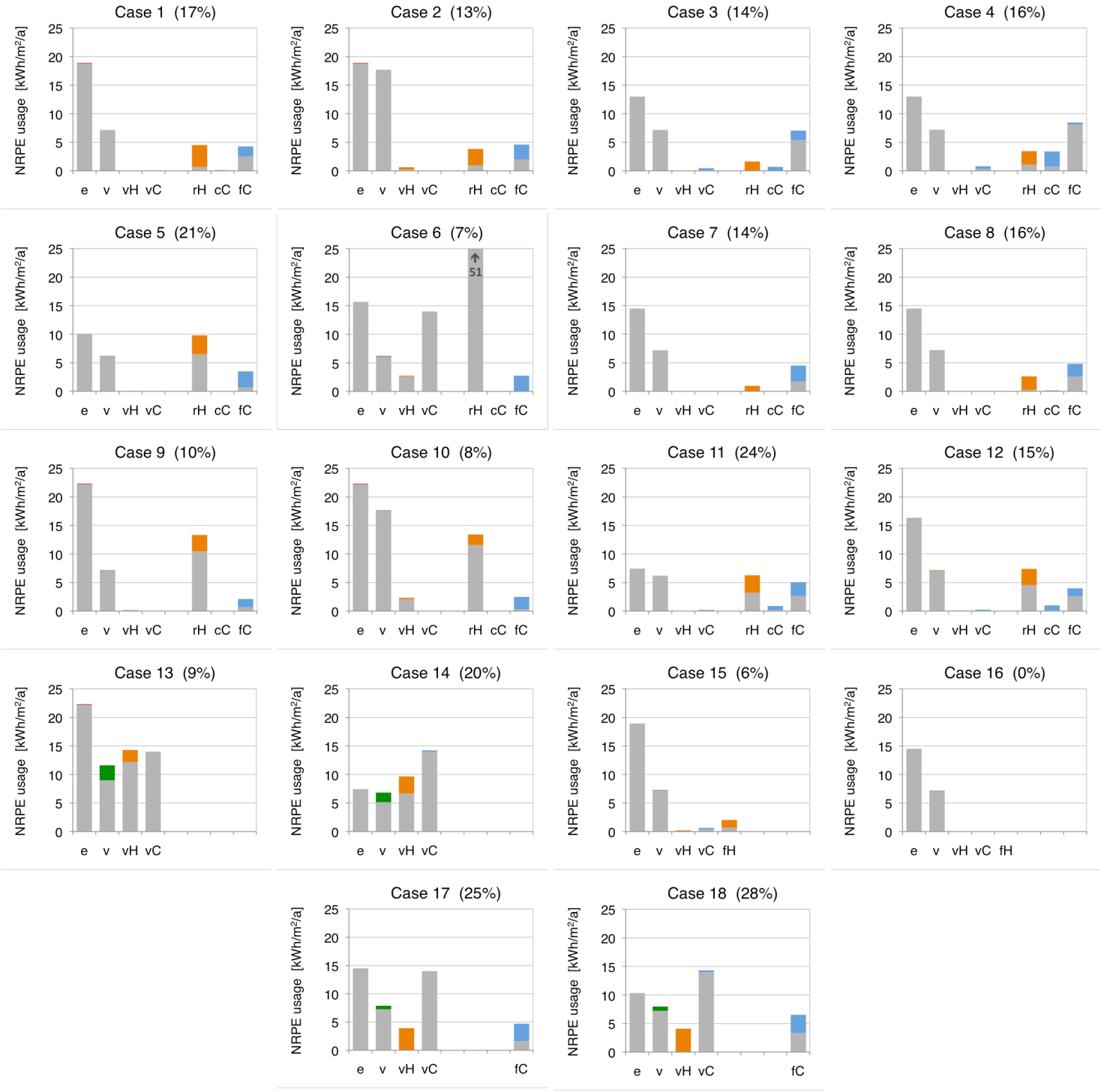

Figure 8.12: Distribution of annual Performance Bound values (PB, grey) and annual savings potentials (RBC3-PB, colored) across building technical sybsystems. Shown are data for Non-Renewable Primary Energy (NRPE) usage and for 18 selected cases representing different Building System variants and Building Standards (cf. Table 8.1). Cases 1-12: Building System variant S2; Cases 13-14, 15–16, 17–18: Building System variant S3, S4 and S5, respectively. NRPE usage is shown for the following subsystems (data points omitted if subsystem not present for the respective Building System variant): e: electric lighting; v: fan operation for mechanical ventilation; vH, vC: heating and cooling by mechanical ventilation, respectively; fH: floor heating; rH: radiator heating; cC, fC: cooled ceiling operated through a mechanical chiller or a through free cooling, respectively. Numbers in brackets on top of each panel give annual total relative savings potentials 100·(RBC3-PB)/RBC3, where RBC3 and PB denote the annual Performance Bound and the annual total NRPE usage for the RBC-3 control strategy, respectively.

8.3.3.4 Mechanisms

In this section we investigate the mechanisms behind the found NRPE savings for heating and cooling. To this purpose we examine the hourly simulations results of two selected cases in more detail.

The first analysis refers to Case 8. As reported earlier (Figure 8.10) this case showed for February a substantial savings potential for heating, but also some savings potential with regard to cooling.

Figure 8.13 shows hourly simulation results for a 16-day time window during February. The simulations were based on the Average Design Reference Year (DRY) weather data for the site SMA/Zurich Fluntern. The February data used in the DRY were actually those from the year 1992.

The top panel of Figure 8.13 summarizes the outdoor meteorological conditions and the room's occupancy status, while the remaining panels juxtapose the simulation results obtained from the PB calculation (blue) with those from the RBC-3 simulation (orange). Note, the x-axis labels and vertical gridlines in all panels mark the beginning of the respective day at 00:00 UTC.

The second panel of Figure 8.13 compares the simulated room temperatures (Troom). It can be seen that the temperatures from the PB were mostly above those from the RBC-3 simulation. In particular, the simulated temperatures under the RBC-3 control often lied at the lower bound (21 ºC) of the thermal comfort range, while the PB temperatures floated within it most of the time.

In order to guarantee thermal comfort the RBC-3 controller repeatedly employed radiator heating (hPowRad, fourth panel), for instance during February 17th and into the morning of February 18th, a period during which outside air temperatures (Tair, top panel) coincided with very low radiation input (RGS) and low internal gains due to the room not being occupied (occup). In contrast to this control behavior, the PB required most of the time no radiator heating at all.

The main reason was due to differences in blind operation (bPos, third panel of Figure 8.13): the PB kept the blinds much more open than the RBC-3 algorithm, thus making better use of the incident radiation for (pre-)heating of the room. Quite differently, RBC-3 aimed at reducing heating power by stronger use of energy recovery as compared to the PB (ercUsgFact, last panel).

A further consequence of the optimal blind control by the PB was the avoidance of situations where energy was required for cooling. E.g., it can be seen that during the night of February 13th to 14th the PB kept the blinds open in order to pre-cool the room in anticipation of the solar (RGS) and internal gains (occup) that were expected for the next day. The pre-cooling was also supported by the shown reduction in the energy recovery usage factor (ercUsgFact) that resulted into a lower inlet air temperature.

In contrast, the RBC-3 strategy managed to keep the room temperature below the upper comfort limit of 25 ºC only with the aid of occasional free cooling pulses (fcUsgFact, second bottom panel of Figure 8.13), as this was e.g. the case during the afternoon of February 14th.

Our second analysis related to summertime cooling and here we considered the simulation results from a 16-day period for Case 1 in August (see also Figure 8.11). The simulations were based on the Average DRY data set for the site LUG/Lugano; the August data were those from the year 1998.

Figure 8.14 summarizes the prevailing meteorological conditions (top panel) plus selected simulation results (remaining panels). In contrast to the previous analysis the blinds positioning is not detailed here because for this control variable the PB and the RBC-3 simulation were found to yield very similar results: both control strategies turned out to avoid solar gains as much as possible by opening the blinds only just as much as needed in order to achieve the minimum required illuminance level when the room was occupied.

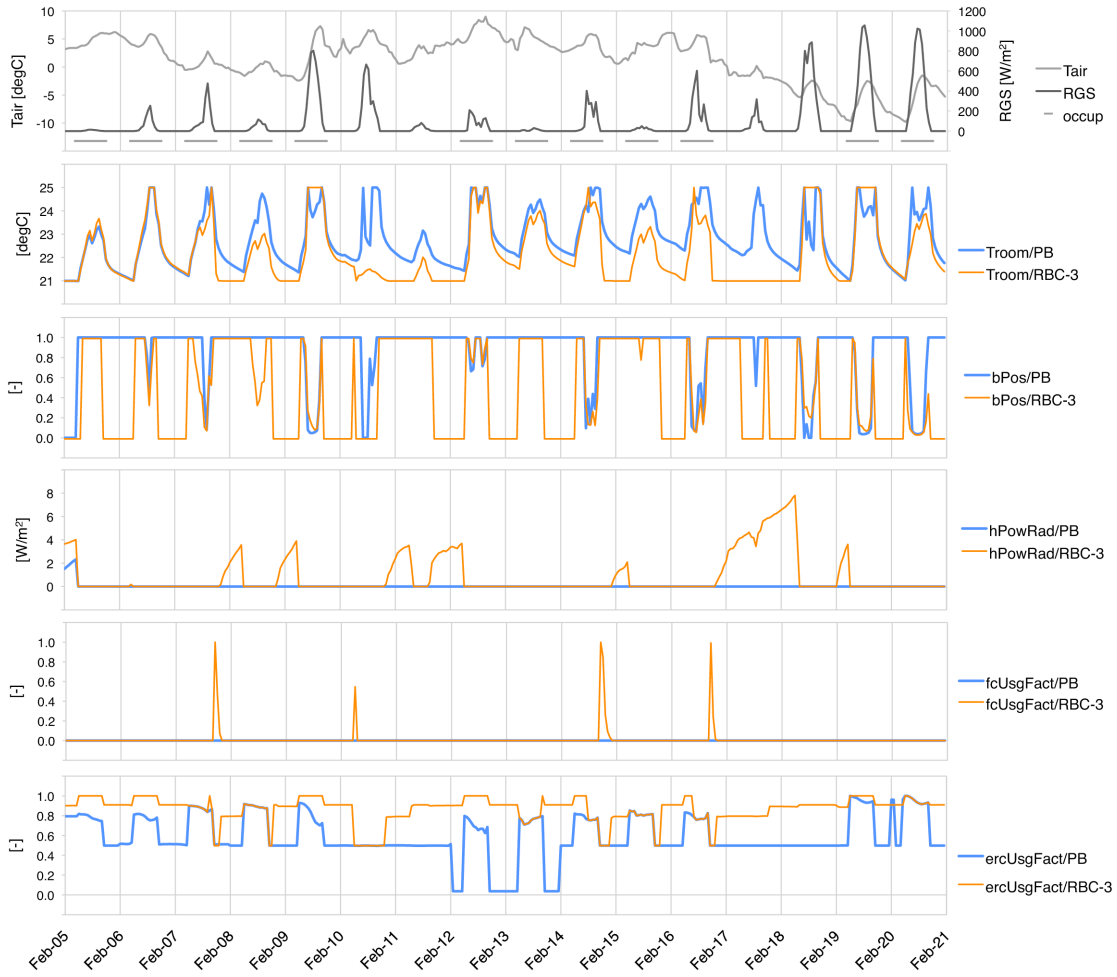

Figure 8.13: Comparison of hourly simulation results for Case 8 (see Table 8.1) in February. PB: Performance Bound simulation; RBC-3: simulation using rule-based control RBC-3. Tair: outdoor air temperature; RGS: global radiation component on a south-facing vertical suface; occup: occupancy status (gray = office working hours); Troom: room temperature; bPos: blinds position (0 = blinds closed); hPowRad: radiator heating power; fcUsgFact: free cooling usage factor (0 = free cooling deactivated); ercUsgFact: energy recovery usage factor (0 = energy recovery deactivated). Delivered power for hPowRad refers to Non-Renewable Primary Energy.

The second panel of Figure 8.14 juxtaposes the simulated room temperatures (Troom). It can be seen that the room temperature from the PB was generally below the one from the RBC-3 simulation. During the two sunny and increasingly warmer periods of August 6th–10th and 14th–16th, respectively, the PB temperatures successively approached the ones simulated under RBC-3.

The third and fourth panel of Figure 8.14 show the cooling power consumed by the mechanical ventilation (cPowMev) and the mechanical chiller (cPowSlab), respectively. It can be seen that as opposed to RBC-3 the PB managed to almost completely avoid the usage of these two energy-intensive devices.

The reason can be seen from the last two panels that illustrate the free cooling usage (fcUsgFact) and the energy recovery intensity (ercUsgFact), respectively: The PB used the free cooling much more extensively than RBC-3 and at different points in time, namely for pre-cooling of the room (e.g., Aug 5th–7th and 12th–14th). To the same purpose the PB also made more extensive use of the energy recovery for cooling than RBC-3. Salient examples are the energy recovery usage peaks of August 4th–6th and 11th–12th, where the PB exploited the fact that nighttime outside air temperature was below the room temperature.

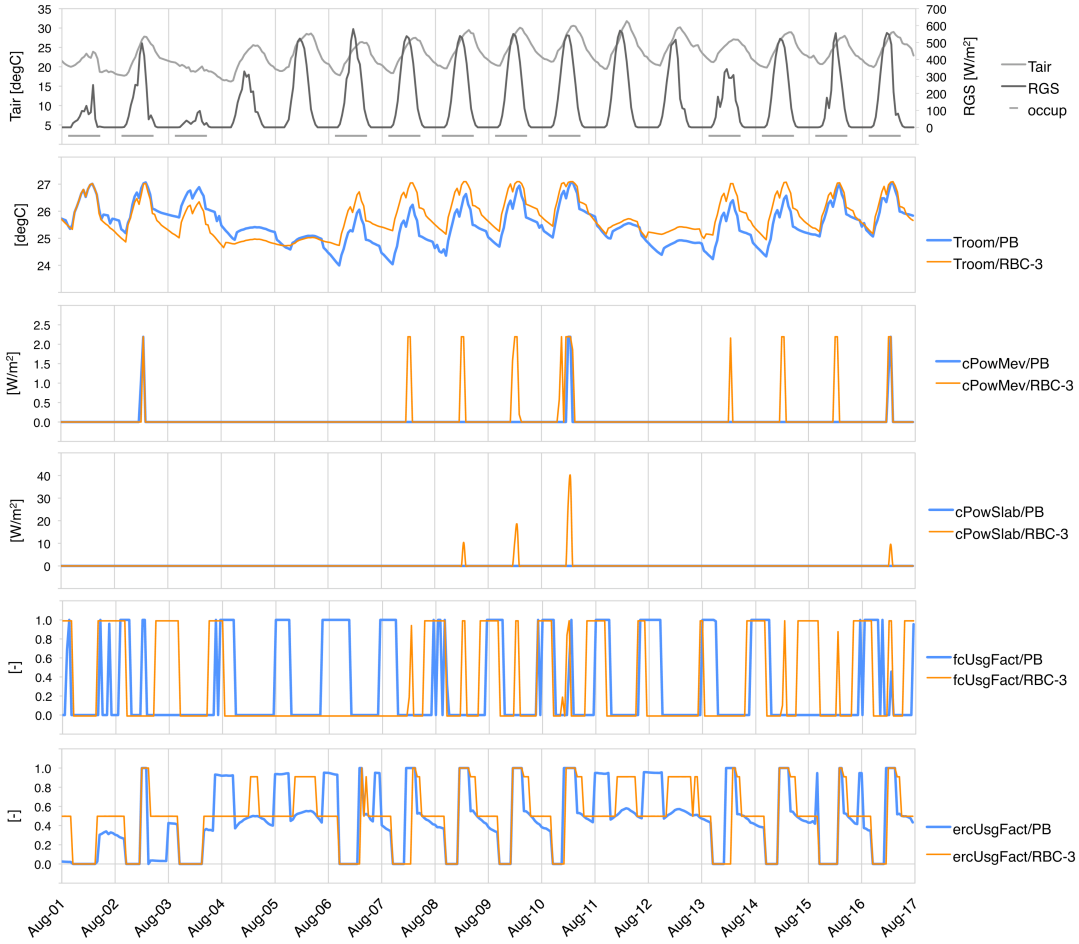

Figure 8.14: Comparison of hourly simulation results for Case 1 (see Table 8.1) in August. PB: Performance Bound simulation; RBC-3: simulation using rule-based control RBC-3. Tair: outdoor air temperature; RGS: global radiation component on a south-facing vertical surface; occup: occupancy status (gray = office working hours); Troom: room temperature; cPowMev: cooling power by mechanical ventilation; cPowSlab: cooling power of mechanical chiller for cooled ceiling; fcUsgFact: free cooling usage factor (0 = free cooling deactivated); ercUsgFact: energy recovery usage factor (0 = energy recovery deactivated). Delivered power for cPowMev and cPowSlab refers to Non-Renewable Primary Energy.

8.3.4 Analysis of Peak Electricity Demand

Figure 8.15 compares the distributions of simulated hourly mean total electric power demand (EPD) between the PB and RBC-3 simulations for the 18 cases given in Table 8.1. It can be seen that for Cases 1–4, 8, 11, 12, 14 and 15 the RCB-3 simulations yielded higher extreme values than the PB. Only in one case, Case 13, the PB gave higher extremes. In the remaining eight cases no notable differences were found between the respective distribution's upper tails.

The 98-, 99- and 100-Percentile (maximum) values of all distribution pairs are compared in Figure 8.16. Again, the aforementioned cases stick out, and it can be seen that the largest relative differences occurred for the annual maximum values and amounted up to 30% (or ca. 6 W/m^2).

A closer analysis (not shown) of the nine cases where the RBC-3 simulations showed more extreme EPD distributions than the PB revealed that the largest EPD values occurred always during the warm season.

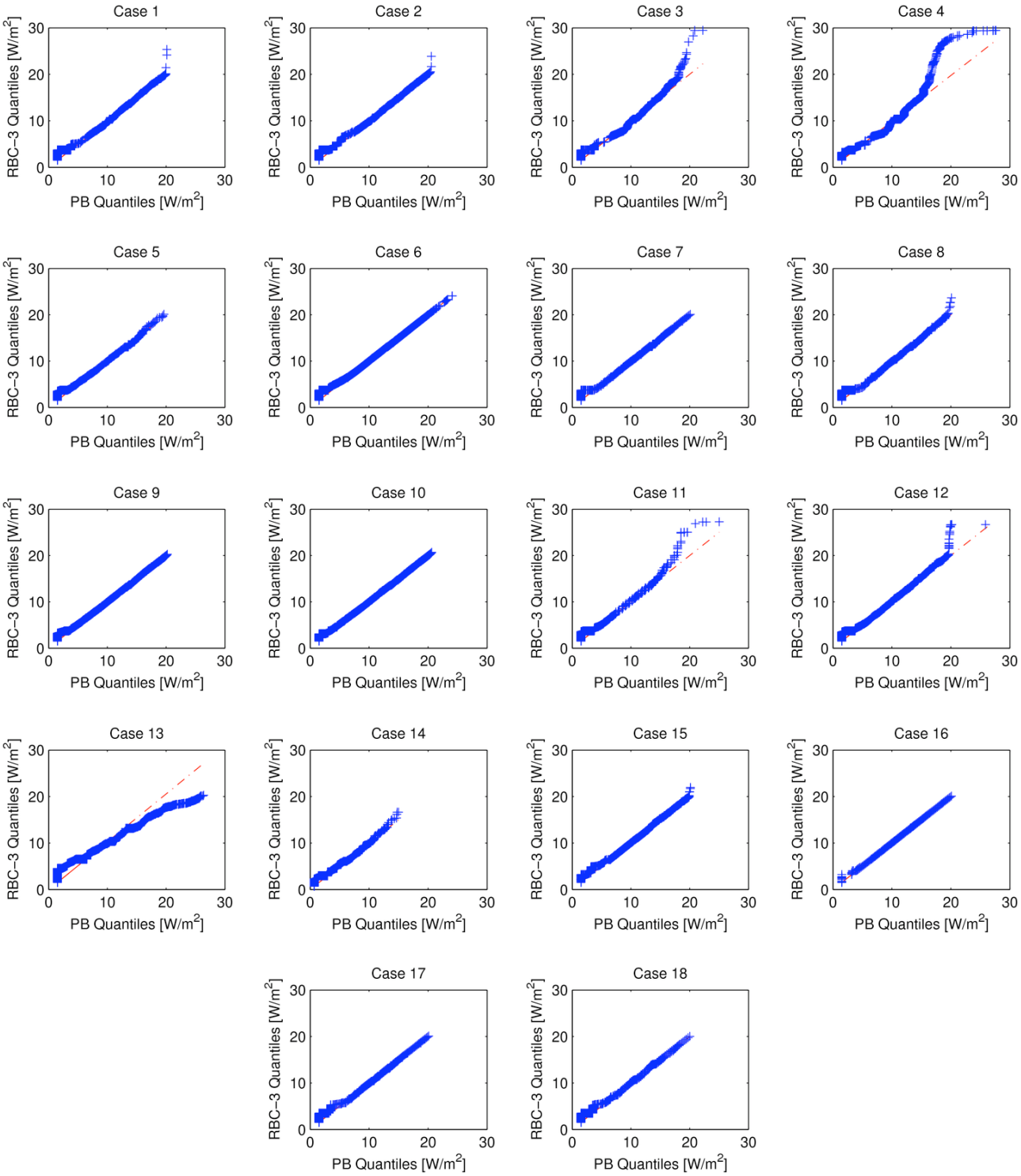

Figure 8.15: Quantile-quantile plots of hourly mean total electric power demand for 18 selected cases representing different Building System variants and Building Standards (cf. Table 8.1). PB: power demand values from the whole-year Performance Bound simulation; RBC-3: power demand values from corresponding simulation using the RBC-3 control strategy. Sample size n = 8759. Cases 1-12: Building System variant S2; Cases 13-14, 15–16, 17–18: Building System variant S3, S4 and S5, respectively.

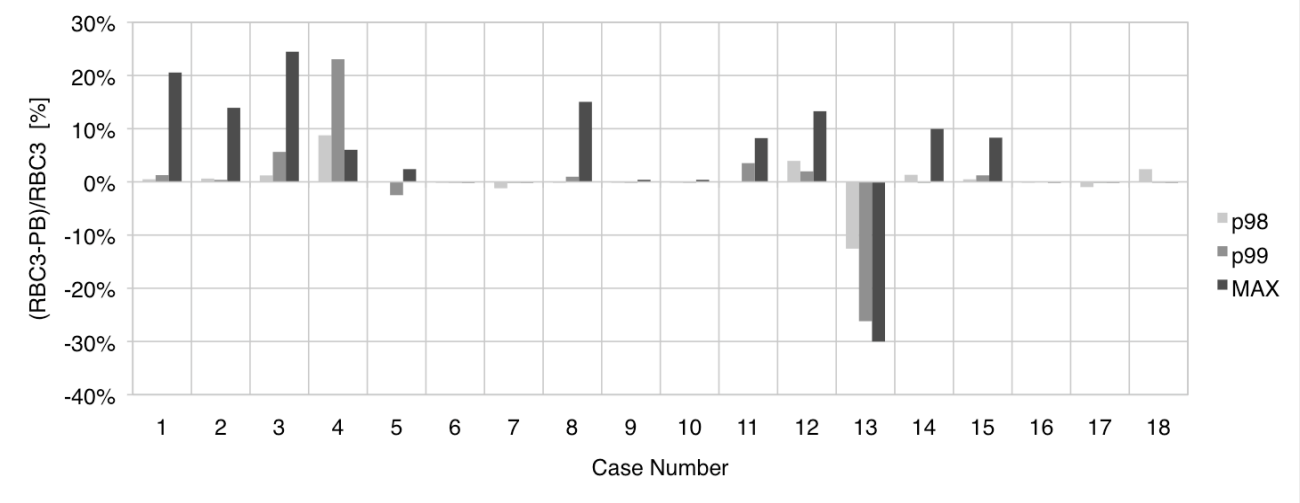

Figure 8.16: Relative differences for the 98-, 99- and the 100-Percentile (MAX) of hourly mean total electric power demand. RBC-3: percentiles from a whole-year simulation using the RBC-3 control strategy; PB: percentiles from the corresponding Performance Bound simulation. Sample size n = 8759, i.e. one percent represents 88 hourly values. Shown are results for 18 selected cases representing different Building System variants and Building Standards (cf. Table 8.1).

Figure 8.17 illustrates a typical summertime episode with extreme EPD values in the RBC-3 simulation. The top panel shows the used meteorological data (site MSM/Marseille-Marignane, year 2006) together with the occupancy status, while the second panel juxtaposes the simulated room temperatures. It can be seen that the RBC-3 simulations yielded generally higher room temperatures, whereas for the PB the room temperature started from a pre-cooled state and warmed successively throughout the week (cf. Figure 8.14).

The third panel in Figure 8.17 compares the computed hourly mean total EPD values. Both simulations yielded a double-peaked diurnal profile with increasing peak levels throughout the week. Note, the shown EPD values contained a contribution from electric lighting in the early morning hours of working days, but this component is not detailed here because it was comparatively small (peak value of 1.2 W/m^2) and identical in the two simulations. The double-peak shape of total EPD was attributable to the operation of the equipment (see Figure 2.4, right).

From the bottom panel of Figure 8.17 can be seen that the trend in the EPD peaks was caused by the increasing power consumption by the mechanical chiller throughout the week. Due to the generally higher room temperature level that was closer to the upper comfort bound of 27 °C this trend was more pronounced in the RBC-3 as compared to the PB simulations.

Now we turn to the special Case 13 that referred to Building System variant S3 (ventilation-only system). Here, the highest EPD values were found to occur in the PB simulations, and during wintertime (analysis not shown).

Figure 8.18 shows selected simulation results for a typical winter episode. The used weather data (top panel) were from site SMA/Zurich Fluntern and the year 2003.

From the second panel of Figure 8.18 can be seen that the two simulations yielded similar room temperatures at the beginning and towards the end of the week. However, in the period January 9^{th}–11^{th} that had particularly cool outdoor conditions and almost no solar gains (top panel) the daytime room temperatures showed strong differences.

The simulated hourly mean total EPD values are detailed in the third panel of Figure 8.18. Total EPD contained identical contributions from electric lighting in both simulations (peak values of 2.2 W/m^2) that are not shown here. Otherwise it can be discerned that the PB simulation showed consistently higher daytime and lower nighttime EPD than the RBC-3 simulation.

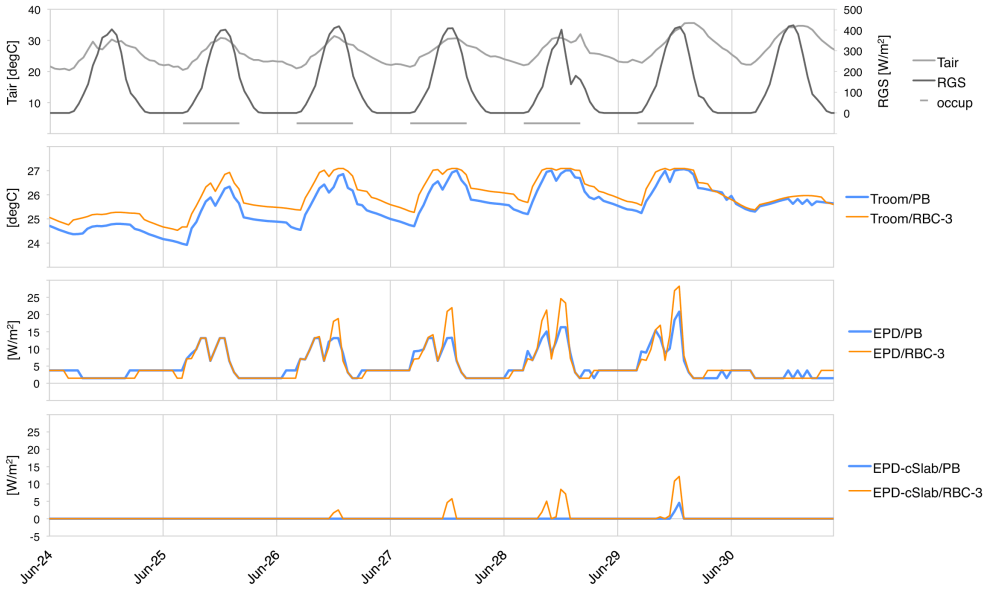

Figure 8.17: Comparison of hourly simulation results for Case 3 (see Table 8.1) in June. PB: Performance Bound simulation; RBC-3: simulation using rule-based control RBC-3. Tair: outdoor air temperature; RGS: global radiation component on a south-facing vertical surface; occup: occupancy status (gray = office working hours); Troom: room temperature; EPD: hourly mean total electric power demand; EPD-cSlab: electric power demand of mechanical chiller for cooled ceiling.

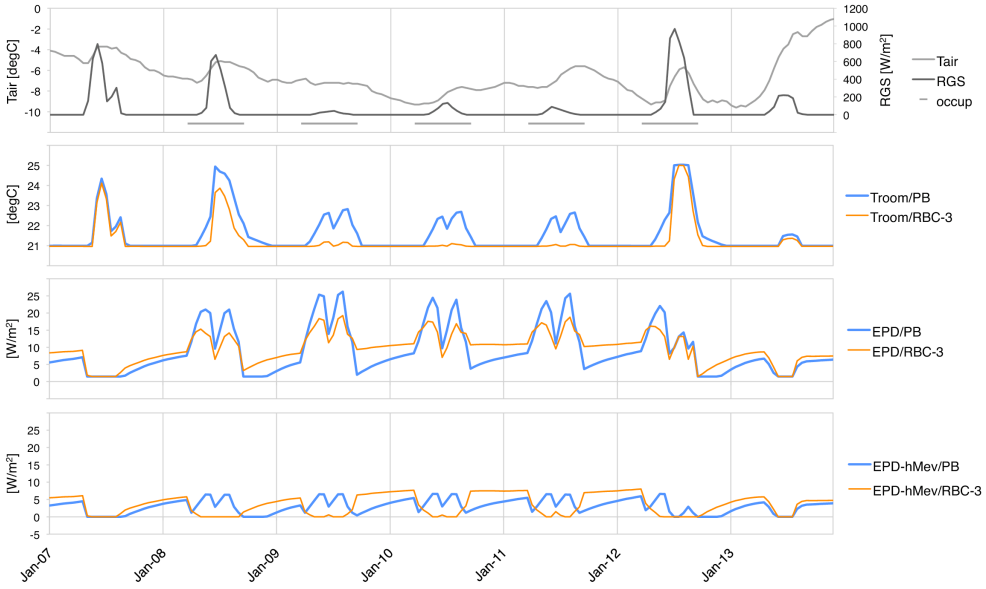

Figure 8.18: Comparison of hourly simulation results for Case 13 (see Table 8.1) in January. PB: Performance Bound simulation; RBC-3: simulation using rule-based control RBC-3. Tair: outdoor air temperature; RGS: global radiation component on a south-facing vertical surface; occup: occupancy status (gray = office working hours); Troom: room temperature; EPD: hourly mean total electric power demand; EPD-hMev: electric power demand for heating by mechanical ventilation.

The reason relates to the very different operation of heating by means of mechanical ventilation in the two simulations (Figure 8.18, bottom panel). Apparently, the energy-optimal solution by the PB consisted in pre-heating the room during daytime (with the aid of internal gains) whereas the RBC-3 controller minimized daytime heating at the cost of having to use more heating power during nighttime and in the early morning hours of the next day. Note that the average power consumption (cf. third panel) over the entire week was lower in the PB (8.9 W/m^2) as compared to the RBC-3 simulation (9.6 W/m^2).

8.4 Discussion

The found savings potentials for the RBC-3 control strategy were highly case-dependent (Figures 8.1, 8.2 and 8.6–8.12). Moreover, it was found that the individual potentials can not be easily predicted from the defining factors such as building site, façade orientation or construction type (Figures 8.3–8.5). These results on the one hand highlight that appropriate modeling and simulation tools are indispensible for the assessment of alternative control strategies on a per-case basis. On the other hand they also confirm our approach of exploring the savings potentials with the aid of a large-scale simulation study.

The database analyzed included some PB simulations that used extra electric lighting for heating (Section 7.3.1.5), and several RBC-3 simulations that showed violations of the upper and lower thermal comfort bounds by up to +38 Kh/a and -198 Kh/a, respectively (Appendix E; see also Figures 8.1 and 8.2). The first problem tended to inflate the NRPE usage by the PB in some cases by up to a few percent (Section 7.3.1.5), whereas the second one was associated with reduced NRPE usage by the RBC-3 controller. The net effect was a conservative estimation of savings potentials. We therefore believe that our overall results were not too much affected by these problems.

The conducted statistical analyses allow us to comment on the hypotheses stated in the introduction:

Hypothesis 1: *"The importance of advanced control increases with the complexity of the building technical system under consideration"*. The rationale behind this statement is that the more complex a given system the more difficult it is to determine a "simple" rule-based strategy (including generic tuning rules, cf. Chapter 3) that comes close to the Performance Bound (PB). Our results support this view to some extent, because on average the largest absolute potential savings were obtained for the most complex Building System variant, variant S2. Interestingly, for this variant the absolute savings potentials also showed the largest variation (Figure 8.1). This result is compatible with the fact that rule-based control is normally tuned to "average" conditions, such that for increasingly complex technical systems the rules can be expected to perform poorly for an increasing fraction of the cases.

Hypothesis 2: *"Intelligent control is particularly favorable in the presence of high energy fluxes"*. This argument is based on the notion that in the presence of higher energies the system responses tend to depend more sensitively on control decisions. Our findings definitely support this statement: the found savings potentials were generally positively correlated with the available solar gains (Figure 8.5) as well as the internal gains level (Figures 8.3 and 8.4). However, the lack of dependency on the solar gains for the Swiss Average Building Standard and Building System variant S3 (bottom right panel in Figure 8.5) presented an exception. This result reflected the compensating effect of a slightly positive correlation for heavy buildings and a slightly negative one for light buildings (analysis not shown). The reasons behind the found behavior for the light buildings are not clear and should be investigated further.

Hypothesis 3: *"Predictive control is more useful for 'heavy' as opposed to 'light' buildings"*. This frequently stated argument is based on the notion that buildings with a high thermal mass have long response times, and are thus particularly suited for predictive control. Our ANOVA results support this statement only for the Swiss Average Building Standard (Figure 8.3, right panels), whereas for the Passive House Building Standard the ANOVA showed for the heavy Construction Type a below-average savings potential (Figure 8.3, left panels). A closer analysis showed that this result depended on the definition of "average" conditions as implied by the specific set of cases considered in this study (Section 8.2.1): the positive effect of high thermal mass was also present for Passive Houses, however only for corner offices with a high window area fraction. This was in line with the results reported in Figure 8.5 which shows that for both Building Standards heavy constructions are only advantageous in the presence of high solar gains. Apparently, advanced control can manage high thermal masses effectively only if there is enough "cheap" energy at disposal.

Figure 8.5 also shows a large amount of variation around this general trend. The variability probably reflects the fact that a building's time constant does not only depend on the thermal mass but also on the transmission losses through the envelope. A further factor that contributed to the richness of the found responses is that heavy buildings tend not only to react "slower" but also to be less sensitive to fast weather and internal gains disturbances than their light counterparts.

Hypothesis 4: *"Predictive control is particularly advantageous during the transition seasons"*. This statement is based on the intuition that during mid-latitude spring and autumn there is a culmination of situations that make "intelligent" switching between heating and cooling necessary. Our results do not provide much support for such a simple argument. Firstly, it was found that total savings potentials were generally irregularly distributed throughout the year. And secondly, in several cases both, heating as well as cooling savings potentials were found to occur simultaneously during wintertime (Figures 8.10 and 8.11). These results show that the transition period between the heating and cooling seasons is building-specific and can hardly be defined based on outdoor climate alone. The lack of general rules is not too discomforting since the Performance Bound calculations can be used to flexibly detect savings potentials whenever they occur throughout the year.

The allocation of the savings potentials to the various technical subsystems (Figure 8.12) showed that the main potentials were associated with the fast heating and cooling devices. Although energy recovery was operated quite differently between the PB and the RBC-3 strategy (Figures 8.13 and 8.14) total energy use for ventilation was generally very similar same for both control approaches (Figure 8.12). The ventilation-only variant S3 presented an exception that deserves further study.

The PB and the RBC-3 strategy showed very similar costs for electric lighting because they both minimized the use of NRPE-intensive electricity by using as much daylight as possible. Note that since the lighting costs present a substantial part of total costs (Figure 8.12) any changes in the prescribed illuminance comfort or lighting parameters would strongly affect the found relative total savings potentials (Figure 8.2).

The origins of the savings potentials could be traced to the predictive behavior of the PB, as opposed to the non-predictive control realized by the RBC-3 strategy (Figures 8.13 and 8.14). The PB results provide a valuable benchmark for the development of enhanced, predictive rule-based strategies that could be used to harvest the found potentials. Our analyses suggest that such strategies should attempt to (i) keep the room temperature closer to the center of the comfort range in order to reduce frequent switching between cooling and heating; and (ii) to pre-heat or pre-cool the building structure with the aid of anticipatory blind movement and free cooling.

As shown in Figures 8.16 and 8.17 predictive control can help to reduce not only energy usage but also (summertime) peak electric power demand. However, Case 13 (Figures 8.16 and 8.18) clearly demonstrates that there are also some tricky exceptions. In view of the complexity of the problem we believe that a general *rule-based* control solution for joint minimization of energy cost and peak electricity power demand is hardly feasible. The most promising (and flexible) approach probably consists in the development of Model Predictive Control algorithms that include appropriate constraints (cf. Section 4.2.4) for peak power limitation.

Finally we note that our results refer to individual building zones or rooms, not whole buildings. Savings potentials for entire buildings might be smaller than for the cases considered here (Table 8.1) since each building can be expected to include also low-potential zones. On the other side, additional savings potentials might emerge from optimized management of energy fluxes between zones. Such investigations would require simulations with a whole building/multi-zone model. These would also allow for a more realistic assessment of peak electricity demand.

8.5 Conclusions

The comparison of the rule based strategy RBC-3 with the Performance Bound (PB) shows that the putative benefits of improved (predictive) control are highly case dependent. Both, the mean and the variability of the absolute savings potentials are largest for the Building System variant S2 (most complex technical system), and smallest for variant S3 (ventilation-only system). Relative savings potentials are for all three Building System variants S1–S3 always higher for the Passive House as compared to the Swiss Average Building Standard.

In general, savings potentials for the RBC-3 strategy tend to increase with higher solar and internal gains. Façade orientation is the most important single factor explaining the variability of the savings potentials, followed by window area fraction and building site. A newly introduced compound measure of annual average solar gains typically explains ~50% of the variance in savings potentials. The consideration of internal gains levels increases the proportion of explained variance by 5-10%.

For the systems considered in this study heavy buildings are only favorable if sufficiently large solar gains are at disposal. Otherwise savings potentials tend to be higher for "light" buildings, where already small energy fluxes can be exploited by improved control.

A detailed investigation of the results for Building System variant S2 showed that energy saving potential is identifiable throughout the year. Improved control implies a shortening of both, the heating as well as the cooling season. For variant S2 the savings are mainly associated with reduced energy usage for radiator heating and free cooling. Energy savings for heating and cooling are often realized simultaneously in one and the same month.

The savings potentials can be traced back to the optimized use of the blinds, free cooling and energy recovery subsystems. Predictive control of these low-cost devices allows to efficiently pre-heat or pre-cool the building structure and to avoid frequent switching between heating and cooling while keeping room temperatures floating more freely within the prescribed thermal comfort range.

Predictive control also appears beneficial with regard to reducing peak electricity demand. From a total of 18 cases investigated in 9 cases was found a reduction, in 8 no change, and in 1 case an increase in the upper few percentiles of the hourly electric power demand values simulated during a year. The last mentioned case shows that energy efficiency and reduction of peak demand can present conflicting objectives and suggests the need for explicit consideration of peak limitation in the control algorithms.

In summary, it was found that the mechanisms determining energy savings potentials and reduced peak electricity demand can be plausibly explained a posteriori. The dynamical behavior of the simulated building systems and their overall energy demand often depend on subtle variations in the timing and magnitude of control actions. This underlines the importance of appropriate tools and data sets for the simulation-based development of improved control solutions. It also points towards possible limitations when one aims to exploit the found theoretical potentials in practice.

This work investigated savings potentials only for one particular control strategy, RBC-3. Nevertheless, given the large number of cases considered and the generality of the mechanisms identified we believe that all in all our findings give a useful insight into the potential of predictive control for the application Integrated Room Automation.

Chapter 9

ANALYSIS OF MODEL PREDICTIVE CONTROL STRATEGIES

by Frauke Oldewurtel, Dimitrios Gyalistras, Colin. N. Jones,
Alessandra Parisio and Manfred Morari

Cite as:

Oldewurtel, F., Gyalistras, D., Jones, C.N., Parisio, A. & Morari, M. (2010). Analysis of Model Predictive Control Strategies. In: Gyalistras, D. & Gwerder, M. (eds.): *Use of weather and occupancy forecasts for optimal building climate control (OptiControl): Two years progress report*. Terrestrial Systems Ecology ETH Zurich, Switzerland and Building Technologies Division, Siemens Switzerland Ltd., Zug, Switzerland, pp 135–151. ISBN 978-3-909386-37-6..

9.1 Introduction

Chapter 8 demonstrated a considerable theoretical potential for improvement of control performance thanks to the use of predictive control. In this chapter we investigate how far this potential could be exploited by using the Model Predictive Control (MPC) strategies introduced earlier (Chapter 4). Besides control performance we also explore some other properties of these strategies.

We address the following questions:

Q1: What is the added value of Certainty Equivalence MPC?

Q2: What is the added value of stochastic MPC?

Q3: How much does the quality of weather predictions matter for MPC?

Q4: How robust is MPC to model parameter mismatch?

Q5: How can a desired thermal comfort level be adjusted with MPC?

The formulation of these questions was guided by the first four assessment criteria given in Chapter 1 (Table 1.1), as follows:

Q1 and Q2 are related to the assessment criterion no. 1 ("achievable control performance"). For the corresponding analyses we employed MPC using weather forecasts from the COSMO-7 numerical weather prediction model (see Chapter 6). As benchmarks we used the Performance Bound (PB) and the non-predictive, rule-based control (RBC) strategy RBC-4 (see Chapter 3).

Q3 was motivated by the fact that the success of MPC in real applications depends on the quality of the information available at each time step as an input to the model-based optimization. Q3 went with the assessment criterion no. 3 ("robustness on building type, disturbances, user interactions"). Here we focused on the varying quality of weather predictions due to the use of different forecast methods. Otherwise we assumed that the building's state and the future internal gains are perfectly known at begin of each optimization step.

Q4 dealt with the fact that the quality of the model that is incorporated in the controller is also essential in the practical application of MPC. The question goes with criterion no. 2 ("robustness on control parameter settings"): we considered the effect of uncertainty in the MPC model parameters. The building's state and the future weather and internal gains were assumed to be perfectly known at begin of each optimization step.

Question Q5 finally related to criterion no. 4 ("flexibility and tuning effort in the engineering process"). We investigated the tuning of the thermal comfort level because of its obvious importance.

Below we first present our assessment strategy and the simulations undertaken (Section 9.2), followed by a presentation of the results (Section 9.3), a discussion (Section 9.4), and our conclusions (Section 9.5).

9.2 Materials and Methods

9.2.1 Simulation Experiments

In order to answer the five questions we conducted several sets of simulation experiments, as summarized in Table 9.1. Below we discuss the table in more detail.

Experiment/ Question	*HL-Ctrl*	*LL-Ctrl*	*WP*	*KF*	*HL-Tuning*	*Cost Function*	*Year*	*Period*	*Case Nos.*	*Set-backs*
E1/ Q1	PB CE RBC-4	EL EL RBC	– W4 –	– x –	– – –	MC	2007	Jan-Dec	01–18	no
E2/ Q2	SMPC	EL	W4	x	–	NRPE	2007	Jan-Dec	01, 02, 03, 07, 17, 18	no
E3/ Q3	CE	– – – –	W1 W2 W3 W4	– – – x	– – – –	NRPE	2007	Jan-Dec	01–18	no
E4/ Q4	CE	EL	W4	x	–	NRPE	2007	Jan-Dec	01	no
E5/ Q5	PB CE SMPC RBC-4	EL EL EL RBC	– W4 W4 –	– x x –	– x x –	NRPE	2007	Jan	01	no

Table 9.1: Overview of simulation experiments. HL-Ctrl: High-level controller; LL-Ctrl: Low-level controller; WP: Weather Prediction type; KF: Kalman Filter for local correction of weather forecasts at building site; PB: Performance Bound; CE: Certainty Equivalence Model Predictive Control; SMPC: Chance Constrained Stochastic Model Predictive Control; RBC-4: Rule-based control no. 4; EL: low-level control for electric lighting only; RBC: Standard low-level control for rule-based controllers; x/–: used/not used; W1–W4: See Table 9.2. Case Nos.: see Table 9.3.

High-level controller: Four different controllers were considered: the Performance Bound (PB), the Certainty Equivalence MPC (CE), the Chance Constrained Stochastic MPC (SMPC) and the Rule-Based Control no. 4 (RBC-4). RBC-4 was chosen because it was a rule-based controller that allows moving of the blinds once every time step (every hour), in exactly the same manner as this is the case for CE and SMPC. This ensured a fair comparison. In reality blind movements once an hour are already very frequent, and alternative restrictions to blind movement could have been formulated. We chose this particular restriction because it could be easily implemented within our modeling framework.

Low-level controller: PB, CE and SMPC had no low-level controller, or only a very simple one that regulated only electric lighting (EL), as described below. RBC-4 had the generic, ideal RBC low-level controller described in Section 3.3. The EL controller was introduced for two reasons: (1) Initial investigations showed that the errors present in the weather forecasts for the next time step(s) lead to a frequent violation of the illuminance level in the room. In reality, a constant light level control would prevent these violations happening. Therefore, an (ideal) illuminance correction was implemented that adjusted the illuminance level to the minimum required level, depending on occu-

pancy status. (2) The EL controller also solved the problem that electric lighting was sometimes used as a fast heating device (see Chapter 7).

Weather predictions: We used hourly weather input data for the years 2006 and 2007, and a series of weather prediction methods, as described in Table 9.2.

WP Method	*Description*
W1	Persistence prediction: The weather is predicted by using the measurements from the past 24 hours for the prediction horizon of usually 24 hours. In order to prevent a big jump between the weather actually experienced during the last hour and the predicted weather for the first hour, the prediction for the first predicted hour is given by the measured data from the last hour.
W2	"Direct model output": The gridpoint-scale predictions by the COSMO-7 numerical weather prediction model of MeteoSwiss are used.
W3	"Postprocessing": The COSMO-7 outputs are postprocessed with a newly developed statistical method developed at MeteoSwiss (Section 6.4). Update cycle: 12 h.
W4	"Postprocessing + local Kalman filter": Same as W3, but in addition a local Kalman filter is employed that uses measurements from the building site to improve the COSMO-7 forecast. Update cycle: 1h.
W5	"Direct model output + local Kalman filter": Same as W2, but in addition usage of a local Kalman filter. Update cycle: 1h.

Table 9.2: Overview of weather prediction methods.

Kalman filter: A simple Kalman filter/predictor for the local correction of the radiation-related disturbances was used, as outlined in Section 4.5.1. The local Kalman filter assumes the availability of corresponding measurements at the building site and was tuned separately for weather prediction methods W2 and W3 (see Table 9.2) as follows: firstly, tuning was done for a building zone with South oriented façade separately for each location considered. Secondly, the mean values of the tuning parameters over all locations were computed. These values were finally applied to all locations and all façade orientations. Note, there were two sets of local Kalman filter parameters, one for the W2 and one for the W3 predictions.

Tuning of high-level controllers: Tuning (for adjustment of thermal comfort level) was explored only for the CE and SMPC controllers. For SMPC there exists a single tuning parameter α that can be used for tuning. As default value 0.01 was used which corresponded to the definition of the chance constraint that the comfort band should be respected in 99% of the cases. For CE there exists no single tuning parameter. Instead, tuning was done by varying the width of the thermal comfort range employed in the optimization: a tighter comfort range should result in a more conservative behavior and less violations of the original comfort range, and a broader one in a less conservative behavior and more violations.

Cost function: Optimizations were partially done by optimizing over Non-Renewable Primary Energy (NRPE) usage and partially by optimizing over Monetary Costs (MC). MC was erroneously employed in some cases due to a mistake in the setup of the experiments. Here we report however only NRPE usage, as derived by post-processing of the MC results. This procedure tended to modestly overestimate the NRPE usage that would have been obtained under an optimization for NRPE (see Chapter 7). Optimization was done with an hourly time step and a prediction horizon of 24h. For dealing with the chance constraints the deterministic equivalent described in Chapter 4 was used. The feedback matrix of the affine disturbance feedback was first optimized over and then fixed for the remaining optimization. For this the average over six feedback matrices was computed.

Cases sets: Simulations were done for a set of buildings cases, as summarized in Table 9.3. The cases were selected to reflect frequent and interesting building setups, with typical to large theoretical savings potentials thanks to predictive control (cf. Chapter 8, Table 8.1).

		Cases Set						
Case No	*Site*	*BSV*	*BS*	*FO*	*CT*	*WAF*	*IGL*	*VS*
1	LUG	2	sa	S	h	wl	ih	W
2	LUG	2	sa	S	h	wl	ih	V
3	MSM	2	sa	S	h	wl	ih	W
4	MSM	2	sa	S	l	wl	ih	W
5	SMA	2	pa	SW	h	wh	ih	W
6	SMA	2	sa	SW	h	wl	ih	W
7	SMA	2	pa	S	h	wh	ih	W
8	SMA	2	pa	S	l	wh	ih	W
9	SMA	2	sa	S	h	wl	ih	W
10	SMA	2	sa	S	h	wl	ih	V
11	WHW	2	pa	SW	h	wh	ih	W
12	WHW	2	sa	S	h	wl	ih	W
13	SMA	3	sa	S	h	wl	ih	W
14	WHW	3	pa	SW	h	wh	il	W
15	LUG	4	sa	S	h	wl	ih	W
16	SMA	4	pa	S	h	wh	ih	W
17	SMA	5	pa	S	h	wh	ih	W
18	WHW	5	pa	S	h	wh	ih	W

Table 9.3: Selected cases for assessment of Model Predictive Control strategies. BSV: Building System variant; BS: Building Standard; FO: Façade Orientation; CT: Construction Type; WAF: Window Area Fraction; IGL: Internal Gains Level; VS: Ventilation; sa: Swiss average; pa: passive house; h: heavy construction type; l: light construction type; wl: low window area fraction; wh: high window area fraction; il: low internal gains level; ih: high internal gains level; V: non-air quality controlled ventilation; W: CO_2-controlled ventilation.

Night/weekend set-backs: All simulations for Cases Set 1 assumed the presence of set-backs during non-working hours (Table 2.7).

Some further settings that were used in all conducted simulation experiments were: (i) The internal heat gains due to occupancy and equipment were assumed to be perfectly known over the entire optimization horizon; (ii) All MPC model states were assumed to be observable and perfectly measured.

9.2.2 Comparison Procedure

The performance was always assessed both in terms of annual total NRPE usage versus annual amount of thermal comfort violations, as well as NRPE usage versus annual number of violations.

The amount of violations was defined as the sum of the violations of the upper and lower bounds of the thermal comfort range and it was given in Kh. Tolerable violations are 20Kh/a for the lower bound and 50Kh/a for the upper bound, i.e. total amount of 70Kh/a. The distribution of the violations was not investigated, but in general the violations of the upper bounds were found to be more frequent. The considered number of violations was given by the sum of the upper and lower bound violations. In this case only the violations by more than 0.1K were counted since violations below this threshold were mainly due to numerical inaccuracies.

It was necessary to assess both energy and violations, because a given strategy can result in many violations and a small energy use, or vice versa, and it might even be possible to change this combination by tuning. Thus, if a strategy has more violations but a smaller energy use as compared to another strategy, no clear decision is possible which of the two strategies is superior. Only when both, energy use and the violations are less (or more) a clear decision is possible. Figure 9.1 summarizes the situation.

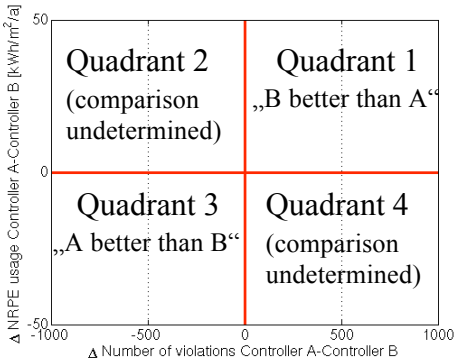

Figure 9.1: Overview of possible outcomes of controller comparison.

When comparing NRPE between two controllers A and B we considered absolute, as well as relative deviations (Δ). The relative deviations were given as 100(A-B)/PB, where A, B, and PB denote the NRPE usage of the respective control strategy. Unless stated differently all reported results refer to annual total NRPE usage.

9.3 Results

9.3.1 What Is The Added Value of Certainty Equivalence MPC (Q1)?

In order to answer Q1 we compared CE with PB and RBC-4 (Experiments E1 in Table 9.1).

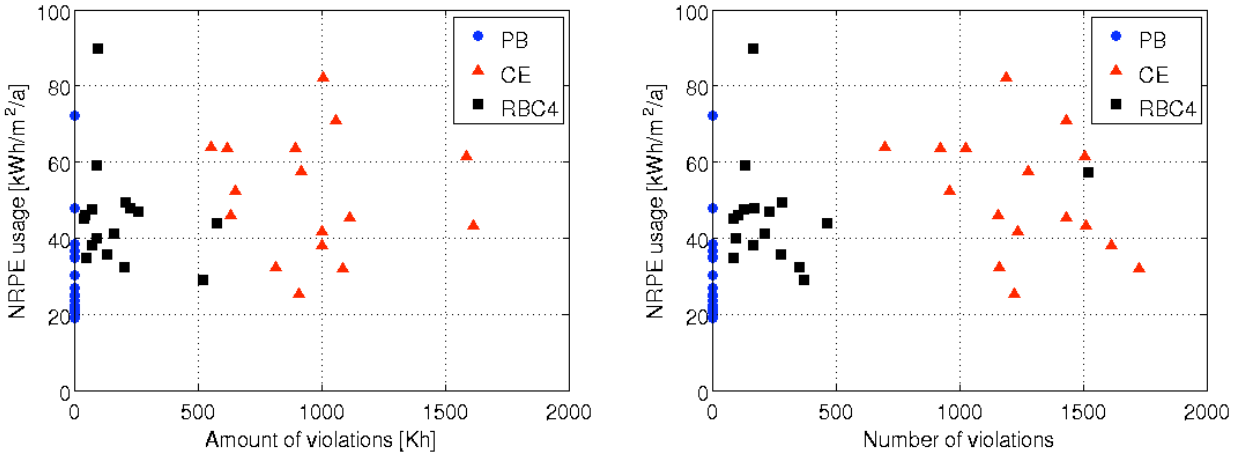

Figure 9.2: Comparison of PB, CE and RBC-4 in terms of NRPE usage versus amount of violations (left) as well as number of violations (right).

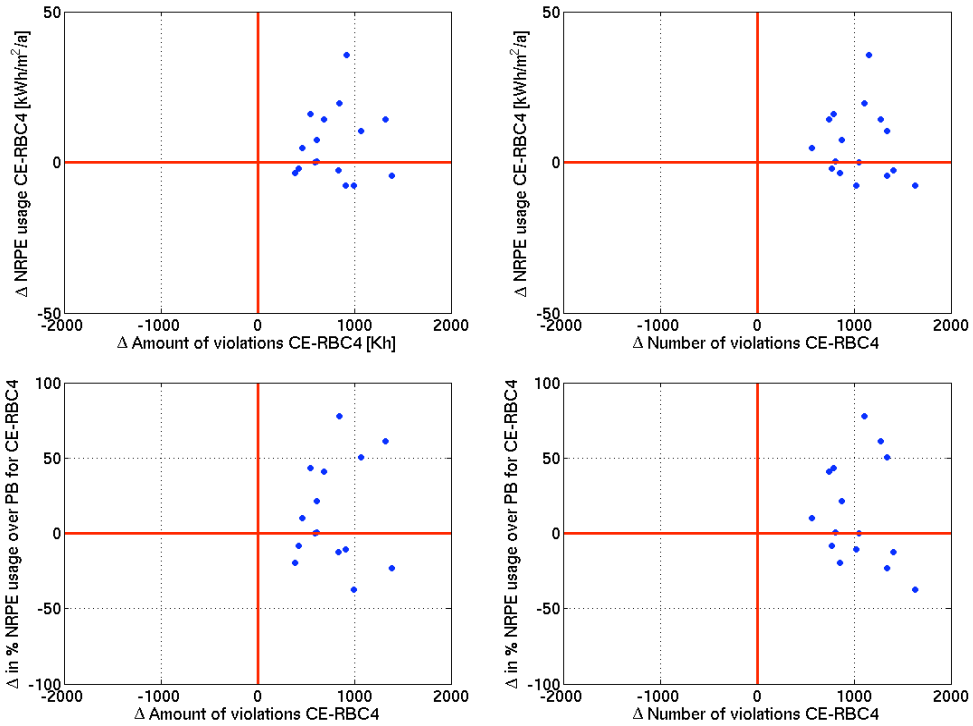

Figure 9.3: Comparison of CE and RBC-4 in terms of absolute (top) and relative (bottom) ΔNRPE usage versus differences in amount of violations (left), as well as in number of violations (right).

Figure 9.2 compares PB, CE, and RBC-4 in terms of NRPE usage and violations. It can be seen that PB showed practically no violations. CE, and RBC-4 used more energy than PB and both had many violations. When comparing RBC-4 and CE for all cases, both, RBC-4 as well as CE, exceeded 70 Kh/a, but CE violated this threshold more clearly. The number of violations were also typically larger for CE. Note, for both RBC-4 and CE the data points for the cases 4 and 8 are not shown because they were far beyond the axes ranges of the plots.

Figure 9.3 provides a pairwise comparison of the CE and RBC-4 results. As it stands, CE was for at least half the cases performing worse than RBC-4, and for the rest of cases the comparison was undetermined. (Note that cases 4 and 8 are omitted again).

9.3.2 What Is The Added Value of Stochastic MPC (Q2)?

In order to assess the possible added value of SMPC as compared to the simpler CE controller we considered PB, CE, RBC-4 and SMPC from the Cases Set (Experiments E1 and E2 in Table 9.1). Note for SMPC only cases 1,2,3,7,17, and 18 were available.

Figure 9.4 gives an overview of the obtained results. The results of PB, RBC-4 and CE are identical with those in Figure 9.2. SMPC resulted in clearly less violations than CE and for the available cases also had a comparable or smaller NRPE use. The amounts of violation were always < 70 Kh/a (the tolerable amount of violations defined in Section 9.2.2).

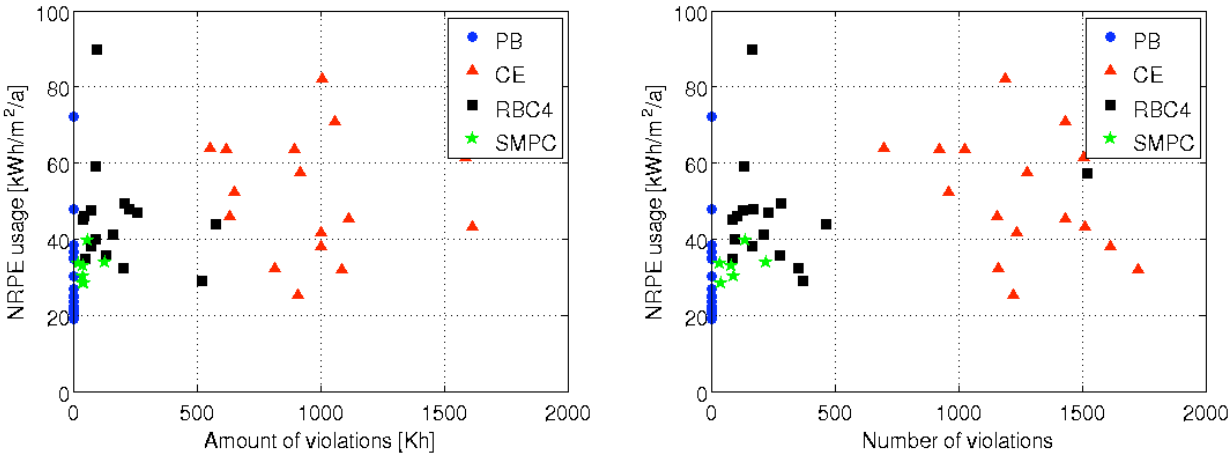

Figure 9.4: Comparison of PB, CE and SMPC in terms of NRPE usage versus amount of violations, (left) as well as in terms of NRPE usage and number of violations (right).

The comparison of SMPC and RBC-4 is more detailed in Figure 9.5 which shows a pairwise comparison for the six available cases. It is evident that SMPC performed significantly better than RBC-4 both in terms of NRPE usage and violations. The NRPE usage of SMPC was smaller by up to 22%.

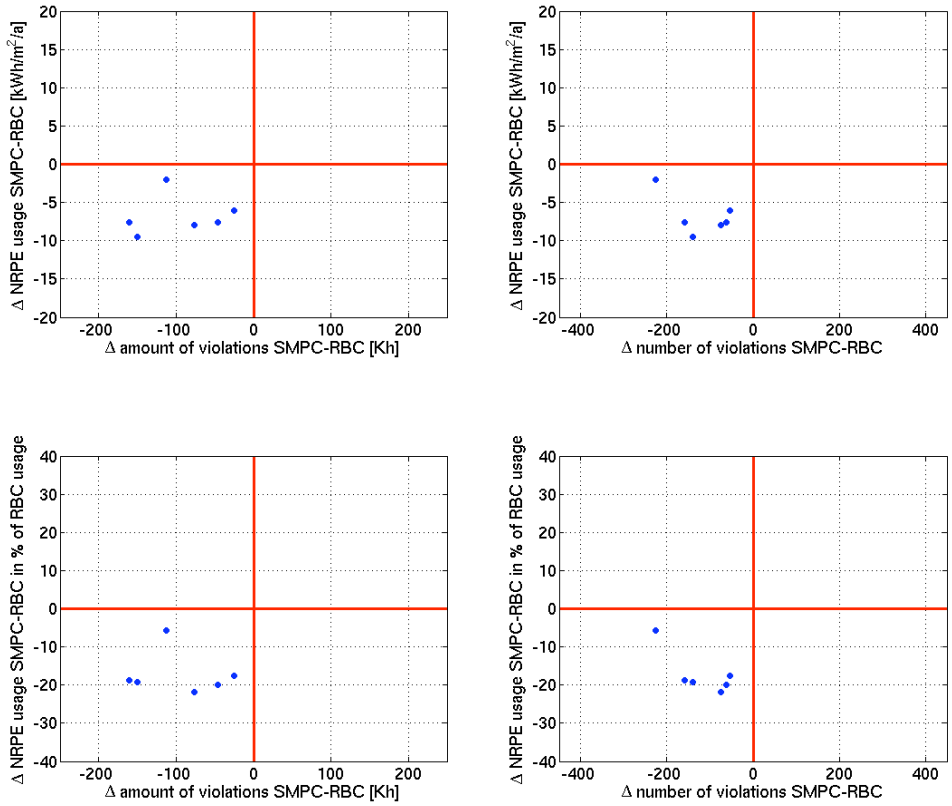

Figure 9.5: Comparison of SMPC and RBC-4 in terms of absolute (top) and relative (bottom) ΔNRPE usage versus differences in amount of violations (left), as well as in number of violations (right). Cases shown: 01, 02, 03, 07, 17, 18.

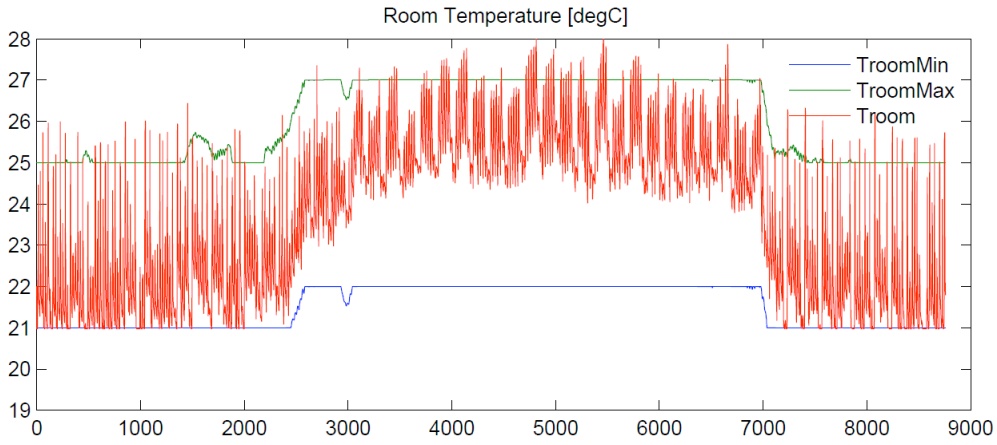

Figure 9.6: Annual evolution of the room temperature for Case 03, with controller RBC-4.

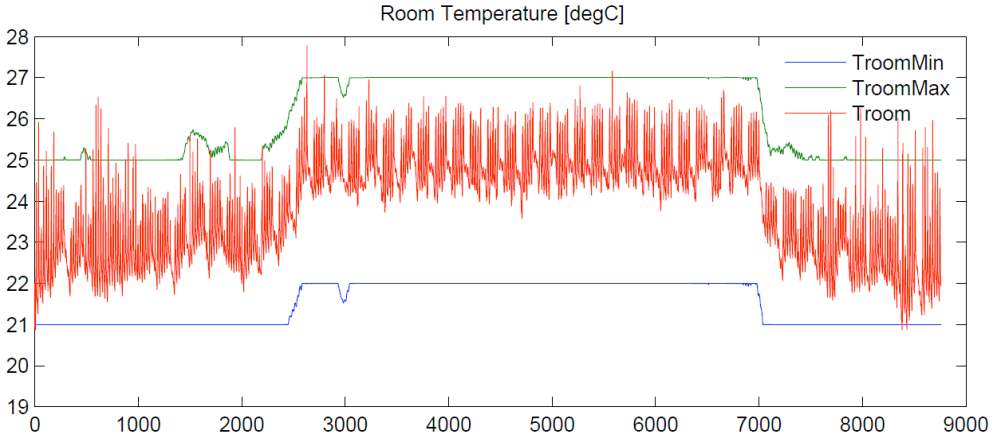

Figure 9.7: Annual evolution of the room temperature for Case 03, with controller SMPC.

Figures 9.6 and 9.7 depict the annual evolutions of the room temperature for Case 03 with the RBC-4 and SMPC controllers, respectively. It can be seen that RBC-4 yielded much larger high-frequency variations than SMPC. With the RBC-4 controller often the upper and lower bound of the comfort range were reached within one and the same day. With the SMPC controller the room temperature showed on average much smaller diurnal variations.

9.3.3 How Much Does The Quality Of The Weather Predictions Matter For MPC (Q3)?

To investigate the influence of the quality of the weather predictions, CE was run for Cases Set 2 with the four different weather predictions W1, W2, W3, and W4 (Experiment E3 in Table 9.1).

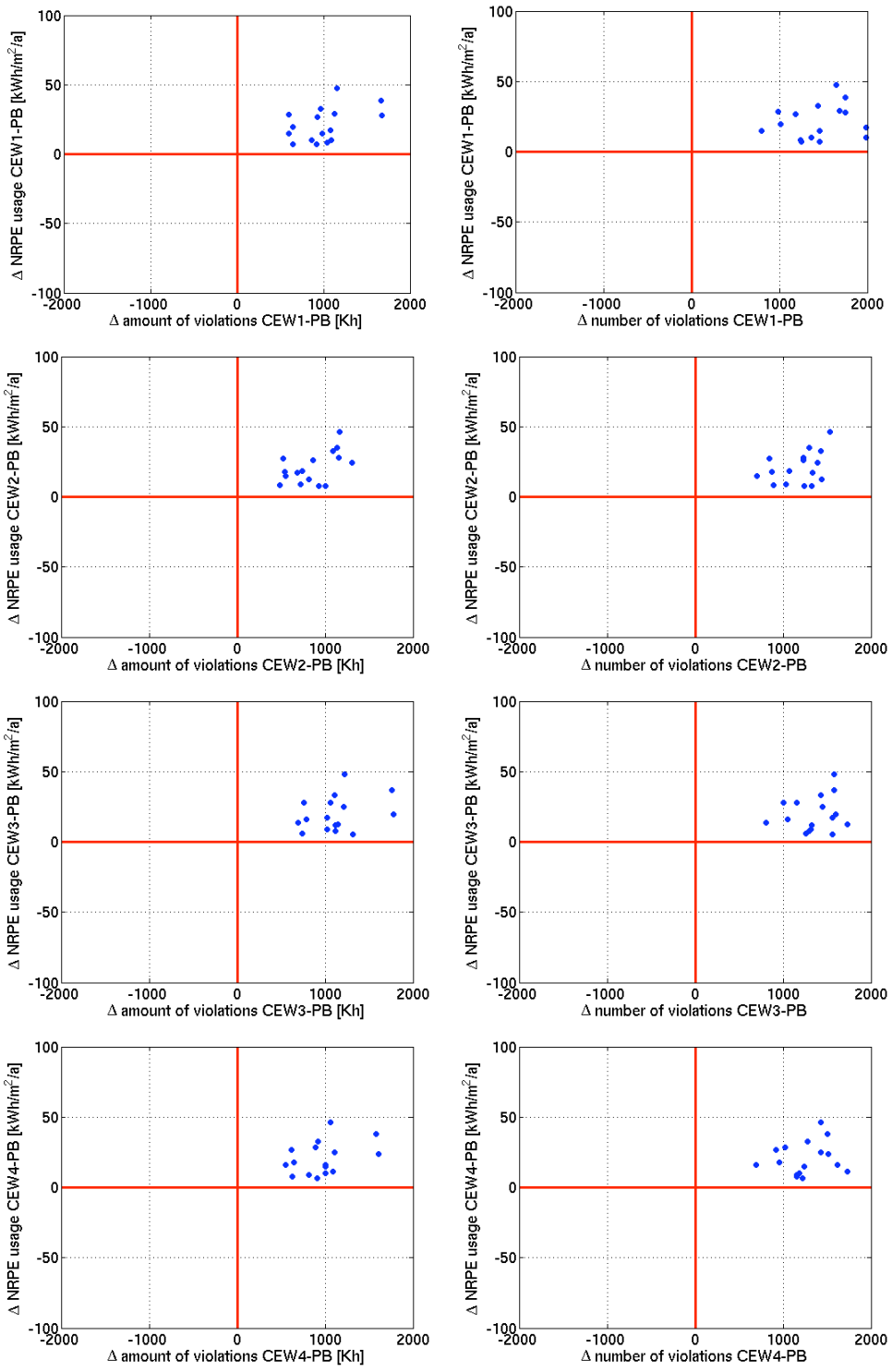

Figure 9.8: Comparison of CEW1, CEW2, CEW3, and CEW4 absolute ΔNRPE usage versus differences in amount of violations (left), as well as in number of violations (right).

Figure 9.8 depicts the differences in NRPE usage relative to PB for CEW1– CEW4 (from top to bottom) versus the differences in amount of violation to PB (left) and the differences in number of violations to PB (right). (The abbreviation CEW*n* means CE simulated with prediction method W*n*). All cases lie in Quadrant 1 meaning that PB was always superior. Apart from that the performance seems similar on the first sight.

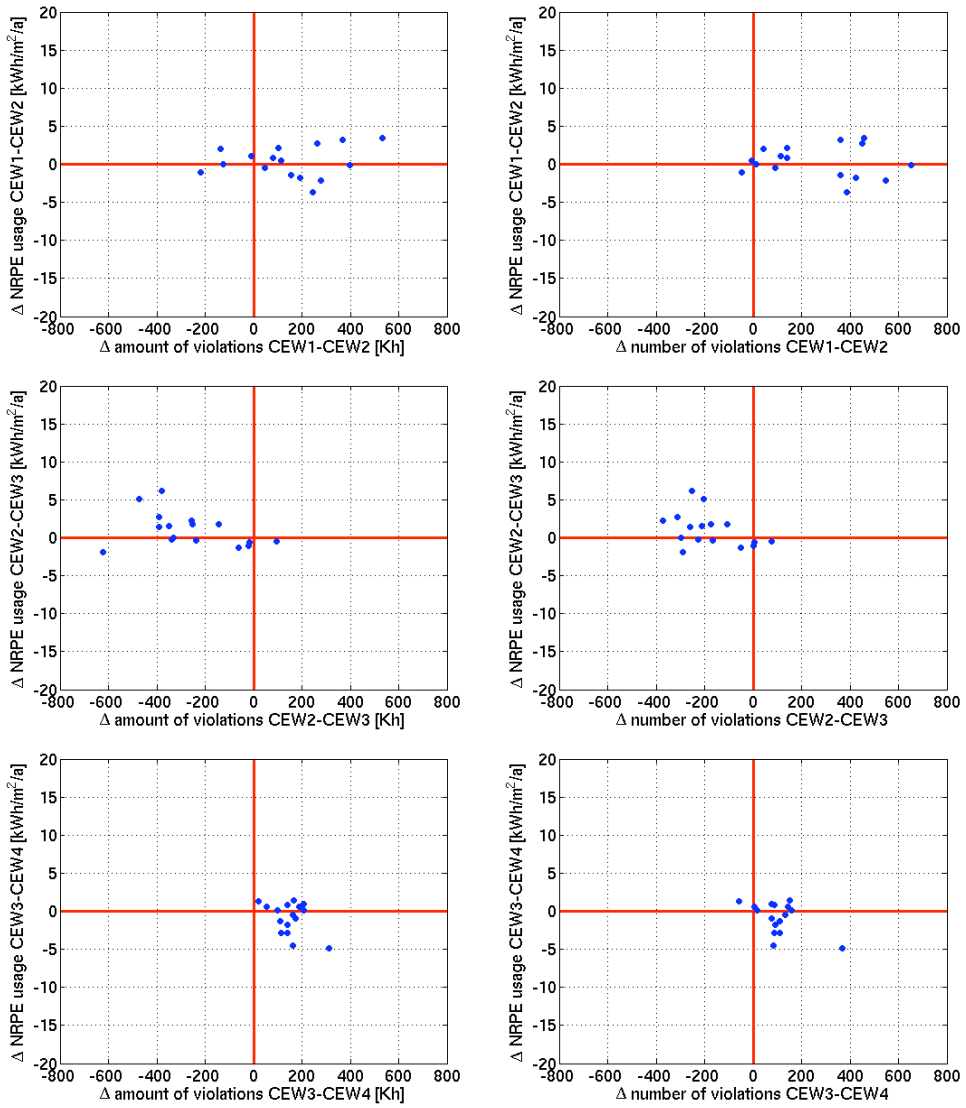

Figure 9.9: Comparison of CEW1-CEW2, CEW2-CEW3, and CEW3-CEW4 in terms of relative ΔNRPE usage versus differences in amount of violations (left), as well as in number of violations (right).

The changes in the CE controller performance due to the progression from W1 through W2 and W3 to W4 are shown in Figure 9.9.

From W1 to W2: 6 (left) or 7 (right) of 16 shown cases lie in the first quadrant, which means that using the COSMO-7 operational weather forecast was clearly better than using a persistence forecast. 9 (left) and 7 (right) cases, respectively, were found in Quadrants 2 and 4, where no clear decision was possible, and only one case each lies in the third quadrant, meaning that the persistence prediction yielded the better results.

From W2 to W3: Results are mainly in the second quadrant meaning that with the statistical post-processing of the COSMO-7 output the NRPE usage was reduced but more violations were caused. Few results in the third quadrant suggest that due to the statistical post-processing the control behavior deteriorated somewhat.

From W3 to W4: Results are in the first and fourth quadrant indicating that with the local Kalman filter the control behavior in about half the cases improved and that in the other cases the amount of violations was reduced at the expense of having more NRPE usage.

9.3.4 How Robust Is MPC To Model Parameter Mismatch (Q4)?

To investigate the robustness of the MPC strategies on model parameter mismatch we conducted experiment E4 (cf. Table 9.1). The parameters in the controller model were changed as listed in Table 9.4. The choice of parameters and their range of variation were determined such as to represent the uncertainty in the building properties' knowledge of HVAC designers in practice. The parameters were selected as being the most critical ones and the employed changes corresponded to the typical estimation uncertainty.

Experiment	*Mismatch*	*Involved Parameters*	*Change*
BPvar1	U-values windows	Utilwin0, dUtilwin	+10%
BPvar2	U-values windows	Utilwin0, dUtilwin	-10%
BPvar3	Heat transmission coefficients	hFloor, hCeil, hiW1,hiW2, hoW1, hoW2	+15%
BPvar4	Heat transmission coefficients	hFloor, hCeil, hiW1,hiW2, hoW1, hoW2	-15%
BPvar5	Energy recovery efficiency ventilation	epsERC	+15%
BPvar6	Energy recovery efficiency ventilation	epsERC	-15%
BPvar7	Building mass	Cs1...Cs5, CiW1...CiW3, CoW1...CoW3	+10%
BPvar8	Building mass	Cs1...Cs5, CiW1...CiW3, CoW1...CoW3	-10%
BPvar9	g-value and visual transmission windows	solGFact1, tauVisFact1	+10%
BPvar10	g-value and visual transmission windows	solGFact1, tauVisFact1	-10%

Table 9.4: Changes in controller model to investigate robustness on building parameters.

The sensitivity to individual mismatches was investigated by changing the parameters one at a time to the highest and lowest deviation. The resulting altered models were used in the CE controller, whereas the plant model representing the real building was left unchanged.

The CE simulation of Case 01 (set no. 2) with the perfect controller model was used as the reference for comparison.

An overview of the resulting behaviors with the modified controller model is given in Figure 9.9. In the left panel, the NRPE usage, and the amount and number of violations of the 10 experiments are plotted. The dashed lines indicate the levels of the reference simulation. The right panel depicts the respective relative changes to the reference in percent.

It can be seen that the energy costs among all investigated cases of model parameter mismatch were within a few percent, the amount of violations differed by no more than 9% and the numbers of violations did not differ by more than 14%.

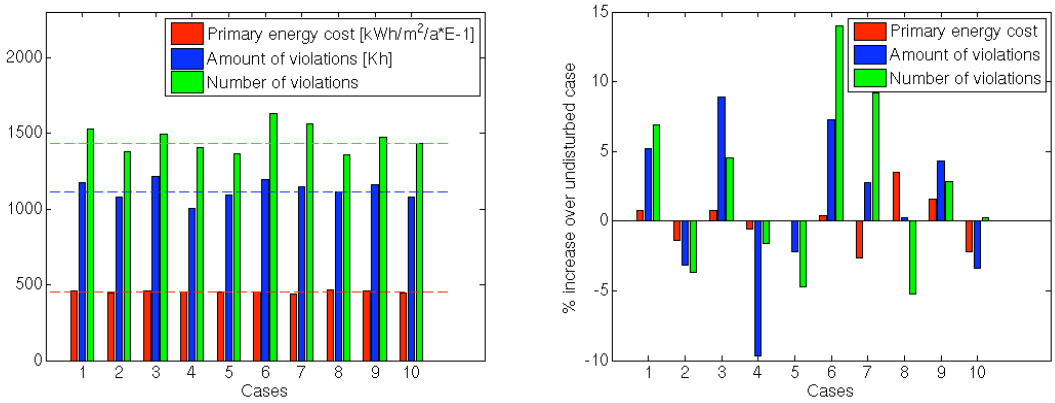

Figure 9.10: Absolute performance indicators of the modified models (left), and their relative deviations from the reference case (right). Note, NRPE usage in the left panel is given in 0.1 kWh/m²/a.

9.3.5 How Can The Desired Thermal Comfort Level Be Adjusted In MPC (Q5)?

The tuning of CE and SMPC was investigated for Case 01 from the Cases Set and the duration of one month (January, see also Table 9.1, Experiment E5). CE was run with different upper and lower bounds for the controller, and SMPC was run with different values of the tuning parameter α.

Figure 9.11 shows the NRPE usage versus the amount of violations with the different tuning settings. One can see that for both controllers it was possible to move along the tradeoff curve via tuning. The control performance is the better, the closer to the origin a curve lies. SMPC performed clearly better than both, CE and RBC-4; the RBC-4 data point was approximately on the tradeoff curve of CE.

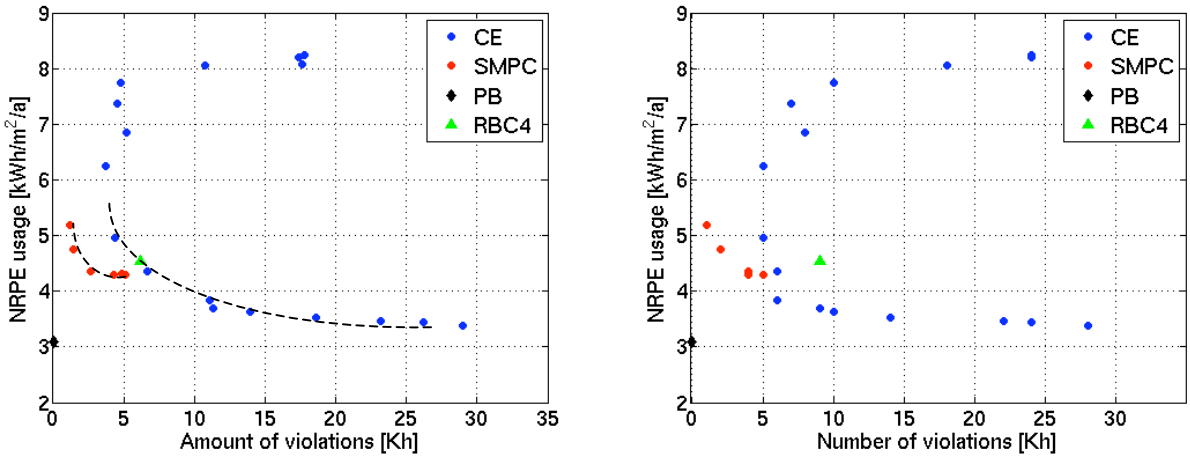

Figure 9.11: Tuning curves of SMPC and CE for Case 01 in January.

It should be noted for the CE curve that from a certain point on a further reduction of the comfort band yielded again an increase in the number and amount of violations. Hence it was not possible to reduce the amount of violations to the same level as for SMPC, even with more NRPE usage.

Figures 9.12 and 9.13 show the simulated room temperatures with RBC-4 and SMPC, respectively. It can be seen that SMPC kept the temperature in the middle of the comfort range, and that it yielded smaller diurnal temperature variations. For most days the simulated daily temperature amplitude was smaller than 2K. Quite differently, for RBC-4 in one third of the days the difference between the daily temperature extremes was larger than the comfort bandwidth of 4K, i.e. within one and the same day both the upper and lower bound of the comfort band were reached. This situation was never observed for SMPC.

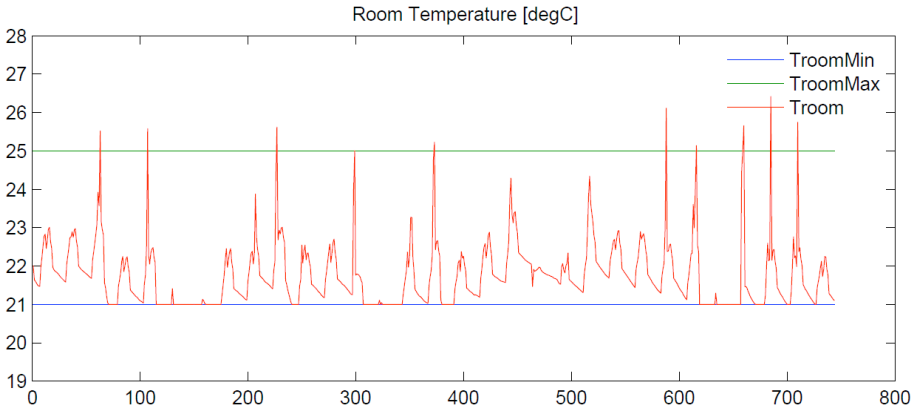

Figure 9.12: Room temperature of Case 01 for January with RBC-4.

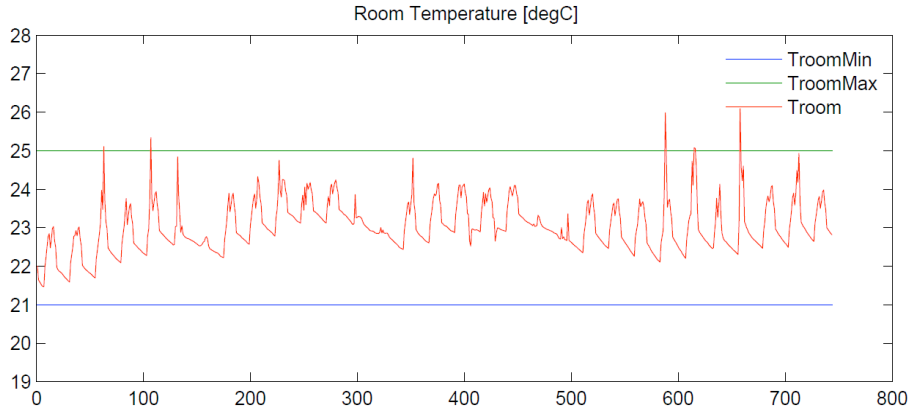

Figure 9.13: Room temperature of Case 01 for January with SMPC.

9.4 Discussion

For the assessment of the MPC controllers the newly developed rule-based control strategy RBC-4 was taken as a reference because it allowed for the same freedom in blind movement (once per hour) as the MPC controllers. An alternative would have been the state-of-the-art strategy RBC-1 (see Chapter 3). A closer analysis showed that in half of the 18 cases considered here (cases 01–03, 06, 09, 10, 12, 13, 15 from the Cases Set, see Table 9.3) the RBC-4 strategy performed clearly better than RBC-1 (results not shown). For the remaining cases RBC-1 performed better, suggesting that our results (Figs. 9.2–9.4) have to some extent underestimated the achievable performance by non-predictive rule-based control. Future studies should therefore better consider as a reference strategy “best of RBC-1 and RBC-4”. First such analyses (not shown) suggested however that the conclusions drawn from the comparison of RBC-4 and SMPC (Figs. 9.5-9.7) remain valid.

When comparing RBC-4 with CE, there were cases where RBC-4 was clearly superior, and others where CE was using less NRPE but had more violations (see Fig. 9.3). The neglect of the uncertainty present in the weather predictions by CE apparently resulted in many violations, many more than typically would be tolerated in office buildings.

When comparing with RBC-4 one has to note that RBC-4 is running with a low-level-controller that is instantaneously and ideally rejecting any disturbances, whereas the MPC strategies are run with an hourly time step and thus have their control inputs fixed at the begin of each hour. It can therefore be expected that the comfort performance of CE can be significantly improved (at the expense of higher energy use) if a low-level controller is added.

The results obtained with CE have shown that the uncertainty in the weather prediction has a significant impact. SMPC takes the uncertainty in the weather prediction directly into account and was found to be superior to CE when the two strategies were tuned to the same amount of energy use and a small amount of thermal comfort violations (Fig. 9.11).

Moreover, our results indicate that SMPC performs significantly better than RBC-4 (Figs. 9.5–9.7, 9.12, and 9.13). SMPC was found to outperform RBC-4 both in terms of NRPE usage and in terms of the amount and number of violations (Fig. 9.5, 9.11). Note that this was achieved without using a low-level controller – the SMPC control inputs were fixed on an hourly basis. The obtained improvement in performance as compared to CE was only due to the fact that the uncertainty in the weather prediction was taken into account.

A further advantage of SMPC relates to the resulting dynamics for the room temperature. As can be seen from Figs. 9.6 vs. 9.7 and 9.12 vs. 9.13, SMPC yielded much smaller diurnal temperature amplitudes. This behavior can be considered more favorable because the occupants are exposed to much smaller temperature variations during the day.

In general the comparability of control strategies was complicated by the fact that controller performance needs to be measured in terms of both, energy usage, and some thermal comfort violation statistics. In order to facilitate comparability we introduced “delta” plots, as described in Fig. 9.1. However, data points that are found in the second and fourth quadrant – i.e., one strategy uses less energy than the other, but has more violations – make further investigations necessary. One possibility consists in adjusting the controllers to the same amount of comfort violations via tuning. The tunability of CE and SMPC was demonstrated in Fig. 9.11.

Tuning for CE was accomplished by assuming a tighter comfort range in the controller. Tightening of the comfort range makes the controller more conservative, i.e. it is producing less violations at the cost of spending more energy. Interestingly, the same level of constraint violations possible with SMPC could not be reached with CE. From a certain point on further tightening of the comfort range was found to lead to an increase of NRPE usage (Fig. 9.11). The reason was that the assumed comfort range was so small that the soft constraints upon the room temperature were active all the time such that the controller could not react properly anymore.

The tuning for SMPC is much simpler and was done by changing a single parameter that is describing the probability level of constraint violation. With this tuning knob, the user can easily adjust the system between ‘high comfort/high energy usage’ mode to ‘low comfort/low energy usage’ mode.

Although both, CE and SMPC can be tuned, the resulting tradeoff curve by CE (Fig. 9.11) was on the right hand side of the tradeoff curve of SMPC, which means that at some point CE cannot reach a smaller amount of violations even if it spends more energy. This also holds for SMPC, but at a smaller level of violations. One should also note that when SMPC was run with the predefined tuning value of $\alpha = 0.01$ (and a properly tuned local Kalman filter) it already complied with the defined tolerable value of 70 Kh/a for comfort violations (Fig. 9.4).

As described in Chapter 4, the controller models used for MPC were assumed to be perfect so far, i.e. equal to the models used to simulate the building behavior. The sensitivity to model parameter mismatch is very important for all MPC strategies, since in reality a perfect model of the building will not be available. All model parameters can however be estimated from physical parameters (Chapter 5). The results shown in Fig. 9.10 suggest that the control performance is quite robust within the expected range of model parameter mismatch. There is an increase in violations, but this can be dealt with by tuning. Further work should be done on a randomized study in order to account for the fact that in reality estimation errors apply to several parameters simultaneously and that these errors can be correlated.

From Fig. 9.9 can be seen that the operational weather predictions obtained from the COSMO-7 numerical weather prediction model generally helped to improve control performance compared to the use of a persistence forecast. As discussed in Chapter 6 the impact of further statistical post-processing of the COSMO-7 direct model output (DMO) was positive throughout for air and wet-bulb temperature, but depended on the season for the global radiation components. This might explain the undetermined results obtained in 9.3.3 from the comparison of the control performance with "DMO" (W2) and "Postprocessing" (W3) as disturbance input. Consequently, the impact of errors in the radiation predictions on the control performance might be of dominating importance and therefore need to be further investigated. Moreover, for our simulations we used throughout an optimization horizon of 24h, and the use of a longer horizon should also be investigated.

The importance of the local Kalman filter can be seen from Fig. 9.9. The local Kalman filter can be expected to become even more important in practice when systematic errors must be accounted for (shadowing effects of neighboring buildings etc.).

In the Cases Set (Table 9.3) there were only two building cases (Cases 04 and 08), that had a light construction type. In all simulations undertaken with the CE and RBC-4 controllers these two cases produced outliers in the results, that were behaving notably different from the rest of the cases, both in terms of NRPE usage and comfort violations. Possibly, this behavior has also been caused by the used scant dimensioning for the maximum available heating and cooling power (Chapter 2.3.2). Further investigations are needed in order to understand this result.

9.5 Conclusions

The newly developed Chance Constrained Stochastic Model Predictive Control (SMPC) strategy is clearly superior to the non-predictive rule-based controller RBC-4. The CE MPC strategy performs in some cases comparable to RBC-4, for others cases it is worse.

SMPC not only outperforms RBC-4 in terms of Non-Renewable Primary Energy (NRPE) usage and thermal comfort statistics, but it also yields much more favorable room temperature dynamics showing smaller diurnal temperature variations.

The uncertainty present in local weather predictions has a significant effect on CE controller performance. CE could be improved by using a low-level controller as in RBC-4, since the primary problem of the CE strategy is the abundant comfort violations that a low-level controller can reject.

Operational weather forecasts with the numerical weather prediction model COSMO-7 give an improvement of the control performance as compared to persistence forecasts. The use of statistically post-processed COSMO-7 predictions results in lower NRPE usage but at the cost of more thermal comfort violations.

Use of a local Kalman filter for the correction of the COSMO-7 weather forecasts at the building site seems to have a small beneficial effect. The impact of the COSMO-7 post-processing and how it intervenes with the local Kalman filter at the building site needs to be investigated further.

Our results further suggest that the performance of MPC controllers is robust against model parameter mismatch.

SMPC and CE can both be tuned to adjust the thermal comfort. The tuning of SMPC is particularly easy to accomplish and involves but one plausible parameter, the probability level of constraint violation. When tuned to comparable levels of energy use and a small amount of comfort violations SMPC proved superior to CE.

This page has intentionally been left blank.

Chapter 10

PROJECT STATUS

by Dimitrios Gyalistras and Markus Gwerder

Cite as:

Gyalistras, D. & Gwerder, M. (2010). Project Status. In: Gyalistras, D. & Gwerder, M. (eds.): *Use of weather and occupancy forecasts for optimal building climate control (OptiControl): Two years progress report*. Terrestrial Systems Ecology ETH Zurich, Switzerland and Building Technologies Division, Siemens Switzerland Ltd., Zug, Switzerland, pp 153–158. ISBN 978-3-909386-37-6.

10.1 Overview

During its first two years the OptiControl project has successfully answered many important questions related to the potential, utility and feasibility of predictive building control. Moreover, from a more methodical point of view, the project has pioneered research at the interface of buildings, applied meteorology, modeling/simulation, and control. These results have only been possible thanks to the excellent collaboration between all project participants and the unique combination of expertise in the project team.

The project combined elements of basic engineering research, development, and technology deployment. Research always involves elements of surprise, and the scientific investigation of the predictive control of modern, automated building systems revealed to be much more challenging than initially expected. The main reasons related to the very high complexity of the systems considered and the large number of variants and choices involved.

It has been a major success of the project of having found ways and methods to deal with this complexity, and as a result of being able to provide important insights into the relevant mechanisms and problem areas. This in turn paves the way towards the development of a new generation of controllers offering an unprecedented efficiency, flexibility and quality of control.

A first important project result consisted in the development and successful application of a general methodology, as well as corresponding software tools and data sets for the systematic, quantitative assessment of building control. To our knowledge this result is groundbreaking. Its importance is likely to increase in the future due to the growing demand for advanced, robust control strategies that shall ensure a correct and efficient operation of buildings. Such strategies can only be developed and analyzed with the aid of appropriate modeling and simulation tools.

In our simulation-based analyses we have considered a wide range of system variants and building cases for the Integrated Room Automation (IRA) application. The definition of a meaningful experimental set-up and the determination of appropriate models, approximations, and parameter values have been elaborate and demanding. Relevant building types, control operation types, locations, and types of heating, cooling, ventilation, blind and lighting subsystems were identified, the subsystems were sized properly, and meaningful energy usages/costs were specified.

For IRA, we have demonstrated a substantial, yet highly case-dependent potential for predictive control. The conducted large-scale simulation studies gave insight into the comparative performance of a range of state-of-the-art control approaches, as well as on the role of key factors affecting the control performance (e.g., set-backs, or variations in thermal comfort range width). To our knowledge, the depth and width of these quantitative results is unprecedented.

A new family of Model Predictive Control (MPC) algorithms has been developed that has been tailored to the needs of building control. These algorithms differ in their degree of sophistication, computing requirements, and robustness to disturbances and modeling errors.

Presently we are about to refine the newly developed MPC algorithms and to investigate their properties in detail. This goes in parallel with pushing forward our investigations of the use and added value of weather forecasts. A further ongoing activity is the development of rule-based predictive control algorithms. The implications of our single building zone results for whole buildings also need to be investigated further.

Substantial work remains to be done in order to make the novel control strategies suitable for use in practice. This includes the extension of our MPC solutions to the multi-zone case and an appropriate consideration of occupancy/internal heat gains that so far have not been treated in as much detail as originally planned.

Phase/ Milestone/ Deliverable	Description	Target month	Status
Phase I	**Initial Exploration and Sensitivity Analyses**		
M 1	Study sites, meteorological inputs, occupancy inputs, building types and HVAC systems defined.	**9**	achieved (IRA)
M 2	Targets and constraints for control strategies defined. Reference cases and simulation experiments defined.	**9**	achieved (IRA)
M 3	Software for preparation of weather data and weather forecasts implemented, initial data sets prepared.	**9**	achieved
M 4	Occupancy data sets prepared, first iteration of occupancy submodel implemented.	**11**	partially achieved occupancy data sets prepared, but no occupancy prediction considered
M 5	Simulation models for the selected building types and HVAC systems prepared.	**11**	achieved (IRA)
M 6	Predictive control schemes selected and adapted for building climate control (performance bound).	**11**	achieved (IRA)
M 7	Added value of weather forecasts and/or occupancy information explored.	**13**	partially achieved (IRA) first results for added value of weather forecasts, no occupancy prediction considered
M 8 + D1	Case studies for in-depth investigations selected.	**15**	achieved/delivered (IRA)
Phase II	**In-Depth Investigations**		
M 9	Procedure for the delivery of optimal local weather forecasts at building sites developed and tested.	**19**	achieved procedure developed and evaluated, possible improvements identified
M 10	Improved methods for the acquisition and modelling of occupancy data implemented.	**19**	not achieved occupancy prediction was not considered
M 11	Models of selected buildings and HVAC systems developed and tested.	**19**	achieved (IRA)
M 12 + D2	Predictive control strategies tailored to the case studies.	**19**	achieved/delivered (IRA)
M 13	Utility of probabilistic weather forecasts investigated.	**21**	not achieved no investigations done so far
M 14	Role of disturbances and forecast errors analyzed, control approach made more robust.	**23**	achieved (IRA)
M 15 + D3	Supervisory control and manual or automatic tuning methods investigated.	**23**	partially achieved/delivered (IRA) necessity to improve and analyze tuning procedure
M 16 + D4	Added value of the refined control approaches for the selected case studies determined.	**25**	partially achieved/delivered (IRA) control strategies still under development, evaluation ongoing
Phase III	**Demonstration**		
M 17	Demonstrator building and HVAC/energy systems selected.	**27**	achieved a potential demonstrator building has been identified and preparations are on the way
M 18 + D5	Control scheme plus monitoring and test strategies for demonstrator building defined.	**27**	–
M 19	System delivering operational weather forecasts at demonstrator building installed.	**27**	–
M 20	System exploiting occupancy information installed.	**27**	–
M 21 + D6	Control scheme implemented and fine-tuned.	**29**	–
M 22 + D7	Tests and experiments at demonstrator building completed.	**35**	–
M 23	Overall benefit-cost analysis completed.	**37**	–
M 24 + D8	Synthesis of overall project accomplished.	**39**	–

Table 10.1: Overview of project Milestones and Deliverables, as defined in the project description of August 2007 and its revision of May 2008.

During the last 6 months there also has been intensive preparation for the third project year (Phase III, demonstration in a real building). A demonstrator subproject has already been drafted in cooperation with a new candidate project partner, Dr. A. Seerig from Gruner AG, Basel.

Table 10.1 gives a more formal overview of the project status in terms of the Milestones and Deliverables. It can be seen that 10 of 16 milestones due at the end of the second project year have been fully achieved, and that 4 further ones have been partially achieved. The first milestone of Phase III could even be reached earlier than scheduled.

The following two sections discuss the achievements and the major challenges identified during the first two years in more detail.

10.2 Achievements

1. **Selection of building automation applications.** Two major classes of applications, namely (i) Integrated Room Automation (IRA), and (ii) the generic control of energy fluxes and energy storages related to buildings (Generic Flux Control, GFC) were identified as promising candidates for predictive control. The IRA application has been treated first, and for this application 5 major building system variants were identified and prioritized.
2. **Development of a general methodology for assessing building control schemes.** The methodology consists of (i) problem definition (system, cost functions, constraints etc.); (ii) determination of the so-called Performance Bound (PB, the best possible solution for a given problem assuming perfect forecasts and models); (iii) comparison of control algorithms among each other and with the PB (identification of improvement potentials); and (iv) assessment of Model Predictive Control under increasingly realistic conditions based on the stepwise relaxation of the idealized assumptions present in the PB calculations.
3. **Development of a general modeling and simulation environment.** The developed "Building Automation and Control Laboratory" (BACLab) software is a distributed building modeling and simulation environment tailored to the analysis of (predictive) building control schemes. BACLab consists of generic, portable, and reusable components that provide interfaces to specialized databases (see below). It supports structured problem definitions, the integration of alternative control schemes, and the execution of systematic, large-scale simulation studies, including the post-analysis of the obtained results.
4. **Development of building and HVAC/lighting/blinds models for IRA.** Simulation models operating at an hourly or sub-hourly time step were derived, implemented, tested and validated for a wide range of building types and for various heating, cooling, ventilation, blinds and lighting subsystems.
5. **Development of a building systems server and database**. The so-called BuSy server is a web service supporting the distributed modeling and simulation of buildings and HVAC systems. In particular it provides an interactive (web browser) and an automated (remote simulation client) interface to the so-called BuSyDB, a database supporting the retrieval of structured parameter data sets for a wide range of buildings and IRA building systems.
6. **Database with weather forecasts and observations for building control applications.** Algorithms for the disaggregation of hourly global radiation into the direct and diffuse part, and the derivation of global radiation components on vertical oriented surfaces were implemented in the MeteoSwiss operational processing and dissemination software. These and other relevant weather observations and according predictions from the COSMO-7 numerical weather prediction model furnish the extensive, interactively (web browser) as well as automatically (remote simulation client) accessible OptiControl Weather and occupancy Data Base (OCWDB).

7. **Improvement of local weather forecasts for building control applications.** Statistical methods were developed to improve the accuracy of all relevant local weather forecasts from numerical weather prediction models. The quality of global radiation and radiation components as predicted by the COSMO-7 model was analyzed and characterized for correction. Systematic differences could be substantially reduced for all variables with the developed schemes. Hourly 2m temperature and wet-bulb temperature predictions were also improved physically by changes in the COSMO model diagnostics (operationally introduced in August 2008).
8. **Preparation of standard internal heat gain profiles relevant for IRA.** Standard internal heat gain profiles for offices were prepared and integrated in the OCWDB.
9. **Definition of benchmark control schemes for IRA.** State of the art non-predictive, rule-based control strategies for IRA were selected next to the Performance Bound as benchmark control schemes to measure the performance of the newly developed control algorithms.
10. **Development of rule-based control algorithms and associated tuning rules for IRA.** The rule-based control strategies were implemented within the BACLab software. Automated tuning rules to automatically determine control parameter values as a function of characteristic building parameters were developed. The rules can also be used in practice for manual tuning. Simulation studies proved that applying the new rule-based control strategy RBC-3 results in substantial energy (cost) savings compared to state of the art rule-based control (RBC-1). In many cases, control performance of RBC-3 was found to be close to the Performance Bound.
11. **Development of predictive control algorithms for IRA.** Model predictive control (MPC) schemes were selected, adapted for building climate control and implemented within the BACLab software. Several MPC variants were examined; besides the classical certainty equivalence approach new stochastic MPC controllers were developed.
12. **Design of simulation experiments for IRA.** Study sites, occupancy inputs, building types and HVAC/lighting/blinds systems were defined that span many of the most important IRA configurations. The assessment targets regarding comfort and energy (costs) were specified. Constraints for control strategies (e.g. limited heating/cooling power) were defined using, among other things, appropriate dimensioning procedures.
13. **Large-scale Performance Bound simulation study for IRA.** The minimum possible primary energy and monetary cost under perfect conditions were determined for a wide range of building set-ups and climatic conditions. Differences were compared among narrow vs. wide comfort range width, for constant comfort range vs. night/weekend set-back of comfort range, and for different ventilation strategies. Besides their immediate relevance, these results were useful to put the found primary energy (or cost) savings thanks to improved control into context.
14. **Comprehensive simulation based assessment of rule-based controllers for IRA.** The performance of 4 rule-based controllers was assessed for a large number of cases by comparison of the obtained results (i) under each other, and (ii) with the respective Performance Bound simulations. This showed the controller's absolute performance and range of applicability (building types, HVAC/lighting/blinds systems). The investigations also provided insight into the importance of blind control and revealed the potential of predictive control.
15. **In-depth analysis of potential of predictive control approaches for IRA.** Investigations for a carefully selected set of promising cases assessed the achievable control performance when using realistic weather forecasts. Systematic simulations were also conducted to assess the robustness of MPC on control parameter settings and the robustness on model parameter mismatch.
16. **Preparations for application Generic Flux Control (GFC).** First ideas and modeling approaches for the application GFC were discussed. Specific GFC applications were pre-selected.

17. **Identification of suitable demonstrator building for IRA.** A range of academic research groups, as well as building planers, operators and owners were contacted in the search for an appropriate object. The CCEM-CH demonstrator cell, plus buildings from the portfolios of the ETH Zurich and the company Gruner AG were evaluated in more detail. At last we were able to identify a particularly suitable object for testing of the newly developed control algorithms, a representative office building close to Basle, Switzerland.
18. **Publication and dissemination activities.** Our work has resulted in a series of papers, posters and conference contributions. There have also been several articles in brochures and magazines, indicative of a broader interest in our activities. A comprehensive compilation of project results can be found at the project's web site (www.opticontrol.ethz.ch).

10.3 Challenges

Specification of benchmark control. In order to represent the state of the art in control and to measure possible improvements thanks to novel control schemes, rule-based reference control strategies had to be specified and implemented and also appropriate tuning rules for control parameter values had to be found. These tasks proved very challenging but could be solved to a large part (see points 9 and 10 above). Yet, implementations of rule-based strategies supporting night/weekend set-back, as well as good reference strategies for building systems that include floor heating and TABS are still missing within the BACLab software.

Comparability of control strategies for IRA. The investigated control schemes (RBC-1 to RBC-3, CE-MPC, CCS-MPC, PB) differ in two important points: (i) the degrees of freedom for blind movement and (ii) the treatment of low-level control. E.g., blind movement for RBC-1 is restricted to once an hour and to only three different blind positions whereas there is no restriction in blind movement in the performance bound (PB). For the MPC approaches – with the exception of electric lighting – no low-level control has been taken into account so far. In order to enable or enhance the comparability between the different control strategies, new rule-based control variants were elaborated already, and more have to be elaborated.

Making novel control strategies suitable for the use in practice. This issue causes a delay in the project timetable, and this fact needs to be considered in the further planning. The following elements considered necessary for a successful implementation of new control approaches in a real building still need to be addressed: (i) initial tuning procedure and tuning in operation; (ii) state estimation for model predictive controllers, (iii) internal heat gain prediction and (iv) correction of weather forecasts for local conditions at the building site.

Integration of novel control algorithms in commercial BAC systems. Building automation and control (BAC) systems typically have a hierarchical control structure featuring high-level and low-level control. To facilitate the integration of predictive control schemes in such systems, the new algorithms should preferably replace only the high-level part of existing controllers, thus keeping the interface between high- and low level control unchanged. This was precisely how the rule-based control strategies RBC-x were implemented within the BACLab software, and a similar approach is needed for the MPC strategies. A further challenge is the application of MPC to multiple building zones.

These challenges are being addressed in our current work. For example, a prototype algorithm for the correction of weather forecasts at the building site has already been implemented in BACLab, and a generally applicable solution is currently being developed. Also, possible solutions for predictive rule-based controllers, as well as the coupling of MPC and low-level controllers are currently being examined in two coordinated semester works at ETH/IfA and Siemens BT.